SH
11
A2 F53
FISH

U.S. Department
of Commerce

Volume 117
Number 4
October 2019

Fishery Bulletin

SHOUT
SHARE
IT

U.S. Department of Commerce

Wilbur L. Ross Jr.
Secretary

National Oceanic and Atmospheric Administration

Neil A. Jacobs
Acting Administrator

National Marine Fisheries Service

Chris Oliver
Assistant Administrator
for Fisheries

Fishery Bulletin (ISSN 0090-0656) is published quarterly by the Scientific Publications Office, National Marine Fisheries Service, NOAA, 7600 Sand Point Way NE, Seattle, WA 98115-0070.

Although the contents of this publication have not been copyrighted and may be reprinted entirely, reference to source is appreciated.

The Secretary of Commerce has determined that the publication of this periodical is necessary according to law for the transaction of public business of this Department. Use of funds for printing of this periodical has been approved by the Director of the Office of Management and Budget.

For Sale by the Superintendent of Documents, U.S. Government Publishing Office, Washington, DC 20401. Subscription price per year: $32.00 domestic and $44.80 foreign. Cost per single issue: $19.00 domestic and $26.60 foreign. **See back for order form.**

Fishery Bulletin

Scientific Editor
José I. Castro
National Marine Fisheries Service, NOAA
263 13th Avenue South
Saint Petersburg, Florida 33701

Managing Editor
Kathryn Dennis
Scientific Publications Office
National Marine Fisheries Service, NOAA
1845 Wasp Boulevard, Building 176
Honolulu, Hawaii 96818

Associate Editor
Cara Mayo
Scientific Publications Office
National Marine Fisheries Service, NOAA
7600 Sand Point Way NE
Seattle, Washington 98115-0070

Editorial Board

Henry L. Bart Jr.	Tulane University, New Orleans, Louisiana
Matthew D. Campbell	National Marine Fisheries Service, Pascagoula, Mississippi
Shannon L. Cass-Calay	National Marine Fisheries Service, Miami, Florida
William B. Driggers III	National Marine Fisheries Service, Pascagoula, Mississippi
Gretchen L. Grammer	South Australian Research and Development Institute, Adelaide, Australia
Richard Langton	National Marine Fisheries Service, Walpole, Maine (retired)
Richard S. McBride	National Marine Fisheries Service, Woods Hole, Massachusetts
Richard L. Merrick	National Marine Fisheries Service, Falmouth, Massachusetts (retired)
Richard D. Methot	National Marine Fisheries Service, Seattle, Washington
Lisa J. Natanson	National Marine Fisheries Service, Narragansett, Rhode Island
Joseph M. Quattro	University of South Carolina, Columbia, South Carolina
Mark S. Peterson	University of Southern Mississippi, Ocean Springs, Mississippi
John F. Walter III	National Marine Fisheries Service, Miami, Florida
Bruce Wright	Aleutian Pribilof Island Association, Anchorage, Alaska

***Fishery Bulletin* website: https://spo.nmfs.noaa.gov/fb.htm**

Fishery Bulletin carries original research reports on investigations in fishery science, engineering, and economics. It began as the Bulletin of the United States Fish Commission in 1881; it became the Bulletin of the Bureau of Fisheries in 1904 and the *Fishery Bulletin* of the U.S. Fish and Wildlife Service in 1941. Separates were issued as documents through volume 46; the last document was no. 1103. Beginning with volume 47 in 1931 and continuing through volume 62 in 1963, each separate appeared as a numbered bulletin. A new system began in 1963, with volume 63, in which papers are bound together in a single issue. Beginning with volume 70, number 1, January 1972, *Fishery Bulletin* became a periodical, issued quarterly. In this form, it is available by subscription from the Superintendent of Documents, U.S. Government Publishing Office, Washington, DC 20401. It is also available free in limited numbers to libraries, research institutions, and state and federal agencies and in exchange for other scientific publications.

U.S. Department of Commerce
Seattle, Washington

Volume 117
Number 4
October 2019

Fishery Bulletin

Contents

Articles

277–290 **Joseph D. Schmitt, Brandon K. Peoples, Aaron J. Bunch, Leandro Castello, and Donald J. Orth**

Modeling the predation dynamics of invasive blue catfish (*Ictalurus furcatus*) in Chesapeake Bay

291–302 **Lyndsey S. Lefebvre, Cherisa L. Friedlander, and John C. Field**

Reproductive ecology and size-dependent fecundity in the petrale sole (*Eopsetta jordani*) in waters of California, Oregon, and Washington

Short contribution

303–307 **Dalin N. D'Alessandro and Deborah A. Duffield**

Salmonid passive integrated transponder tags and coded wire tags found in the forestomach of a harbor porpoise (*Phocoena phocoena*) in southwestern Washington

Articles

308–321 **Kevin J. Kolmos, David M. Wyanski, D. Byron White, and Paulette P. Mikell**

Temporal changes in the life history of snowy grouper (*Hyporthodus niveatus*) off North and South Carolina, and factors that influence spawning dynamics

322–336 **Joseph M. O'Malley, Corey B. Wakefield, Zack S. Oyafuso, Ryan S. Nichols, Brett Taylor, Ashley J. Williams, Maria Sapatu, and Michael Marsik**

Effects of exploitation evident in age-based demography of 2 deepwater snappers, the goldeneye jobfish (*Pristipomoides flavipinnis*) in the Samoa Archipelago and the goldflag jobfish (*P. auricilla*) in the Mariana Archipelago

SMITHSONIAN
FEB 19 2020
LIBRARIES

The National Marine Fisheries Service (NMFS) does not approve, recommend, or endorse any proprietary product or proprietary material mentioned in this publication. No reference shall be made to NMFS, or to this publication furnished by NMFS, in any advertising or sales promotion that would indicate or imply that NMFS approves, recommends, or endorses any proprietary product or proprietary material mentioned herein or that has as its purpose an intent to cause directly or indirectly the advertised product to be used or purchased because of this NMFS publication.

The NMFS Scientific Publications Office is not responsible for the contents of the articles.

337–347 Katie V. Anweiler, Karl Brenkert, Tanya L. Darden, Eric J. McElroy, and Michael R. Denson
Effects of temperature and hypoxia on the metabolic performance of juvenile striped bass (*Morone saxatilis*)

348–359 Karissa O. Lear, Gregg R. Poulakis, Rachel M. Scharer, Adrian C. Gleiss, and Nicholas M. Whitney
Fine-scale behavior and habitat use of the endangered smalltooth sawfish (*Pristis pectinata*): insights from accelerometry

360–371 Rebecca K. May, S. Gregory Tolley, Rachel M. Scharer, Bass Dye, Felix Jose, and Gregg R. Poulakis
Automated monitoring of fine-scale movements of the endangered smalltooth sawfish (*Pristis pectinata*)

372–385 H. Kevin Brown, Blake Price, Laura Lee, M. Scott Baker Jr., and Sara E. Mirabilio
Simple gear modifications for achieving greater than 40% bycatch reduction in an estuarine shrimp trawl fishery

386 Acknowledgment of reviewers

387–390 Guidelines for authors

National Marine Fisheries Service
NOAA

Fishery Bulletin
established in 1881

Spencer F. Baird
First U.S. Commissioner of Fisheries and founder of *Fishery Bulletin*

Modeling the predation dynamics of invasive blue catfish (*Ictalurus furcatus*) in Chesapeake Bay

Joseph D. Schmitt (contact author)[1]
Brandon K. Peoples[2]
Aaron J. Bunch[3]
Leandro Castello[1]
Donald J. Orth[1]

Email address for contact author: jschmitt@usgs.gov

[1] Department of Fish and Wildlife Conservation
Virginia Polytechnic Institute and State University
106 Cheatham Hall
Blacksburg, Virginia 24060
Present address for contact author:
Lake Erie Biological Station
U.S. Geological Survey
6100 Columbus Avenue
Sandusky, Ohio 44870

[2] Department of Forestry and Environmental Conservation
Clemson University
256 Lehotsky Hall
142 Jersey Lane
Clemson, South Carolina 29634

[3] Region 1 Office
Virginia Department of Game and Inland Fisheries
3801 John Tyler Memorial Highway
Charles City, Virginia 23030

Abstract—Blue catfish (*Ictalurus furcatus*) have been widely introduced throughout the United States and are invasive in Chesapeake Bay. Despite this proliferation, little is known about the diet of this large, predatory catfish. We used stratified random sampling to collect stomachs from 14,488 blue catfish in Chesapeake Bay. Canonical correspondence analysis (CCA) was used to identify key drivers of the diet of blue catfish, and generalized additive models (GAMs) were used to explore trends in rates of predation by blue catfish on depleted or commercially valuable native species, including American shad (*Alosa sapidissima*), blueback herring (*A. aestivalis*), alewife (*A. pseudoharengus*), American eel (*Anguilla rostrata*), and blue crab (*Callinectes sapidus*). Results of CCA reveal that diets were significantly correlated with season, salinity, and total length (TL) of blue catfish, and those from our GAMs reveal the circumstances associated with greater predation on these species. For example, we found that *Alosa* species were most susceptible to predation by large catfish (>600 mm TL) in freshwater areas during the month of April. This paper describes methods for identifying times, locations, and other circumstances that are associated with maximal predation rates upon certain taxa. The information gained from these approaches can be used to inform management strategies, with the goal of reducing effects of predation on specific organisms.

Manuscript submitted 8 February 2019.
Manuscript accepted 9 September 2019.
Fish. Bull. 117:277–290 (2019).
Online publication date: 19 September 2019.
doi: 10.7755/FB.117.4.1

The views and opinions expressed or implied in this article are those of the author (or authors) and do not necessarily reflect the position of the National Marine Fisheries Service, NOAA.

Invasive species are key drivers of the global biodiversity crisis (Vitousek et al., 1997; Mack et al., 2000), can cause enormous economic losses (Pimentel, 2011), and can result in native species declines and extinctions (McGee et al., 2015). Invasive fish species have been a chronic problem at the global scale, yet there are considerable knowledge gaps pertaining to their impacts on recipient ecosystems (Cucherousset and Olden, 2011). Some introduced fish species appear to be benign, but others have deleterious ecological effects, restructuring native communities through competitive interactions or direct predation (Helfman, 2007; Albins and Hixon, 2008). Because of these potential impacts, description of the diet is important in understanding how an invader may affect a given ecosystem (Brandner et al., 2013; Dick et al., 2014).

The blue catfish (*Ictalurus furcatus*) is the largest catfish species (Ictaluridae) in North America and is one of the most prolific invasive fish species in Atlantic slope drainages of the southeastern United States (Fuller and Neilson, 2018). Blue catfish have been widely stocked outside of their native range (Mississippi River basin) for recreational fishing purposes (Graham, 1999), and they were introduced to tidal rivers in Virginia during the 1970s (Greenlee and Lim, 2011). Blue catfish populations grew rapidly during the late 1990s, prompting concern and subsequent management action (Fabrizio et al., 2018). Populations of blue catfish have since expanded from tidal freshwater areas into oligohaline and mesohaline portions of several tidal tributaries of Chesapeake Bay (Greenlee and Lim, 2011). This expansion is problematic because these brackish areas serve as spawning and nursery habitat for many native marine and estuarine species (MacAvoy et al., 2009; Magoro et al., 2015).

Over several decades, populations of native fish taxa, including the Atlantic

sturgeon (*Acipenser oxyrinchus*), the American shad (*Alosa sapidissima*), *river herring*, a collective term for the blueback herring (*A. aestivalis*) and the alewife (*A. pseudoharengus*), and the American eel (*Anguilla rostrata*), have declined in Chesapeake Bay (Haro et al., 2000; Niklitshek and Secor, 2005; Limburg and Waldmen, 2009). Chesapeake Bay is far from pristine, and anthropogenic activities have resulted in major ecological changes, including the widespread loss of aquatic macrophytes, increased turbidity, and frequent hypoxic and anoxic events (Kemp et al., 2005). Scientists and fisheries managers are now concerned that predation by invasive blue catfish may lead to further declines of depleted native fish species. Although blue crab (*Callinectes sapidus*) are not rare, there is concern about predation pressure on this species because it supports lucrative commercial fisheries in Virginia, Maryland, and Delaware (Paolisso, 2002). Other studies have shown that blue catfish are consuming the aforementioned fish and crab species, with the exception of Atlantic sturgeon (Schmitt et al., 2017, 2019). Previous research has revealed that blue catfish in Chesapeake Bay have remarkably broad diets that include vegetation, numerous fish species, mollusks, crustaceans, birds, terrestrial mammals, reptiles, amphibians, and various invertebrates, yet the factors that drive dietary variation have not yet been identified (Schmitt et al., 2019). Furthermore, the predation dynamics of blue catfish on depleted species like the American shad and American eel have not been described.

Although a substantial body of literature is dedicated to factors that influence the establishment of invasive species (Catford et al., 2009; Blackburn et al., 2011), fewer works have focused on the impact phase of invasion (Fei et al., 2016), and most studies produce speculative results (Simberloff et al., 2013). This is especially the case for invasive fish species, for which more observational and experimental studies are urgently needed (García-Berthou, 2007; Layman and Allgeier, 2012; Brandner et al., 2013). Diet studies are not necessarily direct measures of impact, but they are useful for determining which organisms are most likely to be affected by an introduced predator (Caut et al., 2008; Layman and Allgeier, 2012). Diet studies can also be used to determine when and where depleted species are most vulnerable to predation by an invader, information that can be used to guide management efforts (Schmitt et al., 2017).

This study fulfilled 2 main objectives. First, we used multivariate modeling to determine the significance and relative influence of several factors that were suspected to influence the food habits of blue catfish. We hypothesized that diets would vary spatiotemporally, as these tidal systems support diverse assemblages that change in space and time due to salinity preference and seasonal migration patterns (Wagner and Austin, 1999; Jung and Houde, 2003). We also expected diets to vary with catfish size, as previous work has demonstrated that blue catfish undergo ontogenetic diet shifts from omnivory to piscivory at larger sizes (500–900 mm total length [TL], depending on the river; Schmitt et al., 2019). Second, we incorporated any significant factors from the first objective into models of predation on American shad, river herring, American eel, and blue crab. These models were then used to elucidate the circumstances that result in greater predation on these depleted or economically valuable native taxa. This information can be used to direct management efforts, which we discuss later.

Materials and methods

Study area

Chesapeake Bay is the largest estuary in the continental United States and has a long history of commercial and recreational exploitation (McHugh and Bailey, 1957; Richards and Rago, 1999). Although blue catfish are now found in all major tributaries of Chesapeake Bay (Schloesser et al., 2011), many populations are still in the early stages of establishment and support low densities of fish (Aguilar et al., 2017). We therefore focused our efforts on the James, Pamunkey, Mattaponi, and Rappahannock Rivers in eastern Virginia (Fig. 1). These rivers were stocked with hundreds of thousands of blue catfish between 1973 and 1985 and now contain well-established populations that include mature individuals (Greenlee and Lim, 2011; Bunch et al., 2018).

Field methods

Each river was divided into 3 strata according to average fall surface salinities during 1985–2016 by using data from the Chesapeake Bay Program's Water Quality Database (available from website). The 3 strata included tidal freshwater stretches (Practical Salinity [S_P]: 0.0–0.5), oligohaline stretches (S_P: 0.6–5.0), and mesohaline stretches (S_P: 5.0–18.0). We stratified each river by autumn salinities because density stratification is less problematic during fall (Shiah and Ducklow, 1994). Each stratum was divided into 2-km sections, which were numbered, and then a random number generator was used to select each sampling location. During April–October, a minimum of 2 randomly selected sections were sampled monthly within each stratum for all 4 rivers, with both nearshore and main-channel sampling occurring when possible. Most blue catfish were sampled by using low-frequency, pulsed direct current electrofishing (5–25 Hz, 100–400 V) because it captures blue catfish of all sizes (Bodine and Shoup, 2010) and is extremely effective in Virginia's tidal rivers (Greenlee and Lim, 2011; Schmitt and Orth, 2015). In higher salinities, pulsed alternating current electrofishing was occasionally used, and anode design, voltage, and pulse frequency were adjusted on the basis of water conductivity and other environmental conditions.

Upon capture, fish were immediately placed in a 568-L aerated livewell, and stomach contents were extracted within 30 min of capture to prevent regurgitation (Garvey and Chipps, 2012). Stomach contents were extracted either by excising the stomachs or with pulsed gastric lavage, which is highly effective for extracting stomach contents from blue catfish (Waters et al., 2004). Date, time,

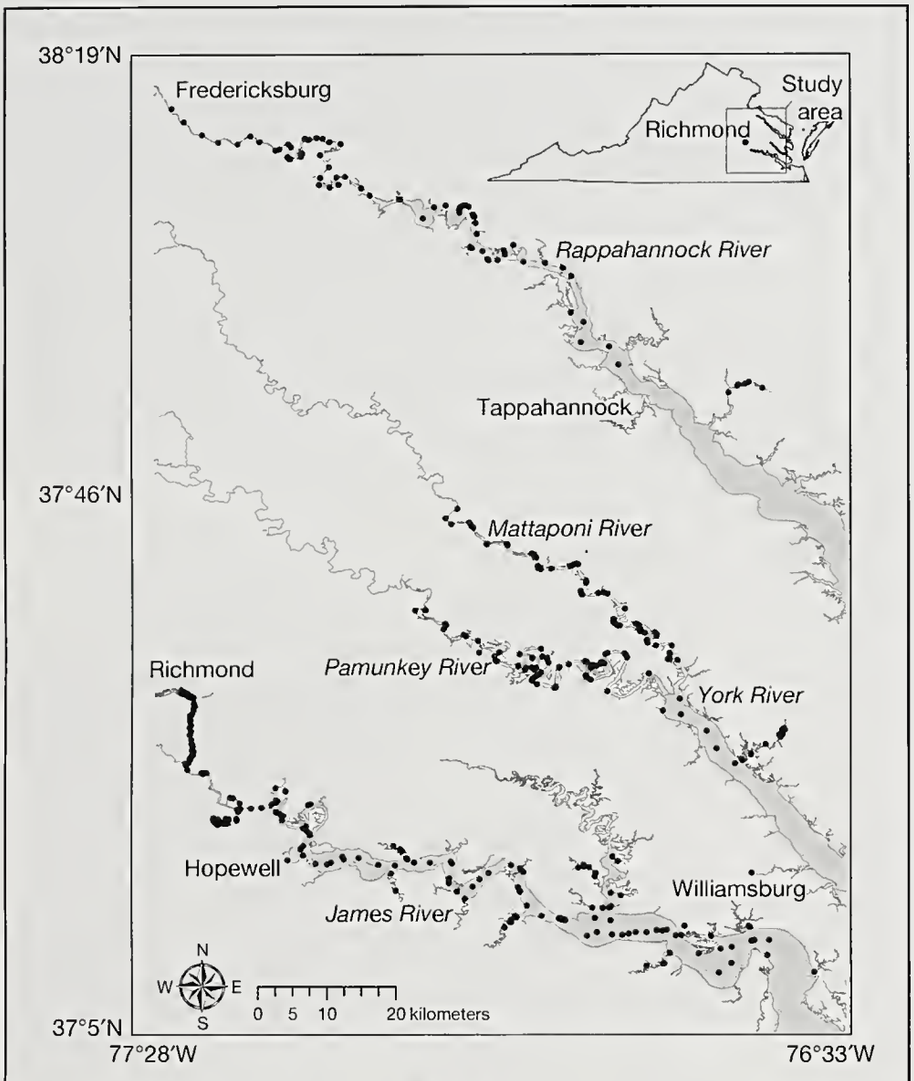

Figure 1

Map of eastern Virginia showing the 542 locations (black circles) in 4 major tidal rivers where blue catfish (*Ictalurus furcatus*) were collected from April through October in 2013–2016 for analysis of the contents of their stomachs (n=14,488). From north to south, rivers sampled were the Rappahannock, Mattaponi, Pamunkey, and James Rivers. The Mattaponi and Pamunkey Rivers converge to form the York River.

water temperature, salinity, and coordinates were recorded for each sampling event. Fish weight (in grams) and TL (in millimeters) were also recorded, and stomach contents were placed on ice and later frozen.

Laboratory methods

Prior to examination, stomachs were thawed, and stomach contents were blotted dry with a paper towel (Schmitt et al., 2017). Prey items were then weighed, counted, and identified to the lowest possible taxon. Digested fish remains that lacked morphological distinctiveness were identified by using DNA barcoding techniques. The use of DNA barcoding enabled us to identify 70–80% of fish prey that were unidentifiable by gross morphology, excluding instances in which only bones or scales remained. Our DNA barcoding methods are described in Moran et al. (2016) and Schmitt et al. (2017, 2019).

Modeling diet drivers for blue catfish

Populations of blue catfish extend from tidal fresh water into mesohaline waters in Chesapeake Bay, where species assemblages change along the salinity gradient (Wagner and Austin, 1999; Jung and Houde, 2003). Seasonality affects the availability of some prey resources, such as adults of *Alosa* species, which enter tidal rivers during spring to spawn (Waldman, 2013), or blue crab, which migrate seasonally (Aguilar et al., 2005). Moreover, blue catfish exhibit ontogenetic trophic niche shifts, with differently sized fish consuming different prey (Schmitt et al., 2017). We therefore hypothesized that the diet of blue catfish would vary with season, salinity, and catfish size.

We explored overall patterns in the diet of blue catfish by using canonical correspondence analysis (CCA; ter Braak, 1986). This analysis is a form of multivariate ordination in which a matrix of response variables is "regressed" (constrained) on a matrix of independent variables; it is the multivariate analog of multiple linear regression. It is often used for analyzing relationships between species assemblages and multidimensional environmental data (ter Braak and Verdonschot, 1995), but CCA has also been used for assessing feeding patterns (Clifton and Motta, 1998; Jaworski and Ragnarsson, 2006). Because we were interested in general diet patterns, we first grouped all diet items into 6 broader categories: fish species, mollusks, crustaceans, other invertebrates, vegetation, and *other* (e.g., anthropogenic debris, terrestrial mammals, birds, and other rare items). Each CCA was based on the binary presence–absence of diet items (i.e., frequency of occurrence) because it is less biased than other diet measures and is preferred for assessing feeding patterns (Baker et al., 2014; Buckland et al., 2017). Predictor variables included salinity zone, TL (rounded to the nearest 100 mm), and season (also coded as 3 dummy variables).

We assessed whole-model and variable-wise statistical significance with F-tests, and significance was assessed by using an alpha threshold of 0.05. Magnitude of relationship groupings of individual fish and constraining variables or diet items were assessed on the basis of loading scores (an analog of correlation coefficients, centered at 0 and ranging from −1 to 1). Because previous studies

showed river-specific variability in diet, dietary ontogeny, growth, and population structure, we conducted a separate CCA for each river (Hilling et al., 2018; Schmitt et al., 2019). Each CCA was completed in the package vegan (vers. 2.4-4; Oksanen et al., 2017), which is an extension of the statistical software R, vers. 3.4.3 (R Core Team, 2017).

Predation models for species of concern

We used binomial generalized additive models (GAMs), which are semiparametric generalizations of logistic regression (Hastie and Tibshirani, 1990), to examine relationships between the binary occurrence of depleted alosines (American shad and river herring), blue crab, and American eel in the diet of blue catfish by predictor variables identified in each CCA. This approach was especially useful for identifying when and where predation by blue catfish on these species of concern was most likely. Again, the GAMs were based on occurrence data because it is the best metric for assessing predation and is often more reliable than other diet measures (Baker et al., 2014; Buckland et al., 2017). A GAM is flexible because it assumes only that functions are additive and relationships are smooth (Guisan et al., 2002). A GAM, like a generalized linear model, uses a link function to establish a relationship between the mean of the response variable and a "smoothed" function of the explanatory variables, making it robust to scattered or correlated data (Lin and Zhang, 1999). Separate GAMs were constructed for American eel, depleted *Alosa* species (American shad and river herring), and blue crab. Each GAM included smoothing functions for *predator length* and *salinity*, yet *month* and *river* were treated as categorical factors (Wood, 2006). Although interannual variation is likely an important driver of dietary patterns, stomach contents for each month were pooled across years (e.g., contents for June in 2013, 2014, 2015, and 2016 were combined into the single category for June) to increase sample sizes. This pooling was a necessary step because circumstances that were out of our control (equipment failure and weather) resulted in limited sampling during some combinations of month and year (e.g., June 2014).

Each model was created by using the R package mgcv, vers. 1.8.28 (Wood, 2017), with default values unless otherwise specified. Each model was constructed as follows:

$$\text{logit}(P) = \beta_0 + f_1(\textit{predator length}) + f_2(\textit{salinity}) + \textit{month} + \textit{river},$$

where logit = the binomial link function;
P = the probability of a species being consumed;
β_0 = the model intercept; and
f_1–f_2 = the smoothing functions realized by penalized thin plate regression splines (Wood, 2006).

For each covariate, the mgcv package fits a series of penalized regression splines as smoothing functions and supplies degrees of freedom for smooth terms by minimizing generalized cross-validation scores (Wood, 2006). Individual F-tests were then used to determine which predictors contribute significantly to the deviance explained (Wood, 2006). The probability of encountering each species in stomachs of blue catfish was then predicted separately by river to elucidate the conditions that lead to higher predation rates for these species. Overall predictive performance of each model was then assessed by using the area under the receiver operating curve (ROC) in the package ROCR (vers. 1.0-7; Sing et al., 2005) in R. An area under the ROC of 0.5 is equivalent to a random guess, a value of 1.0 indicates perfect model performance, and a value >0.7 indicates adequate model performance (Bewick et al., 2004; Austin, 2007).

Results

Data collection

During 2013–2016, we collected 14,488 blue catfish stomachs at 542 sites on the James, Pamunkey, Mattaponi, and Rappahannock Rivers in eastern Virginia (Fig. 1). In addition, stomachs were collected from several hundred fish that were captured from the York River, which forms at the confluence of the Pamunkey and Mattaponi Rivers near Westpoint, Virginia (Fig. 1). For simplicity, fish captured from the northern half of the York River were allocated to the Mattaponi River sample, and fish captured on the southern half were allocated to the Pamunkey River sample. Of the stomachs collected, 7302 contained food items (50%). Although stomachs (sample size [n]=16,110) were collected year-round (Schmitt et al., 2019), we limited this study to stomachs that were collected by using low-frequency electrofishing following a stratified random sampling protocol (April–October) to avoid spatiotemporal biases.

Major diet drivers for blue catfish

Diets of blue catfish varied by river, salinity, season, and predator TL, and all constraining variables were statistically significant in the CCA (P<0.001; Table 1). For each river, the first 2 CCA axes accounted for a considerable amount of variation in the diet of blue catfish: 80.0% in the James River, 85.0% in the Rappahannock River, 97.4% in the Pamunkey River, and 93.3% in the Mattaponi River. Global F-tests on each CCA for each river were highly significant (P<0.001 for all), and nearly all constraining variables significantly affected the diet of blue catfish in each river (P<0.001), with the exception of salinity zone in the Mattaponi River (P=0.081; Table 1, Fig. 2).

Results of each CCA indicate several key patterns in the diet of blue catfish. First, there were consistent, length-related (i.e., ontogenetic) shifts from omnivory to piscivory in all rivers. Second, blue catfish more frequently preyed on invertebrates or crustaceans during spring than during other seasons and began to consume more fish as the seasons progressed. Third, the predation of various invertebrates is generally associated with lower salinities,

Table 1

Results of the canonical correspondence analyses used to identify key drivers of the diet of blue catfish (*Ictalurus furcatus*) collected in 4 tributaries to Chesapeake Bay in Virginia during 2013–2016. Whole-model and variable-wise statistical significance ($P<0.05$) were evaluated with F-tests. Predictor variables include salinity zone, season, and predator total length. Separate models were developed for each river.

	James River			Rappahannock River			Pamunkey River			Mattaponi River		
Variable	df	F	P	df	F	P	df	F	P	df	F	P
Whole model	4	17.9	<0.001	4	21.6	<0.001	4	21.7	<0.001	4	14.9	<0.001
Salinity zone	1	32.7	<0.001	1	11.8	<0.001	1	46.7	<0.001	1	1.9	0.081
Season	3	21.6	<0.001	2	49.2	<0.001	2	13.3	<0.001	2	43.1	<0.001
Total length	1	8.9	<0.001	1	7.6	<0.001	1	7.8	<0.001	1	11.3	<0.001

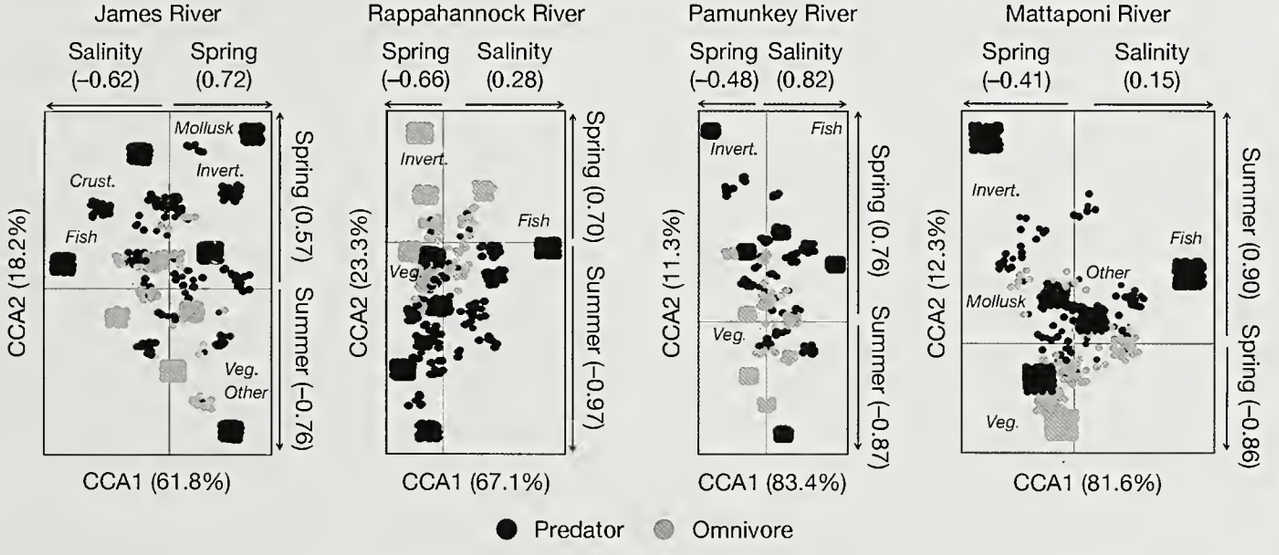

Figure 2

Canonical correspondence analysis (CCA) plots used to identify key drivers of the diet of blue catfish (*Ictalurus furcatus*) collected in 4 tributaries to Chesapeake Bay in Virginia during 2013–2016. Each point represents an individual fish and has been jittered to reduce overlap of individuals with the same combination of diet items. Gray points represent individuals containing vegetation in their stomachs (i.e., omnivores), and black points represent predatory fish. The amount of variation in multivariate diet responses described by each axis is reported in each axis label. Loading scores of independent constraining variables (e.g., season and salinity zone) are presented on the outsides of the plots, instead of traditional arrowed vectors within plots. Constraining variable loading scores on a given axis should be interpreted as directional within plot halves. Only loading scores >0.4 are presented (for all axis loading scores, see Table 2). Text within plots indicates loading scores of diet items, such as other invertebrates (Invert.), crustacean (Crust.), and vegetation (Veg.). Although points have been jittered, they are positioned in the correct quadrants as close as possible to their original coordinates.

but blue catfish shifted toward piscivory in higher salinity areas, especially in the James and Pamunkey Rivers (Fig. 2). Not surprisingly, herbivory was strongly associated with spring and summer in all rivers.

Perhaps most importantly, patterns were not consistent among rivers. For example, herbivory was strongly associated with summer in all rivers except the Rappahannock River, where it was more prevalent in spring. Moreover, distinct length- and season-related breaks were observed in diets of individual blue catfish from some rivers (e.g., the Mattaponi River), but much more overlap occurred in other rivers (e.g., the James River; Fig. 2). All CCA axis loadings of diet items and constraining variables are presented in Table 2.

Predation models for species of concern

Our GAMs demonstrate that predation by blue catfish on species of concern varies by river, salinity, month, and predator TL (Figs. 3–5). All GAMs were globally significant

Table 2

All canonical correspondence analysis (CCA) axis loadings (CCA1 and CCA2) of diet items and constraining variables used to identify patterns in the diet of blue catfish (*Ictalurus furcatus*) collected during 2013–2016 in 4 tributaries to Chesapeake Bay in Virginia—the James, Pamunkey, Mattaponi, and Rappahannock Rivers. Variables include salinity zone, season (spring and summer), and predator total length. Separate models were constructed for each river.

	James		Pamunkey		Mattaponi		Rappahannock	
Variable	CCA1	CCA2	CCA1	CCA2	CCA1	CCA2	CCA1	CCA2
Salinity zone	−0.624	0.303	0.816	−0.312	0.150	0.013	0.284	0.105
Spring	0.720	0.574	−0.482	0.759	−0.415	−0.868	−0.665	0.702
Summer	−0.036	−0.756	−0.420	−0.870	−0.092	0.898	0.029	−0.973
Total length	−0.050	0.530	0.286	−0.289	−0.194	0.391	−0.041	−0.078

(P<0.001), and all predictors were significant (P<0.05), with the exception of salinity in the model for predation on American eel (Table 3). All GAMs had acceptable predictive performance, with areas under the ROC of 0.84–0.86 (Table 2; Pearce and Ferrier, 2000).

Our models demonstrate that depleted alosines, American shad and river herring, were most susceptible to predation by blue catfish in tidal freshwater areas. As many as 4% of stomachs from blue catfish were expected to contain these taxa in certain areas (e.g., tidal freshwater stretches of the James River; Fig. 3). Our model also revealed that large blue catfish consumed more alosines, and as many as 8% of stomachs from 700–1000-mm-TL blue catfish were predicted to contain American shad or river herring in the James River. Seasonally, the probability of predation upon depleted *Alosa* species was greatest in April, with another increase in predation during October. Overall, predicted predation on alosines was highest in the James and Rappahannock Rivers. In the imperiled alosine GAM, river herring were the most commonly consumed species group in both rivers, although American shad were found in more stomachs of blue catfish from the Rappahannock River than in those from the James River (Schmitt et al., 2019).

Our model suggests that predation on blue crab increases at higher salinities. Nearly 30% of stomachs from blue catfish were predicted to contain blue crab in S_P levels >8 in the James River, and predicted percent occurrence of blue crab in stomachs was typically less than 5% in the other rivers. Large blue catfish consumed blue crab more frequently, and model predictions indicate that catfish between 600 and 900 mm TL were most likely to consume blue crab (Fig. 4). Model predictions also indicate that predation on blue crab was greatest during the late summer and into fall (August–October).

Predation on American eel was uncommon, and predicted occurrence in stomachs of blue catfish was <5% in all modeled scenarios (Fig. 5). Predation on American eel was not significantly correlated with salinity (P>0.05), although it was correlated with predator TL and month (P<0.02). Model predictions indicate that medium and large blue catfish (500–900 mm TL) were the most likely to consume American eel. Seasonally, predicted occurrence was highest during spring and fall, particularly in April and October (Fig. 5).

Discussion

In all rivers, the diet of blue catfish varied with season, salinity, or both. These 2 factors also influence the structure of assemblages of organisms in Chesapeake Bay (Wagner and Austin, 1999; Jung and Houde, 2003; Lippson and Lippson, 2006). These relationships are intuitive because species assemblages vary drastically along the salinity gradient and some species are only available seasonally (Wagner and Austin, 1999; Jung and Houde, 2003; King et al., 2005). For example, aquatic macrophytes, which are commonly found in stomachs of blue catfish (Schmitt et al., 2019), are generally only available during the warmer months (Moore et al., 2000). Other potential prey in tributaries of Chesapeake Bay include adult American shad, hickory shad (*A. mediocris*), and river herring that make upstream spawning migrations during spring (Garman and Nielsen, 1992; Schmitt et al., 2017). Additionally, juveniles of these taxa emigrate from these rivers during the late summer and autumn months (Hoffman et al., 2008). Blue crab and American eel also make seasonal movements in these rivers (Wenner and Musick, 1974; Aguilar et al., 2005), and our models revealed increased predation during these migratory periods. Lastly, although interannual variation is likely an important driver of dietary patterns for blue catfish, stomach contents were pooled across years for each month to increase sample sizes for our study. Other diet studies have reported strong interannual trends that mirror fluctuations in prey abundance (Latour et al., 2008).

Multivariate analyses identified consistent, length-related shifts from omnivory to piscivory, a finding consistent with previous work (Schmitt et al., 2017, 2019). In general, small blue catfish feed primarily on macrophytes and benthic invertebrates, and large blue catfish become more piscivorous (see Schmitt et al., 2019). The size at which this shift to piscivory occurs varies from

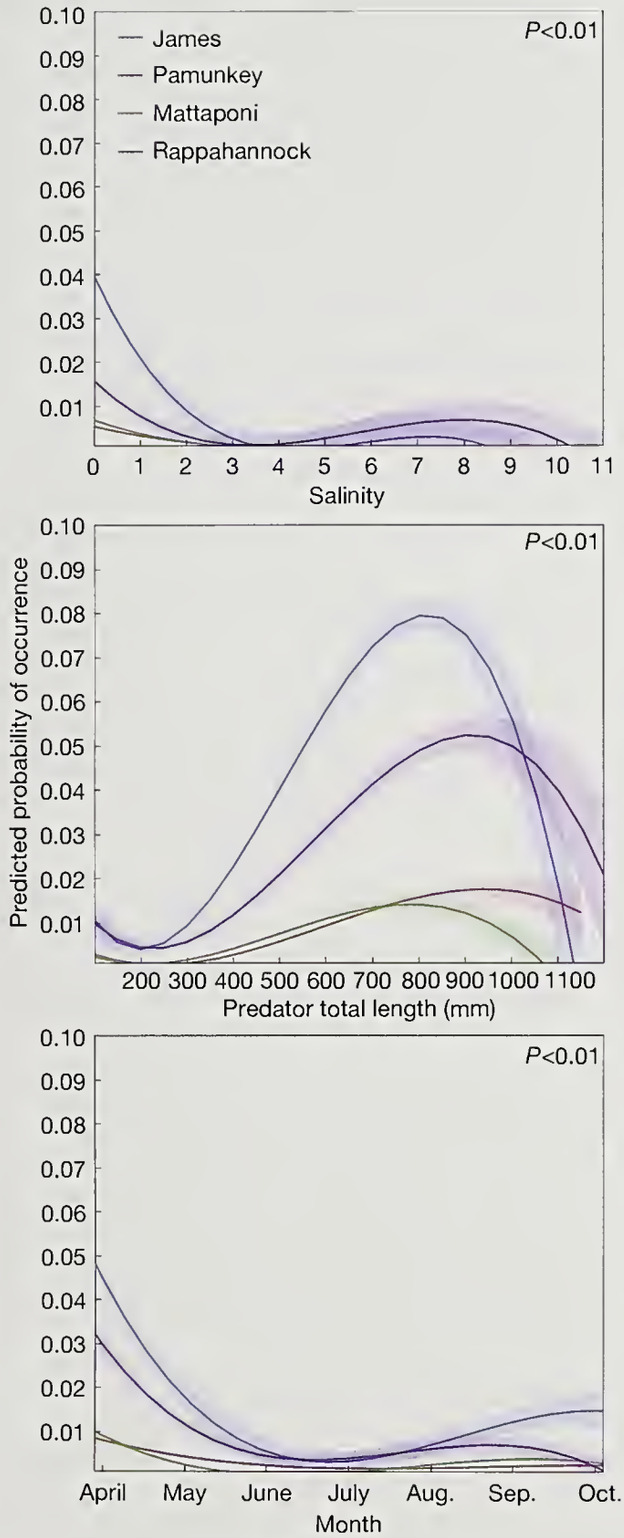

Figure 3

Predictions from the generalized additive model for predation on imperiled alosines by blue catfish (*Ictalurus furcatus*), calculated as probability of occurrence in a catfish stomach, by salinity, predator total length, month, and river. All predictive factors were significant ($P<0.05$). Imperiled alosines include the American shad (*Alosa sapidissima*), blueback herring (*A. aestivalis*), and alewife (*A. pseudoharengus*). Blue catfish were collected in the James, Pamunkey, Mattaponi, and Rappahannock Rivers in eastern Virginia during 2013–2016.

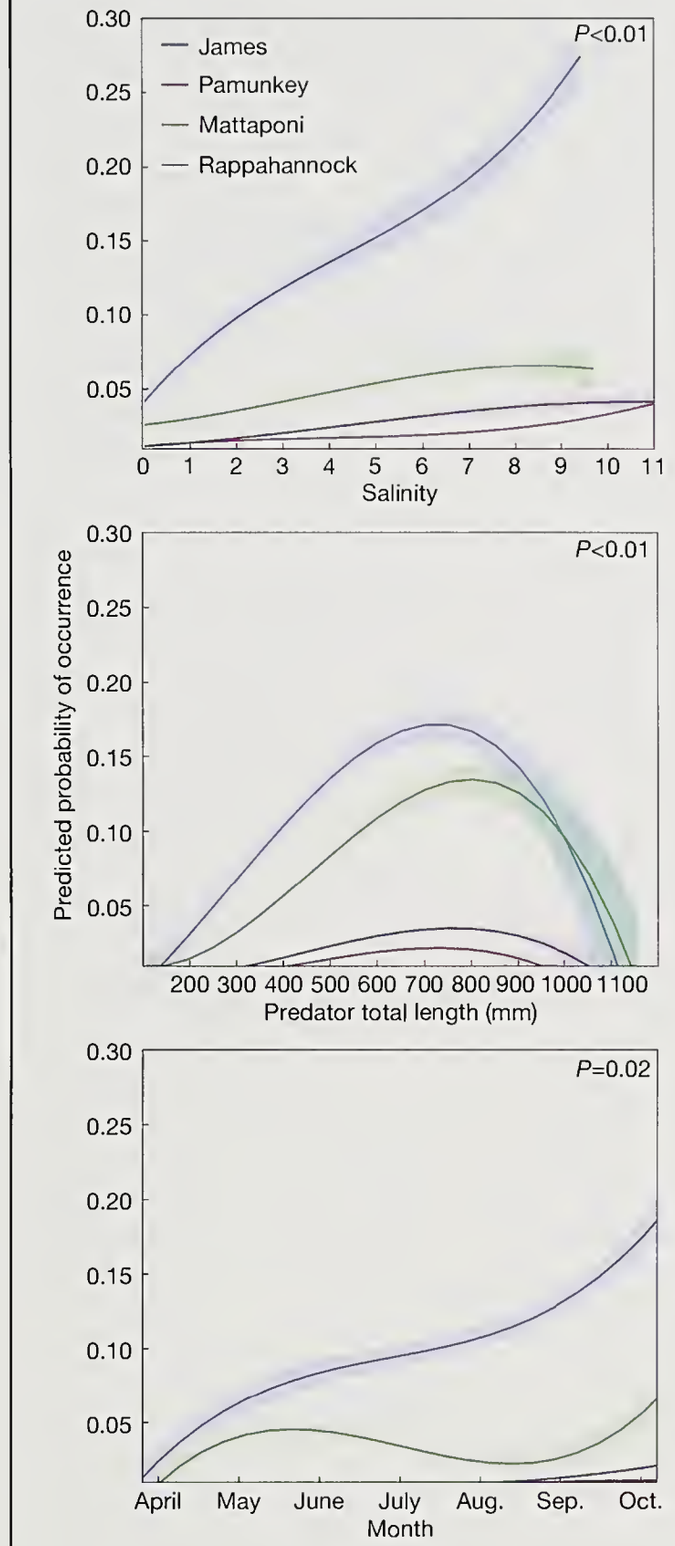

Figure 4

Predictions from the generalized additive model for predation on blue crab (*Callinectes sapidus*) by blue catfish (*Ictalurus furcatus*), calculated as probability of occurrence in a catfish stomach, by salinity, predator total length, month, and river. All predictive factors used in the model were significant ($P<0.05$). Blue catfish were collected in the James, Pamunkey, Mattaponi, and Rappahannock Rivers in eastern Virginia from April through October during 2013–2016.

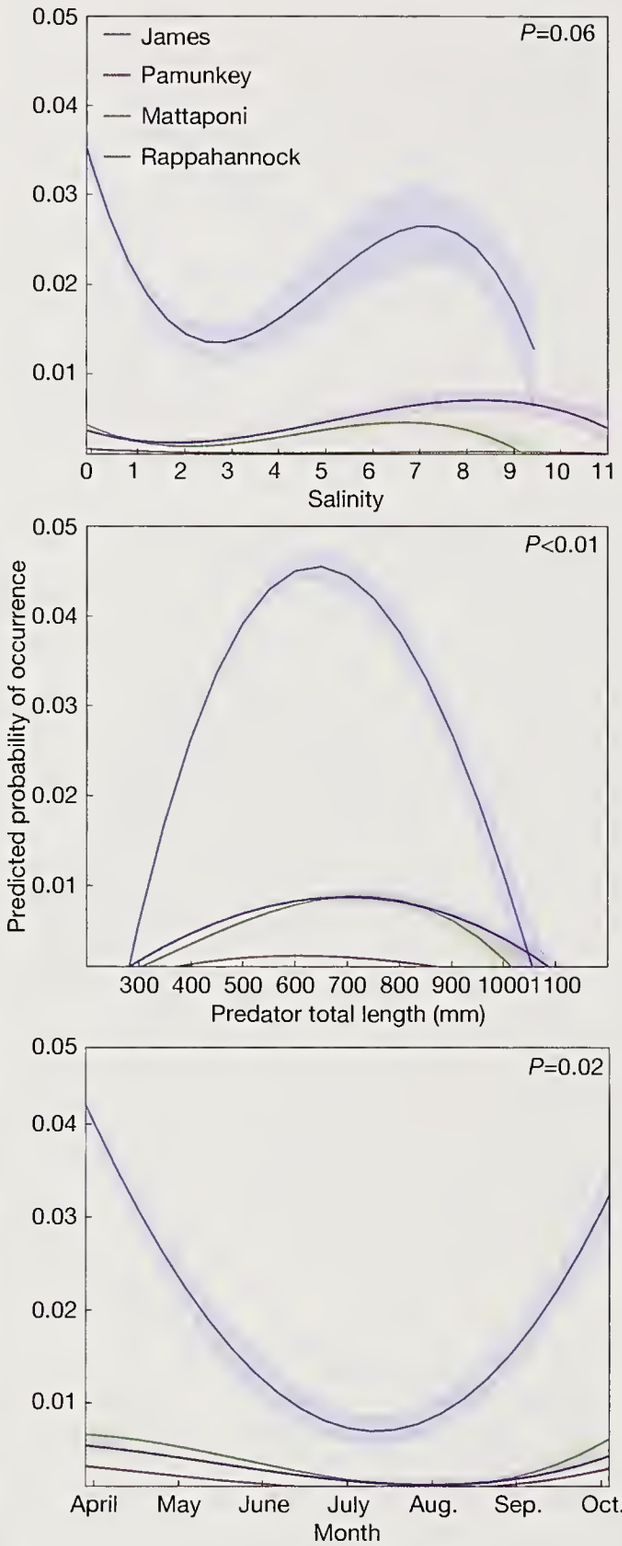

Figure 5

Predictions from the generalized additive model for predation on American eel (*Anguilla rostrata*) by blue catfish (*Ictalurus furcatus*), calculated as probability of occurrence in a catfish stomach, by salinity, predator total length, month, and river. All predictive factors were significant ($P<0.05$), with the exception of salinity ($P=0.06$). Blue catfish were collected in the James, Pamunkey, Mattaponi, and Rappahannock Rivers in eastern Virginia during 2013–2016.

Table 3

Whole-model and variable-wise statistical significance for each generalized additive model (GAM) used to explore trends in rates of predation by blue catfish (*Ictalurus furcatus*) on American eel (*Anguilla rostrata*); imperiled alosines, including American shad (*Alosa sapidissima*), blueback herring (*Alosa aestivalis*), and alewife (*A. pseudoharengus*); and blue crab (*Callinectes sapidus*) in Chesapeake Bay in Virginia during 2013–2016. An asterisk indicates that the value was insignificant ($\alpha=0.05$). Model performance was evaluated by using area under the receiver operating curve (ROC) and deviance explained.

Predictor	American eel	Imperiled alosines	Blue crab
River	$P<0.001$	$P=0.009$	$P<0.001$
Month	$P<0.001$	$P=0.019$	$P=0.017$
Salinity	$P=0.063$*	$P<0.001$	$P<0.001$
Total length	$P=0.023$	$P<0.001$	$P<0.001$
Model fit			
Area under ROC	0.859	0.874	0.843
Null deviance	651.305	698.980	2032.733
Residual deviance	127.875	151.977	440.578
Deviance explained	523.430	547.003	1592.155

500 mm TL (James River) to 900 mm TL (Pamunkey River) and may be driven by the relative abundance of small fish prey in each river (Schmitt et al., 2019). Although large, piscivorous catfish compose a small fraction of each population, they could still have deleterious effects on important native taxa like American shad, river herring, and American eel. Ample evidence indicates that blue catfish feed on locally abundant prey, as other studies have reported that blue catfish are nonselective, opportunistic feeders (Eggleton and Schramm, 2004; Schmitt et al., 2017). These life history traits have been documented in many other estuarine and marine fish species, for which diets are a reflection of the variability of available prey (Beumer, 1978; Livingston, 1984; Ley et al., 1994; Jaworski and Ragnarsson, 2006).

Our GAMs revealed the circumstances that lead to greater predation on species of concern by invasive blue catfish. For American shad and river herring, maximal predation occurred in freshwater areas, a finding that corresponds with those of Schmitt et al. (2017), who reported that predation on depleted alosines peaked in both tidal and non-tidal freshwater segments of the James River. For simplicity, we pooled imperiled alosines for analysis; however, river herring were consumed more frequently than American shad, which are larger and faster-swimming fish (Waldman, 2013). For more detailed, species-specific data, please see Schmitt et al. (2019). For all rivers, the highest predation rates occurred in April, a result that agrees with previous work from the James River (Schmitt et al., 2017). Although some of the alosine prey items were in the late stages of digestion, all of the discernible

specimens captured during spring were mature, spawning adults. The model for American shad and river herring also revealed a small increase in predation during September and October. All alosines consumed during this period were small, and autumn is associated with the outriver migration of juvenile alosines in Atlantic estuaries (Loesch and Lund, 1977; Hoffman et al., 2008; Palkovacs et al., 2014). Therefore, this migratory behavior may make juvenile alosines more susceptible to predation by blue catfish at this time. It is important to note that small, juvenile fish are digested more rapidly than adults (Bromley, 1994) and that, as a result, we may have underestimated predation on juvenile alosines during autumn.

Predation on American shad and river herring was highest for blue catfish ranging in size from 600 to 900 mm TL, although predation probabilities decrease for trophy-sized catfish (≥1072 mm TL; Gabelhouse, 1984). These feeding patterns may be driven by individual diet specialization, where trophy-sized blue catfish are cannibalistic or specialize on gizzard shad (*Dorosoma cepedianum*) as observed by Schmitt et al. (2019). The predicted percent occurrence of alosines in the diet of blue catfish was relatively low in all circumstances (<8% occurrence). It is also important to note that some *Alosa* species can experience high post-spawning mortality because of energetic demands (Glebe and Leggett, 1981), and the presence of alosines in blue catfish stomachs could be, in part, due to scavenging (Schmitt et al., 2019).

Along the Atlantic coast, declines in populations of river herring and American shad began well before the proliferation of blue catfish and must have been initiated by other mechanisms (e.g., declines in populations of American shad began during the 1800s, and river herring populations declined precipitously in the 1960s; Limburg and Waldman, 2009). Alosines face many challenges, including habitat loss, overharvesting, poor water quality, climate change, and impediments that block migratory corridors (Limburg and Waldmen, 2009; Raabe and Hightower, 2014). Moreover, alosines are frequently taken as bycatch in Atlantic herring (*Clupea harengus*) fisheries (Bethoney et al., 2013; Hasselman et al., 2016). Nonetheless, predation by invasive catfish could further destabilize these species, especially if functional response curves are such that predation rates increase at low prey densities (Dick et al., 2014). Interestingly, some signs of recovery have been observed for populations of American shad in the Rappahannock and Potomac Rivers (Cummins[1]; Hilton et al.[2]). Both of these rivers support dense populations of blue catfish, possibly indicating that blue catfish play an insignificant role in the population dynamics of American shad.

Blue catfish predation on blue crab increased with salinity, and this increase was likely driven by the relative density and spatial dynamics of blue crab populations in the James, York, and Rappahannock Rivers. Previous research has indicated that blue crab abundance (measured as the number of blue crab caught per 24 h in fyke nets) was positively correlated with salinity in tidal tributaries of Chesapeake Bay (King et al., 2005). Moreover, low-salinity areas are typically dominated by adult male crab, which, because of their large size, are less susceptible to predation, yet smaller juvenile and female crab become more abundant at higher salinities (Hines et al., 1987). Many of the blue crab we found in stomachs were immature, a finding that correlates well with the observed relationship between salinity and predation on blue crab. Rates of predation on blue crab were highest for blue catfish around 800 mm TL and declined in larger blue catfish. Maximal predation rates occurred during the autumn months in all rivers, although predation on blue crab increased during spring in the Mattaponi River. The autumn months are typically associated with reduced freshwater inflow, which often results in the upriver advancement of the salt wedge (Schubel and Pritchard, 1986). As the salt wedge advances upriver, we would expect there to be greater spatial overlap between blue catfish and blue crab (King et al., 2005). We directly observed this phenomenon in the James River when we found blue crab at high densities along the lower edge of the fall line during August and September. This area is usually home to freshwater species, like the smallmouth bass (*Micropterus dolomieu*) and various sunfish species (*Lepomis* spp.), but the upriver advancement of the salt wedge enables blue crab to colonize this area during extended dry periods.

Blue crab naturally co-occur with blue catfish in estuaries in Louisiana (Baltz and Jones, 2003) and are consumed at higher rates there (up to 50% of stomachs; Perry, 1969) than those observed in Virginia's tidal rivers. In spite of high predation rates, Louisiana continues to sustain valuable blue crab fisheries, and annual harvests exceed those in both Virginia and Maryland (NMFS[3]). This is not surprising because blue crab have complex life histories (Hines et al., 2010) and population dynamics appear to be strongly influenced by abiotic factors (Bauer and Miller, 2010; Colton et al., 2014). Nonetheless, predation of blue crab by blue catfish should be considered in future population models; after all, the predicted percent occurrence of blue crab in stomachs of blue catfish can be quite high (up to 28% in brackish portions of the James River).

For American eel, salinity did not significantly affect predation rates. This result is intuitive because eels readily colonize freshwater, estuarine, and marine habitats and move freely between them (Feunteun et al., 2003; Daverat et al., 2006). Size of blue catfish significantly affected predation rates on American eel, and maximal predation rates were observed for blue catfish between

[1] Cummins, J. 2016. The return of American shad to the Potomac River: 20 years of restoration. Final Report. Interstate Comm. Potomac River Basin, ICPRB Rep. ICP16-5, 23 p. [Available from website.]

[2] Hilton, E. J., R. Latour, P. E. McGrath, B. Watkins, and A. Magee. 2016. Monitoring relative abundance of American shad and river herring in Virginia rivers 2015 annual report, 98 p. Va. Inst. Mar. Sci., Coll. William Mary, Gloucester, VA. [Available from website.]

[3] NMFS (National Marine Fisheries Service). 2017. Fisheries of the United States 2016. NOAA, Natl. Mar. Fish. Serv., Curr. Fish. Stat. 2016, 147 p. [Available from website.]

600 and 800 mm TL. Most of the American eel consumed were yellow-phase (sexually immature adults), although phase determination was often difficult because of tissue degradation from digestion. Month was a significant factor in the model for American eel, and maximal predation rates occurred during spring and fall, especially in April and October. This observation may be related to eel migration patterns driven by seasonal changes in temperature (Welsh et al., 2016; Aldinger and Welsh, 2017). For example, silver-phase American eel (sexually mature adults) make long spawning migrations in autumn, and yellow-phase American eel are known to make punctuated upstream movements as waters warm in spring (Welsh and Liller, 2013). Overall, predation by blue catfish on American eel was rare (predicted percent occurrence was <5% in all circumstances).

Populations of eel species, including the American eel, have declined across the northern hemisphere (Bonhommeau et al., 2008); therefore, blue catfish are unlikely to be drivers of these declines. Population declines may be attributed to many factors, although climate change and the proliferation of an invasive parasitic nematode are likely culprits (Shepard, 2015). Climate change may affect spawning and recruitment success of American eel because of their complex life history (Knights, 2003). Silver-phase eel undergo long spawning migrations to the Sargasso Sea, after which ocean currents transport larvae to nurseries on the continental slope (Wang and Tzeng, 2000). Warming temperatures have been associated with changes in physical oceanographic processes in the North Atlantic Ocean, changes that may negatively affect the survival and transport of eel larvae (Knights, 2003). Furthermore, an exotic parasitic nematode, *Anguillicoloides crassus*, has expanded its distribution across the western Atlantic Ocean. Although this parasite does not cause immediate mortality, it damages the swim bladder and may increase mortality rates as silver-phase eel undergo long-distance spawning migrations (Fazio et al., 2012; Barry et al., 2014).

Several conclusions can be drawn from the results of this study. First, our models revealed that American shad, river herring, and American eel are rarely consumed by blue catfish; however, large catfish (500–1000 mm TL) consume disproportionately more of these taxa. This may explain why results from all models indicate that overall predation on species of concern is highest in the James River, where large blue catfish are most abundant (Greenlee and Lim, 2011; Hilling et al., 2018). Predation on these taxa declines as blue catfish approach trophy size (≥1072 mm TL; Gabelhouse, 1984), and reports from previous work indicate that many trophy-sized blue catfish are cannibalistic or feed on gizzard shad (Schmitt et al., 2019). Although American shad, river herring, and American eel are rarely consumed, blue crab are frequently consumed by large catfish in brackish areas.

These length-based feeding patterns have important implications for management of blue catfish in Atlantic drainages of the United States. In the James River, fishing for large blue catfish is quite popular (Greenlee and Lim, 2011), and many fishing guide services and tackle shops rely on this resource. For individuals involved in these businesses, the status of blue catfish as *invasive* is controversial because several other nonindigenous fish species are not considered invasive in this river, for example, the smallmouth bass and muskellunge (*Esox masquinongy*) in the non-tidal James River and the largemouth bass (*Micropterus salmoides*) and channel catfish (*Ictalurus punctatus*) in the tidal James River. This argument is valid; however, these species exist at much lower densities and are far more spatially restricted than blue catfish. Blue catfish have spread to every major tributary of Chesapeake Bay (Schloesser et al., 2011) and are abundant in brackish areas (Fabrizio et al., 2018). Moreover, population densities in the tidal James River have been estimated to be as high as 70,800 blue catfish/km^2 (Bunch et al., 2018).

Although the results of our study indicate that trophy-sized blue catfish (≥1072 mm TL; Gabelhouse, 1984) do not routinely consume imperiled species, it is likely that these large fish produce disproportionately more offspring than smaller fish (Hixon et al., 2014). Therefore, current regulations that require mandatory release of large blue catfish (e.g., in Virginia, anglers can only keep one blue catfish >813 mm TL per day) could potentially contribute to increases in population densities and further range expansion for this species. Mandatory release regulations may not be ideal; however, high contaminant burdens in large blue catfish can render them unfit for human consumption, particularly in the James and Potomac Rivers (Luellen et al., 2018). Ultimately, it is probable that all future management of blue catfish in Chesapeake Bay will be controversial because differing opinions exist among various user groups and management agencies (Orth et al.[4]).

Eradication programs for invasive species often fail in large, open systems (Britton et al., 2011; Franssen et al., 2014) and are unlikely to succeed for blue catfish in the Chesapeake Bay region (Orth et al.[4]). Nonetheless, increased commercial harvest of large blue catfish (500–1000 mm TL) could reduce their predation on depleted alosines, American eel, and blue crab. In the James and Rappahannock Rivers, size structure of blue catfish is already shifting toward smaller sizes, as growth rates decline and large fish become rarer (Hilling et al., 2018). Currently, harvest of large catfish is limited because of concerns about contaminant burdens (Hale et al.[5]); however, it may be time to consider uses other than as human food for the harvest of these large catfish, including uses for pet foods and fertilizers (Orth et al.[4]). Because blue crab are consumed most commonly in brackish segments of these rivers, managers may want to explore options to incentivize more harvest of blue catfish in these areas.

[4] Orth, D. J., Y. Jiao, J. D. Schmitt, C. D. Hilling, J. A. Emmel, and M. C. Fabrizio. 2017. Dynamics and role of non-native blue catfish *Ictalurus furcatus* in Virginia's tidal rivers, 102 p. Final Report. Va. Dep. Game Inland Fish., Henrico, VA.

[5] Hale, R. C., T. D. Tuckey, and M. C. Fabrizio. 2016. Risks of expanding the blue catfish fishery as a population control strategy: influence of ecological factors on fish contaminant burdens, 48 p. [Available from Va. Inst. Mar. Sci., Coll. William Mary, 1375 Greate Rd., Gloucester Point, VA 23062.]

This study had limitations. First, winter diet information was not included in our modeling exercises because it was not collected in a randomized manner. This omission is problematic because blue catfish consume blue crab during winter, although the spatiotemporal extent of these data is limited (Schmitt et al., 2019). Second, we had limited success capturing blue catfish when using low-frequency electrofishing in brackish areas ($S_P \geq 10$), although blue catfish have been captured in S_P levels as high as 21.5 (Fabrizio et al., 2018). Our limited success in these locations is simply an artifact of low-frequency electrofishing, which becomes ineffective at higher salinities (Bringolf et al., 2005). Predation on blue crab increases with salinity; therefore, we may be underestimating predation by blue catfish on this commercially valuable species. Future studies in Chesapeake Bay should focus on the diet of blue catfish during winter, particularly in brackish areas with S_P levels ≥10.

This study focused on invasive blue catfish in Chesapeake Bay; however, the development of similar models could be useful for other invasive species, especially if the goal is to minimize predation for specific organisms. Although it does not necessarily result in population-level effects (Ney, 1990), predation has been identified as a major driver in the decline of native species richness at the global scale (Mollot et al., 2017). Predation is particularly dangerous for depleted biota because it can impede population recovery and even drive organisms to extinction. No evidence conclusively indicates that blue catfish are driving alosines to extinction (e.g., some signs of recovery have been observed for populations of American shad in the Rappahannock River), yet other invasive predators have driven prey to extinction (Spencer et al., 2016). In these cases, the best approach may be to determine the factors that lead to greater predation on specific biota. This information could also provide guidance for additional harvest of the invader (Schmitt et al., 2017). Models of predation for depleted species could be especially useful for control of invasive predators in large, open systems where eradication is not a viable option (Franssen et al., 2014; Thresher et al., 2014). In these circumstances, targeted harvest may be the best approach, with the goal of "suppress[ing] invasive populations below levels predicted to cause undesirable ecological change" (Green et al., 2014).

Acknowledgments

We thank C. Hilling, B. Peoples, J. Emmel, Z. Moran, J. Woodward, A. Mosely, H. Kim, H. Lee, B. Greenlee, J. Odenkirk, R. Willis, K. Johnson, A. Weaver, Y. Jiao, and S. Smith for their assistance over the course of the study. We thank the anonymous reviewers whose comments resulted in a better manuscript. Data collection was supported by the Virginia Department of Game and Inland Fisheries through a Sport Fish Restoration Grant from the U.S. Fish and Wildlife Service (contract #2012-13705), and the senior author was partially supported through a fellowship from Virginia Sea Grant (R/71856A).

Literature cited

Aguilar R., A. H. Hines, T. G. Wolcott, D. L. Wolcott, M. A. Kramer, and R. N. Lipcius.
2005. The timing and route of movement and migration of post-copulatory female blue crab, *Callinectes sapidus* Rathbun, from the upper Chesapeake Bay. J. Exp. Mar. Biol. Ecol. 319:117–128.

Aguilar, R., M. B. Ogburn, A. C. Driskell, L. A. Weigt, M. C. Groves, and A. H. Hines.
2017. Gutsy genetics: identification of digested piscine prey items in the stomach contents of sympatric native and introduced warmwater catfishes via DNA barcoding. Environ. Biol. Fish. 100:325–336.

Albins, M. A., and M. A. Hixon.
2008. Invasive Indo-Pacific lionfish *Pterois volitans* reduce recruitment of Atlantic coral-reef fishes. Mar. Ecol. Prog. Ser. 367:233–238.

Aldinger, J. L., and S. A. Welsh.
2017. Diel periodicity and chronology of upstream migration in yellow-phase American eels (*Anguilla rostrata*). Environ. Biol. Fish. 100:1–10.

Austin, P. C.
2007. A comparison of regression trees, logistic regression, generalized additive models, and multivariate adaptive regression splines for predicting AMI mortality. Stat. Med. 26:2937–2957.

Baker, R., A. Buckland, and M. Sheaves.
2014. Fish gut content analysis: robust measures of diet composition. Fish Fish. 15:170–177.

Baltz, D. M., and R. F. Jones.
2003. Temporal and spatial patterns of microhabitat use by fishes and decapod crustaceans in a Louisiana estuary. Trans. Am. Fish. Soc. 132:662–678.

Barry, J., J. McLeish, J. A. Dodd, J. F. Turnbull, P. Boylan, and C. E. Adams.
2014. Introduced parasite *Anguillicola crassus* infection significantly impedes swim bladder function in the European eel *Anguilla anguilla* (L.). J. Fish Dis. 37:921–924.

Bauer, L. J., and T. J. Miller.
2010. Spatial and interannual variability in winter mortality of the blue crab (*Callinectes sapidus*) in the Chesapeake Bay. Est. Coasts 33:678–687.

Bethoney, N. D., B. P. Schondelmeier, K. D. E. Stokesbury, and W. S. Hoffman.
2013. Developing a fine scale system to address river herring (*Alosa pseudoharengus, A. aestivalis*) and American shad (*A. sapidissima*) bycatch in the U.S. Northwest Atlantic mid-water trawl fishery. Fish. Res. 141:79–87.

Beumer, J. P.
1978. Feeding ecology of four fishes from a mangrove creek in north Queensland, Australia. J. Fish Biol. 12: 475–490.

Bewick, V., L. Cheek, and J. Ball.
2004. Statistics review 13: receiver operating characteristic curves. Crit. Care 8:508–512.

Blackburn, T. M., P. Pyšek, S. Bacher, J. T. Carlton, R. P. Duncan, V. Jarošík, J. R. U. Wilson, and D. M. Richardson.
2011. A proposed unified framework for biological invasions. Trends Ecol. Evol. 26:333–339.

Bodine, K. A., and D. E. Shoup.
2010. Capture efficiency of blue catfish electrofishing and the effects of temperature, habitat, and reservoir location on electrofishing-derived length structure indices and relative abundance. North Am. J. Fish. Manage. 30:613–621.

Bonhommeau, S., E. Chassot, B. Planque, E. Rivot, A. H. Knap, and O. Le Pape.
2008. Impact of climate on eel populations of the Northern Hemisphere. Mar. Ecol. Prog. Ser. 373:71–80.

Brandner, J., K. Auerswald, A. F. Cerwenka, U. K. Schliewen, and J. Geist.
2013. Comparative feeding ecology of invasive Ponto-Caspian gobies. Hydrobiologia 703:113–131.

Bringolf, R. B., T. J. Kwak, W. G. Cope, and M. S. Larimore.
2005. Salinity tolerance of flathead catfish: implications for dispersal of introduced populations. Trans. Am. Fish. Soc. 134:927–936.

Britton, J. R., R. E. Gozlan, and G. H. Copp.
2011. Managing non-native fish in the environment. Fish Fish. 12:256–274.

Bromley, P. J.
1994. The role of gastric evacuation experiments in quantifying the feeding rates of predatory fish. Rev. Fish Biol. Fish. 4:36–66.

Buckland, A., R. Baker, N. Loneragan, and M. Sheaves.
2017. Standardising fish stomach content analysis: the importance of prey condition. Fish. Res. 196: 126–140.

Bunch, A. J., R. S. Greenlee, and E. M. Brittle.
2018. Blue catfish density and biomass in a tidal tributary in coastal Virginia. Northeast. Nat. 25:333–340.

Catford, J. A., R. Jansson, and C. Nilsson.
2009. Reducing redundancy in invasion ecology by integrating hypotheses into a single theoretical framework. Divers. Distrib. 15:22–40.

Caut, S., E. Angulo, and F. Courchamp.
2008. Dietary shift of an invasive predator: rats, seabirds and sea turtles. J. Appl. Ecol. 45:428–437.

Clifton, K. B., and P. J. Motta.
1998. Feeding morphology, diet, and ecomorphological relationships among five Caribbean labrids (Teleostei, Labridae). Copeia 1998:953–966.

Colton, A. R., M. J. Wilberg, V. J. Coles, and T. J. Miller.
2014. An evaluation of the synchronization in the dynamics of blue crab (*Callinectes sapidus*) populations in the western Atlantic. Fish. Oceanogr. 23:132–146.

Cucherousset, J., and J. D. Olden.
2011. Ecological impacts of nonnative freshwater fishes. Fisheries 36:215–230.

Daverat, F., K. E. Limburg, I. Thibault, J.-C. Shiao, J. J. Dodson, F. Caron, W. N. Tzeng, Y. Iizuka, and H. Wickström.
2006. Phenotypic plasticity of habitat use by three temperate eel species, *Anguilla anguilla, A. japonica* and *A. rostrata*. Mar. Ecol. Prog. Ser. 308:231–241.

Dick, J. T. A., M. E. Alexander, J. M. Jeschke, A. Ricciardi, H. J. MacIsaac, T. B. Robinson, S. Kumschick, O. L. F. Weyl, A. M. Dunn, M. J. Hatcher, et al.
2014. Advancing impact prediction and hypothesis testing in invasion ecology using a comparative functional response approach. Biol. Invasions 16:735–753.

Eggleton, M. A., and H. L. Schramm Jr.
2004. Feeding ecology and energetic relationships with habitat of blue catfish, *Ictalurus furcatus*, and flathead catfish, *Pylodictis olivaris*, in the lower Mississippi River, U.S.A. Environ. Biol. Fish. 70: 107–121.

Fabrizio, M. C., T. D. Tuckey, R. J. Latour, G. C. White, and A. J. Norris.
2018. Tidal habitats support large numbers of invasive blue catfish in a Chesapeake Bay subestuary. Est. Coasts 41:827–840.

Fazio, G., P. Sasal, G. Mouahid, R. Lecomte-Finiger, and H. Moné.
2012. Swim bladder nematodes (*Anguillicoloides crassus*) disturb silvering in European eels (*Anguilla anguilla*). J. Parasitol. 98:695–705.

Fei, S., Q. Guo, and K. Potter.
2016. Macrosystems ecology: novel methods and new understanding of multi-scale patterns and processes. Landscape Ecol. 31:1–6.

Feunteun, E., P. Laffaille, T. Robinet, C. Briand, A. Baisez, J.-M. Olivier, and A. Acou.
2003. A review of upstream migration and movements in inland waters by anguillid eels: toward a general theory. *In* Eel biology (K. Aida, K. Tsukamoto, and K. Yamauchi, eds.), p. 191–213. Springer, Tokyo, Japan.

Franssen, N. R., J. E. Davis, D. W. Ryden, and K. B. Gido.
2014. Fish community responses to mechanical removal of nonnative fishes in a large southwestern river. Fisheries 39:352–363.

Fuller, P., and M. Neilson.
2018. *Ictalurus furcatus* (Valenciennes in Cuvier and Valenciennes, 1840). Nonindigenous Aquatic Species Database. U.S. Geol. Surv., Gainesville, FL. [Available at website, accessed May 2018.]

Gabelhouse, D. W., Jr.
1984. A length-categorization system to assess fish stocks. North Am. J. Fish. Manage. 4:273–285.

García-Berthou, E.
2007. The characteristics of invasive fishes: what has been learned so far? J. Fish Biol. 71(sd):33–55.

Garman, G. C., and L. A. Nielsen.
1992. Medium-sized rivers of the Atlantic slope. *In* Biotic diversity of the southeastern United States: aquatic communities (C. Hackney, S. Adams, W. Martin, eds.), p. 315–349. John Wiley and Sons, NY.

Garvey, J. E., and S. R. Chipps.
2012. Diets and energy flow. *In* Fisheries techniques, 3rd ed. (A. V. Zale, D. L. Parrish, and T. N. Sutton, eds.), p. 733–779. Am. Fish. Soc., Bethesda, MD.

Glebe, B. D., and W. C. Leggett.
1981. Temporal, intra-population differences in energy allocation and use by American shad (*Alosa sapidissima*) during the spawning migration. Can. J. Fish. Aquat. Sci. 38:795–805.

Graham, K.
1999. A review of the biology and management of blue catfish. Am. Fish. Soc. Symp. 24:37–49.

Green, S. J., N. K. Dulvy, A. M. L. Brooks, J. L. Akins, A. B. Cooper, S. Miller, and I. M. Côté.
2014. Linking removal targets to the ecological effects of invaders: a predictive model and field test. Ecol. Appl. 24:1311–1322.

Greenlee, R. S., and C. N. Lim.
2011. Searching for equilibrium: population parameters and variable recruitment in introduced blue catfish populations in four Virginia tidal river systems. Am. Fish. Soc. Symp. 77:349–367.

Guisan, A., T. C. Edwards Jr., and T. Hastie.
2002. Generalized linear and generalized additive models in studies of species distributions: setting the scene. Ecol. Model. 157:89–100.

Haro, A., W. Richkus, K. Whalen, A. Hoar, W. D. Busch, S. Lary, T. Brush, and D. Dixon.
2000. Population decline of the American eel: implications for research and management. Fisheries 25(9):7–16.

Hasselman, D. J., E. C. Anderson, E. E. Argo, N. D. Bethoney, S. R. Gephard, D. M. Post, B. P. Schondelmeier, T. F. Schultz, T. V. Willis, and E. P. Palkovacs.
2016. Genetic stock composition of marine bycatch reveals disproportional impacts on depleted river herring genetic stocks. Can. J. Fish. Aquat. Sci. 73:951–963.

Hastie, T. J., and R. J. Tibshirani.
1990. Generalized additive models, 352 p. Chapman and Hall, London.

Helfman, G. S.
2007. Fish conservation: a guide to understanding and restoring global aquatic biodiversity and fishery resources, 548 p. Island Press, Washington, D.C.

Hilling, C. D., A. J. Bunch, R. S. Greenlee, D. J. Orth, and Y. Jiao.
2018. Natural mortality and size structure of introduced blue catfish in Virginia tidal rivers. J. Southeast. Assoc. Fish Wildl. Agency 5:30–38.

Hines, A. H., R. N. Lipcius, and A. M. Haddon.
1987. Population dynamics and habitat partitioning by size, sex, and molt stage of blue crabs *Callinectes sapidus* in a subestuary of central Chesapeake Bay. Mar. Ecol. Prog. Ser. 36:55–64.

Hines, A. H., E. G. Johnson, M. Z. Darnell, D. Rittschof, T. J. Miller, L. J. Bauer, P. Rodger, and R. Aguilar.
2010. Predicting effects of climate change on blue crab in Chesapeake Bay. *In* Biology and management of exploited crab populations under climate change (G. H. Kruse, G. L. Eckert, R. J. Foy, R. N. Lipcius, B. Sainte-Marie, D. L. Stram, and D. Woodby, eds.), p. 109–127. Alaska Sea Grant Prog. Rep. AK-SG-10-01. Univ. Alaska Fairbanks, Fairbanks, AK.

Hixon, M. A., D. W. Johnson, and S. M. Sogard.
2014. BOFFFFs: on the importance of conserving old-growth age structure in fishery populations. ICES J. Mar. Sci. 71:2171–2185.

Hoffman, J. C., K. E. Limburg, D. A. Bronk, and J. E. Olney.
2008. Overwintering habitats of migratory juvenile American shad in Chesapeake Bay. Environ. Biol. Fish. 81:329–345.

Jaworski, A., and S. A. Ragnarsson.
2006. Feeding habits of demersal fish in Icelandic waters: a multivariate approach. ICES J. Mar. Sci. 63:1682–1694.

Jung, S., and E. D. Houde.
2003. Spatial and temporal variabilities of pelagic fish community structure and distribution in Chesapeake Bay, USA. Est. Coast. Shelf Sci. 58:335–351.

Kemp, W. M., W. R. Boynton, J. E. Adolf, D. F. Boesch, W. C. Boicourt, G. Brush, J. C. Cornwell, T. R. Fisher, P. M. Glibert, J. D. Hagy, et al.
2005. Eutrophication of Chesapeake Bay: historical trends and ecological interactions. Mar. Ecol. Prog. Ser. 303:1–29.

King, R. S., A. H. Hines, F. D. Craige, and S. Grap.
2005. Regional, watershed and local correlates of blue crab and bivalve abundances in subestuaries of Chesapeake Bay, USA. J. Exp. Mar. Biol. Ecol. 319:101–116.

Knights, B.
2003. A review of the possible impacts of long-term oceanic and climate changes and fishing mortality on recruitment of anguillid eels of the Northern Hemisphere. Sci. Total Environ. 310:237–244.

Latour, R. J., J. Gartland, C. F. Bonzek, and R. Johnson.
2008. The trophic dynamics of summer flounder (*Paralichthys dentatus*) in Chesapeake Bay. Fish. Bull. 106:47–57.

Layman, C. A., and J. E. Allgeier.
2012. Characterizing trophic ecology of generalist consumers: a case study of the invasive lionfish in the Bahamas. Mar. Ecol. Prog. Ser. 448:131–141.

Ley, J. A., C. L. Montague, and C. C. Mclvor.
1994. Food habits of mangrove fishes: a comparison along estuarine gradients in northeastern Florida Bay. Bull. Mar. Sci. 54:881–899.

Limburg, K. E., and J. R. Waldman.
2009. Dramatic declines in North Atlantic diadromous fishes. BioScience 59:955–965.

Lin, X., and D. Zhang.
1999. Inference in generalized additive mixed models by using smoothing splines. J. R. Stat. Soc. Stat. Methodol. Ser. B 61:381–400.

Lippson, A. J., and R. L. Lippson.
2006. Life in the Chesapeake Bay, 3rd ed., 344 p. John Hopkins Univ. Press, Baltimore, MD.

Livingston, R. J.
1984. Trophic response of fishes to habitat variability in coastal seagrass systems. Ecology 65:1258–1275.

Loesch, J. G., and W. A. Lund Jr.
1977. A contribution to the life history of the blueback herring, *Alosa aestivalis*. Trans. Am. Fish. Soc. 106: 583–589.

Luellen, D. R., M. J. LaGuardia, T. D. Tuckey, M. C. Fabrizio, G. W. Rice, and R. C. Hale.
2018. Assessment of legacy and emerging contaminants in an introduced catfish and implications for the fishery. Environ. Sci. Pollut. Res. 25:28355–28366.

MacAvoy, S. E., G. C. Garman, and S. A. Macko.
2009. Anadromous fish as marine nutrient vectors. Fish. Bull. 107:165–174.

Mack, R. N., D. Simberloff, W. M. Lonsdale, H. Evans, M. Clout, and F. A. Bazzaz.
2000. Biotic invasions: causes, epidemiology, global consequences, and control. Ecol. Appl. 10:689–710.

Magoro, M. L., A. K. Whitfield, and L. Carassou.
2015. Predation by introduced largemouth bass *Micropterus salmoides* on indigenous marine fish in the lower Kowie River, South Africa. Afr. J. Aquat. Sci. 40:81–88.

McGee, M. D., S. R. Borstein, R. Y. Neches, H. H. Buescher, O. Seehausen, and P. C. Wainwright.
2015. A pharyngeal jaw evolutionary innovation facilitated extinction in Lake Victoria cichlids. Science 350: 1077–1079.

McHugh, J. L., and R. S. Bailey.
1957. History of Virginia's commercial fisheries. Va. J. Sci. 8(1):42–64.

Mollot, G., J. H. Pantel, and T. N. Romanuk.
2017. Chapter two—the effects of invasive species on the decline in species richness: a global meta-analysis. Adv. Ecol. Res. 56:61–83.

Moore, K. A., D. J. Wilcox, and R. J. Orth.
2000. Analysis of the abundance of submersed aquatic vegetation communities in the Chesapeake Bay. Est. Coasts 23:115–127.

Moran, Z., D. J. Orth, J. D. Schmitt, E. M. Hallerman, and R. Aguilar.
2016. Effectiveness of DNA barcoding for identifying piscine prey items in stomach contents of piscivorous catfishes. Environ. Biol. Fish. 99:161–167.

Ney, J.
1990. Trophic economics in fisheries: assessment of demand-supply relationships between predators and prey. Rev. Aquat. Sci. 2:55–81.

Niklitshek, E. J., and D. H. Secor.
2005. Modeling spatial and temporal variation of suitable nursery habitats for Atlantic sturgeon in the Chesapeake Bay. Est. Coast. Shelf Sci. 64:135–148.

Oksanen, J., F. G. Blanchet, M. Friendly, R. Kindt, P. Legendre, D. McGlinn, P. R. Minchin, R. B. O'Hara, G. L. Simpson, P. Solymos, et al.
2017. vegan: community ecology package. R package, vers. 2.4-4. [Available from website, accessed August 2017.]

Palkovacs, E. P., D. J. Hasselman, E. E. Argo, S. R. Gephard, K. E. Limburg, D. M. Post, T. F. Schultz, and T. V. Willis.
2014. Combining genetic and demographic information to prioritize conservation efforts for anadromous alewife and blueback herring. Evol. Appl. 7:212–226.

Paolisso, M.
2002. Blue crabs and controversy on the Chesapeake Bay: a cultural model for understanding watermen's reasoning about blue crab management. Hum. Organ. 61:226–239.

Pearce, J., and S. Ferrier.
2000. Evaluating the predictive performance of habitat models developed using logistic regression. Ecol. Model. 133:225–245.

Perry, W. G., Jr.
1969. Food habits of blue and channel catfish collected from a brackish-water habitat. Prog. Fish-Cult. 31:47–50.

Pimentel, D.
2011. Biological invasions: economic and environmental costs of alien plant, animal, and microbe species, 2nd ed., 463 p. CRC press, Boca Raton, FL.

Raabe, J. K., and J. E. Hightower.
2014. Assessing distribution of migratory fishes and connectivity following complete and partial dam removals in a North Carolina river. North Am. J. Fish. Manage. 34:955–969.

R Core Team.
2017. R: a language and environment for statistical computing. R Foundation for Statistical Computing, Vienna, Austria. [Available from website, accessed December 2017.]

Richards, R. A., and P. J. Rago.
1999. A case history of effective fishery management: Chesapeake Bay striped bass. North Am. J. Fish. Manage. 19:356–375.

Schloesser, R. W., M. C. Fabrizio, R. C. Latour, G. C. Garman, B. Greenlee, M. Groves, and J. Gartland.
2011. Ecological role of blue catfish in Chesapeake Bay communities and implications for management. Am. Fish. Soc. Symp. 77:369–382.

Schmitt, J. D., and D. J. Orth.
2015. First record of pughead deformity in blue catfish. Trans. Am. Fish. Soc. 144:1111–1116.

Schmitt, J. D., E. M. Hallerman, A. Bunch, Z. Moran, J. A. Emmel, and D. J. Orth.
2017. Predation and prey selectivity by nonnative catfish on migrating alosines in an Atlantic slope estuary. Mar. Coast. Fish. 9:108–125.

Schmitt, J. D., B. K. Peoples, L. Castello, and D. J. Orth.
2019. Feeding ecology of generalist consumers: a case study of invasive blue catfish *Ictalurus furcatus* in Chesapeake Bay, Virginia, USA. Environ. Biol. Fish. 102:443–465.

Schubel, J. R., and D. W. Pritchard.
1986. Responses of upper Chesapeake Bay to variations in discharge of the Susquehanna River. Est. Coasts 9:236–249.

Shepard, S. L.
2015. American eel biological species report, 120 p. U.S. Fish Wildl. Serv., Hadley, MA.

Shiah, F.-K., and H. W. Ducklow.
1994. Temperature and substrate regulation of bacterial abundance, production and specific growth rate in Chesapeake Bay, USA. Mar. Ecol. Prog. Ser. 103:297–308.

Simberloff, D., J.-L. Martin, P. Genovesi, V. Maris, D. A. Wardle, J. Aronson, F. Courchamp, B. Galil, E. García-Berthou, M. Pascal, et al.
2013. Impacts of biological invasions: what's what and the way forward. Trends Ecol. Evol. 28:58–66.

Sing, T., O. Sander, N. Beerenwinkel, and T. Lengauer.
2005. ROCR: visualizing classifier performance in R. Bioinformatics 21:3940–3941.

Spencer, R.-J., J. U. Van Dyke, and M. B. Thompson.
2016. The ethological trap: functional and numerical responses of highly efficient invasive predators driving prey extinctions. Ecol. Appl. 26:1969–1983.

ter Braak, C. J. F.
1986. Canonical correspondence analysis: a new eigenvector technique for multivariate direct gradient analysis. Ecology 67:1167–1179.

ter Braak, C. J. F., and P. F. M. Verdonschot.
1995. Canonical correspondence analysis and related multivariate methods in aquatic ecology. Aquat. Sci. 57:255–289.

Thresher, R. E., K. Hayes, N. J. Bax, J. Teem, T. J. Benfey, and F. Gould.
2014. Genetic control of invasive fish: technological options and its role in integrated pest management. Biol. Invas. 16:1201–1216.

Vitousek, P. M., C. M. D'Antonio, L. L. Loope, M. Rejmanek, and R. G. Westbrooks.
1997. Introduced species: a significant component of human-caused global change. N.Z. J. Ecol. 1:1–16.

Wagner, C. M., and H. M. Austin.
1999. Correspondence between environmental gradients and summer littoral fish assemblages in low salinity reaches of the Chesapeake Bay, USA. Mar. Ecol. Prog. Ser. 177:197–212.

Waldman, J.
2013. Running silver: restoring Atlantic rivers and their great fish migrations, 304 p. Lyons Press, Guilford, CT.

Wang, C. H., and W. N. Tzeng.
2000. The timing of metamorphosis and growth rates of American and European eel leptocephali: a mechanism of larval segregative migration. Fish. Res. 46:191–205.

Waters, D. S., T. J. Kwak, J. B. Arnott, and W. E. Pine III.
2004. Evaluation of stomach tubes and gastric lavage for sampling diets from blue catfish and flathead catfish. North Am. J. Fish. Manage. 24:258–261.

Welsh, S. A., and H. L. Liller.
2013. Environmental correlates of upstream migration of yellow-phase American eels in the Potomac River drainage. Trans. Am. Fish. Soc. 142:483–491.

Welsh, S. A., J. L. Aldinger, M. A. Braham, and J. L. Zimmerman.
2016. Synergistic and singular effects of river discharge and lunar illumination on dam passage of upstream migrant yellow-phase American eels. ICES J. Mar. Sci. 73:33–42.

Wenner, C. A., and J. A. Musick.
1974. Fecundity and gonad observations of the American eel, *Anguilla rostrata*, migrating from Chesapeake Bay, Virginia. Can. J. Fish. Aquat. Sci. 31:1387–1391.

Wood, S. N.
2006. Generalized additive models: an introduction with R, 416 p. Chapman and Hall/CRC, Boca Raton, FL.
2017. Generalized additive models: an introduction with R, 2nd ed., 476 p. Chapman and Hall/CRC, Boca Raton, FL.

National Marine
Fisheries Service
NOAA

Fishery Bulletin
established in 1881

Spencer F. Baird
First U.S. Commissioner
of Fisheries and founder
of *Fishery Bulletin*

Reproductive ecology and size-dependent fecundity in the petrale sole (*Eopsetta jordani*) in waters of California, Oregon, and Washington

Lyndsey S. Lefebvre (contact author)[1,2]
Cherisa L. Friedlander[2]
John C. Field[2]

Email address for contact author: lyndsey.lefebvre@noaa.gov

[1] Institute of Marine Sciences
University of California Santa Cruz
1156 High Street
Santa Cruz, California 95064
Present address for contact author: Integrated Statistics Inc.
Population and Ecosystems Monitoring and Analysis Division
Northeast Fisheries Science Center
National Marine Fisheries Service, NOAA
166 Water Street
Woods Hole, Massachusetts 02543

[2] Fisheries Ecology Division
Southwest Fisheries Science Center
National Marine Fisheries Service, NOAA
110 McAllister Way
Santa Cruz, California 95060

Abstract—The petrale sole (*Eopsetta jordani*) is a commercially and ecologically important flatfish found throughout the continental shelf from California through British Columbia, Canada. Although stock assessments are routinely conducted along the West Coast of the United States for this population, these assessments have depended on limited data for estimating reproductive output. In this analysis, the reproductive strategy for this species was revisited, fecundity estimates were updated, and size-dependent fecundity relationships were established from fish collected off California and the Pacific Northwest. Results of histological analysis indicate that petrale sole exhibit a determinate batch spawning strategy, with potential annual fecundity (PAF) set prior to the release of eggs over the course of several spawning events. Both PAF and relative PAF (weight-specific fecundity) increased significantly with maternal length and weight. Regional differences in the strength of the relationship between relative PAF and size indicate that the maternal effect is stronger in the Pacific Northwest; however, more data are necessary to confirm regional patterns. Because reproductive output was not proportionate with female size, fisheries managers should consider using relative PAF in determining the reproductive potential of this stock.

Manuscript submitted 15 November 2018.
Manuscript accepted 10 September 2019.
Fish. Bull. 117:291–302 (2019).
Online publication date: 30 September 2019.
doi: 10.7755/FB.117.4.2

The views and opinions expressed or implied in this article are those of the author (or authors) and do not necessarily reflect the position of the National Marine Fisheries Service, NOAA.

The petrale sole (*Eopsetta jordani*) is a commercially important flatfish in the family Pleuronectidae (right-eyed flounders). Although their range extends from Baja California, Mexico, to the western Gulf of Alaska, their greatest abundance and commercial significance is generally from Santa Barbara, California, through British Columbia, Canada (Alverson and Chatwin, 1957; CDFW, 2013). Female petrale sole grow considerably larger than males and can reach a maximum total length (TL) of 70 cm (although fish larger than 60 cm are rarely encountered) and live up to 31 years (Haltuch et al., 2013; Stawitz et al., 2016). Hannah et al. (2002) estimated the length at 50% maturity at 33 cm (corresponding to an age of 5 years) for fish collected off Oregon. Petrale sole migrate seasonally between shallow feeding grounds (with depths of 70–200 m), where they disperse across the continental shelf from March through October, and deeper spawning grounds (with depths of 290–440 m), where they form discrete aggregations along the outer shelf during late fall and winter (November–February) (Ketchen and Forrester, 1966; CDFW, 2013; Stawitz et al., 2016). Tagging data indicate that individuals are capable of dispersing several hundred miles, although most individuals have high fidelity to winter spawning habitats (Ketchen and Forrester, 1966; Pedersen, 1975).

The petrale sole fishery off the U.S. Pacific coast has a long history, having started in the late 1800s off California and Oregon (CDFW, 2013). The first stock assessments in U.S. waters evaluated only populations north of Cape Blanco, Oregon, because of data constraints (Turnock et al., 1993; Sampson and Lee, 1999), but recent stock assessments have assumed a single coast-wide stock (Haltuch and Hicks, 2009; Haltuch et al., 2013). The petrale

sole is currently treated as a single stock in waters of Canada for management purposes (Starr and Fargo, 2004), although it is believed that there are 2 distinct stocks in British Columbia (Ketchen and Forrester, 1966; Starr and Fargo, 2004). Stock depletion was evident as early as the 1950s and 1960s in waters of both the United States (Haltuch et al., 2013) and Canada (Ketchen and Forrester, 1966), following increasing landings and targeting of petrale sole on their winter spawning grounds. Recent stock assessments indicate that the population in the United States was below target levels (25% of the unfished spawning output) from 1962 through 2014 and below the overfished level (12.5% of the estimated unfished spawning output) from 1979 through 2011 (Haltuch et al., 2013; Stawitz et al., 2016), although the stock was not declared overfished until 2009. Following subsequent reductions in allowable catch, and due in part to strong recruitment events, the stock abundance increased sharply from 2009 through 2015, and the stock was declared rebuilt in 2014 (Stawitz et al., 2016).

High priority research recommendations in recent petrale sole stock assessments engendered new studies on the reproductive biology of the stock and on spatial variability in growth and recruitment (Haltuch et al., 2011, 2013; Stawitz et al., 2016). The only published estimates of fecundity for petrale sole come from collections in the 1950s off California (Porter, 1964), and the reproductive strategy of this species was established solely on the basis of visual (macroscopic) evaluation of the ovaries. Annual fecundity estimates in that study ranged from 150,000 to 1.49 million eggs, and females were presumed to exhibit a determinate total spawning strategy (Murua and Saborido-Rey, 2003), releasing all eggs in a single spawning event annually. Relationships between maternal size and relative fecundity (the number of eggs per gram of maternal somatic weight) were not examined. Subsequently, stock assessments for this species have assumed that fecundity is proportional to maternal length.

In response to research recommendations in recent stock assessments and in cooperation with The Nature Conservancy and commercial fishermen, mature female petrale sole were collected from spawning grounds off Central California (Morro Bay) in the 2014–2015, 2015–2016, and 2016–2017 reproductive seasons (August–February) to estimate annual fecundity. Collections were expanded in the 2015–2016 and 2016–2017 reproductive seasons to include samples caught off Oregon and Washington with cooperation from the West Coast Groundfish Bottom Trawl Survey of the Northwest Fisheries Science Center (NWFSC), National Marine Fisheries Service (NMFS) (Keller et al., 2012), and from Washington Department of Fish and Wildlife (WDFW) commercial port samplers. Histological analysis of ovarian tissue was used to determine the reproductive strategy of petrale sole and to identify suitable samples for inclusion in fecundity analyses. The relationships between fecundity and maternal size were established or updated, and regional differences between fish collected off California and those from waters of the Pacific Northwest (Oregon and Washington) were examined. The majority of samples collected for this study came from commercial fishermen who targeted fish on their spawning grounds. Because maturity estimates from fish collected on spawning grounds can be biased (Murua and Saborido-Rey, 2003), we did not attempt to update maturity ogives in this study.

Materials and methods

Sample collection

A total of 401 female petrale sole were collected from commercial and survey bottom-trawl operations off California (number of samples [n]=291), Oregon (n=1), and Washington (n=109) between August and February of the 2014–2015, 2015–2016, and 2016–2017 reproductive seasons (Table 1, Fig. 1). The majority (n=250) were collected off Morro Bay by commercial fishermen in all 3 sampling years. Sixty females were collected by WDFW port samplers in Puget Sound, Washington, from commercial and tribal bottom trawlers, 40 in August 2015, 10 in December 2016, and 10 in January 2017. The remaining fish (n=91) were collected by the NWFSC West Coast Groundfish Bottom Trawl Survey off the coasts of Washington and Oregon and off part of California (from Bodega Bay south to Point Conception) from August through October in the 2015–2016 and 2016–2017 reproductive seasons.

Fish collected by commercial fishermen in Morro Bay were stored on ice and landed 1–5 days after capture. On average, 40 fish per landing were selected to represent the entirety of the size range of the catch. Fish were transported to the Fisheries Ecology Division of the Southwest Fisheries Science Center (SWFSC) and processed within 24 h of landing. Total weight (TW, in grams) and TL (in millimeters) were recorded, and sagittal otoliths were removed for age analysis. Ovaries were excised, weighed (in grams), and assigned a macroscopic development stage (Table 2). Initially, the blind- and eyed-side ovarian lobes were weighed and recorded separately. A paired t-test conducted on 136 stage-2 and -3 ovaries demonstrated that weights did not significantly vary between blind- and eyed-side ovarian lobes (P=0.35, df=145).

Fish collected by WDFW were processed at an unknown time after capture, and those collected by the NWFSC were processed immediately after capture. For both collections, sagittal otoliths were removed; TL (in centimeters) and TW (in grams) were recorded; and one or both ovarian lobes (depending on their size and ability to fit in storage containers) were excised, placed individually into muslin bags, and fixed in 10% neutral buffered formalin. Ovaries were processed at the SWFSC within 1–6 months from the date of collection. Ovaries were removed from the formalin, assigned a macroscopic stage, blotted dry, and weighed (in grams). When only one ovarian lobe was present, the weight was doubled to estimate total gonad weight; a macroscopic stage-based correction

Table 1

Summary information for catches of petrale sole (*Eopsetta jordani*) during 2014–2017 off California and the Pacific Northwest (Oregon and Washington), including number of samples by month, mean size in total length (TL), and mean age in years. An asterisk (*) indicates a sample included in fecundity analyses. Standard deviations (SDs) of means are given in parentheses. Blank cells indicate that no samples were available.

	No. of samples				
	California			Pacific Northwest	
Month	2014–15	2015–16	2016–17	2015–16	2016–17
August		10 (7)*		9	25 (3)*
September		81 (27)*	8 (1)*	42 (11)*	14
October		40 (7)*	40 (6)*		
December	12	39 (1)*			10 (7)*
January	20	1			10 (1)*
February	40				
Total	72	171	48	51	59
Size range (mm TL)	336–555	330–600	305–545	300–520	280–450
Mean size (SD)	441 (39)	487 (47)	463 (40)	429 (55)	442 (69)
Age range (years)	4–14	5–20	4–14	3–10	4–15
Mean age (SD)	7.7 (2.0)	10.6 (3.5)	8.0 (2.0)	6.6 (1.9)	10.0 (3.1)
No. of samples aged	72	147	30	40	20

factor was applied to account for differences in fresh and preserved gonad weights (stage 2: F_{est}=1.02P–3.66; stage 3: F_{est}=0.99PW+5.30; F_{est} is the estimated fresh weight [in grams], and PW is the preserved weight [in grams]). No correction factor was necessary for ovaries of macroscopic stages 1, 4, and 5).

A small piece of tissue was removed from all ovaries for histological analysis. Between 2 and 6 weighed subsamples (0.25–1.00 g) for fecundity analyses and 1 unweighed sample for archives were collected from stage-2 and -3 ovaries by gently teasing oocytes from fresh ovarian tissue (see the "Fecundity" section below for details). Ages were determined from otoliths through the break-and-burn technique by the aging lab at the NWFSC in Newport, Oregon. Ages were estimated from all otoliths from commercial and WDFW collections; from NWFSC collections, ages were estimated only from otoliths of fish that were used to estimate fecundity (n=16).

Histological analysis

Ovarian tissue samples were fixed in 10% neutral buffered formalin for at least 48 h before being rinsed in water and stored in 70% ethanol. Tissues selected for histological analyses were processed according to standard histological techniques, by using paraffin as a blocking medium and staining and counterstaining sections with hematoxylin and Eosin Y (Humason, 1972). All stage-2 (n=142) and stage-3 (n=48) ovaries were selected to determine their suitability for inclusion in fecundity analyses. These samples, along with haphazardly selected representatives of macroscopic stages 1 (n=12), 4 (n=12), and 5 (n=16), were used to detail the reproductive cycle of petrale sole. Histological sections were examined at 40–250× magnification by using a compound microscope. Each ovary was assigned an ovarian phase on the basis of the stage of the leading oocyte cohort, incidence and state of atresia, and presence of postovulatory follicle (POF) complexes (Tables 2 and 3). Ovarian phases were based on descriptions of oocyte development in Wallace and Selman (1981) and Lowerre-Barbieri et al. (2011), and standard terminology suggested by Brown-Peterson et al. (2011) was used for them. To examine the size range of oocyte stages, mean maximum oocyte diameters were recorded from histological slides of 99 individuals: the diameter of the largest oocyte of the leading cohort in each of 5 fields of view was measured by using an ocular micrometer, and diameters were averaged to obtain the mean maximum oocyte diameter (Table 3). Estimates of sizes of hydrated oocytes were made from preserved whole tissue mounts from 5 stage-3 ovarian samples by using a compound microscope and ocular micrometer (Table 3).

To verify homogenous ovarian development, histology samples were collected and processed from the anterior, middle, and posterior portion of blind- and eyed-side ovarian lobes (6 total) from 15 females (stage-2 [n=8] and stage-3 [n=7] ovaries). Slides were read without reference to identification number, ovarian lobe, or location. Oocyte stage of the leading cohort was recorded, and histological phase was assigned. Because there were no

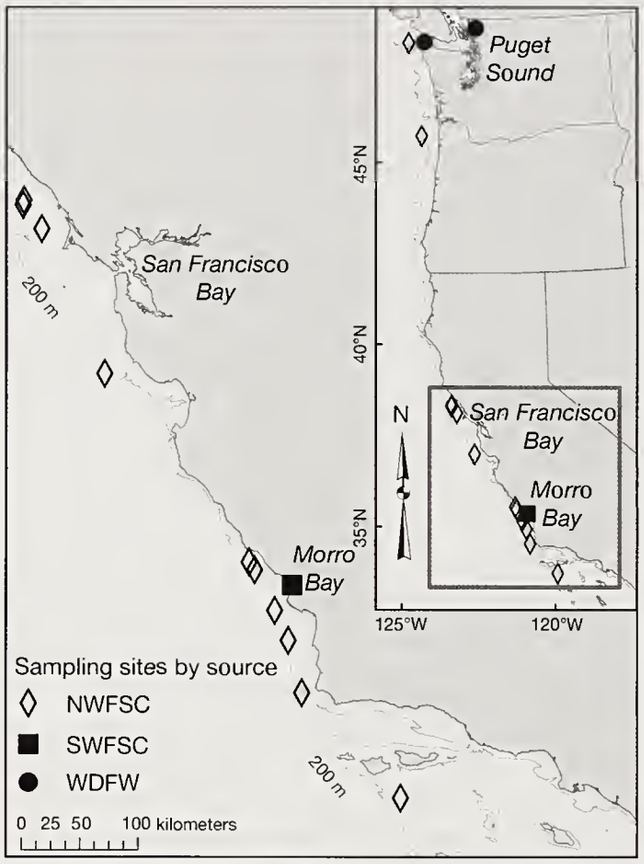

Figure 1

Map of locations where petrale sole (*Eopsetta jordani*) were captured during 2014–2017 off California, Oregon, and Washington. Northwest Fisheries Science Center (NWFSC) locations represent bottom-trawl survey stations; Southwest Fisheries Science Center (SWFSC) and Washington Department of Fish and Wildlife (WDFW) locations are ports of landings. Map provided by R. Miller (SWFSC).

differences among slides from the same individual, thereafter, tissue was collected from the middle portion of a randomly selected ovarian lobe.

Fecundity

Determination of fecundity strategy Fecundity strategy was determined by examination of ovarian histological sections and diagrams of oocyte size–frequency distribution for ovaries of macroscopic stages 2 and 3. Histological observations of POFs concomitant with oocytes undergoing vitellogenesis or maturation indicated that petrale sole spawned multiple times a season (batch spawning). Furthermore, the presence of a hiatus between primary and secondary growth oocytes in ovaries from fish for which spawning was imminent (with the leading oocyte cohort at late stages of vitellogenesis or further developed) and in ovaries from repeat spawners (with the leading oocyte cohort at late stages of vitellogenesis or further developed and POF present) indicated that fecundity was determinate (potential annual fecundity [PAF] set prior to the first spawning event) (Murua and Saborido-Rey, 2003).

To confirm that fecundity was determinate and to define the minimum trailing oocyte stage (least developed secondary growth oocyte present) threshold for fecundity analyses, oocyte size–frequency distributions were examined from archival samples of 20 ovaries of macroscopic stages 2 and 3 (10 of each stage). Oocytes were teased from tissue and placed into welled chambers. Photomicrographs were recorded at 70× magnification by using a digital camera (MU800[1], AmScope, Irvine, CA) mounted to a stereo microscope. Measurements of oocyte diameters were automated from photomicrographs by using the ObjectJ plugin (vers. 1.03x, University of Amsterdam, available from website) and associated modified macros (available from website) for image analysis software ImageJ (vers. 1.50i, National Institutes of Health, available from website; Schneider et al., 2012). Automated measurements recorded from damaged oocytes or detritus were manually removed. Primary growth oocytes clustered together and were difficult to tease apart. Because the maximum size for primary growth oocytes was 150 µm (on the basis of measurements from 10 stage-3 ovaries; Table 2), a lower limit of 150 µm was established for automated measurements. A minimum of 500 secondary growth oocytes per sample were measured. A gap between primary and secondary oocytes was observed (Fig. 2B) when the trailing oocytes had reached the secondary vitellogenic stage (Vtg2) (meaning no secondary growth oocytes were less developed than Vtg2). Recruitment from the reserve of primary growth oocytes to the spawning stock was considered complete at this time.

Fecundity processing and analyses Only macroscopic-stage-2 ovaries (n=132) were considered for fecundity processing and analysis to determine PAF prior to any spawning events. Macroscopic-stage-3 ovaries were not used for fecundity analysis because of the observation of POFs (evidence of prior spawning) in all stage-3 ovaries examined histologically. Histological sections from macroscopic-stage-2 ovaries were examined for the presence of POFs (n=0) and to ensure recruitment of oocytes for the reproductive season was complete. Any samples with trailing oocytes earlier than Vtg2 (n=56) were excluded because of the possibility for incomplete recruitment of oocytes to the potential spawning stock. A total of 70 samples (California: n=49; Pacific Northwest: n=21) were included in fecundity analyses.

Homogenous oocyte density (oocytes per gram of ovarian weight) throughout the ovary was verified by comparing densities from subsamples collected from the anterior, middle, and posterior third of each ovarian lobe from 6 macroscopic-stage-2 ovaries collected in the 2015–2016 reproductive season. The results of a nested analysis of variance indicate that oocyte density did not vary

[1] Mention of trade names or commercial companies is for identification purposes only and does not imply endorsement by the National Marine Fisheries Service, NOAA.

Table 2

Macroscopic stage and histological phase descriptions of ovarian development in petrale sole (*Eopsetta jordani*). Oocyte stages used in this study are based on descriptions in Wallace and Selman (1981) and Lowerre-Barbierie et al. (2011), and terminology follows Brown-Peterson et al. (2011), with modifications specific to petrale sole. BV=blood vessel; CT=connective tissue; GVB=germinal vesicle breakdown; GVM=germinal vesicle migration; HO=hydrated oocyte; LC=leading oocyte cohort; MB=muscular bundle; PG=primary growth oocyte; and POF=postovulatory follicle complex; Vtg1, Vtg2, and Vtg3 represent the primary, secondary, and tertiary vitellogenic oocytes, respectively.

Macroscopic stage	Macroscopic description	Histological phase	Subphase	Histological description
1 (Immature)	Ovaries are small and elongate, pale or flesh-colored with no black pigmentation, and tear easily.	Immature		Lamellae are tight and generally well organized with only PG present. No atresia or prominent BV, MB, or CT present. Ovarian wall is thin.
2 (Developing)	Oocytes are visible, giving ovary a uniformly granular appearance. Ovary is well vascularized and opaque.	Developing	Early developing	LC is at Vtg1 or Vtg 2. Minor atresia may be present. By the end of this stage, there is a distinct hiatus between primary and secondary growth oocytes. *Note: there appears to be no distinct cortical alveolar stage oocytes in petrale sole.*
		Spawning capable	Late developing	LC is at Vtg3, GVM, or GVB stage. Generally, when ovary is at this stage, the earliest secondary growth oocyte stage is Vtg2 or later. Minor atresia may be present, and there is no evidence of recent spawning (no POFs present)
3 (Ripe or running ripe)	Large, translucent hydrated eggs visible, scattered throughout ovary. Hydrated eggs may run under slight pressure.		Actively spawning	LC may be Vtg3, GVM, GVB, or HO. At least one stage of POF present and readily distinguishable from older atresia. Standing stock of secondary growth oocytes at the Vtg3. Moderate delta and gamma atresia may be present.
4 (Spent)	Ovaries are flacid; brown, or dark red in color and may have excess ovarian fluid. Residual oocytes (vitellogenic or hydrated) may or may not be visible.	Regressing		PG are the most advanced nonatretic oocyte present; if present, secondary growth oocytes are undergoing alpha or beta atresia. Lamellae appear loose and disorganized. Initially, POFs are readily distinguishable from other atretic material. BV, MB, and CT are prominent.
5 (Resting)	Ovaries are reduced in size, are firmer to the touch (compared to spent), are pink in color, have no discernable oocytes, and have a gelatinous texture.	Regenerating		PG dominate. Some beta atretic oocytes may be present but delta and gamma atresia dominate. Lamellae more organized compared with "regressing" ovary. BV, MB, and CT are prominent. Ovarian wall is thick.

significantly between lobes (P=0.88) or location within lobes (P=0.97). Subsequently, 2 fecundity subsamples were collected from the middle portion of either the blind- or eyed-side ovarian lobe.

In the 2015–2016 reproductive season, weighed subsamples for fecundity analyses were 0.5–1.0 g. Upon preliminary analysis of these samples, subsample weights were reduced to 0.25–0.50 g in the 2016–2017 season. All oocytes in weighed subsamples were counted by using a stereomicroscope, and oocyte density was calculated as quotient of the oocyte count and subsample weight. Potential annual fecundity was estimated gravimetrically by multiplying the oocyte density by the ovarian weight. Relative PAF was calculated as the quotient of PAF and somatic weight (total weight minus ovarian weight). Estimates from the 2 subsamples were averaged, and the coefficient of variation was calculated. Samples were excluded from further analyses when the coefficient of variation exceeded 0.15 (n=5). Fecundity estimates are potential values because any potential down-regulation through atresia was not accounted for.

Estimates of PAF and relative PAF were developed to evaluate the effects of maternal size on egg production. For most finfish, absolute fecundity increases geometrically

Table 3

Modifications specific to petrale sole (*Eopsetta jordani*) for oocyte stages described by Wallace and Selman (1981) and Lowerre-Barbieri et al. (2011). Oocytes were measured from prepared histological slides, except for hydrated oocytes, which were measured from whole mount samples. *n*=number of samples measured.

Oocyte stage	Petrale sole modification	Size (μm)	*n*
Primary growth	Include oogonia and perinuclear oocytes.	<150	150
Cortical alveolar	A distinct cortical alveolar stage is rare in petrale sole: cortical alveoli mostly appear concurrently with vitellogenin.	140–180	7
Primary vitellogenic (Vtg1)	Initial accumulation of small yolk granules occurs peripherally and mostly concurrently with cortical alveoli. Little to no oil droplet accumulation.	140–325	81
Secondary vitellogenic (Vtg2)	Small yolk granules completely fill cellular space. Little to no oil droplet accumulation.	250–650	234
Tertiary vitellogenic (Vtg3)	Oil droplets begin to appear and increase in size and numbers throughout this stage.	450–775	121
Germinal vesicle migration	Migration of the nucleus occurs concurrently with initial yolk coalescence (larger yolk granules).	625–775	27
Germinal vesicle breakdown	The nuclear membrane breaks down as yolk continues to coalesce, forming pale-pink "plates" within the oocyte. Oil begins to coalesce into a single droplet.	625–850	12
Hydrated	Yolk and lipids are completely coalesced.	>1200	20

with length and weight and is best described as a power function:

$$PAF = aL^b \text{ or} \quad (1)$$

$$PAF = aW^b, \quad (2)$$

where L is the total length (in millimeters) and W is the somatic weight (in grams). The parameters a and b for each equation are the intercept and slope, respectively, of the linear natural-log-transformed least-squares regression fit to the data:

$$\log(PAF) = \log(a) + (b \times \log(L)) \text{ or} \quad (3)$$

$$\log(PAF) = \log(a) + (b \times \log(W)). \quad (4)$$

The value for a was reported after back-transformation by using the bias correction term $\exp(\sigma^2/2)$. Values for P and the coefficient of determination (r^2) were reported for the log-transformed equation. Relative PAF (PAF_{rel}) was described as a linear function of female L or W:

$$PAF_{rel} = c + (d \times L) \text{ or} \quad (5)$$

$$PAF_{rel} = c + (d \times W), \quad (6)$$

where c and d are the intercept and slope, respectively, of the least-squares regression fit to the data. To understand potential geographic effects, we compared the performance of models relating fecundity (PAF or relative PAF) to maternal size in the following ways: 1) without considering region (California or Pacific Northwest) as a covariate, 2) allowing for region-specific intercepts along with a shared effect of size (i.e., classic analysis of covariance), or 3) allowing for region-specific effects of size (i.e., modeling an interaction between region and maternal size). We used the difference between Akaike information criterion (AIC) values for 2 nested models (ΔAIC) to select the most parsimonious models for each combination of size and fecundity predictors. Although in all cases the use of ΔAIC resulted in selection of the model with an interaction between region and size as the best description of the data, we also present results for the size-only model because the use of this model could be more appropriate for stock assessments that do not distinguish among regions.

All statistical analyses were conducted by using R (vers. 3.4.3; R Core Team, 2017) with a significance level of 0.05.

Results

Female petrale sole collected off California ranged in size from 305 to 600 mm TL (mean: 472 mm TL [standard deviation (SD) 48]) and in age from 4 to 20 years (mean: 9.4 years [SD 3.3]) (Table 1). Fish collected off Washington and Oregon measured 280–520 mm TL (mean: 436 mm TL [SD 63]) and had ages from 3 to 15 years (mean: 7.7 years [SD 2.8]) (Table 1). All macroscopic stages of ovarian development were observed in fish collected from California (Fig. 3); the only immature fish were collected in NWFSC bottom-trawl surveys. At the earliest collections, the majority of females had stage-2 ovaries. Spawning was first evident in September, and peak spawning occurred in December, as determined by the percentage of females with stage-3 ovaries. By January, the majority of females had completed spawning and had stage-4 ovaries. The reproductive season appeared to start later in Pacific Northwest collections, with the majority of ovaries found at stage 2 in December and the first stage-3 ovaries collected in January.

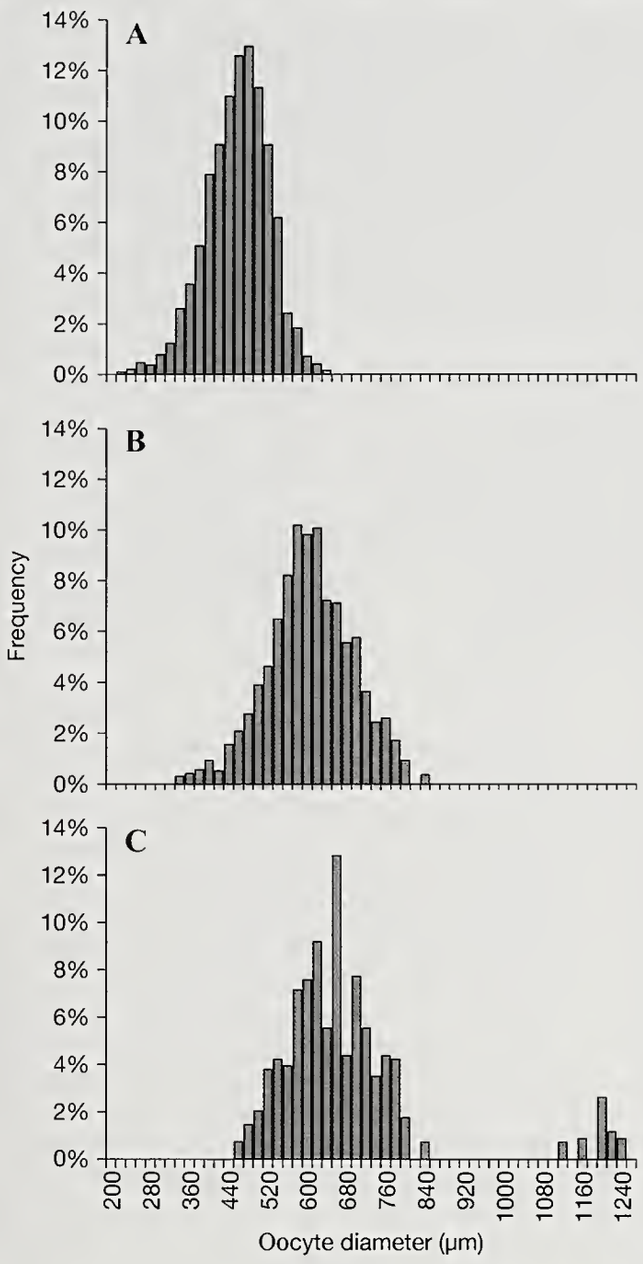

Figure 2

Representative examples of oocyte size–frequency distribution diagrams for ovarian samples taken from petrale sole (*Eposetta jordani*) collected off California, Oregon, and Washington in 2014–2017. Primary growth oocytes, which were <150 um, are not included, and all oocytes are at the primary vitellogenic oocyte stage or further advanced. (**A**) An example of when recruitment of oocytes for the year was nearing completion, from a macroscopic-stage-2 ovary sampled in August. (**B**) An example of oocytes fully recruited before spawning has commenced, from a macroscopic-stage-2 ovary sampled in October. (**C**) An example of a female that had initiated spawning, from a macroscopic-stage-3 ovary sampled in October. The gap between primary and secondary growth oocytes evident in panels B and C indicates a determinate fecundity pattern for petrale sole.

Histological examination of ovarian tissues confirmed macroscopic assignment of developmental stages (Fig. 4) and provided evidence of the fecundity pattern and spawning strategy of petrale sole. Increasing size of perinucleolar stage oocytes signaled the earliest development. Interestingly, there appeared to be no distinct cortical alveolar oocyte stage, with cortical alveoli appearing concomitantly with vitellogenin (yolk protein). Oocytes developed somewhat asynchronously until a mid-vitellogenic state (Vtg2) because, presumably, recruitment from primary growth reserves was ongoing. Oocytes then developed synchronously to the tertiary vitellogenic stage (Vtg3), after which individual clutches underwent final maturation sequentially (observed histologically as ovaries with primary growth and Vtg3 oocytes with groups of oocytes at various stages of final maturation [e.g., germinal vesicle migration, germinal vesicle membrane breakdown, or hydration]). Once the leading cohort reached the Vtg3 stage, earlier vitellogenic stages were not observed (indicating recruitment from the primary growth stage was complete). This oogenesis pattern indicates that petrale sole exhibited a determinate fecundity pattern. The fecundity pattern was corroborated with examination of diagrams of oocyte size–frequency distribution that show a distinct gap between primary and secondary growth oocytes (Fig. 2).

The presence of POFs (from prior spawning events) with hydrating oocytes (destined for imminent spawning) and late vitellogenic oocytes (for future spawning activity) demonstrated that petrale sole exhibited batch spawning behavior (Fig. 4D) (Murua and Saborido-Rey, 2003). The exact number of spawning events could not be determined because the duration of POFs were unknown in this species; however, 2 or 3 distinct stages of POFs were found in many histological sections from ovaries with both vitellogenic and hydrating oocytes, indicating that at least 4 or 5 spawning events for an individual were common and that more were possible. Atresia of secondary growth oocytes appeared to be rare during the reproductive season, indicating minimal fecundity down regulation. A small percentage (14%, or 1 of 7) of ovaries in the regressing phase appeared to be resorbing the final batch of oocytes at the end of the season.

Fecundity models including the interaction term of length or weight and region were the best fit on the basis of AIC (Table 4). Total PAF of the fish examined in this study ranged from 458,000 to over 3 million eggs and was significantly related to maternal size (Table 5, Fig. 5). Relative PAF values ranged from 481 to 1639 eggs per gram of somatic weight and was significantly related to maternal size in the combined and Pacific Northwest regional models (Table 5, Fig. 5); however, the slope parameter in the California regional model was not significantly different from zero (Table 4). The difference in the regional slopes for relative PAF means that a 56-cm-TL fish produced 1.25 times as many eggs per gram as a 40-cm-TL fish in California but produced 2.37 times as many eggs per gram as a 40-cm-TL fish off Washington and Oregon. This regional difference in the fecundity relationship appears to be driven by lower relative PAF for smaller

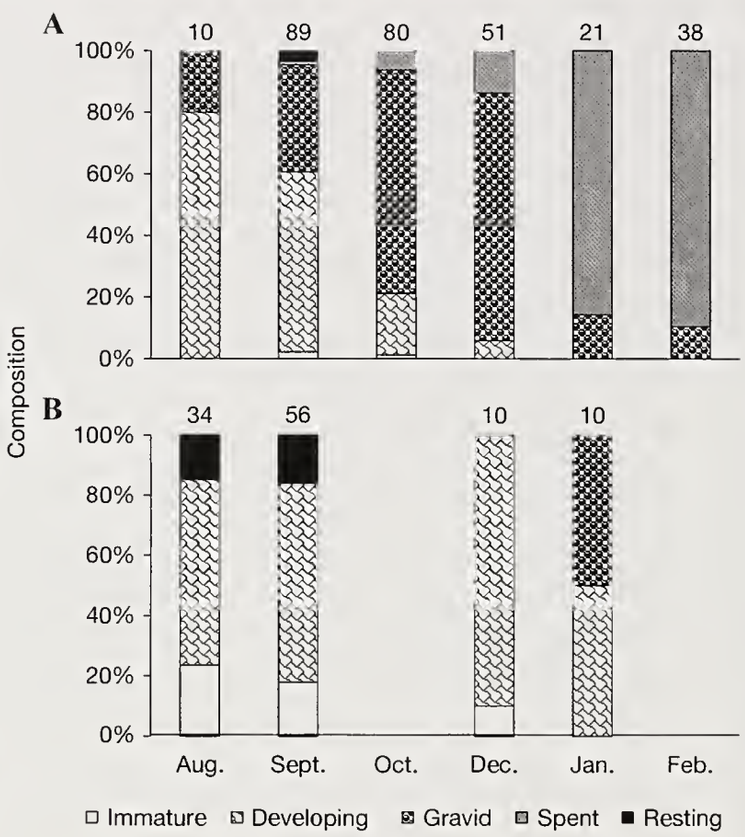

Figure 3

Composition of the macroscopic stages of ovarian development, by month, in petrale sole (*Eopsetta jordani*) collected off (**A**) California and (**B**) the Pacific Northwest (Oregon and Washington) in 2014–2017. The numerals above bars indicate number of samples.

fish in the data from the Pacific Northwest region relative to those from California. When all data are pooled, a 56-cm-TL fish produces 1.60 times as many eggs per gram as a 40-cm-TL fish.

Discussion

Accurate reproductive data are necessary for stock assessments. Even when the biology of a species is well understood, parameters such as fecundity exhibit spatiotemporal variation as a response to environmental conditions and body condition (McElroy et al., 2013; Beyer et al., 2015), and population shifts in egg production may occur over time as the demographics of a stock change (for example, when the number of small females increases) (Rideout and Morgan, 2007). Therefore, it is important to periodically revisit and review these types of data.

Maximum estimates of PAF (>3 million eggs) for petrale sole along the West Coast of the United States were found to be more than double previous estimates (1.45 million eggs; Porter, 1964). Through histological examination of ovarian tissue and analysis of oocyte size–frequency distributions, it was determined that petrale sole employed a determinate batch spawning strategy, as opposed to the determinate total spawning strategy suggested by Porter (1964). This updated understanding of the petrale sole's reproductive biology renders Porter's fecundity estimates obsolete because those data likely include samples from females that had already initiated spawning for the season. Porter (1964) observed hydrated oocytes ("ripe eggs") scattered throughout ovaries but assumed the fish spawned all eggs in a single event annually in part because of the homogeneity in size of the remaining oocytes. The homogeneity that Porter (1964) observed is explained by our observation of all oocytes contributing to PAF developing to the late stages of vitellogenesis prior to the first spawning event (evidenced histologically by all secondary growth oocytes being in late stages of vitellogenesis without evidence of spawning activity [no POFs present]), with individual batches advancing sequentially (evidenced histologically by the presence of POFs, hydrating oocytes, and late-stage vitellogenic oocytes). Furthermore, Porter (1964) noted that, although most oocytes appeared to develop synchronously, there were some samples in which multiple sizes of oocytes were visible. He assumed that they would be resorbed and, therefore, did not include them in his fecundity estimates. However, on the basis of our observations, it is possible that oocyte recruitment was ongoing in those cases and, therefore, PAF would have been underestimated from those individuals. Interestingly, Porter (1964) did also observe regional differences in fecundity: fish from Eureka (Northern California) had a slightly greater number of eggs at length than those from Oregon, a finding consistent with what we observed in differences in relative PAF between small fish from Morro Bay (Central California) and those from Oregon and Washington.

Histological analysis in which hematoxylin and Eosin Y staining was used also demonstrated the lack of a distinct cortical alveolar stage oocyte in petrale sole. Primary growth (perinuclear stage) oocytes move into secondary growth with the appearance of cortical alveoli, a change that is triggered by the hormone gonadotropin (Wallace and Selman, 1981). In most fish, this oocyte stage is a distinct one that occurs prior to the appearance of vitellogenin; however, in petrale sole in our study, cortical alveoli appeared at the same time as the vitellogenin. Although rarely documented, the lack of a cortical alveolar stage has been observed in pollock (*Pollachius virens*) (Skjæraasen et al., 2016). This observation has little relevance in the context of our study; however, it is important to note that, although many aspects of oogenesis and reproductive biology can be generalized across teleosts, a great variety of reproductive patterns exist.

Previous reproductive studies of petrale sole were focused on fish collected primarily off Oregon and to a lesser extent Washington (Harry, 1959; Porter, 1964;

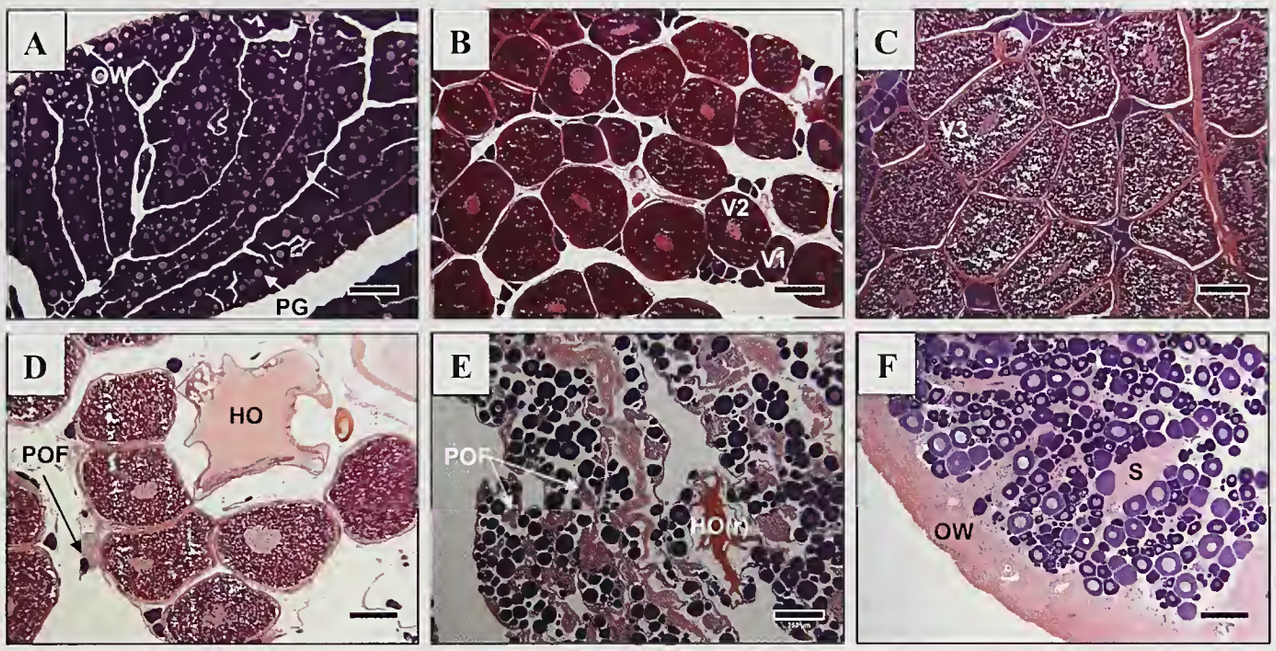

Figure 4

Photomicrographs from histological slides of ovarian tissue from petrale sole (*Eopsetta jordani*) collected in 2014–2017 off California, Oregon, and Washington, showing all phases of development: (**A**) immature, characterized by thin ovarian wall (OW), no stroma, and primary growth oocytes (PGs); (**B**) developing, characterized by oocytes at the mid-vitellogenic stage without evidence of spawning; (**C**) spawning capable, characterized by late vitellogenic oocytes without evidence of spawning; (**D**) actively spawning, characterized by hydrated oocytes (HOs) and postovulatory follicles (POFs); (**E**) regressing, characterized by POFs and only PGs; and (**F**) regenerating, characterized by a thick OW, only PGs, and thick stroma (S). V1=primary vitellogenic oocytes; V2=secondary vitellogenic oocyte; V3=tertiary vitellogenic oocyte; and HO(r)=residual HO. The bars indicate a scale of 250 µm.

Hannah et al., 2002). The reproductive season of petrale sole observed off California in this study, with a peak in December, overlapped with that observed previously for petrale sole in Oregon by Harry (1959), with a peak in December–January, and for those in Oregon and Washington by Porter (1964), with spawning occurring sometime between December and March; however, the season ended earlier in California, with most spawning activity concluding by January. With our limited collections from the waters of the Pacific Northwest, the onset of spawning appears to occur later in more northerly waters, with data from other sources indicating a 1-month lag compared with the timing of spawning observed for petrale sole in California (Haltuch[2]). Seasonal differences in the onset and intensity of upwelling are well known between California waters and those of the Pacific Northwest (e.g., Parrish et al., 1981), and such differences have been linked to shifts in the timing and the duration of spawning for other species of flatfish, such as the English sole (*Parophrys vetulus*) (Kruse and Tyler, 1983). Latitudinal variation in biological traits, such as growth and maturity, are common in many other commercially important fish species (Sampson and Al-Jufaily, 1999; McBride et al., 2013), and both temporal and spatial differences in growth for many species of groundfish on the West Coast of the United States, including the petrale sole, have been previously characterized (Stawitz et al., 2015; Gertseva et al., 2017).

In addition to providing more accurate estimates of PAF, maternal size was shown to significantly affect estimates of relative PAF in petrale sole, such that larger females contributed disproportionately more in terms of egg production compared with smaller females, as is common across fish taxa (e.g., Hixon et al., 2014; Barneche et al., 2018). Furthermore, regional variation in fecundity relationships were observed in this study. In California, the slope of the maternal size–fecundity relationship was less steep (and not statistically different from zero), compared with fish from the Pacific Northwest (Table 4, Fig. 5). This finding may be a reflection of differences in spawning season, such that fish off California have a longer spawning season and, therefore, can extend their reproductive efforts over a wider temporal range. However, the entirety of the spawning season was not studied sufficiently in the Pacific Northwest to verify that durations of the spawning seasons differ regionally. The observed differences in the slopes of the fecundity relationships appear to be driven by the data from small females, with larger females having similar fecundity estimates in both regions. Although

[2] Haltuch, M. 2018. Personal commun. Northwest Fish. Sci. Cent., Natl. Mar. Fish. Serv., NOAA, 2725 Montlake Blvd. East, Bldg. South, Seattle, WA 98112-2097.

Table 4

Selection criteria and parameters of the models for potential annual fecundity (PAF) and relative potential annual fecundity (PAF_{rel}) at length and weight in petrale sole (*Eopsetta jordani*). The base models consider only size (total length [TL] in millimeters or somatic weight [SW] in grams). Colons represent interactions between variables, and an asterisk (*) indicates the regional model that best fits the data on the basis of Aikake information criterion (AIC). Also provided are coefficients of determination (r^2), *P*-values, and values for the difference between Akaike information criterion (AIC) values for 2 nested models (ΔAIC).

Fecundity relationship	Model	r_2	*P*-value	ΔAIC
PAF (length)	TL	0.78	<0.001	23.92
	TL + Region	0.81	<0.001	16.66
	TL + Region + TL:Region*	0.85	<0.001	0.00
PAF (weight)	SW	0.75	<0.001	32.93
	SW + Region	0.81	<0.001	14.66
	SW + Region + SW:Region*	0.85	<0.001	0.00
PAF_{rel} (length)	TL	0.24	<0.001	16.88
	TL + Region	0.38	<0.001	5.03
	Tl + Region + TL:Region*	0.44	<0.001	0.00
PAF_{rel} (weight)	SW	0.13	0.001	23.68
	SW + Region	0.31	<0.001	8.94
	SW + Region + SW:Region*	0.40	<0.001	0.00

Table 5

Fecundity ranges and fecundity relationship model parameters for petrale sole (*Eopsetta jordani*) collected during 2014–2017 off California and the Pacific Northwest (Oregon and Washington). The potential annual fecundity parameter *a* is reported after back calculating from the log of length or weight by using the bias correction term $\exp(\sigma^2/2)$. The 95% confidence intervals for all parameters (*a*, *b*, c, and *d*) are listed in parentheses. An asterisk (*) denotes a result that was not significant. Lengths were measured as total lengths. *n*=number of samples.

		Potential annual fecundity (no. of oocytes)					Potential annual relative fecundity (no. oocytes per gram somatic weight)				
			Length (mm)		Weight (g)			Length (mm)		Weight (g)	
Region	*n*	Range	*a*	*b*	*a*	*b*	Range	*c*	*d*	c	*d*
Combined	70	458,442–3,003,377	9.03×10^{-7} (2.5×10^{-8}, 3.19×10^{-5})	4.55 (3.97, 5.13)	58.63 (14.55, 236.18)	1.39 (1.20, 1.58)	481–1639	−373.56 (−956.04, 212.92)	2.85 (1.65, 4.06)	678.4 (476.67, 880.13)	0.22 (0.09, 0.35)
California	49	839,318–3,003,377	2.86×10^{-4} (7.24×10^{-6}, 1.13×10^{-2})	3.63 (3.03, 4.22)	487.71 (122.50, 1925.87)	1.11 (0.92, 1.30)	833–1639	343.1 (−287.10, 974.48)	1.49* (0.02*, 2.78*)	963.29 (754.88, 11171.70)	0.07 (−0.06, 0.20)
Pacific Northwest	21	458,442–2,558,064	1.16×10^{-10} (4.51×10^{-15}, 3.00×10^{-6})	5.99 (4.35, 7.63)	3.38 (0.09, 526.84)	1.76 (1.26, 2.26)	481–1189	−1296.78 (−3048.06, 454.06)	4.57 (0.77, 8.19)	201.11 (−361.42, 763.67)	0.45 (0.09, 0.81)

intriguing, these relationships are based on a limited number of samples, particularly in large fish from the Pacific Northwest, and should be refined further before conclusions on regional variation can be drawn. Still, the observation that egg production is not proportional to maternal size in the combined model indicates that spawning stock biomass may not be an appropriate predictor of total egg production. Until regional values are established, the combined fecundity relationships (Table 4) are likely to be more appropriate for estimating total egg production in stock assessments.

A thorough understanding of the reproductive biology of a species is vital to providing accurate data for stock assessment models. For as long as the petrale sole has been assessed, fecundity appears to have been underestimated because of an incomplete understanding of the reproductive strategy of this species. The stronger size-dependent relationship observed in our data indicates that previous

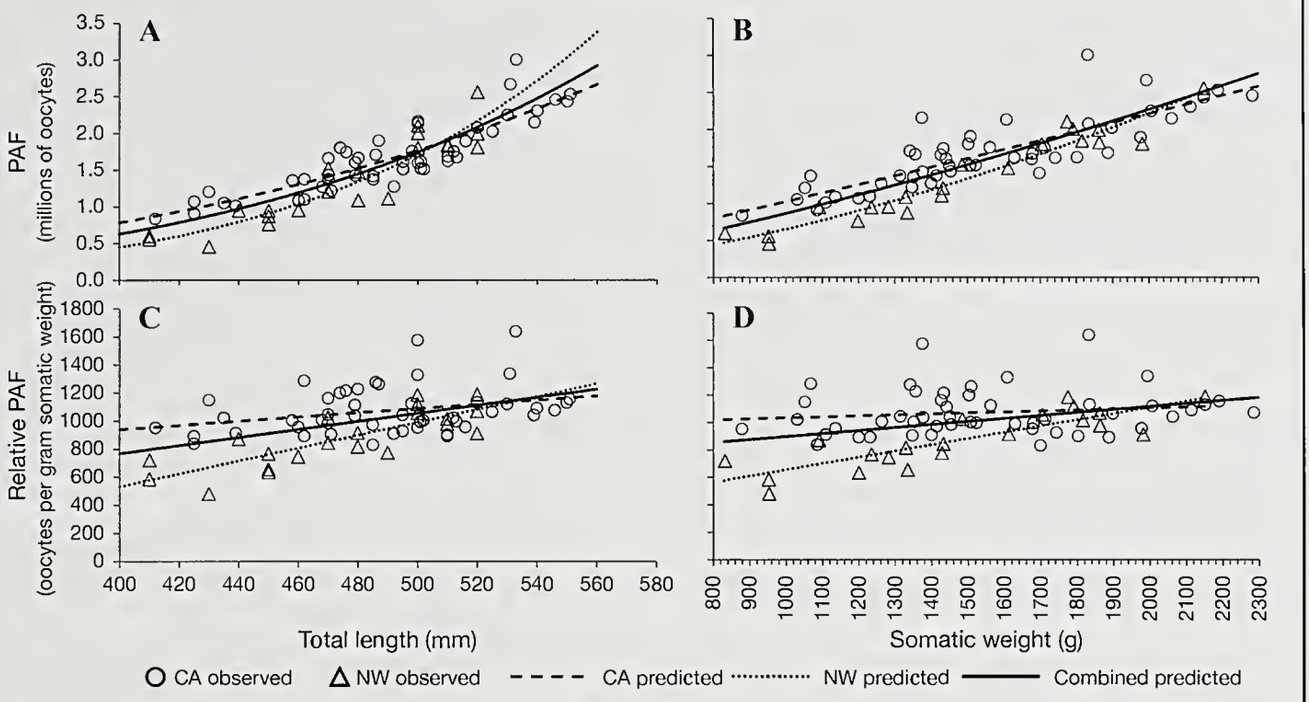

Figure 5

Potential annual fecundity (PAF) as a function of maternal (**A**) length and (**B**) somatic weight and relative PAF as a function of maternal (**C**) length and (**D**) somatic weight in petrale sole (*Eopsetta jordani*) sampled during 2014–2017 off California (CA) and the Pacific Northwest (NW, Oregon and Washington). Circles and triangles indicate observed values, and dashed, dotted, and solid lines indicate values predicted by models for each region and with regions combined.

stock assessments of petrale sole conducted along the West Coast of the United States may have overestimated relative spawning output because they did not fully account for the increased relative egg production of larger individuals that would have been present in an unfished population. Moreover, the observation that female petrale sole produce not one, but several, batches of eggs throughout a given spawning season may have implications for how catch and effort data are evaluated from the winter fisheries (which take place on spawning grounds). However, given the uncertainties regarding potential differences in the relative fecundity relationship over space, additional research to better quantify reproductive output of this commercially important species would be ideal. Given the importance of this stock in commercial fisheries in both the United States and Canada, future studies into the reproductive ecology of petrale sole should include and pool data from a broader latitudinal range, including waters in California, the Pacific Northwest, and Canada, to better understand patterns of variability in fecundity and life history.

Acknowledgments

We are grateful to R. and T. Seitz (South Bay Wild, Astoria, OR), M. Gleason and S. Rienecke (The Nature Conservancy), and M. Head (NWFSC) for their cooperation in collecting commercial and survey samples; P. MacDonald (NWFSC) for providing ages; E. Dick (SWFSC) for statistical assistance; and the processing crew and numerous interns for help developing the data. This manuscript was improved with comments from S. Beyer (SWFSC), M. Haltuch (NWFSC), and 3 anonymous reviewers. Funding was provided by the NMFS Cooperative Research Program.

Literature cited

Alverson, D. L., and B. M. Chatwin.
1957. Results from tagging experiments on a spawning stock of petrale sole, *Eopsetta jordani* (Lockington). J. Fish. Res. Board Can. 14:953–974.

Barneche, D. R., D. R. Robertson, C. R. White, and D. J. Marshall.
2018. Fish reproductive-energy output increases disproportionately with body size. Science 360:642–645.

Beyer, S. G., S. M. Sogard, C. J. Harvey, and J. C. Field.
2015. Variability in rockfish (*Sebastes* spp.) fecundity: species contrasts, maternal size effects, and spatial differences. Environ. Biol. Fish. 98:81–100.

Brown-Peterson, N. J., D. M. Wyanski, F. Saborido-Rey, B. J. Macewicz, and S. K. Lowerre-Barbieri.
2011. A standardized terminology for describing reproductive development in fishes. Mar. Coast. Fish. 3:52–70.

CDFW (California Department of Fish and Wildlife).
2013. Status of the fisheries report: an update through 2011, 224 p. Calif. Dep. Fish Wildl., Monterey, CA. [Available from website.]

Gertseva, V., S. E. Matson, and J. Cope.
2017. Spatial growth variability in marine fish: example from Northeast Pacific groundfish. ICES J. Mar. Sci. 74:602–1613.

Haltuch, M. A., and A. Hicks.
2009. Status of the U.S. petrale sole resource in 2008, 148 p. Pac. Fish. Manage. Counc., Portland, OR. [Available from website.]

Haltuch, M. A., A. Hicks, and K. See.
2011. Status of the U.S. petrale sole resource in 2010, 175 p. Pac. Fish. Manage. Counc., Portland, OR. [Available from website.]

Haltuch, M. A., K. Ono, and J. Valero.
2013. Status of the U.S. petrale sole resource in 2012, 234 p. Pac. Fish. Manage. Counc., Portland, OR. [Available from website.]

Hannah, R. W., S. J. Parker, and E. L. Fruh.
2002. Length and age at maturity of female petrale sole (*Eopsetta jordani*) determined from samples collected prior to spawning aggregations. Fish. Bull. 100:711–719.

Harry, G. Y., Jr.
1959. Time of spawning, length at maturity, and fecundity of the English, petrale, and Dover soles (*Parophrys vetulus*, *Eopsetta jordani*, and *Microstomus pacificus*, respectively). Fish. Comm. Oregon., Res. Briefs 7(1):5–13.

Hixon, M. A., D. W. Johnson, and S. M. Sogard.
2014. BOFFFFs: on the importance of conserving old-growth age structure in fishery populations. ICES J. Mar. Sci. 71:2171–2185.

Humason, G. L.
1972. Animal tissue techniques, 3rd ed., 468 p. W. H. Freeman, San Francisco, CA.

Keller, A. A., J. R. Wallace, B. H. Horness, O. S. Hamel, and I. J. Stewart.
2012. Variations in eastern North Pacific demersal fish biomass based on the U.S. west coast groundfish bottom trawl survey (2003–2010). Fish. Bull. 110:205–222.

Ketchen, K. S., and F. C. R. Forrester.
1966. Population dynamics of the petrale sole, *Eopsetta jordani*, in waters off western Canada. Fish. Res. Board Can., Bull. 153, 204 p.

Kruse, G. H., and A. V. Tyler.
1983. Simulation of temperature and upwelling effects on the English sole (*Parophrys vetulus*) spawning season. Can. J. Fish. Aquat. Sci. 40:230–237.

Lowerre-Barbieri, S. K., K. Ganias, F. Saborido-Rey, H. Murua, and J. R. Hunter.
2011. Reproductive timing in marine fishes: variability, temporal scales, and methods. Mar. Coast. Fish. 3:71–91.

McBride, R. S., M. J. Wuenschel, P. Nitscheke, G. Thorton, and J. R. King.
2013. Latitudinal and stock-specific variation in size- and age-at-maturity of female winter flounder, *Pseudopleuronectes americanus*, as determined with gonad histology. J. Sea Res. 75:41–51.

McElroy, W. D., M. J. Wuenschel, Y. K. Press, E. K. Towle, and R. S. McBride.
2013. Differences in female individual reproductive potential among three stocks of winter flounder, *Pseudopleuronectes americanus*. J. Sea Res. 75:52–61.

Murua, H., and F. Saborido-Rey.
2003. Female reproductive strategies of marine fish species of the North Atlantic. J. Northwest Atl. Fish. Sci. 3:23–31.

Parrish, R. H., C. S. Nelson, and A. Bakun.
1981. Transport mechanisms and reproductive success of fishes in the California Current. Biol. Oceanogr. 1:175–203.

Pedersen, M. G.
1975. Movement and growth of petrale sole (*Eopsetta jordani*) tagged off Washington and southwest Vancouver Island. J. Fish. Res. Board Can. 32:2169–2177.

Porter, P.
1964. Notes on fecundity, spawning, and early life history of petrale sole (*Eopsetta jordani*), with descriptions of flatfish larvae collected in the Pacific Ocean off Humboldt Bay, California. M.S. thesis, 98 p. Humboldt State Coll., Arcata, CA.

R Core Team.
2017. R: a language and environment for statistical computing. R Foundation for Statistical Computing, Vienna, Austria. [Available from website, accessed January 2018.]

Rideout, R. M., and M. J. Morgan.
2007. Major changes in fecundity and the effect on population egg production for three species of north-west Atlantic flatfishes. J. Fish Biol. 70:1759–1779.

Sampson, D. B., and S. M. Al-Jufaily.
1999. Geographic variation in the maturity and growth schedules of English sole along the U.S. west coast. J. Fish Biol. 54:1–17.

Sampson, D. B., and Y. W. Lee.
1999. An assessment of the stocks of petrale sole off Washington, Oregon, and Northern California in 1998, 99 p. Pac. Fish. Manage. Counc., Portland, OR. [Available from website.]

Schneider, C. A., W. S. Rasband,, and K.W. Eliceiri.
2012. NIH Image to ImageJ: 25 years of image analysis. Nat. Methods 9:671–675.

Skjæraasen, J. E., J. A. Devine, J. A. Godiksen, M. Fonn, H. OtterÅ, O. S. Kjesbu, B. Norberg, Ø. Langangen, and Ø. Karlsen.
2016. Timecourse of oocyte development in saithe *Pollachius virens*. J. Fish Biol. 90:109–128.

Starr, P. J., and J. Fargo.
2004. Petrale sole stock assessment for 2003 and recommendations for management in 2004. Can. Sci. Advis. Secr., Res. Doc. 2004/036, 80 p. [Available from website.]

Stawitz, C. C., T. E. Essington, T. A. Branch, M. A. Haltuch, A. B. Hollowed, and P. D. Spencer.
2015. A state-space approach for detecting growth variation and application to North Pacific groundfish. Can. J. Fish. Aquat. Sci. 72:1316–1328.

Stawitz, C. C., F. Hurtado-Ferro, P. Kuriyama, J. T. Trochta, K. F. Johnson, M. A. Haltuch, and O. S. Hamel.
2016. Stock assessment update: status of the U.S. petrale sole resource in 2014, 210 p. Pac. Fish. Manage. Counc., Portland, OR. [Available from website.]

Turnock, J., M. Wilkins, M. Saelens, and C. Wood.
1993. Status of West Coast petrale sole in 1993. *In* Status of the Pacific coast groundfish fishery through 1993 and recommended biological catches for 1994: stock assessment and fishery evaluation, p. G1–G42. Pac. Fish. Manage. Counc., Portland, OR. [Available from website.]

Wallace, R. A., and K. Selman.
1981. Cellular and dynamic aspects of oocyte growth in teleosts. Am. Zool. 21:325–343.

National Marine
Fisheries Service
NOAA

Fishery Bulletin
established in 1881

Spencer F. Baird
First U.S. Commissioner
of Fisheries and founder
of *Fishery Bulletin*

Salmonid passive integrated transponder tags and coded wire tags found in the forestomach of a harbor porpoise (*Phocoena phocoena*) in southwestern Washington

Dalin N. D'Alessandro (contact author)
Deborah A. Duffield

Email address for contact author: dalin@pdx.edu

Department of Biology
Portland State University
P.O. Box 751
Portland, Oregon 97207

Abstract—A dead adult harbor porpoise (*Phocoena phocoena*) was found on the Long Beach Peninsula in Washington on 22 August 2012. The harbor porpoise was skeletonized, with the forestomach being the only organ that remained. The forestomach contained 5 passive integrated transponder (PIT) tags and 91 coded wire tags (CWTs). The PIT tags were from juvenile Chinook salmon (*Oncorhynchus tshawytscha*) from 3 hatcheries in the Columbia River Basin. Of the 91 CWTs, 88 tags were identified as having come from juvenile Chinook salmon from Columbia River Basin hatcheries and 3 tags came from unidentified fish from hatcheries in Oregon. The 88 CWTs represent a number of hatcheries along the Columbia and Snake Rivers in Idaho, Washington, and Oregon. The tagged juveniles were released in the spring and summer of 2012. This report is the first one of Chinook salmon PIT tags and CWTs being recovered from a harbor porpoise in the Pacific Northwest, and it is one of few records of harbor porpoises eating salmon. The presence of these tags and the number of tags in the forestomach of a harbor porpoise indicate that juvenile Chinook salmon might be a more important component of the diet of harbor porpoises in the Pacific Northwest than previously thought.

Manuscript submitted 10 February 2019.
Manuscript accepted 19 September 2019.
Fish. Bull. 117:303–307 (2019).
Online publication date: 4 October 2019.
doi: 10.7755/FB.117.4.3

The views and opinions expressed or implied in this article are those of the author (or authors) and do not necessarily reflect the position of the National Marine Fisheries Service, NOAA.

Passive integrated transponder (PIT) tags and coded wire tags (CWTs) inserted into Chinook salmon (*Oncorhynchus tshawytscha*) of the Columbia River Basin in the Pacific Northwest were recovered from the forestomach of a harbor porpoise (*Phocoena phocoena*) in 2012. Although the Columbia River Basin primarily comprises parts of Idaho, Oregon, Washington, southeastern British Columbia, Canada, and western Montana and small parts of Nevada, Utah, and Wyoming (Fig. 1), the primary areas represented by these tags include Idaho, Oregon, and Washington. The Columbia River Basin is further divided into smaller basins by the Regional Mark Processing Center as part of the Regional Mark Information System (RMIS), a collective database of records of releases of anadromous salmonids tagged with CWTs, recoveries of CWTs, and the locations of these events (available from website). Only the basins associated with tags recovered from the harbor porpoise are identified in Figure 1.

During routine beach surveillance on 22 August 2012, staff of the Northern Oregon/Southern Washington Marine Mammal Stranding Program, Portland State University, found a 140-cm adult harbor porpoise (*Phocoena phocoena*) of unknown sex on the Long Beach Peninsula in southwestern Washington (46.44191, −124.06052) (Fig. 1). The animal was heavily scavenged and skeletonized, with only the forestomach remaining of the internal organs. The skull and forestomach were collected. The entire right occipital area of the skull was fractured in a circular pattern, due to either scavenging or trauma. Examination of the forestomach contents revealed 5 PIT tags and 91 CWTs (Table 1). All tags were submitted for identification to the Oregon Department of Fish and Wildlife (ODFW) Columbia River Management Program in Clackamas, Oregon.

The PIT tags were identified as having come from juvenile fall-run Chinook salmon from hatcheries in the Columbia River Basin that were tagged in April 2012 and released in May 2012. The CWTs were from juvenile Chinook salmon that originated from Columbia River Basin hatcheries and that were from various runs but primarily from fall runs, and all tagged Chinook salmon were released in the spring and summer of 2012 (Table 2, Fig. 1).

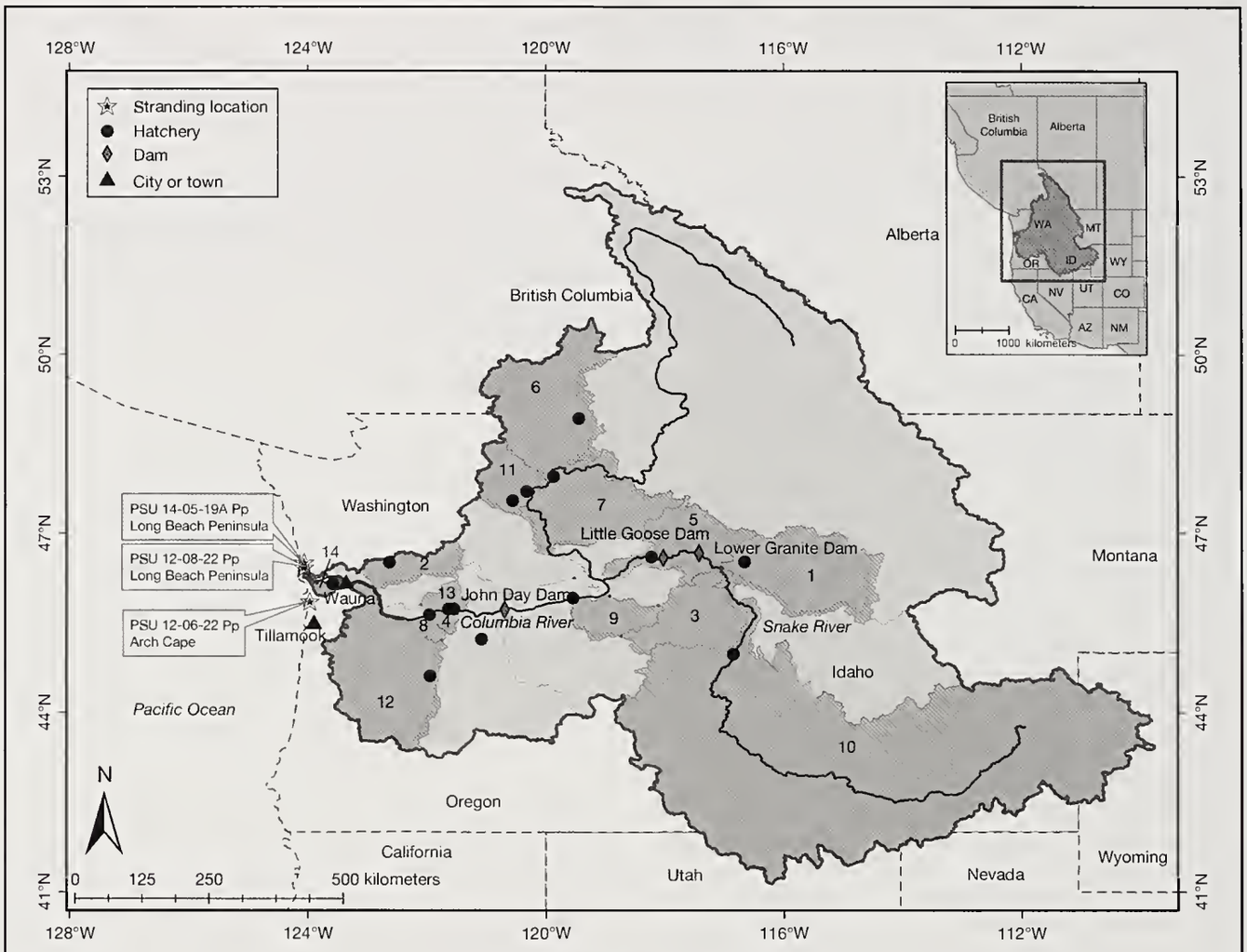

Figure 1

Map of the Columbia River Basin (light and dark gray areas) in the Pacific Northwest where juvenile Chinook salmon (*Oncorhynchus tshawytscha*) were tagged with passive integrated transponder (PIT) tags and coded wire tags and released in 2012 and where 2 juvenile steelhead (*O. mykiss*) were tagged with PIT tags and released in 2012 (n=1) and 2013 (n=1). Tags were recovered from 3 harbor porpoises (*Phocoena phocoena*) that were stranded in 2012 (n=2) and 2014 (n=1). All but 2 of the 98 tags came from 1 harbor porpoise (PSU 12-08-22 Pp). Locations where the PIT tags were detected along the river system, at the dams (gray diamonds) and at the city of Wauna (black triangle), are also shown. The Columbia River Basin is divided into smaller basins in the Regional Mark Information System, and numbers on the map indicate the basins where Chinook salmon were released: 1) Clearwater River, Idaho, 2) Cowlitz River, Washington, 3) Grand Ronde and Imnaha Rivers and Asotin Creek in Oregon and Washington, 4) Hood River, Oregon, 5) Lower Snake River, below Clarkston, Washington, 6) Methow and Okanogan Rivers, Washington, 7) Columbia River, from Priest Rapids Dam to Grand Coulee in Washington, 8) Sandy River, Oregon, 9) Umatilla River, Oregon, 10) Upper Snake River, above Lewiston, Idaho, 11) Wenatchee and Entiat Rivers and Lake Chelan in Washington, 12) Willamette River, Oregon, 13) Wind and White Salmon Rivers, Washington, and 14) Youngs Bay and Clatskanie River in Oregon. Data sources for base map: Esri, HERE, Garmin, OpenStreetMap contributors, and the GIS user community.

Although PIT tags and CWTs have been found in dead, stranded pinnipeds in our area, which covers the outer coast from Tillamook, Oregon, to the Long Beach Peninsula, in 10 years of responding to strandings and stomach content analysis of over 150 stomachs, only 2 other harbor porpoises were found to have salmonid tags in their stomachs. One harbor porpoise, an adult male, had 1 salmonid tag (PIT tag no. 3D9.1C2DB7C94B) from a hatchery winter-run steelhead (*O. mykiss*) in his stomach. This harbor porpoise (Fig. 1) became stranded on 8 June 2012 at Arch Cape, Oregon (45.85530, −123.96366). The second harbor porpoise was also an adult male that had 1 salmonid tag (PIT tag no. 3D9.1C2DDB82D3) from a wild summer-run steelhead in his stomach. This harbor porpoise became stranded on 19 May 2014 on the Long Beach Peninsula (46.48693, −124.06025). This report provides the names of the hatcheries, stock locations, release dates, and basins associated with releases of tagged Chinook salmon and steelhead for the tags recovered from the harbor porpoises in our area. In addition, tag numbers associated with the recovered PIT tags and the CWTs are provided so that queries of the online

Table 1

Summary of information for coded wire tags (CWTs) and the juvenile Chinook salmon (*Oncorhynchus tshawytscha*) from hatcheries in the Columbia River Basin in which the CWTs had been inserted. These CWTs were found in the forestomach of a dead, stranded harbor porpoise (*Phocoena phocoena*) recovered from the Long Beach Peninsula in southwestern Washington on 22 August 2012. The code *09blank* may or may not be associated with Chinook salmon because no data are available. ID=Idaho; WA=Washington; OR=Oregon; NFH=National Fish Hatchery. Data source: Regional Mark Information System (RMIS, available from website). Stock location names are given exactly as they appear in the RMIS.

Release location	Stock location	Hatchery	Run (return to freshwater)	Total no. of CWTs	CWT numbers
ID	Snake River	Oxbow Hatchery	Fall	5	100201
ID	Lyons Ferry Hatchery	Nez Perce Tribal Hatchery	Late fall	6	220216, 220224
ID, WA	Lyons Ferry Hatchery	Lyons Ferry Hatchery	Late fall	19	220324, 220325, 220326, 220327, 220328, 220329
WA	Spring Creek 29.0159	Little White Salmon NFH	Fall	4	055233, 055260
WA	Snake River–Lower 33.0002	Lyons Ferry Hatchery	Fall	3	636417, 636418
WA	Spring Creek 29.0159	Spring Creek NFH	Fall	13	055399, 055404, 055527, 055528
WA	Cowlitz River 26.0002	Cowlitz Salmon Hatchery	Spring	1	635273
WA	Wenatchee River 45.0030	Dryden Pond	Summer	1	635776
WA	Wells Hatchery	Entiat NFH	Summer	1	055364
WA	Methow and Okanogan	Similkameen Hatchery	Summer	1	635690
WA	Wells Hatchery	Wells Hatchery	Summer	2	636370
OR	Big Creek Hatchery	Big Creek Hatchery	Fall	18	090566, 090567, 090582, 090583
OR	Columbia River Tules	Bonneville Hatchery	Fall	3	090571
OR	Snake River–Lower 33.0002	Irrigon Hatchery	Fall	3	636419
OR	Snake River	Irrigon Hatchery	Late fall	2	090587
OR	Umatilla River	Umatilla Hatchery	Fall	5	090585, 090586
OR	Santiam River North Fork	Marion Forks Hatchery	Spring	1	090526
OR	Unknown	Unknown	Unknown	3	09blank

databases, Columbia Basin PIT Tag Information System (available from website) and RMIS, can be performed for more information. The CWT numbers also identify specific batches of fish releases.

Materials and methods

The forestomach of the skeletonized harbor porpoise was collected on 22 August 2012 and transported to the Marine Mammal Laboratory at Portland State University for analysis. The forestomach was completely desiccated; therefore, a single cut to the forestomach was made longitudinally, and the contents were removed by hand. The forestomach lining was inspected for any additional contents that may have adhered to the stomach wall, and remaining contents were gently removed with forceps. Contents included PIT tags and CWTs. All of the tags were delivered to the ODFW Columbia River Management Program, where the tags were read by laboratory staff. Staff of the ODFW provided to us spreadsheets, created in Microsoft Excel[1] (Microsoft Corp., Redmond, WA), that contain hatchery-related data for individual tags. For any CWT records that lacked data because information was not entered into the database, we later downloaded data from the RMIS website. In addition, we queried PIT tag codes and downloaded the associated records from the Columbia Basin PIT Tag Information System website to verify that additional information had not subsequently been added to the online records.

Results and discussion

Five PIT tags and 91 CWTs were recovered from the forestomach of the dead, stranded harbor porpoise from the Long Beach Peninsula. The PIT tags came from juvenile fall-run Chinook salmon representing 3 hatcheries in the Columbia River Basin: Lyons Ferry Hatchery in Washtucna, Washington, Oxbow Fish Hatchery in Oxbow, Oregon, and Irrigon Hatchery in Irrigon, Oregon. Between 3 May and 29 May 2012, these Chinook salmon were released at 3 different locations: Lyons Ferry Hatchery; the acclimation facility at Pittsburg Landing, Idaho; and Snake River, from Salmon River to Hells Canyon in Oregon and Idaho. Two of the tagged Chinook salmon (PIT tag nos. 3D9.1C2DE01E19 and 3D9.1C2DE025DA) were released in the same group on 22 May 2012, one of which was detected at the juvenile bypass system of the Lower Granite Dam (Fig. 1) in southeastern Washington on

[1] Mention of trade names or commercial companies is for identification purposes only and does not imply endorsement by the National Marine Fisheries Service, NOAA.

Table 2

Locations and dates of releases of juvenile Chinook salmon (*Oncorhynchus tshawytscha*) tagged with coded wire tags (CWTs) and released from hatcheries in the Columbia River Basin in 2012. These CWTs were found in the forestomach of a dead, stranded harbor porpoise (*Phocoena phocoena*) recovered from the Long Beach Peninsula in southwestern Washington on 22 August 2012. Also provided are the runs of the Chinook salmon and the basins where they were released. The code *09blank* may or may not be associated with Chinook salmon because no data are available. ID=Idaho; WA=Washington; OR=Oregon. Data source: Regional Mark Information System (available from website).

CWT numbers	Run (return to freshwater)	Basin	Release date range
100201	Fall	Upper Snake River, above Lewiston, ID	3 May
220216, 220224	Late fall	Clearwater River, ID	8 May–12 June
220324, 220325, 220326, 220327	Late fall	Upper Snake River, above Lewiston	21–23 May
220328, 220329	Late fall	Clearwater River	21–23 May
055233, 055260	Fall	Wind River, White Salmon River, WA	13 April
636417	Fall	Lower Snake River, below Clarkston, WA	29–30 May
636418	Fall	Grande Ronde River, Imnaha River, Asotin Creek, OR and WA	29–30 May
055399, 055404, 055527, 055528	Fall	Wind River, White Salmon River	11–13 April
635273	Spring	Cowlitz River, WA	26 March–2 April
635776	Summer	Wenatchee River, Entiat River, Lake Chelan, WA	25 April
055364	Summer	Wenatchee River, Entiat River, Lake Chelan	17 April
635690	Summer	Methow River, Okanogan River, WA	16 April–7 May
636370	Summer	Columbia River, from Priest Rapids Dam to Grand Coulee, WA	16–29 May
090566, 090567, 090582, 090583	Fall	Youngs Bay, Clatskanie River, OR	7 May
090571	Fall	Sandy River, OR	18 May
636419	Fall	Grande Ronde River, Imnaha River, Asotin Creek	24 May
090587	Late fall	Upper Snake River, above Lewiston	22–24 May
090585, 090586	Fall	Umatilla River, OR	23 May
090526	Spring	Willamette River, OR	15 March
09blank	Unknown	Unknown	Unknown

16 June 2012. A third PIT-tagged Chinook salmon (PIT tag no. 3D9.1C2DDEE358) also was released on 22 May 2012 but not as part of the same group as the 2 Chinook salmon noted previously. This third fish was detected at 2 other locations: the juvenile bypass system of Little Goose Dam in southeastern Washington on 4 June 2012 and the juvenile bypass system of John Day Dam, at the boundary of Oregon and Washington formed by the Columbia River, on 18 June 2012. The 2 remaining PIT-tagged Chinook salmon (PIT tag nos. 3D9.1C2DD706F1 and 3D9.1C2E0A858F) were not detected in other systems during their outmigration to the Pacific Ocean.

Of the 91 CWTs, 88 tags came from juvenile Chinook salmon from hatcheries in the Columbia River Basin that were released between 15 March and 12 June 2012 (Tables 1 and 2). These 88 CWTs represent 32 different tag batch numbers from 15 hatcheries located in Idaho, Washington, and Oregon. The juveniles were from fall (number of tagged fish [*n*]=81), spring (*n*=2), and summer (*n*=5) runs. The Chinook salmon were from the brood year 2011, except for 2 spring-run and 3 summer-run Chinook salmon that were from the brood year 2010. The remaining 3 CWTs were coded *09blank*, indicating that they were from a hatchery in Oregon with no other information available.

Each of the PIT-tagged Chinook salmon also may have had a CWT, and the CWT numbers that would have been used for these salmon (090587, 100201, 636417, and 220324 or 220325; Bumgarner[2]; Rosenberger[3]) did match numbers from CWTs recovered from the harbor porpoise's forestomach (Table 1). Two of the PIT-tagged Chinook salmon would have received the same CWT number (090587) because they were part of the same group (Rosenberger[3]), and 2 tags with this CWT number were recovered from the harbor porpoise's forestomach. Given that 5 of the recovered CWTs may have come from PIT-tagged Chinook salmon, the minimum number of individual juvenile Chinook salmon consumed by this harbor porpoise is 86.

On the basis of the release dates of the juvenile Chinook salmon, the date and location of the stranding of the harbor porpoise, and the migration behavior of hatchery Chinook salmon, particularly those from the fall runs that tend to

[2] Bumgarner, J. 2018. Personal commun. Snake River Lab, Fish Program, Sci. Div., Wash. Dep. Fish Wildl., 401 South Cottonwood St., Dayton, WA 99328.

[3] Rosenberger, S. 2018. Personal commun. Idaho Power Co., 1221 West Idaho St., Boise, ID 83702.

migrate in huge schools in the tributaries (Kern[4]), it is possible that the juvenile Chinook salmon tagged with the tags found in the harbor porpoise had gathered in large densities at the mouth of the Columbia River before heading into the Pacific Ocean. This gathering would have made them more vulnerable to one or more foraging events by the harbor porpoise. These foraging events were likely opportunistic because literature review does not support the notion that salmonids are regular prey in the diet of harbor porpoises along the west coast of North America (Scheffer and Slipp, 1948; Wilke and Kenyon, 1952; Scheffer, 1953; Jones, 1981; Treacy[5]; Gearin et al., 1994; Walker et al.[6]). However, Treacy[5] identified salmonid remains in 1 harbor porpoise recovered from the Columbia River area, and Gearin et al. (1994) identified remains of coho salmon (*O. kisutch*) in 1 harbor porpoise that was taken in a Chinook salmon set net in Washington.

Other than the PIT tags and CWTs in the harbor porpoise stranded in August 2012 and the PIT tags found in 2 other harbor porpoises, we have not found any salmonid CWTs or PIT tags in the more than 150 stomachs that we have examined since 2007 from dead harbor porpoises stranded within our area from northern Oregon to southern Washington. One PIT tag that had been inserted into a juvenile winter-run steelhead from a hatchery in the Columbia River Basin was recovered from the forestomach of an adult male harbor porpoise that was stranded on 8 June 2012 in Arch Cape, 30 miles south of the Columbia River plume. This steelhead came from the Oak Springs Hatchery in Maupin, Oregon, and was released in an acclimation pond of the sand trap in the East Fork Hood River in Oregon on 9 May 2012. This fish was not detected elsewhere downstream of its release site. The other PIT tag was recovered from the stomach of an adult male harbor porpoise that was stranded on 19 May 2014 on the Long Beach Peninsula, just north of the Columbia River plume. This PIT tag came from a wild summer-run steelhead that was tagged and released in Idaho on 7 September 2013. This wild steelhead was detected on 6 May 2014 at the juvenile bypass facility of the Lower Granite Dam in southeastern Washington and on 10 May 2014 near Wauna, Oregon.

Although Chinook salmon have been identified as prey for other marine mammals, such as the California sea lion (*Zalophus californianus*), Steller sea lion (*Eumetopias jubatus*), harbor seal (*Phoca vitulina*), and killer whale (*Orcinus orca*), in the Puget Sound region of Washington (see Chasco et al., 2017), this report is the first one of known predation of juvenile Chinook salmon by a harbor porpoise in the Pacific Northwest, adding to the knowledge of feeding habits of harbor porpoises.

[4] Kern, C. 2012. Personal commun. Fish Div., Oregon Dep. Fish Wildl., 4034 Fairview Ind. Dr. SE, Salem, OR 97302.

[5] Treacy, S. D. 1985. Feeding habits of marine mammals from Grays Harbor, Washington to Netarts Bay, Oregon. *In* Marine mammals and their interactions with fisheries of the Columbia River and adjacent waters, 1980–1982, p. 149–198. NOAA, Natl. Mar. Fish. Serv., Northwest Alaska Fish. Sci. Cent. NWAFC Processed Rep. 85-04. [Available from website.]

[6] Walker, W.A., M. B. Hanson, R. W. Baird, and T. J. Guenther. 1998. Food habits of the harbor porpoise, *Phocoena phocoena*, and Dall's porpoise, *Phocoenoides dalli*, in the inland waters of British Columbia and Washington. *In* Marine Mammal Protection Act and Endangered Species Act implementation program 1997 (P. S. Hill, B. Jones, and D. P. DeMaster, eds.), p. 63–75. NOAA, Natl. Mar. Fish. Serv., Alaska Fish. Sci. Cent. AFSC Processed Rep. 98-10. [Available from website.]

Acknowledgments

We would especially like to thank C. Kern of the ODFW for providing information regarding the PIT tags and CWTs, assisting us with interpretation of tag data, and addressing other general hatchery-related questions. We are also grateful for the tag coordinators who provided data related to PIT tags. Lastly, a huge thank you to M. Hughes from the Biology Department at Portland State University for her efforts in generating the map.

Literature cited

Chasco, B., I. C. Kaplan, A. Thomas, A. Acevedo-Gutiérrez, D. Noren, M. J. Ford, M. B. Hanson, J. Scordino, S. Jeffries, S. Pearson, et al.
2017. Estimates of Chinook salmon consumption in Washington State inland waters by four marine mammal predators from 1970 to 2015. Can. J. Fish. Aquat. Sci. 74:1173–1194.

Gearin, P. J., S. R. Melin, R. L. DeLong, H. Kajimura, and M. A. Johnson.
1994. Harbor porpoise interactions with a Chinook salmon set-net fishery in Washington State. *In* Gillnets and cetaceans: incorporating the proceedings of the symposium and workshop on the mortality of cetaceans in passive fishing nets and traps (W. F. Perrin, G. P. Donovon, and J. Barlow, eds.), p. 427–438. Rep. Int. Whaling Comm. Spec. Issue 15. [Available from website.]

Jones, R. E.
1981. Food habits of smaller marine mammals from Northern California. Proc. Calif. Acad. Sci. 42:409–433.

Scheffer, V. B.
1953. Measurements and stomach contents of eleven delphinids from the Northeast Pacific. Murrelet 34:27–30.

Scheffer, V. B., and J. W. Slipp.
1948. The whales and dolphins of Washington State with a key to the cetaceans of the west coast of North America. Am. Midl. Nat. 39(2):257–337.

Wilke, F., and K. W. Kenyon.
1952. Notes on the food of fur seal, sea-lion, and harbor porpoise. J. Wildl. Manage. 16:396–397.

National Marine
Fisheries Service
NOAA

Fishery Bulletin
established in 1881

Spencer F. Baird
First U.S. Commissioner
of Fisheries and founder
of *Fishery Bulletin*

Temporal changes in the life history of snowy grouper (*Hyporthodus niveatus*) off North and South Carolina, and factors that influence spawning dynamics

Kevin J. Kolmos (contact author)
David M. Wyanski
D. Byron White
Paulette P. Mikell

Email address for contact author: kolmosk@dnr.sc.gov

Marine Resources Research Institute
South Carolina Department of Natural Resources
P.O. Box 12559
Charleston, South Carolina 29422

Abstract—The snowy grouper (*Hyporthodus niveatus*) is a commercially valuable deepwater grouper that is managed by the South Atlantic Fisheries Management Council. This study updates life history parameters of snowy grouper caught off North and South Carolina from 1979 through 2012 by commercial and research vessels (number of fish sampled: 5314). On the basis of samples collected in 2008–2012, size at age has decreased since the 1990s, and size and age at maturity have increased in comparison with data pooled from the 1980s and 1990s. However, no significant changes in size and age at sex transition were noted between the 2000s and the 1980s–1990s. This study confirmed that snowy grouper are protogynous and that the spawning season in this region is broader than previously reported. In addition, we found that spawning frequency varied with size and age and was influenced by lunar phase, with most spawning occurring around the new moon. Results indicate that snowy grouper in the study area have started a slow recovery from overfishing.

Manuscript submitted 21 November 2018.
Manuscript accepted 30 September 2019.
Fish. Bull. 117:308–321 (2019).
Online publication date: 24 October 2019.
doi: 10.7755/FB.117.4.4

The views and opinions expressed or implied in this article are those of the author (or authors) and do not necessarily reflect the position of the National Marine Fisheries Service, NOAA.

The snowy grouper (*Hyporthodus niveatus*) is a commercially valuable deepwater species that occurs in the western Atlantic Ocean from Massachusetts to Brazil, including Bermuda, the Bahamas, Cuba, and the Gulf of Mexico (Heemstra et al., 2002), with occasional occurrence off the eastern coast of Canada (Scott and Scott, 1988). This species is thought to be a protogynous hermaphrodite (Moore and Labisky, 1984; Wyanski et al., 2000), but conclusive evidence has not been produced. Along the coast of the southeastern United States, adult snowy grouper are predominantly found on the upper continental slope at depths of 137–259 m, whereas juveniles are more common at shallower depths (Moore and Labisky, 1984). Wyanski et al. (2000) noted a positive correlation between total length (TL) and water depth off North and South Carolina. Most fishing for this species occurs in habitats characterized by rocky ledges, cliffs, and swift currents (Matheson and Huntsman, 1984). Off the southeastern United States, snowy grouper are captured primarily in commercial fisheries with bottom longlines and snapper reels (Parker and Mays, 1998; Wyanski et al., 2000).

Snowy grouper are prone to being overfished (Huntsman et al., 1999) because they are slow growing (Matheson and Huntsman, 1984; Moore and Labisky, 1984; Wyanski et al., 2000) and late maturing, between the ages of 3 and 8 years (Moore and Labisky, 1984; Wyanski et al., 2000). Estimates of their maximum age range from 27 to 29 years (Moore and Labisky, 1984; Wyanski et al., 2000). This range is reasonable, given the maximum age of 27 years reported in a project report for an age validation study (Harris[1]) that measured radiocarbon (^{14}C), from atmospheric testing of nuclear weapons during 1950–1970, in sagittal otolith cores of 21 snowy grouper examined by Wyanski et al. (2000). Results of the validation study were accepted as the best available evidence during the

[1] Harris, P. J. 2013. Validation of ages for species of the deepwater snapper/grouper complex off the southeastern coast of the United States. Southeast Data, Assessment, and Review SEDAR36-RD07, 12 p. [Available from website.]

most recent stock assessment (SEDAR, 2013), although the study had the limitations 1) of not having a reference chronology from the study area, the southeastern United States, and 2) of small sample sizes during the years that the rate of increase for ^{14}C in the surface waters of the oceans was at its maximum. Periodicity of increment formation was determined indirectly by Wyanski et al. (2000) by using marginal increment analysis.

Landings varied widely during 1981–2005, mostly because of the flexibility of commercial fishermen to shift between fisheries (e.g., from bottom longline for deepwater reef fish to pelagic longline for swordfish in 1984–1985) to optimize earnings (Low et al.[2]). This period was characterized by minimal fisheries regulation, given that there were no regulations affecting snowy grouper through 1988 and that the regulations implemented by the South Atlantic Fisheries Management Council after 1988 (e.g., trawling ban, depth restriction for bottom longlining, annual quota, and trip limit) had minimal impact on catches of this species (SEDAR, 2013; SAFMC[3]). In 2009, the South Atlantic Fisheries Management Council allocated 95% of the total allowable catch to the commercial sector through Amendment 15B to the fishery management plan for snapper and grouper off the coasts of North Carolina, South Carolina, Georgia, and Florida (Federal Register, 2009). Two assessments of the snowy grouper population have been conducted by using the Southeast Data, Assessment, and Review process: a benchmark assessment on snowy grouper in 2004 (SEDAR, 2004) and a standard assessment in 2013 (SEDAR, 2013). The results of the assessment completed in 2004 indicate that the population off the southeastern United States was overfished and was undergoing overfishing, a status that resulted in further reductions in commercial quotas and trip limits to reduce fishing mortality starting in 2006 (SEDAR, 2013). The latest assessment, conducted in 2013, determined that the population was not experiencing overfishing but remained overfished.

Nearly 2 decades have elapsed since the life history of the population of snowy grouper along the Atlantic coast of the southeastern United States was investigated by Wyanski et al. (2000) by using samples collected primarily from the commercial fishery during 1979–1995. By comparing characteristics of the population between the 1980s and 1990s, Wyanski et al. (2000) documented a few indicators of an overfished population, and those signals were confirmed by the benchmark stock assessment in 2004 (SEDAR, 2004). The leading indicators were 1) significant increases in size at age, 2) predominance (81%) of fish at ages 1–6 in bottom longline samples collected in the 1990s, the majority (56%) of which were immature females, and 3) a decrease in mean length of fish landed in the bottom longline fishery from 65–80 cm TL to 50–60 mm TL without any notable change in depth of capture.

Updates of life history parameters for snowy grouper are needed to fill existing information gaps and provide critical data for stock assessments in support of the sustainable management of this species. Reproductive parameters such as sex composition need further investigation because of a small sample size in previous studies; the analysis by Wyanski et al. (2000) included only 82 specimens collected during 1993–1994, none of which were >900 mm TL. The results of this study provide updated estimates of life history parameters, such as size at age, age at maturity, spawning seasonality, and age at sex transition. We discuss the potential effects of management measures implemented since 2006 on the life history parameters of the population of snowy grouper off the southeastern United States. Our histological samples were also examined for evidence to confirm that the snowy grouper is a protogynous hermaphrodite and to investigate the effect of age, size, and lunar phase on spawning.

Materials and methods

Sampling

During 1979–2012, snowy grouper were obtained from commercial boats, research vessels, and recreational charter boats, primarily off North and South Carolina. Fishery-independent samples of reef fish species were collected during cruises conducted as part of the Marine Resources Monitoring Assessment and Prediction (MARMAP) program, the Southeast Area Monitoring and Assessment Program—South Atlantic (SEAMAP-SA), and the Southeast Fishery-independent Survey (SEFIS) with bottom longlines, Kali poles (an off-bottom longline; Russell et al., 1988), snapper reels, rods and reels, and chevron traps (Collins, 1990; Smart et al.[4]). These 3 sampling efforts represent a collaborative survey known as the Southeast Reef Fish Survey, which samples fish on natural reefs from Cape Hatteras, North Carolina, to St. Lucie Inlet, Florida. Kali poles were used only during sampling in the 1980s, and sampling prior to 2010 was conducted solely by the MARMAP program. The SEAMAP-SA and SEFIS began sampling in 2008 and 2010, respectively, and use chevron traps and rods and reels to complement sampling done by the MARMAP program with the same gears.

In the years since the study by Wyanski et al. (2000), the MARMAP program acquired specimens of snowy grouper in 2008–2009 through a Cooperative Research Program grant it received from the National Marine Fisheries Service in partnership with a commercial bottom longline fisherman. From this fisherman's vessel, 1078 snowy grouper

[2] Low, R. A., D. Theiling, and E. B. Joseph. 1987. South Carolina marine fisheries, 1977–1986. South Carolina Wildl. Mar. Res. Dep., Tech. Rep. 67, 78 p. [Available from website.]

[3] SAFMC (South Atlantic Fishery Management Council). 2019. Snapper grouper—fishery management plan. [Available from website, accessed February 2019.]

[4] Smart, T. I., M. J. M. Reichert, J. C. Ballenger, W. J. Bubley, and D. M. Wyanski. 2016. Overview of sampling gears and standard protocols used by the Southeast Reef Fish Survey and its partners. Southeast Data, Assessment, and Review SEDAR50-RD20, 14 p. [Available from website.]

were captured at 32.5–33.0°N and depths of 172–251 m, an area similar (32.3–33.9°N and depths of 155–302 m) to that fished by 3 longline fishermen who captured specimens (number of fish sampled [n]=1361) for the earlier study (see figure 1 in Wyanski et al., 2000).

After collection, whole snowy grouper were weighed to the nearest gram and the maximum TL (from the anterior-most point on the head to the tip of the caudal fin with lobes compressed) and standard length were measured to the nearest millimeter. The left sagittal otolith was removed and stored dry prior to processing (the right sagitta also was removed when time permitted). Samples of gonad tissue were removed and fixed in 10–11% seawater–formalin for later histological processing.

Age and growth

Each otolith was embedded in paraffin (1979–1985) or an epoxy resin (1993–2012) and sectioned (thickness: 0.5–0.7 mm) along a dorsoventral plane through the focus with a single high-concentration diamond wheel on a Buehler[5] IsoMet Low Speed Saw (Buehler, Lake Bluff, IL). Otolith sections were mounted on glass slides with thermoplastic or a liquid mounting medium and examined under a Nikon dissecting microscope (Nikon Corp., Tokyo, Japan) (magnification: 7.5–63×) with reflected and transmitted light. Sample sections read before 1996 were covered with cedar wood oil prior to examination.

Otolith sections were examined by 2 readers independently and reexamined jointly when differences in age estimation occurred; aging was done without knowledge of specimen length and date or location of capture (Harris et al., 2002). If disagreement on age persisted, the specimen was eliminated from age and growth analyses. Age analyses were based on counts of annual increments (one opaque and one translucent zone). We examined 2364 specimens from 1996 through 2012 and used samples from Wyanski et al. (2000) as a historical data set (n=2263).

Reproduction

Histological processing of gonadal tissues followed standard hematoxylin and eosin techniques. The posterior portion of each gonad was fixed for 7–14 d in a 10–11% seawater–formalin solution buffered with marble chips then transferred to 50% isopropanol for 7–14 d. Reproductive tissue was processed in automated tissue processors and blocked in paraffin. Three transverse sections (thickness: 6–8 µm) were cut from each sample with a rotary microtome, mounted on glass slides, stained with double-strength Gill's hematoxylin, and counterstained with Eosin Y. Sections were viewed under a Nikon compound microscope (Nikon Corp.) (magnification: 20–400×) by 2 readers without knowledge of specimen length or age and date or location of capture. The readers independently determined sex and reproductive phase by using histological criteria described by Wyanski et al. (2000) and Harris et al. (2004); terminology follows a recent review by Brown-Peterson et al. (2011). If the assessments differed between readers for a section, it was viewed jointly by the readers. A specimen was eliminated from reproductive analyses when disagreement on its sex or reproductive phase persisted. To ensure that inactive females were assigned correctly to either the immature phase or the regenerating phase, the length–frequency histograms of suspected immature and early developing or regenerating females were compared with the histograms for females with evidence of definite maturity (i.e., those that were developing, spawning capable, or regressing). The criteria put forward by Sadovy and Shapiro (1987) and Sadovy de Mitcheson and Liu (2008) were used for the diagnosis of hermaphroditism.

Specimens with developing, spawning-capable, regressing, or regenerating gonads were considered sexually mature. Females of uncertain maturity were excluded from all reproductive analyses (Wyanski et al., 2000). Juvenile females were excluded from sex composition analyses to restrict data to the adult population (Coleman et al., 1996), and specimens undergoing sex transition (female to male) were considered males, unless noted, because these specimens would likely have spawned as males in the next spawning season (Sadovy and Shapiro, 1987). In addition, sex composition analyses were restricted to data from gear types that effectively sample the adult population (i.e., Kali poles and longlines). Females were considered spawners if they possessed maturing oocytes (i.e., fusing of yolk globules, germinal vesicle migration and breakdown, and hydration), ovulated eggs, or postovulatory follicle complexes. Spawning indicators were based on stages that are thought to last approximately 60 h—12 h for oocyte maturation and hydration and 48 h for postovulatory follicle complexes (Hunter and Goldberg, 1980; Fitzhugh et al., 1993). We use *spawning frequency* and *spawning interval* as defined in Lowerre-Barbieri et al. (2011). *Spawning proportion*, called *spawning fraction* by Lowerre-Barbieri et al. (2011), is the proportion of adult females that were spawning daily. Values of spawning proportion were proportionally reduced to a 24-h period. Batches were determined by multiplying the proportion of spawners by duration of the spawning season.

Lunar phase analyses were performed to determine if the lunar cycle influenced the periodicity of spawning in snowy grouper. We combined all samples from all gear types that were collected during 1982–2012 and had stamps with the exact date and time of their collection. The new moon day was defined as day 0, and the full moon was defined as day 15. Individual specimens (n=371) were given a lunar day based on the new moon date for that month and year, their time of capture, and their reproductive phase. For specimens undergoing oocyte maturation (excluding hydration), lunar day was calculated as capture date + 1 d because spawning would have most likely taken

[5] Mention of trade names or commercial companies is for identification purposes only and does not imply endorsement by the National Marine Fisheries Service, NOAA.

place in the 24 h after capture. For specimens with vitellogenic oocytes or with hydrated oocytes, lunar day was equal to their date of capture. For specimens with postovulatory complexes, lunar day was determined to be the capture date – 1 d because spawning would have occurred in the 24–48 h prior to capture. The effect of lunar day on spawning probability (no. of spawners to no. of active females, i.e., presence of vitellogenic oocytes) was analyzed by using a generalized additive model (GAM), with binomial error distribution and logit link function. No other covariates were included in the model.

Analyses

Analyses were completed with statistical software R, vers. 3.0.2 (R Core Team, 2013), Microsoft Excel 2013 (Microsoft Corp., Redmond, WA), and SAS (vers. 9.4; SAS Institute Inc., Cary, NC), and results were deemed significant if $P<0.05$. Mean values of length, age, and length at age were compared between periods by using analysis of variance. All lengths in the text refer to maximum TL. Gear selectivity was assessed with density analysis of TL to determine how data from various gear types could be pooled for temporal comparisons related to age and growth; comparisons focused on 2 or 3 of the following periods: 1982–1985, 1993–1994, and 2008–2012 (hereafter referred to as the *1980s*, *1990s*, and *2000s*). Density analyses and the Kolmogorov–Smirnov test were used to compare length and age distributions between periods. Nonlinear regression analysis was used to fit the von Bertalanffy growth function (von Bertalanffy, 1938) to length at age data by period. Following Wyanski et al. (2000), TLs were weighted by the inverse of the number of fish at each age, by period and overall, to moderate the effect of large and small sample sizes on the estimates of growth parameters from the von Bertalanffy growth function.

All available reproductive samples from all gears were pooled for reproductive analyses, primarily to increase sample size. Pooling data from the 1980s and 1990s was necessary to increase sample size for the temporal aspect of analyses of sexual maturity and sex transition. Additional samples (n=85) from the period 1979–1981 were used in maturity and spawning proportion analyses. For maturity analyses, pooling data over decades also ensured that more specimens, especially those within the range of size and age at which maturity was reached, were included in the temporal comparison (1980s and 1990s versus 2000s); these smaller specimens are caught more frequently with chevron traps, which were not used in the 1980s. To estimate length at 50% maturity ($L_{50,\,mat}$) and age at 50% maturity ($A_{50,\,mat}$), a generalized linear model with a logit, probit, c-log, or Cauchy link was fit to maturity data in RStudio, vers. 3.5.2 (RStudio, 2018); length and increment data were not binned. The same analyses were run to estimate the length ($L_{50,\,male}$) and age ($A_{50,\,male}$) at 50% sex transition to male. The selected model had the lowest Akaike information criterion (Akaike, 1973). Significance was evaluated at the 5% error level by using the likelihood ratio chi-square (χ^2) test. In spawning analyses, data for sizes of fish from the spawning season (April–September) were grouped into 100-mm-TL bins starting from 501–600 mm TL and ending with a terminal group of ≥901 mm TL; analyses were performed overall and within months. The same spawning analyses were performed on ages of fish from the spawning season and grouped into 2-year bins starting from ages 3–4 and ending with a terminal group of ages ≥11 years. Lunar effects on spawning were investigated with a GAM.

Results

Age and growth

All specimens (n=5314) were collected between 29.66°N and 34.73°N and at depths of 18–302 m, but only 7 specimens were collected south of 31°N. We aged 2192 specimens during 1996–2012, making our total number of aged specimens 4342 when adding historical data from Wyanski et al. (2000). Ages in the combined data set ranged from 1 to 35 years, and lengths ranged from 130 to 1137 mm TL. Males ranged in age from 6 to 32 years (mean: 13.0 years [standard error (SE) 0.5]; median: 12 years) and in size from 620 to 1090 mm TL (mean: 899 mm TL [SE 6.5]; median: 901 mm TL), whereas females ranged in age from 1 to 35 years (mean: 6.7 years [SE 0.1]; median: 6 years) and in size from 208 to 1113 mm TL (mean: 611 mm TL [SE 2.9]; median: 619 mm TL). Transitional specimens ranged in age from 5 to 12 years (mean: 8.4 years [SE 0.6]; median: 8 years) and in size from 627 to 895 mm TL (mean: 803 mm TL [SE 18.3]; median: 826 mm TL).

To determine whether to combine length and age data for the 4 prevalent hook-and-line gear types, a density analysis was performed on TL by gear type for all periods combined (Fig. 1). Results indicate that the overall size range of snowy grouper was similar among gear types, but snapper reels caught a higher proportion of individuals <450 mm TL than the other gear types because this gear is fished in shallower depths and catches smaller fish (Wyanski et al., 2000). Given the notable difference in the size selectivity of snapper reels, data from the remaining 3 gear types (long bottom longline, short bottom longline, and Kali pole) were combined, because of their relatively similar size selectivity, and used in further analyses of age and growth (Table 1). Another reason for combining the data is the similarity of the fishing hook sizes (#5–7) used in each longline gear and the Kali pole gear (Russell et al., 1988; Harris et al., 2004; Smart et al.[4]). The inclusion of data from only one period for short bottom longlines (2000s) and Kali poles (1980s) in the pooled data did not influence the temporal comparisons because a Kolmogorov–Smirnov test of data from long bottom longlines between each period was significant ($P<0.001$) for size and age, indicating that the differences between periods are explained by time, not gear type.

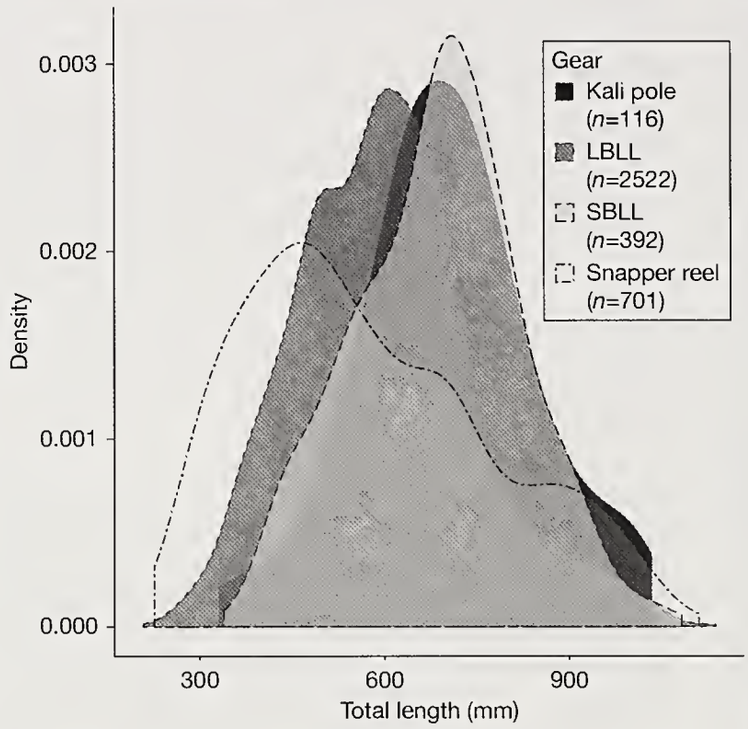

Figure 1

Density plots of total length for all snowy grouper (*Hyporthodus niveatus*) captured during 1979–2012, off North and South Carolina, with 4 gear types: Kali pole, long bottom longline (LBLL), short bottom longline (SBLL), and snapper reel. The unit for density is the relative proportion of fish that were caught with a particular gear type. n=number of fish sampled.

The results of analyses of size and age distributions, mean length, mean age, and size at age all indicate significant differences among periods. Density plots comparing TL by period show similarities in overall size range; however, a Kolmogorov–Smirnov test revealed that the size, as well as age, distributions were significantly different among periods (P<0.001; Fig. 2, A and B). In addition, both mean TL and mean age differed significantly among periods (Tukey's honestly significant difference: adjusted P<0.001). The mean size and age of fish increased from 584 mm TL and 5.5 years in the 1990s to 632 mm TL and 6.8 years in the 2000s (Table 2); however, these values are noticeably less than the means of 714 mm TL and 11.8 years for samples from the 1980s. Size at age of specimens caught only with bottom longline gear (long and short) was significantly different between the 2 recent periods, the 1990s versus the 2000s, for ages 3–12, except it remained the same for age 4 (minimum n>20, P<0.05). A significant decrease in size at age was detected for age 3 and ages 6–12, with size at age increasing only for age 5 (Table 3).

The analyses of von Bertalanffy growth parameters revealed some differences among periods (Fig. 3, Table 4). Growth curves for the 1990s and 2000s had the same growth coefficient (k=0.12), with a slight decrease of the asymptotic length (L_∞) in the 2000s. The 1980s had the lowest k value (0.085) and the lowest L_∞ (1004 mm TL) (Table 4).

Sexual pattern

Conclusive evidence for the diagnosis of sexual pattern has not been presented previously for snowy grouper. We confirmed that this species is a protogynous hermaphrodite by the capture of individuals having gonads with 1) α-stage atresia in vitellogenic oocytes within developing male tissue and 2) sperm sinuses in the gonadal wall (Fig. 4). The results of

Table 1

Number of snowy grouper (*Hyporthodus niveatus*) for which otoliths and gonads were examined per period by gear type. Specimens were caught off North and South Carolina as part of fishery-independent (FI) and fishery-dependent (FD) surveys during 3 periods: 1982–1985, 1993–1994, and 2008–2012. Values in the "Other" row represent the total numbers combined for the following gear types: hook and line, University of Rhode Island high-rise trawl, blackfish trap, experimental trap, Florida trap, and unknown.

		Number of fish					
		Otoliths examined			Gonads examined		
Gear type	Source	1980s	1990s	2000s	1980s	1990s	2000s
Long bottom longline	FI	53	0	5	70	0	5
	FD	22	1215	999	0	146	1074
Short bottom longline	FI	0	0	379	0	0	389
Kali pole	FI	94	0	0	82	0	0
Snapper reel	FI	115	1	0	204	1	0
	FD	57	308	10	1	22	0
Chevron trap	FI	0	78	83	0	77	82
Other	FI	10	2	15	11	2	16
Total		351	1604	1491	368	248	1566

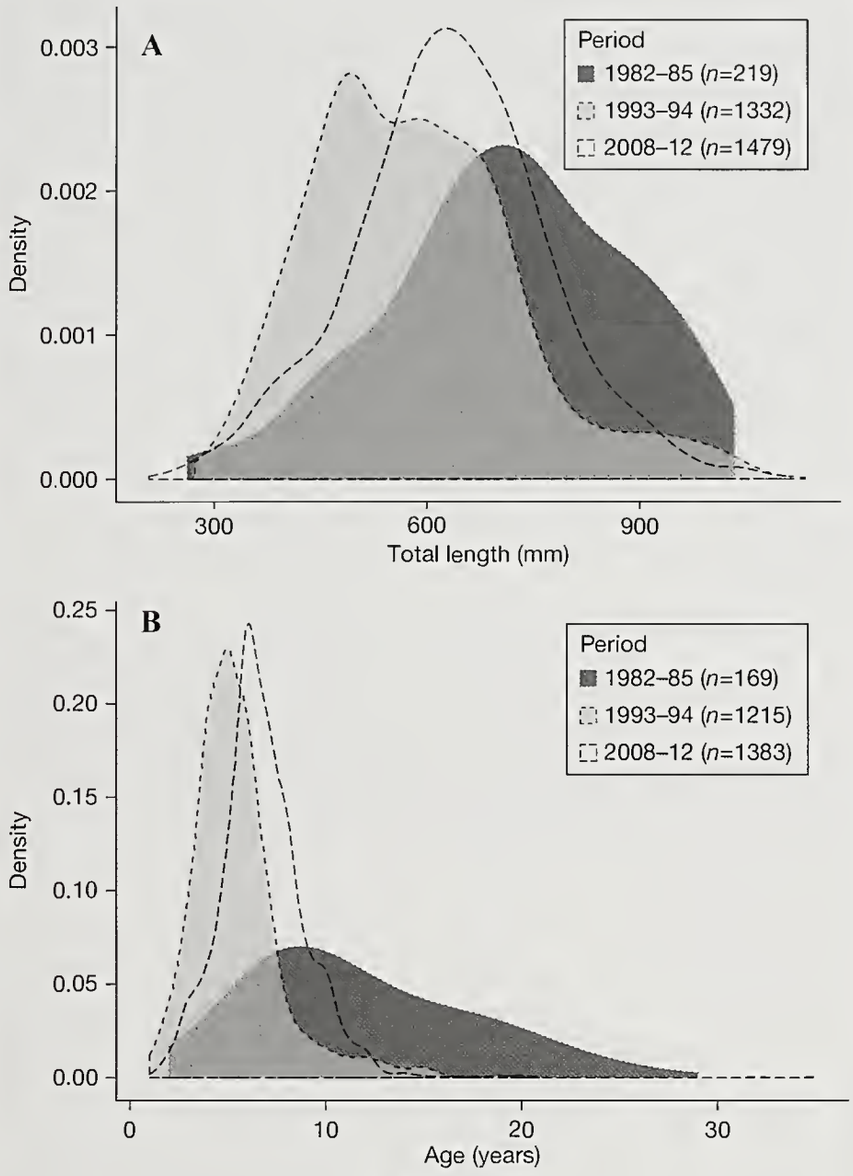

Figure 2

Density plots of (**A**) total length and (**B**) age by period for all snowy grouper (*Hyporthodus niveatus*) captured off North and South Carolina during 3 periods: 1982–1985, 1993–1994, and 2008–2012. Ages are counts of annual increments (one opaque and one translucent zone) from otolith readings. The unit for density is the relative proportion of fish that were caught during a particular period. *n*=number of fish sampled.

comparisons of the age distribution and the median age of females and males (transitional specimens excluded) from all years also indicate protogyny (Fig. 5). Of the 16 fish that were older than age 20, 31% were female and 69% were male. The median age of females was 6 years, half the median age of 12 years for males.

Maturity and sex composition

We examined histological sections of gonad tissue from 1566 snowy grouper collected during 2008–2012, making our total number of histological samples 2324 when adding historical data from Wyanski et al. (2000). Correct assignment of females from the period 2008–2012 to the immature and regenerating reproductive phases was indicated by the presence of only 5 specimens in the regenerating phase (457–517 mm TL) that were smaller than the total length (525 mm TL) of the smallest definitely mature specimen (i.e., specimen in the developing, spawning-capable, or regressing phases). There were 19 specimens <525 mm TL (1.3% of 1467 females examined) that could not be definitively categorized as immature or regenerating.

Female size and age at maturity were assessed for the overall data set (i.e., all gears and all years) and by period. The smallest mature female was 457 mm TL, whereas the largest immature female was 787 mm TL. In the observed data, gonads in a reproductive phase indicative of sexual maturity were present in 4% of females at age 3, in 44% at age 5, in 75% at age 7, and in 100% at ages >13 years. The $L_{50,\ mat}$ was 578 mm TL (logit link: n=1853, 95% confidence interval [CI] 475–702 mm TL). Because of low sample sizes, data from the 1980s and 1990s were combined to conduct a temporal analysis of $L_{50,\ mat}$. There was a significant increase in $L_{50,\ mat}$ from 529 mm TL (logit link: n=564, 95% CI 314–893 mm TL) in the 1980s and 1990s to 596 mm TL (logit link: n=1289, 95% CI 474–747 mm TL) in the 2000s (χ^2 test: P<0.001; Fig. 6A). The overall youngest mature female was age 3, whereas the oldest immature female was age 13. The $A_{50,\ mat}$ was 5.5 years (Cauchy link: n=1637, 95% CI 4.0–7.6 years). To conduct a temporal analysis of $A_{50,\ mat}$, data from the 1980s and 1990s were again combined because of low sample sizes. There was a significant increase in $A_{50,\ mat}$ from 5.0 years (logit link: n=425, 95% CI 3.2–7.6 years) in the 1980s and 1990s to 5.8 years (logit link: n=1212, 95% CI 3.2–7.6 years) in the 2000s (χ^2 test: P<0.001) (Fig. 6B).

Trends in length and age at sex transition to male were examined for the overall data set and by period. The overall estimates of $L_{50,\ male}$ and $A_{50,\ male}$ for all gear types were 886 mm TL (logit link: n=2038, 95% CI 688–1143 mm TL) and 17.0 years (probit link: n=1755, 95% CI 14.0–21.9 years), respectively. Estimates of $L_{50,\ male}$ were similar between periods, 880 mm TL in the 1980s and 1990s combined (logit link: n=657, 95% CI 593–1309mm) and 894 mm TL in the 2000s (logit link: n=1360, 95% CI 633–1269mm TL; χ^2 test: P=0.52). There was a decrease in $A_{50,\ male}$ from 18.0 years (logit link: n=473, 95% CI 11.8–27.8 years) in

Table 2

Summary statistics for the total lengths and ages of snowy grouper (*Hyporthodus niveatus*) collected off North and South Carolina during 3 periods: 1982–1985, 1993–1994, and 2008–2012. Ages are counts of annual increments (one opaque and one translucent zone) from otolith readings. Data were combined for 3 gear types: Kali pole, long bottom longline, and short bottom longline. *n*=number of fish examined; SE=standard error of the mean.

	Total length (mm)				Age			
Period	*n*	Median	Mean	SE	*n*	Median	Mean	SE
1980s	219	720	714	11	169	10	11.8	0.4
1990s	1332	572	584	4	1215	5	5.5	0.1
2000s	1479	634	632	4	1383	7	6.8	0.1
All periods	3030	614	617	3	2767	6	6.6	0.1

Table 3

Mean sizes at age of snowy grouper (*Hyporthodus niveatus*) collected off North and South Carolina during 3 periods: 1982–1985, 1993–1994, and 2008–2012, by age and period. Data were combined for 3 gear types: Kali pole, long bottom longline (LBLL), and short bottom longline (SBLL). Also included are results of analysis of variance conducted for mean total length at age between the 1990s and 2000s by using data for LBLL and SBLL gear. Ages are counts of annual increments from otolith readings. SE=standard error of the mean; *n*=number of fish examined.

	LBLL, SBLL and Kali pole									LBLL and SBLL	
	1982–1985			1993–1994			2008–2012			1990s vs. 2000s	
Age	Mean	SE	*n*	Mean	SE	*n*	Mean	SE	*n*	*P*-value	*n*
2	418	–	1	381	8.9	46	361	19.9	16	0.296	62
3	423	96.0	2	427	6.2	111	396	9.7	61	0.004	172
4	393	127.5	2	492	4.5	250	500	13.7	78	0.520	328
5	515	36.5	8	564	4.5	286	582	7.5	163	0.025	449
6	523	39.4	11	627	5.0	241	612	4.4	364	0.029	605
7	604	23.4	19	673	6.6	126	648	5.6	262	0.006	388
8	640	26.7	19	739	12.2	42	689	6.9	201	0.002	243
9	644	28.2	7	818	19.2	27	725	11.5	87	<0.001	114
10	729	17.1	18	909	14.5	19	770	10.1	85	<0.001	104
11	678	27.3	9	905	30.3	13	821	20.1	27	0.024	40
12	760	31.3	11	932	23.5	14	823	23.8	23	0.004	37

the 1980s and 1990s to 13.9 years (logit link: n=1282, 95% CI 9.6–20.8 years) in the 2000s, but differences were not significant (χ^2 test: P=0.92). The proportion of males (including transitional specimens) in all samples was 0.12. A temporal analysis, restricted to 3 gear types (long bottom longline, short bottom longline, and Kali pole), of sex composition revealed that few males were present at lengths ≤800 mm TL in samples across 3 decades, with the proportions of males at that size ranging from 0.00 to 0.06 (Table 5). In samples from the 2000s, an increasing trend in the proportions of males at larger sizes was observed, with values ranging from 0.32 at lengths of 801–900 mm TL to 0.86 at lengths of 1001–1100 mm TL. These values were similar to, although slightly lower than, those for samples from the 1980s.

Spawning

Spawning season was determined by comparing dates of capture to the presence of spawning indicators. Samples collected during 2008–2012 revealed a similar spawning season (April through September) to that reported by Wyanski et al. (2000). Five specimens with evidence of imminent (oocyte maturation) or recent spawning (post-tovulatory complexes) were collected in October 2008 and in January and March 2009, indicating that the

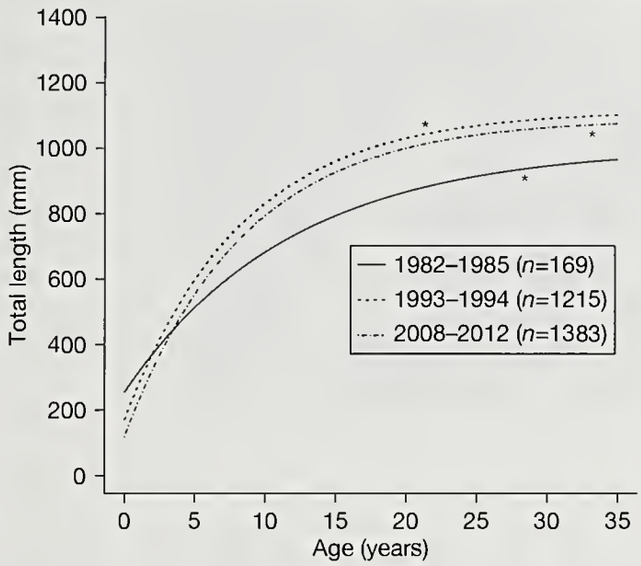

Figure 3

The von Bertalanffy growth curves for snowy grouper (*Hyporthodus niveatus*) captured off North and South Carolina during 3 periods: 1982–1985, 1993–1994, and 2008–2012. Ages are counts of annual increments from otolith readings. The asterisk (*) above each line denotes the oldest fish aged for that period. *n*=number of fish examined.

Table 4

Mean estimates of parameters of the von Bertalanffy growth function, the theoretical maximum length (L_∞), growth coefficient (k), and initial condition parameter (t_0), for snowy grouper (*Hyporthodus niveatus*) collected off North and South Carolina during 3 periods: 1982–1985, 1993–1994, and 2008–2012. Data were combined for 3 gear types: Kali pole, long bottom longline, and short bottom longline. *n*=number of fish examined; SE=standard error of the mean.

Period	*n*	L_∞	SE	k	SE	t_0	SE
1980s	169	1004	47	0.085	0.015	−3.44	1.03
1990s	1215	1115	12	0.120	0.004	−1.37	0.12
2000s	1383	1090	10	0.119	0.004	−0.95	0.12
All periods	2767	980	5	0.126	0.003	−1.85	0.13

potential spawning season is from late January through early October.

Spawning activity varied by size and age. An analysis of spawning proportion in relation to TL revealed that there was less spawning in the smallest fish (501–600 mm TL), with this length bin having the lowest proportion of spawners (0.06), a generally shorter spawning season (2–5 weeks), and the smallest number of batches (8) compared with those of larger fish (Table 6). Spawning proportion and number of batches increased with fish length, reaching the maximum values of 0.18 in the bin for fish ≥901 mm TL and 27 batches in the bin for fish 801–900 mm TL. There was a slight decrease to 24 batches at lengths ≥901 mm TL, possibly because of the shorter spawning season in this size class. For all length bins, the lowest spawning proportions occurred at the beginning (April) and end (September) of the spawning season (Fig. 7A). In addition, the positive relationship between spawning proportion and fish length was evident throughout the spawning season.

Analyses also were completed on effects of age on spawning proportion (Table 7). The youngest snowy grouper (ages 3–4) had the lowest proportion of spawners (0.03), with the proportion increasing to 0.11 at ages 5–6 and leveling out to 0.14–0.15 at ages >6 years. Because the spawning season also is shorter at younger ages, spawning frequency similarly increased, from 15 batches at ages 5–6 to 22–24 batches at older ages; the number of batches for ages 3–4 could not be calculated as a result of the small sample size. Spawning interval decreased slightly with age, from 9 d at ages 5–6 to 7 d at older ages. Similar to results from analyses of the length data, a general pattern of the lowest values of spawning proportion occurring at the beginning (April) and end (September) of the spawning season was observed for snowy grouper at ages >5 years (Fig. 7B). In the youngest age bin (3–4 years), spawners were captured only in July.

Spawning patterns indicate a lunar periodicity (GAM: n=371; χ^2 test: 91.3, $P \leq 0.001$). Overall, the GAM explained 26.7% of the deviance in spawning probability (coefficient of multiple determination [R^2]=0.312). On the basis of occurrence of spawners, spawning was least likely to occur around the full moon period (lunar days 15–18), whereas most spawning occurred between the waning crescent and waxing crescent phases, with a peak during the period of the new moon (lunar days 0–3 and 22–28) (Fig. 8). No adult female fish were collected on lunar days 6–8.

Discussion

The results of analyses of life history parameters support the conclusion of the most recent stock assessment that the population of snowy grouper off North and South Carolina has started a slow recovery from an overfished status: spawning stock biomass (SSB) is less than SSB at maximum sustainable yield (MSY). Results from analyses of age and growth, sex composition, and maturity all indicate a positive response to regulations to reduce fishing effort (i.e., further reductions in trip limit and annual quota for commercial sector) that were implemented after the previous assessment (SEDAR, 2013). Wyanski et al. (2000) proposed that the plasticity observed in growth between the early 1980s and the period 1993–1994 represented a density-dependent response to an increase in fishing mortality. Given that regulations implemented since 1994, and especially since 2006, have reduced fishing mortality, examination of life history samples collected

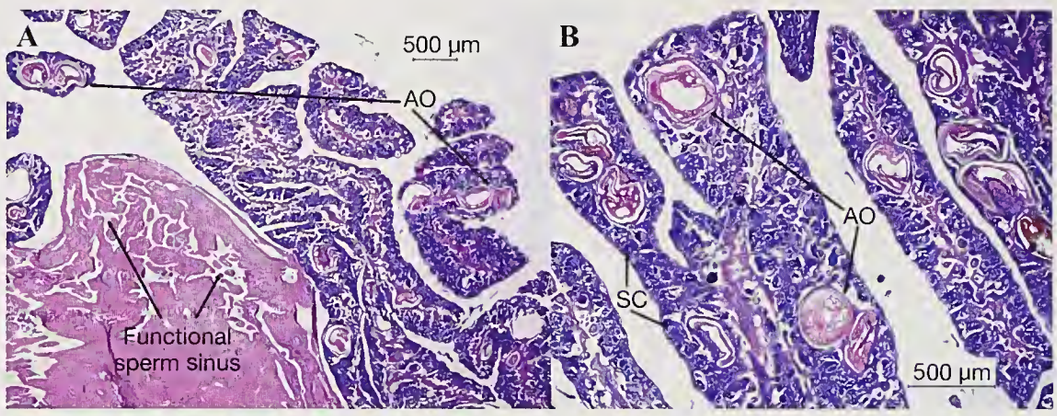

Figure 4

Images of gonadal tissue from a specimen of snowy grouper (*Hyporthodus niveatus*) that was transitioning from female to male, showing (**A**) functional sperm sinuses and atretic oocytes (microscope magnification: 20×) and (**B**) atretic oocytes within spermatogenic tissue (microscope magnification: 40×). This specimen was captured on 27 August 2008 off South Carolina at a total length of 834 mm and age of 7 years. AO=α-stage atretic oocyte; SC=spermatocytes.

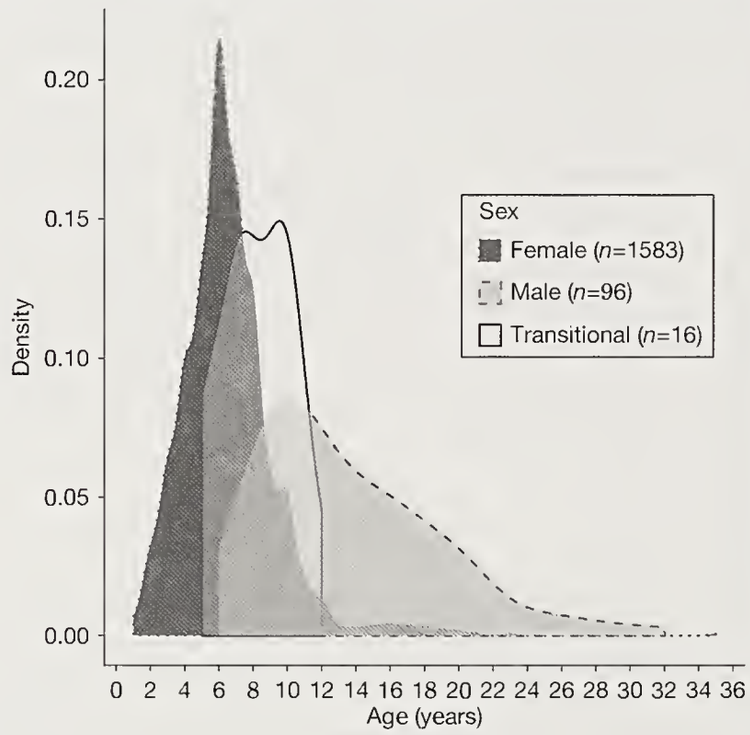

Figure 5

Density plots of age by sex for snowy grouper (*Hyporthodus niveatus*) captured off North and South Carolina during 1982–1985, 1993–1994, and 2008–2012. Ages are counts of annual increments from otolith readings. The unit for density is the relative proportion of fish in each sex category. *n*=number of fish examined.

from snowy grouper captured during 2008–2012 revealed evidence of population recovery. Since the mid-1990s, SSB has increased gradually, but the biomass target has not been reached as of the terminal year of 2012 (SEDAR, 2013). However, overfishing, when the fishing mortality rate is greater than the fishing morality rate at MSY, occurred only once in the last 6 years (2007–2012) of the assessment period, after sustained overfishing that had been happening since the mid-1970s. In the previous assessment conducted in 2004, the population was found to be both overfished and undergoing overfishing (SEDAR, 2004).

Age and growth

The results of this study indicate that there were noticeable differences in both size and age distributions over time. Results of our analyses indicate that the population has responded more quickly size-wise than age-wise. Density plots of size during each period show a substantial shift to smaller individuals (<500 mm TL) from the 1980s to the 1990s, with a lower number of larger individuals (>800 mm TL) during the 1990s (Fig. 2A). However, data from the 2000s reveal a symmetrical bell-shaped curve that encompasses both smaller and larger individuals. A population in which all size classes are represented would be better able to respond to factors that influence survivorship and recruitment, and the snowy grouper population is trending in that direction. The age distributions are not as encouraging. The number of older individuals (>10 years) decreased dramatically in the population from the 1980s to the 1990s. In addition, although there was a slight increase in the proportion of older individuals from the 1990s to the 2000s, the low number of older individuals is of concern (Fig. 2B). A higher proportion of older

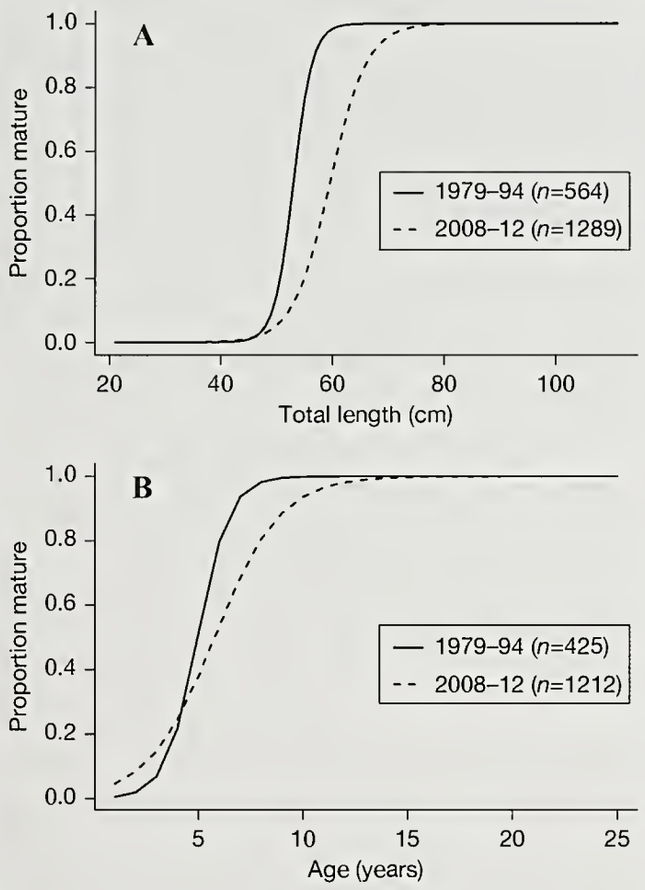

Figure 6

Proportion of female snowy grouper (*Hyporthodus niveatus*) that were mature, by (**A**) total length and (**B**) age. Ages are counts of annual increments from otolith readings. Specimens were collected off North and South Carolina during 1979–1994 and 2008–2012. For size at maturity from the generalized linear model (GLM), the predicted intercept and slope are −35.51 (standard error [SE] 7.45) and 0.066 (SE 0.014), respectively, for 1979–1994 and −17.36 (SE 1.06) and 0.029 (SE 0.002), respectively, for 2008–2012. For age at maturity from the GLM, the predicted intercept and slope are −5.52 (SE1.07) and 1.130 (SE 0.195), respectively, for 1979–1994 and −3.15 (SE 0.28) and 0.566 (SE 0.044), respectively, for 2008–2012. *n*=number of fish examined.

individuals may be detected if the population is given more time to recover.

The size at age of snowy grouper rose sharply from the 1980s to the 1990s during a time of heavy fishing pressure, but size at age declined in the 2000s once regulations were implemented (Fig. 3). Wyanski et al. (2000) speculated that the increase in the size at age of snowy grouper in the 1990s was the result of moderate to high fishing pressure. Increases in size at age have also been observed for other species, including the gag (*Mycteroperca microlepis*), the red grouper (*Epinephelus morio*), and the red porgy (*Pagrus pagrus*), that were experiencing moderate to high levels of exploitation off the coasts of the southeastern United States in the Atlantic Ocean and Gulf of Mexico (Johnson et al., 1993; Johnson and Collins, 1994; Harris and McGovern, 1997). The significant reversal of this trend from the 1990s to the 2000s is a positive sign for the population of snowy grouper off North and South Carolina. We detected only slight differences in the von Bertalanffy growth parameters between periods, because of the low number of specimens at ages >15 years (21 specimens in the 1990s, 9 specimens in the 2000s; Fig. 3).

Reproduction

Although Moore and Labisky (1984) and Wyanski et al. (2000) presented evidence of protogynous hermaphroditism in snowy grouper, that evidence was not conclusive. In both studies, males were reported to have represented older fish, with ages of 6–27 years (Moore and Labisky, 1984) and ages of 8–29 years (Wyanski et al., 2000). Aspects of population structure (e.g., size distributions and sex composition) generally are not reliable indicators of sexual pattern (Sadovy and Shapiro, 1987); however, a bimodal age–frequency distribution (i.e., males are older than females) is less problematic. The following features of gonad morphology strongly indicate protogyny, as described by Sadovy and Shapiro (1987): 1) membrane-lined central cavities in testes; 2), in transitional individuals, gonads that contain degenerating tissue of one sex and proliferating tissue of the other sex; and 3) atretic bodies within testes that are clearly derived from atretic vitellogenic oocytes, and sperm sinuses in the gonadal wall.

Wyanski et al. (2000) concluded that the presence of primary growth oocytes in 2 gonads with predominantly male tissue and membrane-lined central cavities was indicative of a nearly completed sex transition, but evidence of atretic (α-stage) vitellogenic oocytes and sperm sinuses was not present in the samples they analyzed. We met the criteria set by Sadovy and Shapiro (1987) in 2 specimens caught in August 2008 (Fig. 4). An additional criterion, laboratory observations of functional sex change in identified individuals, put forward by Sadovy de Mitcheson and Liu (2008) has yet to be observed in snowy grouper. We noted that 18 specimens were undergoing sex transition, and most (16) of those fish were collected during the spawning season. In contrast, low numbers of transitional specimens in samples collected during the spawning season led Moore and Labisky (1984) and Wyanski et al. (2000) to speculate that transition likely occurs during the non-spawning period. More samples need to be collected outside the spawning season (April–September) to clearly determine the timing of sex transition.

There was also a significant increase in $L_{50,\,mat}$ from the combined value for the 1980s and 1990s (529 mm TL) to the value for the 2000s (596 mm TL), a potentially density-dependent reaction (Rothschild, 1986) that is an indication of some recovery (Fig. 6A). Changes between periods in $A_{50,\,mat}$ were similar to results for $L_{50,\,mat}$. Values increased by almost a year from the combined $A_{50,\,mat}$ for the 1980s and 1990s (5.0 years) to that for the 2000s (5.8 years), a significant difference (Fig. 6B).

Table 5

Proportion of snowy grouper (*Hyporthodus niveatus*) caught off North and South Carolina that were male, by total length and period. Specimens were collected during the spawning season (April–September) in 3 periods: 1982–1985, 1993–1994, and 2008–2012. Data were combined for 3 gear types: Kali pole, long bottom longline, and short bottom longline. Transitional specimens were considered males because they likely would have spawned as males in their next spawning season. *n*=number of fish examined.

	1980s		1990s		2000s	
Total length (mm)	*n*	Proportion male	*n*	Proportion male	*n*	Proportion male
401–500					1	0.00
501–600	6	0.00	23	0.00	85	0.00
601–700	32	0.00	33	0.00	302	0.01
701–800	40	0.00	16	0.06	267	0.03
801–900	29	0.38	3	0.00	97	0.32
901–1000	26	0.73	0	0.00	34	0.62
1001–1100	6	0.83	0	0.00	7	0.86

Table 6

Proportion of adult female (active and inactive) snowy grouper (*Hyporthodus niveatus*) that were spawning daily, by 100-mm bin for total length. Specimens were collected during spawning season (April–September) off North and South Carolina in 1979–2012. Spawners had at least one indicator of imminent or recent spawning (i.e., oocyte maturation, ovulated eggs, or postovulatory complexes). Sampling period is the time (in days) from which representative samples of data were taken. Values of spawning proportion have been proportionally reduced to a 24-h period.

Total length bin (mm)	Adult females (*n*)	Spawning proportion (24 h)	Sampling period (d)	Spawning season duration (d)	Spawning interval (d)	No. of batches
501–600	130	0.06	178	139	17.1	8
601–700	326	0.13	178	153	8.0	19
701–800	325	0.14	178	177	7.0	25
801–900	94	0.17	175	163	6.0	27
≥901	26	0.18	171	129	5.4	24
Total	901	0.13		152	7.8	19

The spawning seasonality observed in our study is broader than that previously reported for the study area and varies with size and age. That 5 specimens with spawning indicators were collected from October 2008 through March 2009 reveals that at least some snowy grouper can have a longer spawning season than the season of April–September reported by Wyanski et al. (2000). Spawning in October also was reported by Kowal (2010), on the basis of capture of snowy grouper with mature oocytes (i.e., undergoing oocyte maturation) in south Florida and the Florida Keys. It remains unknown if spawning in the fall and winter occurs regularly. Spawning by smaller and younger fish (<600 mm TL and <5 years) tended to occur later in the season and for a shorter period than spawning by larger and older fish (Fig. 7). Larger and older (701–900 mm TL and ≥5 years) individuals had a longer spawning season, and a high proportion of them were spawning throughout the season; therefore, they can produce more batches within the spawning season.

This information is essential for accurate estimates of reproductive potential in the population of snowy grouper off North and South Carolina and indicates that the larger, older females are of greatest importance in reproductive output of this population. Although the spawning proportion increased as individuals grew larger, the duration of the spawning season decreased at sizes >801 mm TL, a possible indication of female preparation for sex transition.

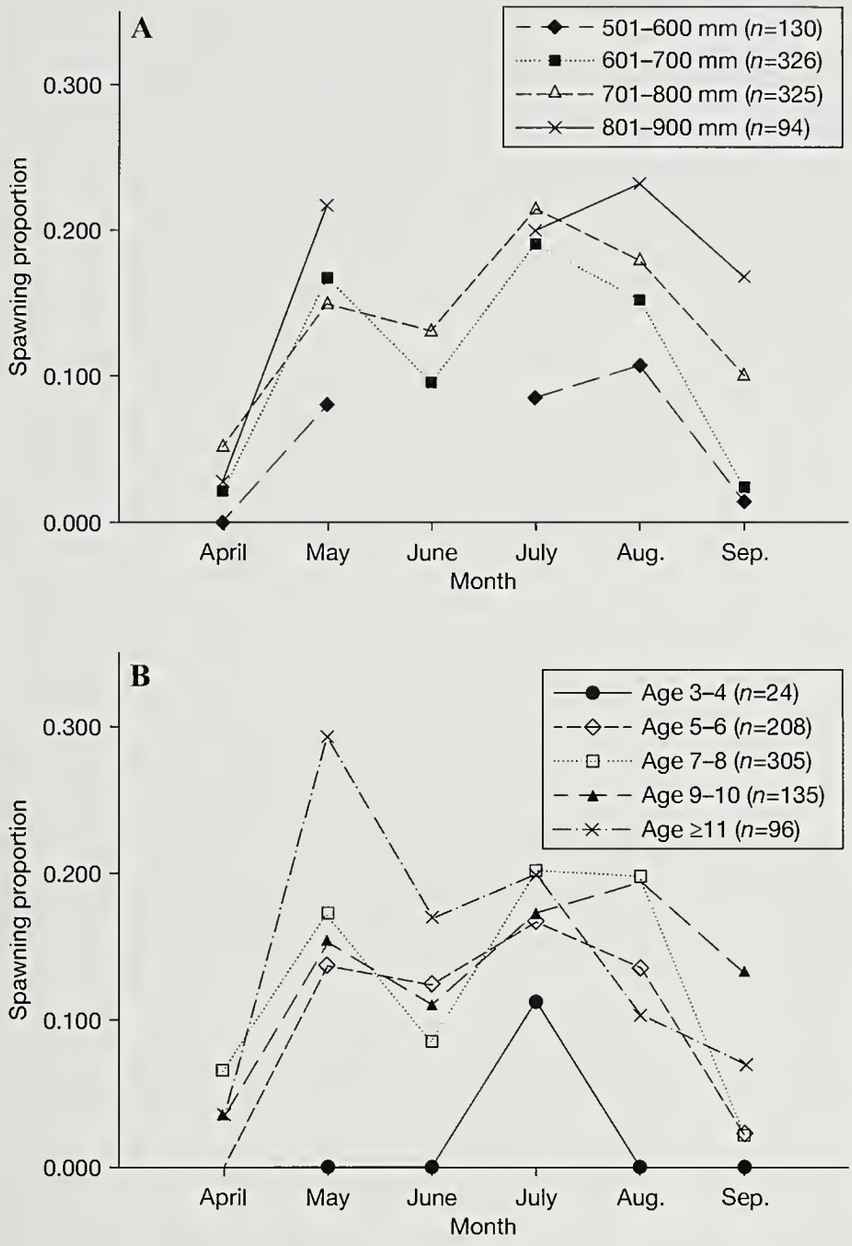

Figure 7

Proportion of adult female (active and inactive) snowy grouper (*Hyporthodus niveatus*) that were spawning daily, (**A**) by 100-mm bin for total lengths and (**B**) by age group (2-year groups for fish 3–10 years old and a terminal group for fish with ages ≥11 years). Note that 2 data points for the month of June in panel A were omitted because of low sample sizes (number of adult females in each group [*n*]<10). Specimens were collected off North and South Carolina during spawning season (April–September) in 1979–2012.

These larger, older females may have been saving energetic resources for sex transition and forgone some spawning events. Recent studies of a closely related serranid and 2 grouper species revealed a similar pattern of reduced spawning frequency in larger, older females. Klibansky and Scharf (2018) proposed that decreased egg production prior to sex transition in black sea bass (*Centropristis striata*) allows females to allocate energy to somatic growth, a switch that would be beneficial during the subsequent male phase. Gamboa-Salazar et al. (2019) observed moderate to strong declines in female spawning frequency relative to age and size in gag and scamp (*M. phenax*), declines that they also have proposed are linked to increasing future reproductive success as males.

In addition to the effects of size and age, spawning in snowy grouper is influenced by lunar phase. This finding is noteworthy for this grouper species because it inhabits deep waters, where less light reaches during spawning. Spawning of snowy grouper occurs more frequently around the new moon (waning crescent to waxing crescent), when there is less moonlight and possibly less predation on eggs (Fig. 8). It makes intuitive sense that this timing would increase survivorship possibly by affecting larval transport and predation. Farmer et al. (2017) conducted an analysis of monthly relationships between lunar phase and spawning and concluded that spawning in snowy grouper most commonly occurred from June through August during waning crescent to full moon periods by using a data set limited to fishery-independent sources for the period 1990–2013. Results of our study based on aggregated data from a longer period, 1982–2012, and on both fishery-independent and fishery-dependent sources indicate a different relationship between spawning and lunar phase. We found that the major peak of spawning in snowy grouper occurs within 5 d, before and after, of a new moon. Farmer et al. (2017) also found that snowy grouper exhibit multiyear use of spawning areas, but the resolution of their data was insufficient to confirm the presence of spawning aggregations. This life history characteristic is important and should be investigated further because the presence of spawning aggregations would increase the vulnerability of snowy grouper to fishing and, therefore, would have implications for the management of this species.

The updated information we provide here on life history parameters of snowy grouper supports the notion that the stock off North and South Carolina is in a slow recovery from overfishing. Given that significant plasticity in life history parameters has been observed over time in this population of snowy grouper, continued monitoring of this stock is necessary to assess its status and to allow managers to accurately adjust future regulations, including commercial quotas and trip limits, with the ultimate goal of maintaining the recovery of this stock.

Table 7

Proportion of adult female (active and inactive) snowy grouper (*Hyporthodus niveatus*) that were spawning daily, by age group. Specimens were collected during spawning season (April–September) off North and South Carolina in 1979–2012. Age groups are based on counts of annual increments from otolith readings. Spawners had at least one indicator of imminent or recent spawning (i.e., oocyte maturation, ovulated eggs, or postovulatory complexes). Sampling period was the time (in days) from which representative samples of data were taken. Values of spawning proportion have been proportionally reduced to a 24-h period. n/a=not applicable.

Age group	Adult females (*n*)	Spawning proportion (24 h)	Sampling period (d)	Spawning season duration (d)	Spawning interval (d)	No. of batches
3–4	24	0.03	160	1	n/a	n/a
5–6	208	0.11	178	130	8.8	15
7–8	305	0.14	178	165	7.1	23
9–10	135	0.15	175	159	6.6	24
11–35	96	0.14	175	157	7.3	22
Total	768	0.13		153	7.6	20

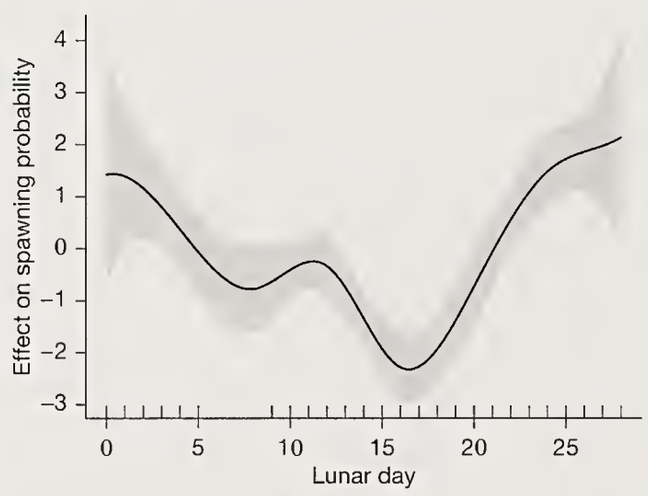

Figure 8

Effect on spawning probability in female snowy grouper (*Hyporthodus niveatus*) by lunar day from the use of the generalized additive model with a binomial error distribution. The gray area represents 95% confidence intervals. Tick marks above the x-axis line represent days for which data were available. The new moon day was defined as day 0, and the full moon was defined as day 15. Data used in the model came from specimens (n=371) captured during the spawning seasons (April–September) in 1981–2012 off North and South Carolina.

Acknowledgments

We sincerely appreciate the efforts of all personnel with the partners (MARMAP, SEAMAP-SA, and SEFIS) of the Southeast Reef Fish Survey, research vessels, Little River Fish House, and Carolina Seafood to collect and process samples. Special thanks go to Captain S. Shelley, F/V *Mollie D*, for collaborating with us. Funding was provided by the NOAA Cooperative Research Program, MARMAP Program (NA11NMF4540174), and SEAMAP-SA Reef Fish Complement (NA11NMF4350043). This is contribution no. 805 of the South Carolina Marine Resources Center.

Literature cited

Akaike, H.
1973. Information theory as an extension of the maximum likelihood principle. *In* Second international symposium on information theory (B. N. Petrov and F. Csaki, eds.), p. 267–281. Akademiai Kiado, Budapest.

Brown-Peterson, N. J., D. M. Wyanski, F. Saborido-Rey, B. J. Macewicz, and S. K. Lowerre-Barbieri.
2011. A standardized terminology for describing reproductive development in fishes. Mar. Coast. Fish. 3:52–70.

Coleman, F. C., C. C. Koenig, and L. A. Collins.
1996. Reproductive styles of shallow-water groupers (Pisces: Serranidae) in the eastern Gulf of Mexico and the consequences of fishing spawning aggregations. Environ. Biol. Fish. 47:129–141.

Collins, M. R.
1990. A comparison of three fish trap designs. Fish. Res. 9:325–332.

Farmer, N. A., W. D. Heyman, M. Karnauskas, S. Kobara, T. I. Smart, J. C. Ballenger, M. J. M. Reichert, D. M. Wyanski, M. S. Tishler, K. C. Lindeman, et al.
2017. Timing and locations of reef fish spawning of the southeastern United States. PLoS ONE 12(3):e0172968.

Federal Register.
2009. Fisheries of the Caribbean, Gulf of Mexico, and South Atlantic; snapper-grouper fishery off the southern Atlantic states; Amendment 15B; reef fish fishery of the Gulf of Mexico. Fed. Regist. 74:58902–58914.

Fitzhugh, G. R., B. A. Thompson, and T. G. Snider III.
1993. Ovarian development, fecundity, and spawning frequency of black drum *Pogonias cromis* in Louisiana. Fish. Bull. 91:244–253.

Gamboa-Salazar, K. R., D. M. Wyanski, W. J. Bubley, and N. Klibansky.
2019. Effects of age and size on spawning and egg production in gag and scamp grouper off the southeastern United States. ICES J. Mar. Sci. fsz174.

Harris, P. J., and J. C. McGovern.
1997. Changes in the life history of the red porgy, *Pagrus pagrus*, from the southeastern United States, 1972–1994. Fish. Bull. 95:732–747.

Harris, P. J., D. M. Wyanski, D. B. White, and J. L. Moore.
2002. Age, growth, and reproduction of scamp, *Mycteroperca phenax*, in the southwestern North Atlantic, 1979–1997. Bull. Mar. Sci. 70:113–132.

Harris, P. J., D. M. Wyanski, and P. T. Powers Mikell.
2004. Age, growth, and reproductive biology of blueline tilefish along the southeastern coast of the United States, 1982–1999. Trans. Am. Fish. Soc. 133:1190–1204.

Heemstra, P. C., W. D. Anderson Jr., and P. S. Lobel.
2002. Serranidae. *In* The living marine resources of the Western Central Atlantic. Vol. 3: bony fishes part 2 (Opistognathidae to Molidae), sea turtles and marine mammals (K. E. Carpenter, ed.), p. 1308–1369. FAO species identification guide for fishery purposes and American Society of Ichthyologists and Herpetologists Spec. Publ. 5. FAO, Rome.

Hunter, J. R., and S. R. Goldberg.
1980. Spawning incidence and batch fecundity in northern anchovy, *Engraulis mordax*. Fish. Bull. 77:641–652.

Huntsman, G. R., J. Potts, R. W. Mays, and D. Vaughan.
1999. Groupers (Serranidae, Epinephelinae): endangered apex predators of reef communities. Am. Fish. Soc. Symp. 23:217–231.

Johnson, A. G., and L. A. Collins.
1994. Age-size structure of red grouper, (*Epinephelus morio*), from the Eastern Gulf of Mexico. Northeast Gulf Sci. 13:101–106.

Johnson, A. G., L. A. Collins, and J. J. Isley.
1993. Age-size structure of gag, *Mycteroperca microlepis*, from the northeastern Gulf of Mexico. Northeast Gulf Sci. 13:59–63.

Klibansky, N., and F. S. Scharf.
2018. Fecundity peaks prior to sex transition in a protogynous marine batch spawning fish, black sea bass (*Centropristis striata*). ICES J. Mar. Sci. 75:1042–1053.

Kowal, K.
2010. Aspects of the life history of the snowy grouper, *Epinephelus niveatus*, in the Gulf of Mexico. M.S. thesis, 70 p. Univ. South Fla., Tampa, FL.

Lowerre-Barbieri, S. K., K. Ganias, F. Saborido-Rey, H. Murua, and J. R. Hunter.
2011. Reproductive timing in marine fishes: variability, temporal scales, and methods. Mar. Coast. Fish. 3:71–91.

Matheson, R. H., III, and G. R. Huntsman.
1984. Growth, mortality, and yield-per-recruit models for speckled hind and snowy grouper from the United States South Atlantic Bight. Trans. Am. Fish. Soc. 113:607–616.

Moore, C. M., and R. F. Labisky.
1984. Population parameters of a relatively unexploited stock of snowy grouper in the lower Florida Keys. Trans. Am. Fish. Soc. 113:322–329.

Parker, R. O., Jr., and R. W. Mays.
1998. Southeastern U.S. deepwater reef fish assemblages, habitat characteristics, catches, and life history summaries. NOAA Tech. Rep. NMFS 138, 41 p.

R Core Team.
2013. R: a language and environment for statistical computing. R Foundation for Statistical Computing, Vienna, Austria. [Available from website, accessed February 2018.]

Rothschild, B. J.
1986. Dynamics of marine fish populations, 277 p. Harvard Univ. Press, Cambridge, MA.

RStudio.
2018. RStudio: integrated development environment for R. RStudio Inc., Boston, MA. [Available from website, accessed February 2018.]

Russell, G. M., E. J. Gutherz, and C. A. Barans.
1988. Evaluation of demersal longline gear off South Carolina and Puerto Rico with emphasis on deep-water reef fish stocks. Mar. Fish. Rev. 50(1):26–31.

Sadovy, Y., and D. Y. Shapiro.
1987. Criteria for the diagnosis of hermaphroditism in fishes. Copeia 1:136–156.

Sadovy de Mitcheson, Y., and M. Liu.
2008. Functional hermaphroditism in teleosts. Fish Fish. 9:1–43.

Scott, W. B., and M. G. Scott.
1988. Atlantic fishes of Canada. Can. Bull. Fish. Aquat. Sci. 219, 731 p.

SEDAR (Southeast Data, Assessment, and Review).
2004. SEDAR 4—stock assessment report 1: stock assessment of the deepwater snapper-grouper complex in the South Atlantic, 574 p. SEDAR, North Charleston, SC. [Available from website.]
2013. SEDAR 36—South Atlantic snowy grouper stock assessment report, 141 p. SEDAR, North Charleston, SC. [Available from website.]

von Bertalanffy, L.
1938. A quantitative theory of organic growth (Inquiries on growth laws. II). Hum. Biol. 10:181–213.

Wyanski, D. M., D. B. White, and C. A. Barans.
2000. Growth, population age structure, and aspects of the reproductive biology of snowy grouper, *Epinephelus niveatus*, off North Carolina and South Carolina. Fish. Bull. 98:199–218.

National Marine
Fisheries Service
NOAA

Fishery Bulletin
established in 1881

Spencer F. Baird
First U.S. Commissioner
of Fisheries and founder
of *Fishery Bulletin*

Effects of exploitation evident in age-based demography of 2 deepwater snappers, the goldeneye jobfish (*Pristipomoides flavipinnis*) in the Samoa Archipelago and the goldflag jobfish (*P. auricilla*) in the Mariana Archipelago

Joseph M. O'Malley (contact author)[1]
Corey B. Wakefield[2]
Zack S. Oyafuso[3]
Ryan S. Nichols[1]
Brett Taylor[4]
Ashley J. Williams[5,6]
Maria Sapatu[7]
Michael Marsik[8]

Email address for contact author: joseph.omalley@noaa.gov

[1] Pacific Islands Fisheries Science Center
National Marine Fisheries Service, NOAA
1845 Wasp Boulevard, Building 176
Honolulu, Hawaii 96818

[2] Science and Research Division
Department of Primary Industries and
Regional Development
39 Northside Drive
Hillarys, Western Australia 6025, Australia

[3] Hawaii Institute of Marine Biology
School of Ocean and Earth Science and Technology
University of Hawaii at Manoa
46-007 Lilipuna Road
Kaneohe, Hawaii 96744

[4] Joint Institute for Marine and Atmospheric Research
University of Hawaii at Manoa
1000 Pope Road, Marine Science Building 312
Honolulu, Hawaii 96822

[5] Oceanic Fisheries Programme
Pacific Community
BP D5
98848 Noumea, New Caledonia

[6] Australian Bureau of Agricultural and
Resource Economics and Sciences
Department of Agriculture
G.P.O. Box 858
Canberra City, Australian Capital
Territory 2600, Australia

[7] Fisheries Division
Ministry of Agriculture and Fisheries
P.O. Box 1874
Apia, Samoa

[8] Pacific Islands Regional Office
National Marine Fisheries Service, NOAA
1845 Wasp Boulevard, Building 176
Honolulu, Hawaii 96818

Abstract—The paucity of species-specific biological information for most exploited Indo-Pacific deepwater snappers (Lutjanidae) limits stock assessment options and management strategies. To improve stock assessments, age-based demographics were estimated for 2 deepwater snapper species, the goldeneye jobfish (*Pristipomoides flavipinnis*) in the Samoa Archipelago and the goldflag jobfish (*P. auricilla*) in the Mariana Archipelago. Each archipelago has locations where fishing had not occurred for at least 30 years, providing a rare opportunity to examine the effects of exploitation on the age and size compositions, growth, and mortality of these species. Overall, age-based data reveal a greater effect of fishing pressure than those based on size. This difference highlights concerns with size-based analyses; when species have protracted asymptotic growth trajectories, the resulting fishing impacts may not be readily apparent in size-based analyses because size and age become decoupled. This decoupling also confounds comparisons of growth among areas with different exploitation levels. Mortality estimates derived from an age-based catch curve for the unfished areas (where total mortality equals natural mortality) were comparable to those produced by using a maximum-age-based natural mortality estimator. The comparison of these methods indicates that the age-based natural mortality estimator is suitable for use in deepwater snapper stock assessments when direct measures of natural mortality are unavailable.

Manuscript submitted 6 June 2019.
Manuscript accepted 1 November 2019.
Fish. Bull. 117:322–336 (2019).
Online publication date: 22 November 2019.
doi: 10.7755/FB.117.4.5

The views and opinions expressed or implied in this article are those of the author (or authors) and do not necessarily reflect the position of the National Marine Fisheries Service, NOAA.

Many Indo-Pacific fisheries that target tropical and subtropical deepwater snappers (Lutjanidae) are considered data poor with limited fisheries information and few reliable, detailed life history studies (Williams et al., 2012, 2013; Newman et al., 2015). The available information indicates that *Pristipomoides* species have long life spans (>30 years), slow to moderate growth rates, and low levels of natural mortality (Newman et al.[1]; Newman and Dunk, 2003; Andrews et al., 2012). These attributes equate to low to medium fisheries potential (Musick, 1999; Newman et al., 2016), a level of potential that makes these species inherently vulnerable to, and slow to recover from, overexploitation (Koslow et al., 2000; Clarke et al., 2003). This combination of limited fisheries data

[1] Newman, S. J., D. Evans, and R. Ashworth. 2000. Assessment of the outer-shelf fishery resources off the Pilbara coast of tropical Western Australia. Final Report to the Fisheries Research and Development Corporation, Proj. No. 97/138, 78 p. Fish. West. Australia, North Beach, Australia. [Available from website.]

and lack of life history information restricts options for quantitative stock assessment and, hence, the accurate determination of stock status needed for sustainable management.

In species of *Pristipomoides*, size and age can become decoupled because asymptotic size is reached at a young age relative to maximum age (Newman et al., 2016). Although fishery-dependent size information is relatively easy and cost effective to obtain compared with age data derived from collecting and analyzing aging structures, this decoupling may result in biased assessments when length data are used to define cohorts within stock assessments. As such, fishing impacts may not be readily identifiable by examining changes in fish size, highlighting the importance of age information. Hence, there is a need for accurate and timely information on age structure and age-based life history of deepwater snappers. Age-based demography furthers our understanding of deepwater snapper life history and facilitates stock assessment models and sustainable harvest strategies for these species (Brodziak et al., 2011a; Newman et al., 2016).

Species-specific life history parameters important for assessments and development of harvest strategies include growth, maturity, maximum size and age, and mortality (Quinn and Deriso, 1999; Maunder et al., 2016). Estimating natural mortality (Pauly, 1980; Then et al., 2015) is particularly important and exceedingly difficult. In data-poor situations, such as those of many deepwater snapper fisheries, total mortality is typically estimated by using catch curve analysis, and natural mortality is calculated indirectly by using empirical formulae (hereafter referred to as *natural mortality estimators*) derived from correlation with life history parameters or maximum age from a collection of species (Pauly, 1980; Kenchington, 2014; Then et al., 2015). Because of the lack of life history information, none of these natural mortality estimators were derived by using information specific to tropical deepwater snappers. The lack of this information is concerning because many studies show life history parameters vary among taxa (Thorson et al., 2014; Nadon and Ault, 2016) and among populations within species (Brown, 1995; Newman et al., 1996; Williams et al., 2007, 2017; Cappo et al., 2013). Further, Kenchington (2014), in a review of indirect methods, postulated that none of these natural mortality estimators are sufficiently precise to use in an analytical stock assessment.

The spatial extents of the Samoa and Mariana Archipelagoes present the opportunity to compare life history and population dynamics between exploited and unexploited populations of deepwater snappers and to test the suitability of natural mortality estimators for assessing deepwater snapper stocks. Deepwater snapper populations surround the populated islands, as well as the uninhabited islands and offshore seamounts, within the Samoa and Mariana Archipelagoes (Fig. 1).

The history of American Samoa's deepwater snapper fishery is detailed in Itano (1996) and WPRFMC[2] and is briefly described here. There were 2 periods of expansion and subsequent decline in landings and effort, both due to the availability of fishing vessels (subsidized by the local government) and advances in technology. The first was in 1972, when the "dory fleet" began the commercial exploitation of shallow-water snappers and emperors (e.g., *Lutjanus* spp. and *Lethrinus* spp.) and, to a limited extent, deepwater snappers (e.g., *Pristipomoides* spp. and *Etelis* spp.) around the populated Tutuila Island and Manua Islands (Tau, Ofu, and Olosega). However, the number of dories quickly declined in 1977 to near zero.

A new period of exploitation began in 1978 with the advent of a new vessel design (called *alia*), which extended fishing to the offshore banks (South Bank, East Bank, Two Percent Bank, Northeast Bank, and Rose Atoll). Significant quantities of deepwater snappers, particularly *Etelis coruscans* and *E. carbunculus*, were landed in the early 1980s. *Etelis carbunculus* is now known to be composed of 2 distinct, non-interbreeding lineages (Andrews et al., 2016). Both species occur in the Samoa Archipelago, and they were likely both captured by fishermen in the 1980s but reported as one species. By 1989, fishing of deepwater snappers stopped on the offshore banks (Moffitt[3]) for reasons generally attributed to typhoons destroying vessels, fishermen leaving the deepwater snapper fishery for other fisheries, and market competition from imported fish (Levine and Allen, 2009). The results of discussions with fishermen and creel surveys (WPacFIN[4,5]) indicate that little to no deepwater snapper fishing has occurred for the past 29 years at the offshore banks of American Samoa but that fishing continues around the populated islands throughout this archipelago.

The deepwater snapper fishery in the Mariana Archipelago occurs primarily in the southern portion of the archipelago from Santa Rosa Reef north to Zeelandia Bank. This area includes offshore banks (Santa Rosa Reef, Galvez Banks, Eleven-Mile Bank, and Esmerelda Bank), populated islands (Guam, Rota, Tinian, and Saipan), and unpopulated islands (Farallon de Medinilla, Anatahan, and Sarigan) (WPRFMC[6]; Fig. 1). The islands to the north of Zealandia Bank (Guguan, Alamagan, Pagan, Agrihan, Asuncion, Maug, and Farallon de Pajaros) have had very little historical and contemporary fishing because of the economics of traveling long distances.

[2] WPRFMC (Western Pacific Regional Fishery Management Council). 2009. Fishery ecosystem plan for the American Samoa Archipelago, 202 p. WPRFMC, Honolulu, HI. [Available from website.]

[3] Moffitt, R. B. 1989. Analysis of the depletion of bottom fishes at 2% Bank, American Samoa. NOAA, Natl. Mar. Fish. Serv., Southwest Fish. Cent., Honol. Lab. Manuscr. Rep. MRF-002-89H, 9 p.

[4] WPacFIN (Western Pacific Fishery Information Network). 2018. Boat-based creel survey of the Am. Samoa Dep. Mar. Wildl. Resour. [Available from website.]

[5] WPacFIN (Western Pacific Fisheries Information Network). 2017. Unpubl. data. Confidential data from boat-based creel surveys. WPacFIN, Pac. Isl. Fish. Sci. Cent., Natl. Mar. Fish. Serv., NOAA. 1845 Wasp Blvd., Bldg. 176, Honolulu, HI 96818.

[6] WPRFMC (Western Pacific Regional Fishery Management Council). 2009. Fishery ecosystem plan for the Mariana Archipelago, 231 p. WPRFMC, Honolulu, HI. [Available from website.]

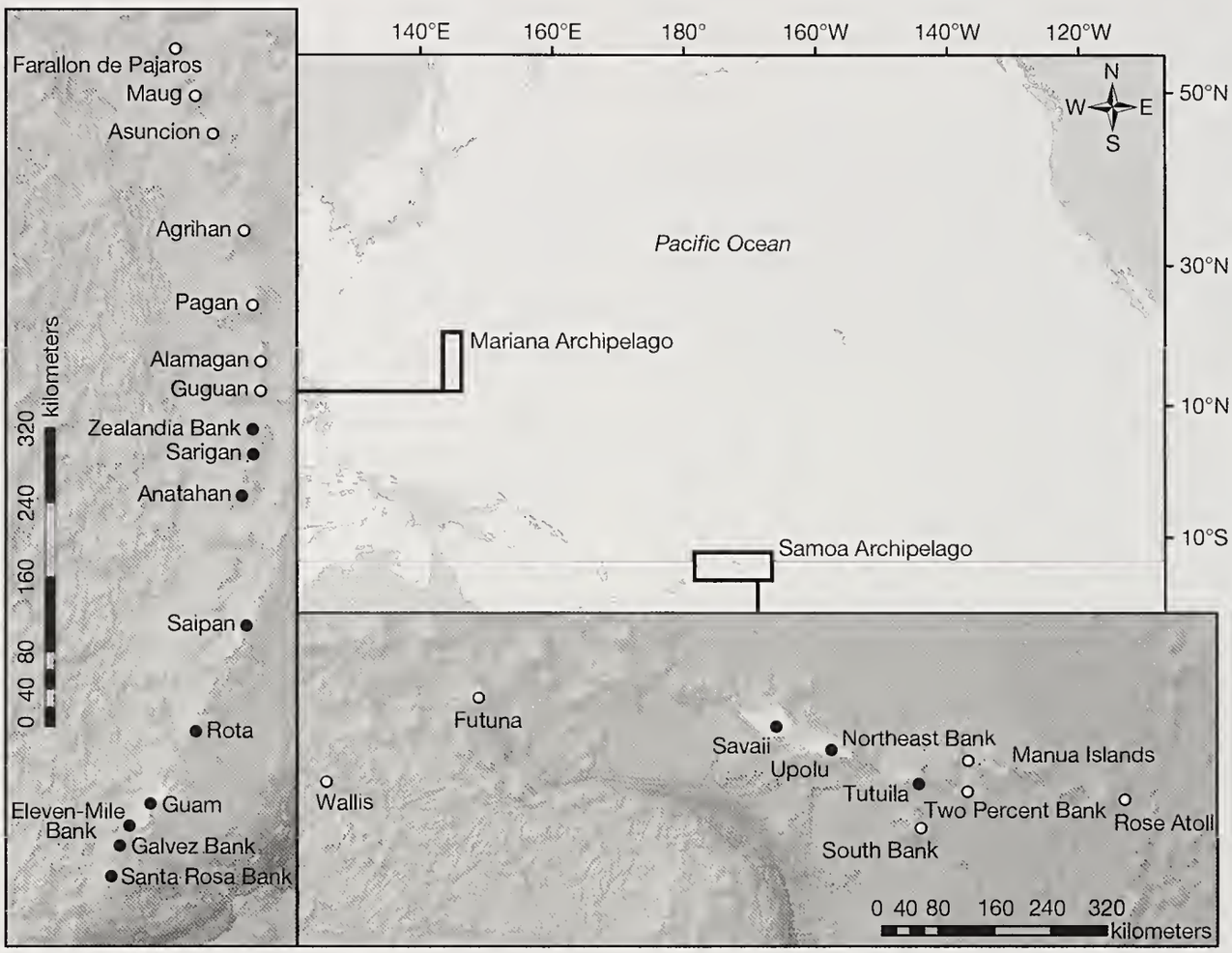

Figure 1

Maps of the Samoa Archipelago, which includes the Territory of Wallis and Futuna Islands, and the Mariana Archipelago highlighting the areas where goldeneye jobfish (*Pristipomoides flavipinnis*) and goldflag jobfish (*P. auricilla*) were collected. Goldeneye jobfish were sampled in March and October 2012 and March 2016 in the Samoa Archipelago, and goldflag jobfish were sampled in June and July 2014 in the Mariana Archipelago. Open circles indicate areas where fishing does not occur, and black circles indicate areas where fishing occurs. Data sources for the base maps: Esri, DeLorme, GEBCO, NOAA NGDC, and other contributors.

The goldeneye jobfish (*Pristipomoides flavipinnis*) and the goldflag jobfish (*P. auricilla*) are part of the deepwater demersal fishery resources of the Indo-Pacific. These snappers are widespread in the tropical and subtropical Pacific Ocean and inhabit rocky seamounts and continental slopes at depths of 90–360 m (Anderson and Allen, 2001). Both species are fished commercially and for subsistence around the populated islands and nearshore banks and seamounts throughout their range. In the U.S. territories of American Samoa, Guam, and the Commonwealth of the Northern Mariana Islands, these species are federally assessed and managed as part of a multi-species complex composed of 17 shallow-water and deepwater snappers, groupers (Epinephelinae), jacks (Carangidae), and emperors (Lethrinidae) (Yau et al., 2016). These assessments use fishery-dependent data from creel surveys in a surplus production model framework.

A recent review of this approach recommended exploring approaches based on life history parameters for the assessment process, if sufficient species-specific data are available. Reliable life history information (e.g., age, growth, and mortality) is currently unavailable for any species in this complex in the Samoa or Mariana Archipelago. Ralston and Williams (1988) estimated von Bertalanffy growth parameters and mortality rates for goldeneye jobfish and goldflag jobfish in the Mariana Archipelago by using the technique of numerical integration of daily growth increments. The resulting estimates indicate that both species had moderate growth rates and were short lived (6.7 and 4.7 years for goldeneye jobfish and goldflag jobfish, respectively). However, concerns about underestimation of fish ages produced by this method have arisen, especially for longer-lived species; therefore, the estimates are considered unreliable (Newman et al., 2016).

The objective of this research was to compare size and age information, length at age, growth, and total and natural mortality rates for 2 deepwater snappers between areas with contrasting fishing histories. The lack of fishing effort for goldeneye jobfish at the offshore banks in American Samoa since the mid-1980s and for goldflag jobfish in the islands of the Mariana Archipelago north of Zealandia Bank allows comparison of life history parameters between exploited and unexploited areas. Moreover, the calculated total mortality rate for an unfished area is equivalent to the natural mortality rate. We compared mortality estimates produced by using an age-based catch curve analysis (for the unfished areas, total mortality equals natural mortality) to those produced by using 2 natural mortality estimators that were developed from comparative life history studies that incorporated maximum ages and growth parameters to predict natural mortality rates (Then et al., 2015). This study is the first detailed age and growth study of an eteline snapper in the Samoa or Mariana Archipelago to use the nascent methods of age-based life history parameters reported in Newman et al. (2015, 2017).

Materials and methods

Sampling

Samples of goldeneye jobfish were collected during research cruises in the Samoa Archipelago in March 2012 and March 2016 and in the Territory of the Wallis and Futuna Islands in October 2012 (Fig. 1). Fish sampled from Wallis and Futuna were added to the samples from the Samoa Archipelago offshore banks (unfished) because of their close proximity and negligible exploitation history (Adams and Chapman[7]). Goldflag jobfish were collected during research cruises in the Mariana Archipelago in June and July 2014. The Guam Biosampling Program of the NOAA Pacific Islands Fisheries Science Center also provided samples from the commercial fishery operating around Guam and nearby offshore banks.

Fish were sampled during research cruises conducted in the Samoa and Mariana Archipelagoes, by using standard vertical drop lines hauled with hydraulic or electric reels from depths between 90 and 300 m. Research sampling in Wallis and Futuna also used vertical drop lines at similar depths between 100 and 400 m (Williams et al., 2017).

Each sampled fish was measured to the nearest millimeter (in fork length [FL]) and weighed to the nearest gram. Gonads were removed and preserved in 10% buffered formaldehyde. Medial transverse sections of the preserved gonads were later embedded in paraffin wax, sectioned at 5 µm, mounted on slides, and stained with Mayer's haematoxylin and eosin. These histological slides were used to determine the sex of each fish. Sagittal otoliths were extracted, cleaned, and stored dry.

Otolith preparation and aging criteria

Thin otolith sections were prepared by first mounting the whole otolith to a glass slide by using thermal adhesive so that the primordium was aligned with the short edge of the slide and the sulcus acusticus was aligned perpendicular to the long edge of the slide. The otolith was ground transversely and perpendicular to the sulcus to within close proximity of the primordium by using 1600-grit diamond-coated lap on a grinding wheel. The otolith was removed from the slide edge and remounted with the previously ground section facing downward; then it was ground to a thickness of 130–150 µm. The resulting thin section was rinsed in 0.5% HCl for 20 s, rinsed with fresh water, dried, and mounted to a clean slide with a glass cover slip.

Aging criteria for goldeneye jobfish and goldflag jobfish were developed by experienced readers of deepwater snapper otoliths during an international workshop on the life history of deepwater snappers and groupers (Newman et al., 2017) and refined during subsequent meetings. Thin sections were examined by using a dissecting microscope under transmitted light at 10–50× magnification. Fish ages were estimated by enumerating visible opaque zones that were assumed to be formed annually. This pattern of otolith material deposition has been validated for other deepwater snappers in the Indian Ocean (Newman and Dunk, 2003) and in the South and North Pacific Oceans (Newman et al., 2016; Wakefield et al., 2017; Williams et al., 2017). Thin otolith sections were read with no knowledge of location, date of capture, or fish size. Final decimal age estimates were determined by using the number of opaque zones, the birth date (peak spawning period: North Pacific, 1 June; South Pacific, 1 December; Moffitt, 1993), and capture date.

Aging precision and bias, and age determination

A subsample of otolith sections (n=50) was read independently by 2 experienced readers (goldeneye jobfish: C. Wakefield and senior author; goldflag jobfish: R. Nichols and senior author). Aging precision (i.e., consistency in replicate otolith readings between readers) was assessed by using a modified form of the Beamish and Fournier (1981) index of average percent error (IAPE) (Wakefield et al., 2017):

$$IAPE = \frac{1}{n}\sum_{j=1}^{n}\frac{(x_{ij} - \tilde{x}_j)}{\tilde{x}_j}, \quad (1)$$

where n = number of samples;
x_{ij} = the ith count of the jth fish; and
$\tilde{x}_j$ = the median count for the jth fish.

[7] Adams, T., and L. Chapman. 2004. Overview of deepwater snapper fisheries in the SPC region. Fourth SPC heads of fisheries meeting, 30 August–4 September. Secr. Pac. Community, Info. Pap. E-IP5, 9 p.

Estimates of aging precision were compared with previously determined levels of acceptance of <5.5% for IAPE (Campana, 2001; Matta and Kimura, 2012), which are applicable to deepwater snappers (Wakefield et al., 2017). Age-bias plots were examined to assess aging bias or the systematic variation in enumerated annuli counts.

The ages of all goldeneye jobfish and goldflag jobfish were estimated from the counts of opaque zones from a single age reader following the established aging criteria, with all samples read twice and at least 2 weeks between readings. Opaque zone counts for each fish were accepted if they were the same between the 2 readings, otherwise a third or, in rare cases, a fourth reading was required until a match was made with a previous count and considered the final age.

Comparison of size and age distributions

Kolmogorov–Smirnov tests were used to compare species-specific differences in the size and age frequency distributions between the sexes and between fished and unfished areas.

Growth trajectories

Species-specific growth of goldeneye jobfish and goldflag jobfish was described with the von Bertalanffy growth function (VBGF; von Bertalanffy, 1938) fitted to the FL at age by using nonlinear least squares regression with constant residual variance:

$$L_t = L_\infty\left(1-e^{-K[t-t_0]}\right), \tag{2}$$

where L_t = the predicted mean FL at age t (in years);
L_∞ = the asymptotic length (in millimeters);
K = the growth coefficient (per year);
t = estimated age (in years); and
t_0 = the theoretical age (in years) at which fish would have zero length.

Allowing the VBGF to estimate t_0 resulted in large negative values in some of the data sets because of the lack of smaller fish (<200 mm FL). Constrained growth models (t_0=0) provided a more realistic representation of growth for the younger age classes.

To examine the effects of sex and fishing pressure on growth, these factors were added as covariates to a constrained (t_0=0) Kimura's (2008) extended VBGF (EVB). In this general fixed-effects nonlinear model, L_∞ and K are modeled as functions of the covariates (β):

$$\begin{pmatrix} L_{\infty i} \\ K_i \end{pmatrix} = \begin{pmatrix} \beta_{0L} + x_{i1}\beta_{1L} + x_{i2}\beta_{2L} \\ \beta_{0K} + x_{i1}\beta_{1K} + x_{i2}\beta_{2K} \end{pmatrix}, \tag{3}$$

where x_{i1} = the sex (female or male) dummy variable (either 0 or 1); and
x_{i2} = the fishing pressure (fished versus not fished) dummy variable for the ith fish.

Models with no effects, just sex, just fishing pressure, and with sex and fishing pressure were compared by using the Akaike information criterion corrected for small sample sizes (AIC_c) (Burnham and Anderson, 2002). Statistical analyses were conducted in the statistical software environment R, vers. 3.5.1 (R Core Team, 2018), with the nls function in the stats package.

Mortality

Estimates of natural mortality of goldeneye jobfish and goldflag jobfish were produced by applying a multinomial catch curve with logistic selectivity to the age composition of the unfished populations. This approach assumes that total mortality is equal or close to that of natural mortality. The mortality and selectivity parameters of age at 50% selectivity for the unfished population (A_{50}^{unf}) and of the difference between the ages at 95% and 50% selectivity for the unfished population (Δ^{unf}) were estimated from the age composition by using a multinomial negative log-likelihood (nLL^{unf}) function:

$$nLL^{unf} = -\sum_{a=1}^{A} C_a^{unf} \log\left(P_a^{unf}\right), \tag{4}$$

where C_a^{unf} = the observed catch in numbers of age-a individuals; and
P_a^{unf} = the expected proportion of age-a individuals in the age composition, calculated as follows:

$$P_a^{unf} = \frac{\hat{C}_a^{unf}}{\sum_{a=1}^{A} \hat{C}_a^{unf}}. \tag{5}$$

Relative catch ($\hat{C}_a^{unf}$) of age-a individuals is the product of survivorship at age a (S_a^{unf}) and gear selectivity at age a (V_a^{unf}). Expected per-recruit survivorship at age in the unfished population (S_a^{unf}) was calculated as a negative exponential function with natural mortality as the only source of mortality:

$$\hat{C}_a^{unf} = S_a^{unf} V_a^{unf}, \tag{6}$$

$$S_a^{unf} = e^{-M(a-1)}, \text{ and} \tag{7}$$

$$V_a^{unf} = \frac{1}{1+e^{\frac{-\log(19)\left(a-A_{50}^{unf}\right)}{\Delta^{unf}}}}. \tag{8}$$

The multinomial catch curve results were compared with results from 2 natural mortality (M) estimators. The first was Hoenig's (1983) updated method, which is based on maximum age (Then et al., 2015):

$$M = 4.899 t_{max}^{-0.916}, \tag{9}$$

where t_{max} = maximum observed age.

The second indirect method was the updated Pauly estimator, which is based on VBGF parameters (Then et al., 2015):

$$M = 4.118 K^{0.73} L_\infty^{-0.33}, \tag{10}$$

where K = the growth coefficient (per year); and
L_∞ = the asymptotic length (in millimeters) estimated by using species-specific final growth estimates.

The estimate of natural mortality from the multinomial catch curve for the unfished populations was used as the value for natural mortality in the associated fished populations. The set of equations used to calculate total mortality in the fished areas is similar to the previous equations (with *f* in the superscript instead of *unf* to indicate the fished areas), with the following modifications:

$$\hat{C}_a^f = S_a^f \frac{F_a}{Z_a}(1 - e^{-Z_a}), \quad (11)$$

$$Z_a = M + F_a, \quad (12)$$

$$F_a = FV_a^f, \text{ and} \quad (13)$$

$$S_a^f = S_{a-1}^f e^{-Z_a}, \quad (14)$$

where $\hat{C}_a^f$ = expected catch in numbers of age-a individuals in the fished areas;
Z_a = age-specific total instantaneous mortality;
F_a = fishing mortality at age;
F = full fishing mortality;
V_a^f = gear selectivity at age a in the fished areas; and
S_a^f = survivorship in the fished areas.

Expected catch in numbers of age-a individuals in the fished areas was calculated by using Baranov's formula: age-specific total instantaneous mortality in the fished areas is the sum of natural mortality and fishing mortality, fishing mortality at age is the product of full fishing mortality and gear selectivity at age a in the fished areas, and survivorship in the fished areas is a negative exponential function of both natural mortality and fishing mortality. Selectivity was also assumed to follow a logistic function with parameters A_{50}^f and Δ^f. Values of natural mortality and total mortality, and the gear selectivity parameters in both regions, were simultaneously estimated by minimizing the sum of nLL^f and nLL^{unf}. The catch curve mortality parameters were estimated within AD Model Builder, vers. 12.0 (Fournier et al., 2012), and asymptotic standard errors were used in the calculations of the 95% confidence intervals (CIs) of the parameter estimates.

Results

Aging precision, and length and age compositions

The measures of precision between readers for opaque zone counts from thin transverse sections of otoliths were within the acceptable ranges for deepwater snappers (Wakefield et al., 2017). The between-reader IAPE was 5.2% for aging of goldeneye jobfish; 47% of the sections had exact agreement between readers, and age estimates were within 1 year for 80% of sections. The IAPE for aging of goldflag jobfish was 4.9%; 32% of the sections had exact agreement between readers, and age estimates were within 1 year for 92% of sections.

The size and age of goldeneye jobfish ranged from 234 to 474 mm FL and from 2 to 28 years old (Table 1, Fig. 2). Maximum estimated ages were similar for males (25 years) and females (28 years) as were the maximum sizes (males: 451 mm FL; females: 474 mm FL). The results of Kolmogorov–Smirnov tests indicate no significant differences between males and females in either size (D=0.231, P=0.828) or age (D=0.154, P=0.995) compositions. Analysis conducted with Kolmogorov–Smirnov tests revealed a significant difference in age compositions between fished and unfished areas (D=0.5556, P<0.001) but not in size compositions (D=0.385, P=0.226). The mean FL for combined sexes differed significantly between fished and unfished areas, with fish in unfished areas 41 mm larger on average than those in fished areas ($F_{1,371}$=0.22, P=0.00). Similarly, the mean age for combined sexes differed

Table 1

Estimates of the annual growth coefficient (K) and asymptotic length (L_∞) from the von Bertalanffy growth function, maximum ages (A_{max}), size ranges, and sample sizes (n), by sex and by area (fished and unfished), for goldeneye jobfish (*Pristipomoides flavipinnis*) sampled from the Samoa Archipelago in 2012 and 2016 and for goldflag jobfish (*P. auricilla*) sampled from the Mariana Archipelago in 2014. The 95% confidence intervals for estimates of K and L_∞ are provided in parentheses. Values of L_∞ and in size ranges are fork lengths in millimeters. Combined=areas (fished and unfished) or sexes combined.

Species	Data set	K	L_∞ (mm)	A_{max}	Size range (mm)	n
P. flavipinnis	Female	0.44 (0.41–0.48)	418.6 (413.0–424.6)	28	234–474	179
	Male	0.51 (0.46–0.56)	404.1 (398.4–409.8)	25	253–451	194
	Fished	0.37 (0.30–0.45)	429.2 (402.5–463.5)	10	234–453	61
	Unfished	0.53 (0.50–0.58)	407.9 (404.4–411.6)	28	315–474	312
	Combined	0.47 (0.44–0.50)	411.5 (407.2–415.6)	28	234–474	373
P. auricilla	Female	0.56 (0.51–0.62)	335.2 (327.8–343.1)	32	225–400	106
	Male	0.53 (0.49–0.58)	358.9 (353.4–364.8)	26	240–403	160
	Fished	0.60 (0.55–0.66)	325.2 (317.6–333.1)	18	164–347	135
	Unfished	0.54 (0.50–0.59)	358.6 (353.6–363.8)	32	225–403	160
	Combined	0.51 (0.48–0.54)	358.5 (347.5–357.5)	32	164–403	295

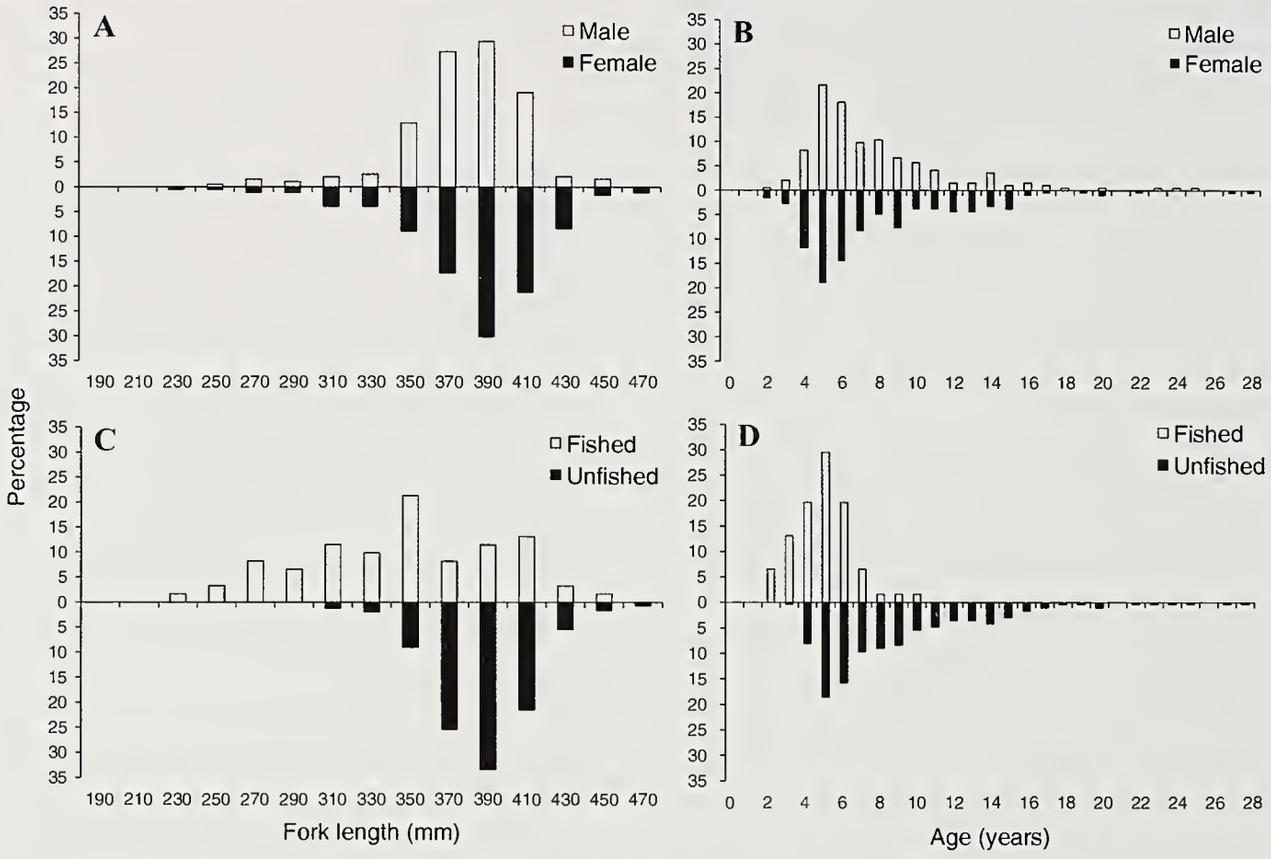

Figure 2

(**A**) Size and (**B**) age compositions for male and female goldeneye jobfish (*Pristipomoides flavipinnis*) sampled in 2012 and 2016 in the Samoa Archipelago and (**C**) size and (**D**) age compositions for goldeneye jobfish sampled from fished and unfished areas in this region.

significantly between fished and unfished areas, with fish in unfished areas 3.7 years older on average than those in fished areas ($F_{1,371}$=7.07, P<0.005). Fish from unfished areas were older and larger relative to those from fished areas. Most notably, age compositions were truncated in fished areas relative to unfished areas. The maximum age in the fished areas was 10 years compared with the maximum age of 28 years in the unfished areas. Furthermore, 30% of the individuals in the unfished areas were older than the oldest fish in the fished areas (10 years).

The size and age of goldflag jobfish ranged from 164 to 403 mm FL and from 2 to 32 years old (Table 1, Fig. 3). The estimated maximum age for males (26 years) was less than that for females (32 years), although the maximum sizes were similar (males: 403 mm; females: 400 mm). Analysis conducted with Kolmogorov–Smirnov tests revealed that the size and age compositions were significantly different between the sexes (size: D=0.328, P<0.0001; age: D=0.234, P=0.001). Within each sex, the results of the Kolmogorov–Smirnov tests indicate significant differences between fished and unfished areas in size compositions (male: D=0.594, P<0.0001; female: D=0.506, P<0.0001) and age compositions (male: D=0.462, P<0.000; female: D=0.322, P=0.006). Mean FLs for males and females were not significantly different between fished and unfished areas (males: $F_{1,158}$=1.08, P=0.37; females: $F_{1,104}$=1.58, P=0.06). However, mean ages for males and females were significantly older in unfished areas by 3.0 years for males and by 4.3 years for females (males: $F_{1,158}$=3.57, P<0.00; females: $F_{1,104}$=6.98, P<0.00). For both sexes, and similar to the results for goldeneye jobfish in the Samoa Archipelago, goldflag jobfish in the Mariana Archipelago were larger and older in the unfished areas relative to those in the fished areas, with a truncated age composition in the fished areas. The maximum ages in the fished and unfished areas were 18 years and 32 years, respectively. Of the samples from the unfished areas, 10% were older than the oldest fish from the fished areas (18 years). However, the oldest fish from the fished areas was sampled from Sarigan, the most remote island in the fished areas. The maximum age from the primary fishing grounds around Guam was 10 years.

Growth

The fit of the EVB model to the age and length data for goldeneye jobfish supported the models with factors for sex and fishing pressure (Table 2). The difference in AIC_c between the best-fit model (sex and fishing pressure) and the model with the next-best fit (just fishing pressure) was 6.13. Females reached a larger L_∞ than males and, consequently,

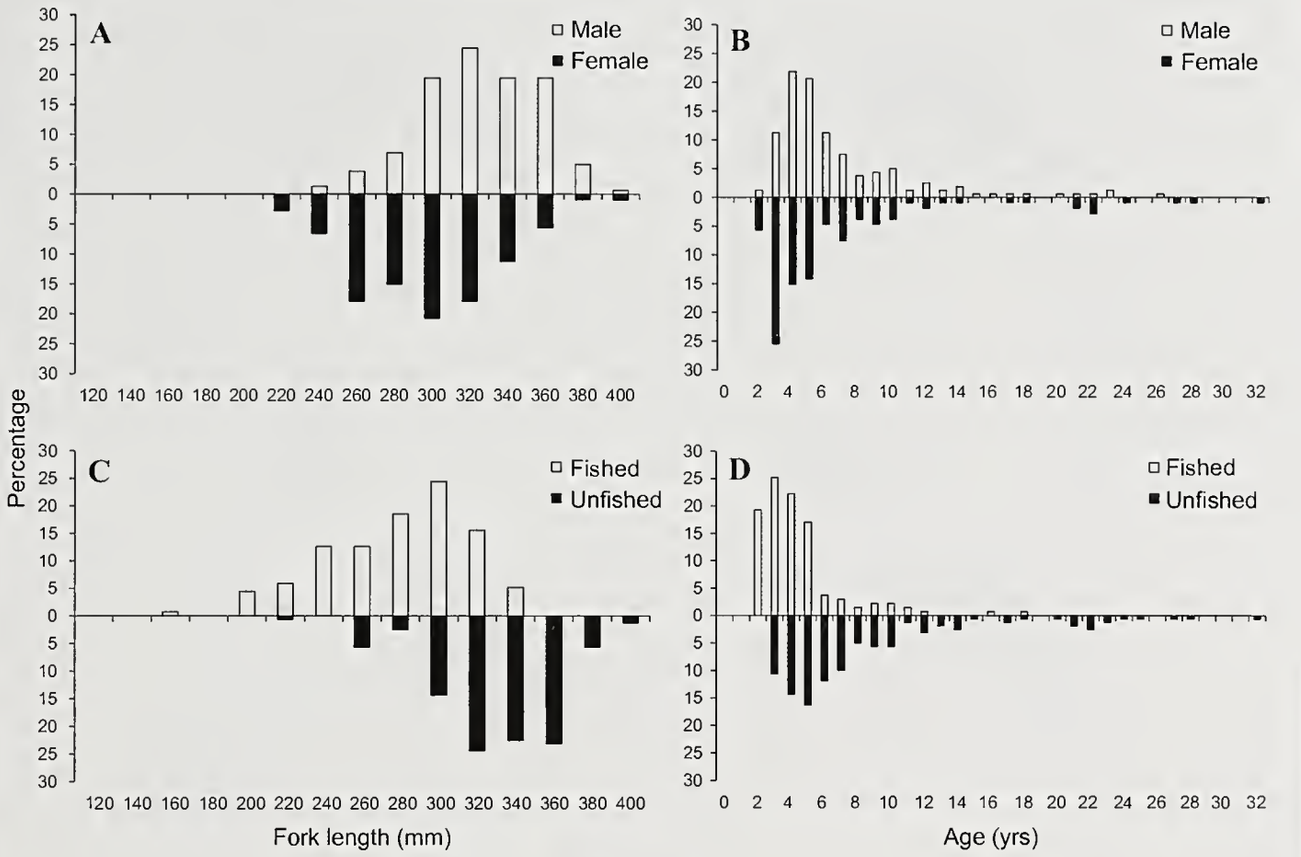

Figure 3

(**A**) Size and (**B**) age compositions for male and female goldflag jobfish (*Pristipomoides auricilla*) sampled in 2014 in the Mariana Archipelago and (**C**) size and (**D**) age compositions for goldflag jobfish sampled from fished and unfished areas in this region.

grew more slowly. However, the difference in L_∞ was small (14.5 mm FL), as were the differences in K (0.07) and in the EVB-predicted FL at age for fish with the most common ages (1.13% for fish 5–6 years old). Significant but small differences were also found between the fished and unfished populations. The L_∞ in the unfished population was 21.3 mm FL smaller, and fish grew slightly faster relative to the fished population. These differences in growth of goldeneye jobfish between fished and unfished areas were further confirmed by 5–6% differences in the EVB-predicted FL at age for fish with the most common ages (5–6 years). Overall, the fitted growth curve for goldeneye jobfish indicates that growth reached an asymptote between ages 6 and 9, corresponding to 20–30% of the maximum age (Fig. 4).

The fit of the EVB model to the age and length data for goldflag jobfish supported the models with factors for sex and fishing pressure (Table 2). The difference in AIC_c between the model fitted with sex and fishing pressure and the model with the next-best fit (just fishing pressure) was 46.9. In this species, males reached a larger L_∞ than females and, consequently, grew more slowly. However, the difference in L_∞ was small (23.7 mm FL), as were the differences in K (0.03) and in the EVB-predicted FL at age for

Table 2

Comparisons of extended von Bertalanffy growth functions fitted to length-at-age data for goldeneye jobfish (*Pristipomoides flavipinnis*) sampled from the Samoa Archipelago in March and October 2012 and in March 2016 and for goldflag jobfish (*P. auricilla*) sampled from the Mariana Archipelago in June and July 2014. Models with no covariates and with sex, fishing pressure, and sex and fishing pressure as covariates were compared by using the Akaike information criterion corrected for small sample sizes (AIC_c). Also provided are the differences in AIC_c between models (ΔAIC_c).

Species	Model	No. of parameters	AIC_c	ΔAIC_c
P. flavipinnis	Sex, fishing	9	3423.3	0.0
	Fishing	6	3429.4	6.1
	Sex	6	3448.0	24.7
	No covariates	3	3456.1	32.8
P. auricilla	Sex, fishing	9	2336.7	0.0
	Fishing	6	2383.6	46.9
	Sex	6	2413.0	76.3
	No covariates	3	2453.6	116.9

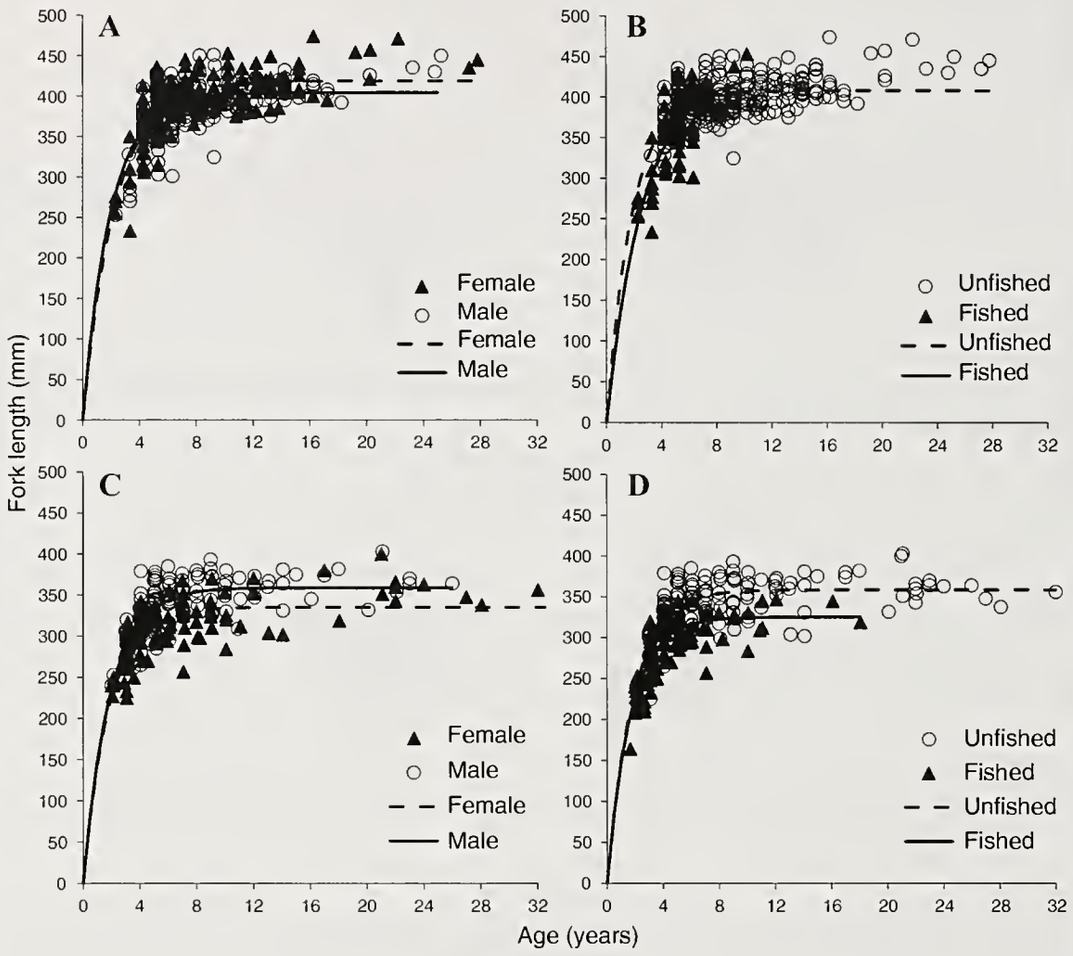

Figure 4

Lengths at age and fitted growth curves from the von Bertalanffy growth function for goldeneye jobfish (*Pristipomoides flavipinnis*) collected in the Samoa Archipelago in 2012 and 2016, by (**A**) sex (female and male) and (**B**) fishing pressure (fished and unfished areas), and for goldflag jobfish (*P. auricilla*) collected in 2014 in the Mariana Archipelago, by (**C**) sex and (**D**) fishing pressure.

fish with the most common ages (4–6% for fish 3–6 years old). Goldflag jobfish had a growth pattern between fished and unfished areas that was the opposite of that observed for goldeneye jobfish in the Samoa Archipelago. They grew more slowly (0.06 difference in K) and reached a larger L_∞ (difference of 33.4 mm FL) in the unfished areas than in the fished areas (Fig. 4, Table 1). These differences in growth of goldflag jobfish between fished and unfished areas were further confirmed by 2–10% differences in the EVB-predicted FL at age for fish with the most common ages (3–6 years). Overall, the fitted growth curve indicates that growth was similar to that of goldeneye jobfish; it reaches an asymptote between ages 6 and 9 or between 20% and 30% of the maximum age (Fig. 4).

Mortality

The multinomial catch curves provide a good fit to the observed age compositions for goldeneye jobfish and goldflag jobfish, as evident in the predicted proportions at age (Fig. 5). The estimated values of total mortality from the unfished areas, assumed to be an estimate of natural mortality, were 0.22 (95% CI: 0.19–0.25) for goldeneye jobfish and 0.18 (95% CI: 0.15–0.21) for goldflag jobfish (Table 3). Use of Hoenig's (1983) updated natural mortality estimator (Then et al., 2015) produced comparable natural mortality estimates for these same unfished areas (goldeneye jobfish: 0.23; goldflag jobfish: 0.20), whereas use of the Pauly estimator (Then et al., 2015) produced lower estimates (goldeneye jobfish: 0.17; goldflag jobfish: 0.18). Using the maximum age natural mortality estimator but substituting the maximum age from the fished areas produced greater estimates of natural mortality for goldeneye jobfish (0.59; maximum age: 10) and goldflag jobfish (0.35; maximum age:18). The values of total mortality from the fished areas, calculated by using the multinomial catch curve, are 0.89 (95% CI: 0.36–1.42) for goldeneye jobfish and 0.42 (95% CI: 0.34–0.50) for goldflag jobfish. The exploitation rates (E), calculated as fishing mortality divided by total mortality, for both species differed greatly depending on whether natural mortality was determined by using the maximum age from the fished or the unfished areas. Using the natural

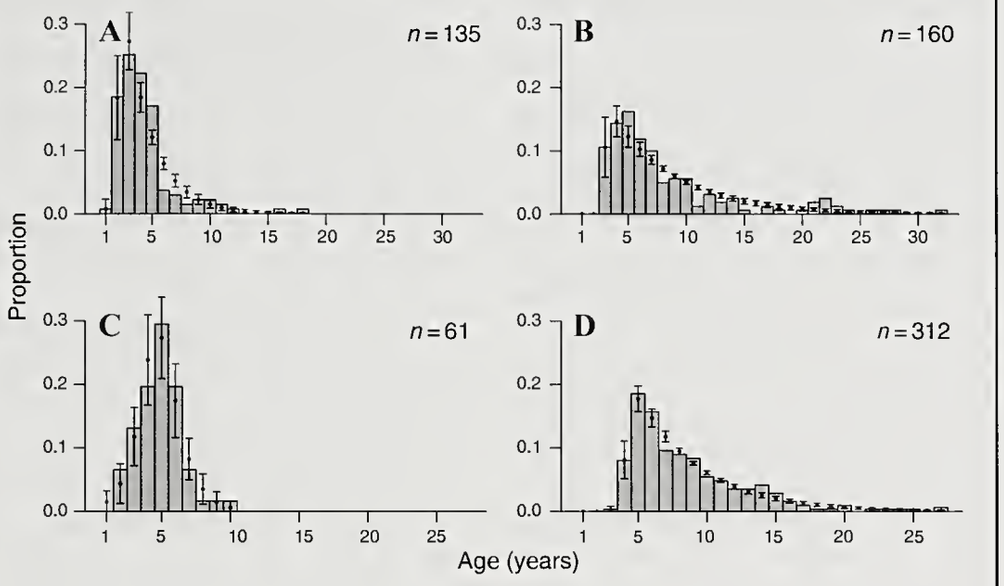

Figure 5

Observed proportions at age (gray bars) of goldflag jobfish (*Pristipomoides auricilla*) collected from (**A**) fished and (**B**) unfished areas in the Mariana Archipelago in 2014 and of goldeneye jobfish (*P. flavipinnis*) collected from (**C**) fished and (**D**) unfished areas in the Samoa Archipelago in 2012 and 2016. Predicted proportions at age (black dots) with 95% confidence intervals (error bars) are superimposed on the gray bars. *n*=number of fish aged.

Table 3

Point estimates of natural mortality (M) and selectivity in fished and unfished areas from catch curve analysis for goldeneye jobfish (*Pristipomoides flavipinnis*) collected from the Samoa Archipelago in 2012 and 2016 and for goldflag jobfish (*P. auricilla*) collected from the Mariana Archipelago in 2014. Parameters include total mortality (Z), age at 50% selectivity (A_{50}), and the difference between ages at 95% and 50% selectivity (Δ). The 95% confidence intervals for estimates are provided in parentheses.

Parameter	*P. flavipinnis*	*P. auricilla*
M	0.22 (0.19–0.25)	0.18 (0.15–0.21)
Z—fished areas	0.89 (0.36–1.42)	0.42 (0.34–0.50)
A_{50}—unfished areas	4.15 (3.95–4.35)	2.95 (2.78–3.11)
Δ—unfished areas	0.73 (0.38–1.09)	0.37 (0.35–0.37)
A_{50}—fished areas	4.85 (3.49–6.22)	2.10 (1.83–2.36)
Δ—fished areas	2.20 (1.32–3.08)	0.74 (0.33–1.15)

mortality estimates from the unfished areas and the total mortality estimate from the fished areas results in a fishing mortality of 0.66 and an E of 0.74 for goldeneye jobfish, whereas using the natural mortality from the fished areas results in a fishing mortality of 0.30 and an E of 0.33. Applying the same calculations to data for goldflag jobfish results in a fishing mortality of 0.21 and an E of 0.51, whereas using the natural mortality from the fished areas results in a fishing mortality of 0.07 and an E of 0.17.

Discussion

The life histories of deepwater snappers and their sensitivity to fishing pressure are poorly understood. This study compared length- and age-based data and growth between sexes and between fished and unfished areas for the goldeneye jobfish and the goldflag jobfish, both important deepwater snapper species, in the North and South Pacific Oceans. Samples from unfished areas presented a rare opportunity to test the suitability of natural mortality estimators for deepwater snappers and offered a different perspective on the population status relative to samples collected exclusively from the fished areas.

Age, growth, and mortality

The estimates of maximum age for goldeneye jobfish (28 years) and goldflag jobfish (32 years) are much older than those originally estimated by using the technique of numerical integration of counts of daily growth increments (Ralston and Williams, 1988). These new estimates are similar to those for congeners, including 21 years for sharptooth jawfish (*P. typus*) from the Pilbara region of Western Australia (Newman et al.[1]), 30 years for goldbanded jobfish (*P. multidens*) from the Kimberley region of Western Australia (Newman and Dunk, 2003), and 42 years for crimson jobfish (*P. filamentosus*) from the Northwestern Hawaiian Islands (Andrews et al., 2012). Considering that the maximum ages reported here for the goldeneye jobfish and goldflag jobfish came from areas

that have experienced some level of historic fishing pressure, it is possible that the true maximum ages may be greater (Newman et al.[1]; Newman and Dunk, 2003). The growth rates were also similar to those of other species of *Pristipomoides*, although the growth coefficients are slightly greater for both species. Estimates of L_∞ and FL at age indicate that, although statistically significant, the differences between the sexes may be inconsequential because of the small differences in the estimates.

Natural mortality, generally considered one of the most difficult population parameters to estimate, is also one of the most critical and influential parameters in stock assessments (Pauly, 1980; Brodziak et al., 2011b; Thorson et al., 2017). Direct, stock-specific methods, although preferred, are typically unfeasible because of prohibitive costs and data requirements. Because of these limitations, previous research on deepwater snappers (Newman et al.[1], 2016; Newman and Dunk, 2003; Burton et al., 2016; Williams et al., 2017) used indirect methods that use empirical and theoretical relationships (Beverton and Holt, 1959; Hoenig, 1983; Jensen, 1996; Then et al., 2015). These methods often suffer from low sample sizes and do not necessarily address spatial variability or taxonomic issues (Kenchington, 2014; Nadon and Ault, 2016). Estimating natural mortality by using a catch curve analysis with information from the unfished areas is considered an improvement over simply assigning a value of natural mortality (Jennings et al., 2001) or estimating it indirectly from empirical or theoretical relationships (Pauly, 1980; Hoenig, 1983; Then et al., 2015). In this study, however, the estimates of natural mortality obtained by using the multinomial catch curve analysis and by using the natural mortality estimator (maximum age method) are comparable, supporting the recommendation by Then et al. (2015) that their maximum age method provides the most reliable indirect estimates of natural mortality. The results of our research also indicate that the maximum age method is applicable for estimating natural mortality of deepwater snappers.

Using age composition data from an unfished area provides a direct estimate of natural mortality and allows the uncertainty in natural mortality to propagate to the total mortality estimate in a fished area (Maunder and Punt, 2013). The quantification of uncertainty for natural mortality also means that it can serve as a prior distribution for natural mortality in future assessments. Simulations by Punt et al. (2001) and Punt and Methot (2004) demonstrated that data collection within unfished areas (e.g., marine protected areas [MPAs]) results in improvement in the estimation of natural mortality. Garrison et al. (2011), who simulated the value of MPAs to estimate life history parameters, reported that using data collected within MPAs was an improvement to estimating natural mortality from fisheries data, although the success of estimating natural mortality was dependent on life history, movement, and model complexity.

The results of our study highlights the value of obtaining age information for longer-lived species and not relying solely on size information for parameter estimation or investigating fishing effects. In both the goldeneye jobfish and goldflag jobfish, the differences in length-based data (size composition and mean FL) between the fished and unfished areas were much smaller than the differences in age-based data (age composition and mean age). Therefore, inferences on fishery-related effects on populations may be underestimated or undetected if only length-based data are available. This is especially true for goldflag jobfish because the oldest fish (18 years) in the fished areas was sampled from Sarigan, the most remote island within the fished areas. The maximum age was 10 years around the populated island of Guam, which along with nearby seamounts and banks is the focal point of the fishery in the Mariana Archipelago.

The poor correlation between length and age occurs for other deepwater snappers that reach L_∞ at a young age relative to their maximum age (Newman et al., 2016). The results of this study indicate that age is a more sensitive and reliable indicator of deepwater snapper exploitation relative to size, likely because of decoupling of age and length. It is critical to consider this aspect when developing monitoring programs, especially if both length and age information are available to assess stock status.

This study's findings also stress the importance of using appropriate life history values as inputs when using natural mortality estimators. The differences in maximum age between the fished and unfished areas were large (goldeneye jobfish: 10 versus 28 years; goldflag jobfish: 18 versus 32 years). Applying the Then et al. (2015) natural mortality estimator (maximum age method) to the fished areas led to a very different result, depending on which maximum age was used: estimates were close to 3 times greater for the fished area maximum age than for the unfished area maximum age. These different estimates of natural mortality contribute to very different exploitation ratios, which may result in inaccurate advice on stock status for fisheries managers. This potential for inaccuracy highlights the need for thoughtful application of natural mortality estimators and reliable estimates of maximum age when using these empirical methods.

An important assumption of the spatial comparisons and the mortality estimates is that samples from the fished and unfished areas were from the same stock, with no movement of adults between areas. This assumption is valid because preliminary research indicates that, with very few exceptions, deepwater snappers generally do not move great distances (Weng, 2013; O'Malley[8]). Also, growth of the deepwater snapper *E. carbunculus* varied across 20° of latitude in the Pacific Ocean (Williams et al., 2017). These authors suggest that these differences in growth were driven by the metabolic theory of ecology because of large differences in temperature. Although the latitudinal gradient across the Samoa Archipelago is very

[8] O'Malley, J. 2015. A review of the cooperative Hawaiian bottomfish tagging program of the Pacific Islands Fisheries Science Center and the Pacific Islands Fisheries Group. NOAA, Natl. Mar. Fish. Serv., Pac. Isl. Fish. Sci. Cent. Admin. Rep. H-15-05, 36 p. [Available from website.]

small (<3°) and unlikely to affect growth, the Mariana Archipelago spans 7° of latitude. An experiment properly designed (with use of replicate and adjacent areas that have different fishing exposure) to evaluate the effects of fishing is required to investigate the potentially confounding environmental factors across the Mariana Archipelago.

Despite the benefits of the direct measurement of natural mortality, this estimate should still be met with some caution because of some assumptions of our modeling approach. Along with assumptions of equilibrium and of natural mortality being constant over age and time, we also assumed that the natural mortality estimated for the unfished areas can be transferred as the value of natural mortality in the fished areas. There are ecological reasons why the transferability assumption may be untenable. In the unfished areas, predation and competition may differ from that in the fished areas, resulting in a larger estimate of natural mortality (Walters et al., 1999; Macpherson et al., 2000; Martell et al., 2005). This larger value for natural mortality, in turn, may result in underestimation of fishing mortality for the fished areas if the back-calculation is made from total mortality. There will always be a risk of providing precise but inaccurate values of natural mortality from a direct method; however, treating natural mortality as a constant would provide overly confident total mortality intervals for the fished areas and bear the same risks of inaccuracy and transferability.

Fishing effects, assessment, and management

The most prominent effect from fishing on these species is the truncated age composition. This is not unexpected in commercial fisheries and is not necessarily an indication of overfishing by itself. However, there are consequences of age truncation, such as a reduction in a population's reproductive potential due to a reduced spawning stock and age-dependent maternal effects (Trippel et al., 1997; Berkeley et al., 2004; Hsieh et al., 2010). Older females spawn higher quality eggs, resulting in higher larval survival than that of their younger counterparts (Vallin and Nissling, 2000; Bobko and Berkeley, 2004; Sogard et al., 2008). They also spawn over a longer period, increasing the probability of their larvae matching optimal environmental conditions that would promote the resiliency of a population (Hsieh et al., 2008; Rodgveller et al., 2012; Rouyer et al., 2012). Loss of older individuals that have experienced several spawning events is detrimental to the reproductive potential of a population, and failure to account for these maternal effects on recruitment may introduce bias into stock assessments (Murawski et al., 2001).

Despite the lack of reliable catch information from the 1980s, ancillary information substantiates the notion that catches of deepwater snappers from the offshore banks of American Samoa were higher prior to 1989 (Itano, 1996; WPRFMC[2]; Moffitt[3]). During recent research cruises, the approximate age of the oldest goldeneye jobfish caught was the same as the number of years since fishing ceased at the offshore banks and contrasts starkly with that of the oldest fish captured in the fished areas. This result indicates that, despite intensive fishing over a short period (10 years) in the 1980s, populations of goldeneye jobfish were able to attain a broader age composition once intense fishing stopped. However, the maximum age may have yet to be realized at the offshore banks if they remain unexploited.

Why growth varied between the fished and unfished areas differently for the goldeneye jobfish and goldflag jobfish is difficult to interpret. The small sample size of goldeneye jobfish from the fished areas is a suspected issue; however, the size and age distributions do not indicate any obvious problems that would bias growth estimates. The absence of smaller and younger fish from the unfished areas could have confounded growth rate comparisons; for this reason, among others, we used the constrained growth models. Density dependence is a strong driver of growth variability (Beverton and Holt, 1957), but evolutionary effects of fishing on growth rates are also plausible (Conover and Munch, 2002; Jørgensen et al., 2007; Enberg et al., 2012). It is difficult to definitively determine or quantify the significance of either, especially the evolutionary effects of fishing on growth rates (Rose et al., 2001; Hilborn and Minte-Vera, 2008). In this case, the apparent differences in growth likely do not indicate an actual fishery-induced change in growth through density dependence or evolutionary changes but, perhaps, are a function of the fishery primarily removing the individuals that have already reached their L_∞ but not removing significant numbers of fish below their L_∞. This is another example of fishing having a greater effect on age than on size.

Goldeneye jobfish and goldflag jobfish are assessed and managed as part of a 17-species complex in the U.S. territories of American Samoa, Guam, and the Commonwealth of the Northern Mariana Islands. Assessing species on the level of a species complex has been criticized because the specific species that are potentially being overharvested or underutilized cannot be distinguished. The results of the assessment conducted in 2016 indicate that the species complex was not being overfished or experiencing overfishing in any of these U.S. territories (Yau et al., 2016). The mortality estimates and truncated age composition from this study indicate that the current status of goldeneye jobfish in fished areas of the Samoan Archipelago and of goldflag jobfish in fished areas of the Mariana Archipelago may not be as optimistic as the status of the species complex. It is plausible that the offshore banks act as a source for the fished areas. This is an avenue for future research. Finally, it must be noted that this study examined goldeneye jobfish throughout the entire Samoa Archipelago, including Wallis and Futuna, whereas the assessment conducted in 2016 used data from only fished areas of American Samoa.

In conclusion, goldeneye jobfish and goldflag jobfish exhibited growth and longevity similar to those of other *Pristipomoides* species with statistically significant but minimal sexual dimorphism in growth. Estimates of age structure and mortality for goldeneye jobfish and goldflag jobfish indicate that these populations are affected by fishing pressure around populated islands, but this impact is

not as apparent in comparisons of size structure. Despite significant age truncation, the effects of fishing pressure on somatic growth were less clear, and the impacts on other life history traits, such as size and age at maturity, remain unknown. The results of this rare opportunity to estimate natural mortality directly indicate that the maximum age estimator of Then et al. (2015) is suitable for deepwater snappers.

Acknowledgments

The authors thank the crew of the NOAA Ship *Oscar Elton Sette* and participants from the Pacific Islands Fisheries Science Center, American Samoa Department of Marine and Wildlife Resources, American Samoa Office of Samoan Affairs, Independent Samoa Ministry of Agriculture and Fisheries, Independent Samoa Ministry of Natural Resources and the Environment, U.S. Embassy, University of Guam, and Commonwealth of the Northern Mariana Islands Department of Fish and Wildlife for providing ground support, permits, and their time. We thank reviewers for helpful comments. Funding was provided by AusAID, the Pacific Community, the French Pacific Fund, and the ZoNéCo.

Literature cited

Anderson, W. D., and G. R. Allen.
2001. Lutjanidae: snappers (jobfishes). *In* FAO species identification guide for fishery purposes. The living marine resources of the Western Central Pacific. Vol. 5. Bony fishes part 3 (Menidae to Pomacentridae) (K. E. Carpenter and V. H. Niem, eds.), p. 2840–2853. FAO, Rome.

Andrews, A. H., E. E. DeMartini, J. Brodziak, R. S. Nichols, and R. L. Humphreys.
2012. A long-lived life history for a tropical, deepwater snapper (*Pristipomoides filamentosus*): bomb radiocarbon and lead–radium dating as extensions of daily increment analyses in otoliths. Can. J. Fish. Aquat. Sci. 69:1850–1869.

Andrews, K. R., A. J. Williams, I. Fernandez-Silva, S. J. Newman, J. M. Copus, C. B. Wakefield, J. E. Randall, and B. W. Bowen.
2016. Phylogeny of deepwater snappers (Genus *Etelis*) reveals a cryptic species pair in the Indo-Pacific and Pleistocene invasion of the Atlantic. Mol. Phylogen. Evol. 100:361–371.

Beamish, R. J., and D. A. Fournier.
1981. A method for comparing the precision of a set of age determinations. Can. J. Fish. Aquat. Sci. 38:982–983.

Berkeley, S. A., M. A. Hixon, R. J. Larson, and M. S. Love.
2004. Fisheries sustainability via protection of age structure and spatial distribution of fish populations. Fisheries 29(8):23–32.

Beverton, R. J. H., and S. J. Holt.
1957. On the dynamics of exploited fish populations, 533 p. Fish. Invest. Minist. Agric. Fish. Food, Fish. Invest. Ser. 2, vol. 19. HMSO, London.
1959. A review of the lifespans and mortality rates of fish in nature, and their relation to growth and other physiological characteristics. *In* Ciba Foundation colloquium on ageing. Vol. 5. The lifespan of animals (G. E. W. Wolstenholme and M. O'Conner, eds.), p. 142–180. J. and A. Churchill Ltd., London.

Bobko, S. J., and S. A. Berkeley.
2004. Maturity, ovarian cycle, fecundity, and age-specific parturition of black rockfish (*Sebastes melanops*). Fish. Bull. 102:418–429.

Brodziak, J., D. Courtney, L. Wagatsuma, J. O'Malley, H.-H. Lee, W. Walsh, A. Andrews, R. Humphreys, and G. DiNardo.
2011a. Stock assessment of the main Hawaiian Islands Deep7 bottomfish complex through 2010. NOAA Tech. Memo. NMFS-PIFSC-29, 176 p.

Brodziak, J., J. Ianelli, K. Lorenzen, and R. D. Methot Jr. (eds.)
2011b. Estimating natural mortality in stock assessment applications. NOAA Tech. Memo. NMFS-F/SPO-119, 38 p.

Brown, J. H.
1995. Macroecology, 284 p. Univ. Chicago Press, Chicago, IL.

Burnham, K. P., and D. R. Anderson.
2002. Model selection and multimodel inference: a practical information-theoretic approach, 2nd ed., 488 p. Springer-Verlag, New York.

Burton, M. L., J. C. Potts, and D. R. Carr.
2016. Age, growth and natural mortality of blackfin snapper, *Lutjanus buccanella*, from the southeastern United States and U.S. Caribbean. Gulf. Caribb. Res. 27:66–73.

Campana, S. E.
2001. Accuracy, precision and quality control in age determination, including a review of the use and abuse of age validation methods. J. Fish Biol. 59:197–242.

Cappo, M., R. J. Marriott, and S. J. Newman.
2013. James's rule and causes and consequences of a latitudinal cline in the demography of John's snapper (*Lutjanus johnii*) in coastal waters of Australia. Fish. Bull. 111:309–324.

Clarke, M. W., C. J. Kelly, P. L. Connolly, and J. P. Molloy.
2003. A life history approach to the assessment and management of deepwater fisheries in the Northeast Atlantic. J. Northw. Atl. Fish. Sci. 31:401–411.

Conover, D. O., and S. B. Munch.
2002. Sustaining fisheries yields over evolutionary time scales. Science 297:94–96.

Enberg, K., C. Jørgensen, E. S. Dunlop, Ø. Varpe, D. S. Boukal, L. Baulier, S. Eliassen, and M. Heino.
2012. Fishing-induced evolution of growth: concepts, mechanisms and the empirical evidence. Mar. Ecol. 33:1–25.

Fournier, D. A., H. J. Skaug, J. Ancheta, J. Ianelli, A. Magnusson, M. N. Maunder, A. Nielsen, and J. Sibert.
2012. AD Model Builder: using automatic differentiation for statistical inference of highly parameterized complex nonlinear models. Optim. Methods Softw. 27:233–249.

Garrison, T. M., O. S. Hamel, and A. E. Punt.
2011. Can data collected from marine protected areas improve estimates of life-history parameters? Can. J. Fish. Aquat. Sci. 68:1761–1777.

Hilborn, R., and C. V. Minte-Vera.
2008. Fisheries-induced changes in growth rates in marine fisheries: are they significant? Bull. Mar. Sci. 83:95–105.

Hoenig, J. M.
1983. Empirical use of longevity data to estimate mortality rates. Fish. Bull. 82:898–903.

Hsieh, C.-H., S. C. Reiss, R. P. Hewitt, and G. Sugihara.
2008. Spatial analysis shows fishing enhances the climatic sensitivity of marine fishes. Can. J. Fish. Aquat. Sci. 65:947–961.

Hsieh, C.-H., A. Yamauchi, T. Nakazawa, and W. F. Wang.
2010. Fishing effects on age and spatial structures undermine population stability of fishes. Aquat. Sci. 72: 165–178.

Itano, D.
1996. The development of small-scale fisheries for bottomfish in American Samoa (1961–1987). SPC Fish. Newsl. 76–77:28–44.

Jennings, S., M. J. Kaiser, and J. D. Reynolds.
2001. Marine fisheries ecology, 432 p. Blackwell Publishing, London.

Jensen, A. L.
1996. Beverton and Holt life history invariants result from optimal trade-off of reproduction and survival. Can. J. Fish. Aquat. Sci. 53:820–822.

Jørgensen, C., K. Enberg, E. S. Dunlop, R. Arlinghaus, D. S. Boukal, K. Brander, B. Ernande, A. Gårdmark, F. Johnston, S. Matsumura, et al.
2007. Ecology: managing evolving fish stocks. Science 318:1247–1248.

Kenchington, T. J.
2014. Natural mortality estimators for information limited fisheries. Fish Fish. 15:53–562.

Kimura, D. K.
2008. Extending the von Bertalanffy growth model using explanatory variables. Can. J. Fish. Aquat. Sci. 65: 1879–1891.

Koslow, J. A., G. W. Boehlert, J. D. M. Gordon, R. L. Haedrich, P. Lorance, and N. Parin.
2000. Continental slope and deep-sea fisheries: implications for a fragile ecosystem. ICES J. Mar. Sci. 57:548–557.

Levine, A., and S. Allen.
2009. American Samoa as a fishing community. NOAA Tech. Memo. NMFS-PIFSC-19, 74 p.

Macpherson, E., A. García-Rubies, and A. Gordoa.
2000. Direct estimation of natural mortality rates for littoral marine fishes using populational data from a marine reserve. Mar. Biol. 137:1067–1076.

Martell, S. J. D., T. E. Essington, B. Lessard, J. F. Kitchell, C. J. Walters, and C. H. Boggs.
2005. Interactions of productivity, predation risk, and fishing effort in the efficacy of marine protected areas for the central Pacific. Can. J. Fish. Aquat. Sci. 62:1320–1336.

Matta, M. E., and D. K. Kimura (eds.).
2012. Age determination manual of the Alaska Fisheries Science Center Age and Growth Program. NOAA Prof. Pap. NMFS 13, 97 p.

Maunder, M. N., and A. E. Punt.
2013. A review of integrated analysis in fisheries stock assessment. Fish. Res. 142:61–74.

Maunder, M. N., P. R. Crone, A. E. Punt, J. L. Valero, and B. X. Semmens.
2016. Growth: theory, estimation, and application in fishery stock assessment models. Fish. Res. 180:1–3.

Moffitt, R. B.
1993. Deepwater demersal fish. *In* Nearshore marine resources of the South Pacific: information for fisheries (A. Wright and L. Hill, eds.), p. 73–95. Inst. Pac. Stud., Suva, Fiji.

Murawski, S. A., P. J. Rago, and E. A. Trippel.
2001. Impacts of demographic variation in spawning characteristics on reference points for fishery management. ICES J. Mar. Sci. 58:1002–1014.

Musick, J. A.
1999. Ecology and conservation of long-lived marine animals. *In* Life in the slow lane: ecology and conservation of long-lived marine animals (J. A. Musick, ed.), p. 1–10. Am. Fish. Soc. Symp. 23.

Nadon, M. O., and J. S. Ault.
2016. A stepwise stochastic simulation approach to estimate life history parameters for data-poor fisheries. Can. J. Fish. Aquat. Sci. 73:1874–1884.

Newman, S. J., and I. J Dunk.
2003. Age validation, growth, mortality, and additional population parameters of the goldband snapper (*Pristipomoides multidens*) off the Kimberley coast of northwestern Australia. Fish. Bull. 101:116–128.

Newman, S. J., D. McB. Williams, and G. R. Russ.
1996. Variability in the population structure of *Lutjanus adetii* (Castelnau, 1873) and *L. quinquelineatus* (Bloch, 1790) among reefs in the central Great Barrier Reef, Australia. Fish. Bull. 94:313–329.

Newman, S. J., C. B. Wakefield, A. J. Williams, J. M. O'Malley, S. J. Nicol, E. E. DeMartini, T. Halafihi, J. Kaltavara, R. L. Humphreys, B. M. Taylor, et al.
2015. International workshop on methodological evolution to improve estimates of life history parameters and fisheries management of data-poor deep-water snappers and groupers. Mar. Policy 60:182–185.

Newman, S. J., A. J. Williams, C. B. Wakefield, S. J. Nicol, B. M. Taylor, and J. M. O'Malley.
2016. Review of the life history characteristics, ecology and fisheries for deep-water tropical demersal fish in the Indo-Pacific region. Rev. Fish Biol. Fish. 26:537–562.

Newman, S. J., C. B. Wakefield, A. J. Williams, J. M. O'Malley, B. M. Taylor, S. J. Nicol, R. S. Nichols, S. A. Hesp, N. G. Hall, N. Hill, et al.
2017. International workshop on advancing methods to overcome challenges associated with life history and stock assessments of data-poor deep-water snappers and groupers. Mar. Policy 79:78–83.

Pauly, D.
1980. On the interrelationships between natural mortality, growth parameters, and mean environmental temperature in 175 fish stocks. ICES J. Mar. Sci. 39:175–192.

Punt, A. E., and R. D. Methot.
2004. Effects of marine protected areas on the assessment of marine fisheries. Am. Fish. Soc. Symp. 42:133–154.

Punt, A. E., A. D. M. Smith, A. J. Davidson, B. D. Mapstone, and C. R. Davies.
2001. Evaluating the scientific benefits of spatially explicit experimental manipulations of common coral trout (*Plectropomus leopardus*) on the Great Barrier Reef, Australia. *In* Spatial processes and management of marine populations. Alaska Sea Grant Rep. 01-02 (G. H. Kruse, N. Bez, A. Booth, M. W. Dorn, S. Hills, R. N. Lipcius, D. Pelletier, C. Roy, S. J. Smith, and D. Witherell, eds.), p. 67–103. Univ. Alaska Sea Grant Coll. Program, Fairbanks, AK.

Quinn, T. J., II, and R. B. Deriso.
1999. Quantitative fish dynamics, 542 p. Oxford Univ. Press, New York.

R Core Team.
2018. R: a language and environment for statistical computing. R Foundation for Statistical Computing, Vienna, Austria. [Available from website, accessed July 2018.

Ralston, S. V., and H. A. Williams.
1988. Depth distributions, growth, and mortality of deep slope fishes from the Mariana Archipelago. NOAA Tech. Memo. NMFS-SWFC-113, 22 p.

Rodgveller, C. J., C. R. Lunsford, and J. T. Fujioka.
2012. Effects of maternal age and size on embryonic energy reserves, developmental timing, and fecundity in quillback rockfish (*Sebastes maliger*). Fish. Bull. 110:36–45.

Rose, K. A., J. H. Cowan Jr., K. O. Winemiller, R. A. Myers, and R. Hilborn.
2001. Compensatory density dependence in fish populations: importance, controversy, understanding and prognosis. Fish Fish. 2:293–327.

Rouyer, T., A. Sadykov, J. Ohlberger, and N. C. Stenseth.
2012. Does increasing mortality change the response of fish populations to environmental fluctuations? Ecol. Lett. 15:658–665.

Sogard, S. M., S. A. Berkeley, and R. Fisher.
2008. Maternal effects in rockfishes *Sebastes* spp.: a comparison among species. Mar. Ecol. Prog. Ser. 360:227–236.

Then, A. Y., J. M. Hoenig, N. G. Hall, and D. A. Hewitt.
2015. Evaluating the predictive performance of empirical estimators of natural mortality rate using information on over 200 fish species. ICES J. Mar. Sci. 72:82–92.

Thorson, J. T., I. G. Taylor, I. J. Stewart, and A. E. Punt.
2014. Rigorous meta-analysis of life history correlations by simultaneously analyzing multiple population dynamics models. Ecol. Appl. 24:315–326.

Thorson, J. T., S. B. Munch, J. M. Cope, and J. Gao.
2017. Predicting life history parameters for all fishes worldwide. Ecol. Appl. 27:2262–2276.

Trippel, E. A., O. S. Kjesbu, and P. Solemdal.
1997. Effects of adult age and size structure on reproductive output in marine fishes. *In* Early life history and recruitment in fish populations (R. C. Chambers and E. A. Trippel, eds.), p. 31–62. Chapman and Hall, London.

Vallin, L., and A. Nissling.
2000. Maternal effects on egg size and egg buoyancy of Baltic cod, *Gadus morhua*: implications for stock structure effects on recruitment. Fish. Res. 49:21–37.

von Bertalanffy, L.
1938. A quantitative theory of organic growth (Inquiries on growth laws. II). Hum. Biol. 10:181–213.

Wakefield, C. B., J. M. O'Malley, A. J. Williams, B. M. Taylor, R. S. Nichols, T. Halafihi, R. L. Humphreys Jr., J. Kaltavara, S. J. Nicol, and S. J. Newman.
2017. Ageing bias and precision for deep-water snappers: evaluating nascent otolith preparation methods using novel multivariate comparisons among readers and growth parameter estimates. ICES J. Mar. Sci. 74:193–203.

Walters, C., D. Pauly, and V. Christensen.
1999. Ecospace: prediction of mesoscale spatial patterns in trophic relationships of exploited ecosystems, with emphasis on the impacts of marine protected areas. Ecosystems 2:539–554.

Weng, K. C.
2013. A pilot study of deepwater fish movement with respect to marine reserves. Anim. Biotelem. 1:17.

Williams, A. J., B. D. Mapstone, and C. R. Davies.
2007. Spatial and interannual patterns in growth of an exploited coral-reef fish. J. Fish Biol. 71:970–992.

Williams, A. J., S. J. Nicol, N. Bentley, P. J. Starr, S. J. Newman, M. A. McCoy, J. Kinch, P. G. Williams, F. Magron, G. M. Pilling, et al.
2012. International workshop on developing strategies for monitoring data-limited deepwater demersal line fisheries in the Pacific Ocean. Rev. Fish Biol. Fish. 22:527–531.

Williams, A. J., K. Loeun. S. J. Nicol, P. Chavance, M. Ducrocq, S. J. Harley, G. M. Pilling, V. Allain, C. Mellin, and C. J. A. Bradshaw.
2013. Population biology and vulnerability to fishing of deepwater Eteline snappers. J. Appl. Ichthyol. 29:395–403.

Williams, A. J., C. B. Wakefield, S. J. Newman, E. Vourey, F. J. Abascal, T. Halafihi, J. Kaltavara, and S. J. Nicol.
2017. Oceanic, latitudinal, and sex-specific variation in demography of a tropical deepwater snapper across the Indo-Pacific region. Front. Mar. Sci. 4:382.

Yau, A., M. Nadon, B. Richards, J. Brodziak, and E. Fletcher.
2016. Stock assessment updates of the bottomfish management unit species of American Samoa, the Commonwealth of the Northern Mariana Islands, and Guam in 2015 using data through 2013. NOAA Tech. Memo. NMFS-PIFSC-51, 54 p.

National Marine
Fisheries Service
NOAA

Fishery Bulletin
established in 1881

Spencer F. Baird
First U.S. Commissioner
of Fisheries and founder
of *Fishery Bulletin*

Effects of temperature and hypoxia on the metabolic performance of juvenile striped bass (*Morone saxatilis*)

Katie V. Anweiler (contact author)[1]
Karl Brenkert[1]
Tanya L. Darden[1]
Eric J. McElroy[2]
Michael R. Denson[1]

Email address for contact author: anweilerk@dnr.sc.gov

[1] Marine Resources Research Institute
South Carolina Department of Natural Resources
P.O. Box 12559
Charleston, South Carolina 29422

[2] Department of Biology
College of Charleston
66 George Street
Charleston, South Carolina 29424

Abstract—Striped bass (*Morone saxatilis*) found in estuaries and rivers of North America face many environmental challenges. These challenges may have led to local extirpations of striped bass, as has been observed in the Ashley River in South Carolina. The link between environmental challenges and extirpation may be physiological capacities, such as standard metabolic rate (SMR), maximum metabolic rate (MMR), and aerobic metabolic scope (AMS). The objective of this study was to determine the effect of temperature and oxygen availability on the metabolic capacities of striped bass, thereby assessing the physiological capability for survival under varying environmental conditions. After being acclimated to water temperatures of 20°C, 25°C, and 32°C, striped bass swam at their acclimation temperature while being acutely exposed to dissolved oxygen (DO) levels of 2.5, 3.0, and 4.0 mg/L. The highest values of SMR, MMR, and AMS were observed at 32°C, a temperature approaching the upper lethal limit. The MMR, AMS, and exhaustion time were significantly reduced at DO concentrations below 4.0 mg/L. These results indicate that juvenile striped bass are metabolically limited as DO concentrations fall below 4.0 mg/L. However, juvenile striped bass in the Ashley River may be minimally affected by this potential challenge because these conditions are rarely observed.

Manuscript submitted 25 February 2019.
Manuscript accepted 7 November 2019.
Fish. Bull. 117:337–347 (2019).
Online publication date: 5 December 2019.
doi: 10.7755/FB.117.4.6

The views and opinions expressed or implied in this article are those of the author (or authors) and do not necessarily reflect the position of the National Marine Fisheries Service, NOAA.

The striped bass (*Morone saxatilis*) is an ecologically and economically important finfish species along the Atlantic coast of North America. Its native range extends from the St. Lawrence River in Canada to the Gulf of Mexico (Setzler et al., 1980). Striped bass have also been introduced into rivers and reservoirs throughout the United States and are a valuable recreational fishery in many areas. North of Cape Hatteras, in North Carolina, up through New England, adults leave their native estuaries and migrate along the coast, ascending into rivers to spawn (ASMFC[1]; Coutant, 1985). South of Cape Hatteras, striped bass rarely undertake coastal migrations and remain associated with rivers and estuaries (Coutant, 1985).

Across the range of this species, dissolved oxygen (DO) concentration and temperature are important water-quality parameters that affect the survival and reproductive success of striped bass (Coutant, 1985; Coutant and Benson, 1990). Both field observations and experimental results from inland impoundments, rivers, and estuaries indicate that striped bass become physiologically stressed by hypoxic conditions of DO levels of approximately 3 mg/L and that they cannot inhabit areas with DO concentrations less than approximately 2 mg/L (Coutant, 1985). Although resource managers and fisheries biologists commonly measure oxygen preferences and limits and develop habitat suitability index models in terms of DO concentration (e.g., ASMFC[1]; Coutant, 1985; Greene et al.[2]; Ruane et al., 2013), it should be noted

[1] ASMFC (Atlantic States Marine Fisheries Commission). 1981. Interstate fisheries management plan for the striped bass of the Atlantic coast from Maine to North Carolina. Atl. States Mar. Fish. Comm., Fish. Manage. Rep. 1, 329 p. [Available from website.]

[2] Greene, K. E., J. L. Zimmerman, R. W. Laney, and J. C. Thomas-Blate. 2009. Atlantic coast diadromous fish habitat: a review of utilization, threats, recommendations for conservation, and research needs. Atl. States Mar. Fish. Comm., Habitat Manage. Ser. 9, 463 p. [Available from website.]

that the gradient in partial pressure of oxygen (PO_2), rather than in DO concentration, drives the rate of oxygen diffusion and, therefore, oxygen uptake for an organism (Farrell and Richards, 2009). The ability of water to hold oxygen decreases with increasing temperature, but the PO_2 at any given oxygen concentration increases with temperature.

Thermal tolerance of striped bass varies by several degrees depending on experimental methodology, differences among fish stocks, geographic location, age of fish, and the ranges of water temperature and oxygen concentration available to the fish (Crance[3]). Merriman (1941) reported a maximum thermal tolerance of 25–27°C on the basis of field distribution records in New England. However, Tagatz[4] found that adult striped bass sampled in North Carolina tolerated temperatures of 0–30°C in the laboratory. Gift (1970) observed a median lethal temperature of 31.5°C for adult striped bass sampled in New Jersey, acclimating them to 20°C and raising the temperature to the lethal level over a period of approximately 24 h. The same experimental procedure showed a higher temperature tolerance for juvenile striped bass, with a median lethal temperature of 37°C. Likewise, Coutant et al. (1984) reported the optimum temperatures for juvenile striped bass (80–300 mm in total length [TL]) as 24–27°C, and Coutant and Carrol (1980) reported an optimal temperature range of 20–24°C for larger juvenile striped bass (430–680 mm TL). These findings agree with the premise that juvenile striped bass are more tolerant of high temperatures than adults.

Nearly all observations of physiological limits of striped bass have been on migratory northern populations (i.e., those above Cape Hatteras), which likely have different physiological tolerances than southern populations (i.e., those below Cape Hatteras) because of their different life history. Southern populations of striped bass are essentially non-migratory (Greene et al.[2]). In South Carolina, populations of striped bass are small, reproductively isolated, and exist either in inland impoundments or in coastal rivers (Bulak et al., 2004; Sessions et al.[5]). The results of field studies exploring habitat preferences in inland impoundments indicate that striped bass choose habitats with temperatures of 20–24°C during the summer and occupy habitats with temperatures up to 26°C when a cooler habitat is unavailable (Schaffler et al., 2002; Young and Isely, 2002). However, the coastal rivers and estuaries that some southern populations inhabit do not have the degree of thermal refuge of inland impoundments. In a coastal river of South Carolina, Bjorgo et al. (2000) observed that striped bass chose habitats with temperatures of 25–27°C during periods when downstream habitats were as much as 5°C higher.

Striped bass will select habitats with water that is warmer than their preferred range when DO concentration is low in cooler water (Farquhar and Gutreuter, 1989). During summer, when temperatures are highest and DO levels are lowest, striped bass select the coolest habitat available with DO concentrations over 2.0–2.5 mg/L (Zale et al., 1990). Water temperatures in summer (June–August) at our study site, the Ashley River in South Carolina, have been 19–33°C (M. Denson, unpubl. data; Fig. 1), with temperatures of 24–31°C being the most frequent (80% of observations). Concentrations of DO typically range from 3.5 to 5.5 mg/L during the summer, with levels ≤4.0 mg/L for 28% of observations and levels ≤3.0 mg/L for 1% of observations. Tolerance of both high temperatures and low DO concentrations is likely important to survival of striped bass in the coastal rivers and estuaries of the southeastern United States.

Temperature is the principal controlling factor of metabolic demand; within an ectotherm's temperature range, metabolism is expected to increase 2–3 fold for every 10°C increase in temperature (Hochachka and Somero, 2002). Aerobic metabolic scope (AMS) is defined as the mathematical difference between the maximum metabolic rate (MMR) and the standard metabolic rate (SMR) (Fry, 1947, 1971). Aerobic metabolic scope represents the metabolic confines within which all aerobic energetic processes (e.g., somatic and gonadal growth, digestion, and activity) must be performed (Fry, 1947, 1971; Neill and Bryan, 1991; Lapointe et al., 2014). Although SMR increases with temperature (Fry and Hart, 1948), MMR levels off, or even decreases, when temperatures become too high (Fry and Hart, 1948; Pörtner and Knust, 2007). Therefore, at high temperatures, AMS is expected to decrease because of tissue oxygen demand outpacing oxygen supply from the environment (Pörtner, 2001, 2002). Many studies have quantified AMS as a proxy for biological performance in a given environment (e.g., Pörtner and Knust, 2007; Farrell et al., 2008; Clark et al., 2011; Lapointe et al., 2014) and have found that the time it takes for a swimming fish to exhaust (i.e., *exhaustion time*) is positively correlated with AMS (Reidy et al., 2000; Metcalfe et al., 2016).

This study is the first to examine the interactive effects of temperature and low DO concentration on aerobic metabolism and swimming performance in southern stocks of striped bass. The objective of this study was to compare changes in AMS during acute exposure to hypoxic treatments (DO levels of 2.5, 3.0, and 4.0 mg/L) in striped bass that were acclimated and exercised at 3 temperatures (20°C, 25°C, and 32°C). These temperatures span the range of the summer thermal regime in the Ashley River, and the DO levels mimic the lower end of DO concentrations observed in this river (Fig. 1). Although environmental PO_2 has a more direct effect on fish oxygen uptake than environmental oxygen concentration, specific oxygen concentrations were chosen on

[3] Crance, J. H. 1984. Habitat suitability index models and instream flow suitability curves: inland stocks of striped bass. U.S. Fish Wildl. Serv., Div. Biol. Serv. Res. Dev. FWS/OBS-82/10.85, 63 p. [Available from website.]

[4] Tagatz, M. E. 1961. Tolerance of striped bass and American shad to changes of temperature and salinity. U.S. Fish Wildl. Serv., Spec. Sci. Rep. Fish. 388, 8 p. [Available from website.]

[5] Sessions, F., S. Lamprecht, J. Bettinger, J. Bulak, and M. Scott. 2015. Striped bass. *In* South Carolina's state wildlife action plan (SWAP) 2015. Suppl. vol.: species of conservation concern. South Carolina Dep. Nat. Resour., Columbia, SC. [Available from website.]

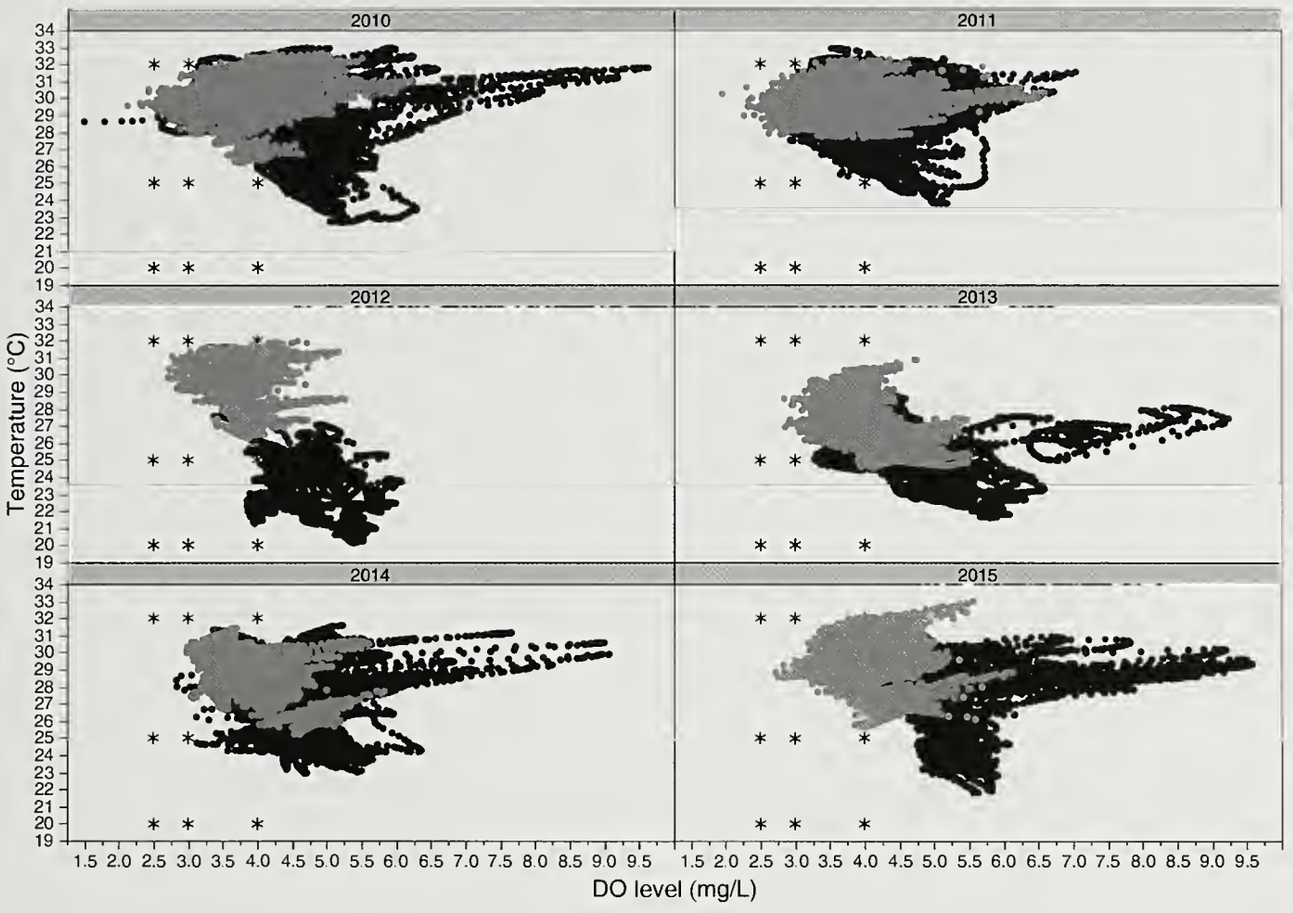

Figure 1

Relationships of temperatures to dissolved oxygen (DO) levels recorded at 2 sites in the Ashley River in South Carolina during the summers (June–August) of 2010–2015. Observations were recorded in 15-min intervals by using 2 YSI 6600EDS V2-2 multiparameter water-quality monitoring devices (or sondes; YSI Inc., Yellow Springs, OH). Sondes were deployed in the Ashley River at river kilometer (rkm) 21 and rkm 39, measured from the river's confluence with Charleston Harbor. Gray dots indicate values recorded at the site at rkm 21, a location that represents a marsh-dominated estuarine habitat. Black dots indicate values recorded at the site at rkm 39, which is a transition zone between estuarine emergent wetland and palustrine forested wetlands. For comparison, asterisks indicate temperatures and DO concentrations used in treatments in this study.

the basis of how natural resource managers monitor systems and estimate fish survival in systems.

Changes in AMS of juveniles due to temperature and DO level were measured to understand how these conditions might affect the survival of stocked fish during their first summer in the Ashley River. Because AMS, when expressed as a function of temperature, typically takes the approximate form of a bell-shaped curve that aligns with organismal performance (Neill and Bryan, 1991; Pörtner and Farrell, 2008; Pörtner, 2010), we predicted that 1) SMR would increase with increasing temperature; 2) MMR, AMS, and exhaustion time would be greatest at 25°C and would be lower at 20°C and 32°C, consistent with the recorded temperature preference for juveniles (Coutant and Carrol, 1980; Coutant et al., 1984); and 3) MMR, AMS, and exhaustion time would decrease with decreasing DO concentration. Hypotheses 2 and 3 are consistent with observations that striped bass avoid DO levels less than 3.0 mg/L and prefer temperatures less than 30°C (Zale et al., 1990; Bjorgo et al., 2000; Schaffler et al., 2002).

Materials and methods

Experimental animals and acclimation conditions

Experiments were conducted at the Marine Resources Research Institute (MRRI), South Carolina Department of Natural Resources (SCDNR), in Charleston, South Carolina. Striped bass larvae (2013 year class) were produced from wild-caught adults from the Santee Cooper reservoirs. Larvae were grown to small juveniles in fertilized, brackish ponds (salinity: ~7) at the SCDNR Waddell Mariculture Center and transported to the MRRI, located in Charleston Harbor. Fish were initially held indoors in circular 1600-L fiberglass tanks in order to acclimate them to feeding routines until they were 1 year old.

Table 1

Results from trials with different treatment combinations conducted on striped bass (*Morone saxatilis*) at the Marine Resources Research Institute, South Carolina Department of Natural Resources, during June–December 2014. Partial pressure of oxygen in water (PO_2), fish wet weight, fish total length (TL), fish relative condition factor (*Kn*), standard metabolic rate (SMR), maximum metabolic rate (MMR), aerobic metabolic scope (AMS), exhaustion time, and fish sample size (n) were measured for each combination of temperature and dissolved oxygen (DO) concentration. Lettered subscripts indicate significant differences between temperature treatments, and numbered subscripts indicate significant differences between DO-level treatments. Standard deviations of means are given in parentheses.

Temp. (°C)	DO level (mg/L)	PO_2 (kPa)	Wet weight (g)	TL (mm)	*Kn*	SMR ($mg \cdot kg^{-1} \cdot h^{-1}$)	MMR ($mg \cdot kg^{-1} \cdot h^{-1}$)	AMS ($mg \cdot kg^{-1} \cdot h^{-1}$)	Exhaustion time (s)	n
20	2.5	5.74_{a} (0.01)	404_{b} (67)	340_{b} (17)	1.00_{a} (0.04)	79_{ab} (15)	$274_{a,1}$ (60)	$194_{a,1}$ (47)	8499_{1} (957)	5
20	3.0	6.89_{b} (0.04)	447_{b} (37)	348_{b} (13)	1.04_{a} (0.04)	73_{ab} (21)	$294_{a,2}$ (36)	$221_{a,2}$ (27)	8994_{1} (1118)	5
20	4.0	9.14_{c} (0.02)	386_{b} (53)	337_{b} (13)	0.99_{a} (0.03)	64_{ab} (13)	$398_{a,3}$ (42)	$334_{a,3}$ (43)	$10{,}954_{2}$ (923)	5
25	2.5	6.27_{d} (0.01)	504_{a} (67)	364_{a} (17)	1.03_{ab} (0.07)	75_{b} (15)	$279_{ab,1}$ (29)	$203_{ab,1}$ (21)	9932_{1} (1497)	7
25	3.0	7.55_{e} (0.01)	512_{a} (43)	366_{a} (14)	1.03_{ab} (0.04)	83_{b} (25)	$311_{ab,2}$ (34)	$227_{ab,2}$ (31)	$10{,}135_{1}$ (1460)	7
25	4.0	10.04_{f} (0.03)	504_{a} (65)	364_{a} (18)	1.03_{ab} (0.08)	66_{b} (9)	$429_{ab,3}$ (80)	$363_{ab,3}$ (77)	$12{,}016_{2}$ (2148)	7
32	2.5	6.83_{b} (0.02)	410_{b} (62)	349_{b} (11)	0.95_{b} (0.09)	106_{a} (34)	$334_{b,1}$ (28)	$227_{b,1}$ (46)	8727_{1} (1147)	5
32	3.0	8.16_{g} (0.01)	436_{b} (19)	353_{b} (10)	0.98_{b} (0.05)	101_{a} (21)	$376_{b,2}$ (28)	$275_{b,2}$ (33)	8710_{1} (1054)	5
32	4.0	10.91_{h} (0.04)	426_{b} (58)	354_{b} (12)	0.95_{b} (0.06)	93_{a} (8)	$530_{b,3}$ (37)	$436_{b,3}$ (35)	$10{,}440_{2}$ (610)	5

Fish were moved to an outside 12,000-L brackish-water flow-through system (salinity: ~5) on 9 April 2014 and held until they were brought indoors for acclimation. While held outside, they experienced natural lighting and temperature conditions similar to those of the Ashley River during spring and summer (ratio of hours of daylight to hours of night: ~12 h:12 h in spring and ~14 h:10 h in summer; temperature range: 20–30°C).

Before each set of experiments was conducted, a subset of striped bass (~50 fish for each temperature treatment) were moved into a circular 1600-L recirculating tank housed in an environmental chamber. Fish were held in lighting conditions with a ratio of 13 h of light to 11 h of dark and were acclimated to the desired salinity (1) and test temperature (20°C, 25°C, or 32°C) before testing. Dechlorinated tap water and Instant Ocean[6] sea salt (Instant Ocean, Blacksburg, VA) were used to make water with a salinity of 1. Fish in the group held in 20°C water were acclimated for a mean of 64 d (standard deviation [SD] 7) and range of 51–75 d, fish in the group held in 25°C water were acclimated for a mean of 26 d (SD 11) and a range of 9–47 d, and fish in the group held in 32°C water were acclimated for a mean of 46 d (SD 15) and a range of 26–70 d. Therefore, acclimation times ranged from 9 d to several weeks. Although 9 d is a relatively short thermal acclimation period, it was considered adequate because the temperature of the outside tank from which fish were collected before each experiment was similar to the temperatures of the experimental tanks (i.e., fish were moved to the 20°C tank in the spring and to the 25°C and 32°C tanks in the summer).

[6] Mention of trade names or commercial companies is for identification purposes only and does not imply endorsement by the National Marine Fisheries Service, NOAA.

To account for any effect of acclimation time on metabolic rates or swimming performance, we included acclimation time as a covariate in the statistical models. During the acclimation period, fish were fed to satiation once daily with a commercially pelleted diet (5.0-mm, slow-sinking Finfish Silver, Zeigler Bros. Inc., Gardners, PA).

Seven days prior to use in a trial, individual fish were transferred from the holding tank into a 70-L rectangular aquarium equipped with an air-driven Hydro-Sponge 1 filter (Aquarium Technology Inc., Decatur, GA) and an air stone to promote water mixing and oxygenation; all fish were held at air saturation >90% and at their test temperature. Water was changed in aquaria daily to prevent buildup of nitrogenous waste. Food was withheld during this 7-d period, which is an adequate amount of time to ensure that digestion and specific dynamic action do not influence oxygen consumption rates (Clark et al., 2013). Five fish held in 20°C water and 5 fish held in 32°C water were tested at each DO level; 7 fish held in 25°C water were tested at each DO level (Table 1).

Oxygen consumption measurements

Standard metabolic rate, MMR, and AMS were determined by using intermittent-flow respirometry at temperatures of 20°C, 25°C, and 32°C and DO concentrations of 4.0, 3.0, and 2.5 mg/L in a full factorial design. The PO_2 of each treatment combination is reported in Table 1. Trials on temperature-acclimated fish were conducted during 19 June–19 December 2014. The day prior to a trial, a single fish was anesthetized directly in its aquarium with Finquel tricaine methanesulfonate (Argent Chemical Laboratories Inc., Redmond, WA) at a concentration of 0.1 g/L. Fish were removed from the aquarium with a dip net and then measured and weighed (Table 1)

before transfer to a 90-L swim tunnel respirometer (Loligo Systems, Tjele, Denmark) containing water at a salinity of 1 and the treatment temperature. Blinders were placed over the front, working portion of the inner chamber to create a darkened environment for the fish and prevent accidental startling from personnel monitoring the swim chamber. Approximately 30 min was allowed for recovery from the effects of anesthesia, and recovery was defined as the return of fish to resting on the bottom of the respirometer in a normal posture and with normal patterns of resting gill ventilation.

After recovery, flow in the tunnel was set to 10 cm/s, and fish were left overnight (~1600–0900). The overnight period allowed fish to recover from any stress due to handling or effects of anesthesia because the results of preliminary overnight trials indicate that oxygen consumption returned to baseline approximately 5 h after transfer. The overnight period also allowed a fish time to orient itself in the swim tunnel against a low-velocity flow. The darkened front portion of the chamber aided fish in using the working portion of the chamber instead of resting against the back grid. During the overnight recovery period, the swim tunnel respirometer was continually flushed with water from the outer bath. An air stone was placed in the outer bath to achieve a constant ambient DO level of over 90%.

On the morning of each trial, a DO galvanic probe (MINI-DO, Loligo Systems; with accuracy of ±1% air saturation) was calibrated with a 2-point calibration method and secured in the inner chamber of the flume through a port. A bright light was placed over the back portion of the swim chamber to further encourage fish to use the darkened portion of the swim chamber. Water in the outer bath was deoxygenated by bubbling nitrogen gas through a high-pressure air stone. A solenoid valve, linked to the DO galvanic probe, controlled the flow of nitrogen gas in the outer chamber. The oxygen saturation in the inner chamber was lowered from the ambient level by continuously flushing in deoxygenated water from the outer bath. The treatment DO level was typically reached within 1 h. Once the treatment DO concentration was reached, fish were held at this concentration for 30 min to allow for acclimation.

After acclimation, flow in the chamber was increased and intermittent respirometry was used to repeatedly measure oxygen consumption. Oxygen consumption measurements were recorded in milligrams per kilogram per hour in 7-min intervals that consisted of a 2-min flush, followed by a 1-min equilibration period then a 4-min measurement period in which oxygen saturation was recorded once every second. The flush cycle served, among other things, to restore oxygen that had been depleted during each equilibration and measurement period. The speed of water flow in the chamber was increased by 15 cm/s every 42–56 min, resulting in 6–8 oxygen consumption measurements at each speed. At least 3 of those measurements were more than 20 min after the speed change; these measurements were required for SMR calculations (see the next section).

Trials ended when the fish was exhausted, which was defined as failure to swim against the current and use of the tail to maintain position against the back screen for at least 15 s. A recent review of methods for eliciting MMR found that the swim-tunnel method is acceptable for species, such as the striped bass, that are active swimmers (Norin and Clark, 2016). The timing of exhaustion was calculated by subtracting the time that we increased speed for the first speed increment of the trial from the time at which the fish became exhausted. After exhaustion, flow in the chamber was decreased to 10 cm/s, water was brought to a DO level of 100%, and fish were left to rest for 15 min before being transferred to the recovery tank. After the fish was removed, the chamber was closed again and 3 measurements of background oxygen consumption were recorded by using the previously described 7-min cycle.

Metabolic calculations

Mean background bacterial oxygen consumption was appreciable at each temperature (20°C: 12.1 mg/h [SD 2.8]; 25°C: 28.9 mg/h [SD 8.9]; and 32°C: 32.6 mg/h [SD 12.3]). Note that these levels represent a substantial portion of the measured oxygen consumption values (39% [SD 12] when measuring SMR and 13% [SD 6] when measuring MMR, averaged across all temperature and DO-level treatments). Although these values are relatively high, they likely occurred because 1) fish were acclimated in the respirometry system for ~12–16 h prior to measurements being recorded and 2) the dechlorinated tap water used to fill the flume was held in 200-L bins for 2–3 d prior to testing to allow it to reach the testing temperature (also see Svendsen et al., 2016). Therefore, the average background bacterial oxygen consumption (computed from the 3 measurements made for that trial) was subtracted from the total recorded oxygen consumption to calculate the oxygen consumption of the fish (Svendsen et al., 2016).

The SMR for each individual was calculated by fitting a linear function to the log of oxygen consumption on swimming speed (Fig. 2) and then by using this function to extrapolate the SMR at a speed of zero (Brett, 1964; Fry, 1971). Only oxygen consumption values measured 20 min after each speed change were used in the calculations for SMR. The MMR was the single maximum oxygen consumption rate achieved by the fish during the entire trial. This reading occurred approximately 50% of the time at the maximum speed step and the other 50% of the time at the speed step just before the maximum. The AMS for each fish was calculated as follows:

$$AMS = MMR - SMR, \quad (1)$$

where AMS = aerobic metabolic scope ($mg \cdot kg^{-1} \cdot h^{-1}$);
MMR = maximum metabolic rate ($mg \cdot kg^{-1} \cdot h^{-1}$); and
SMR = standard metabolic rate ($mg \cdot kg^{-1} \cdot h^{-1}$).

Statistical analysis

All analyses were completed in JMP 13 (SAS Institute Inc., Cary, NC). Differences in weight and relative condition factor (Kn; Le Cren, 1951) between treatments were analyzed

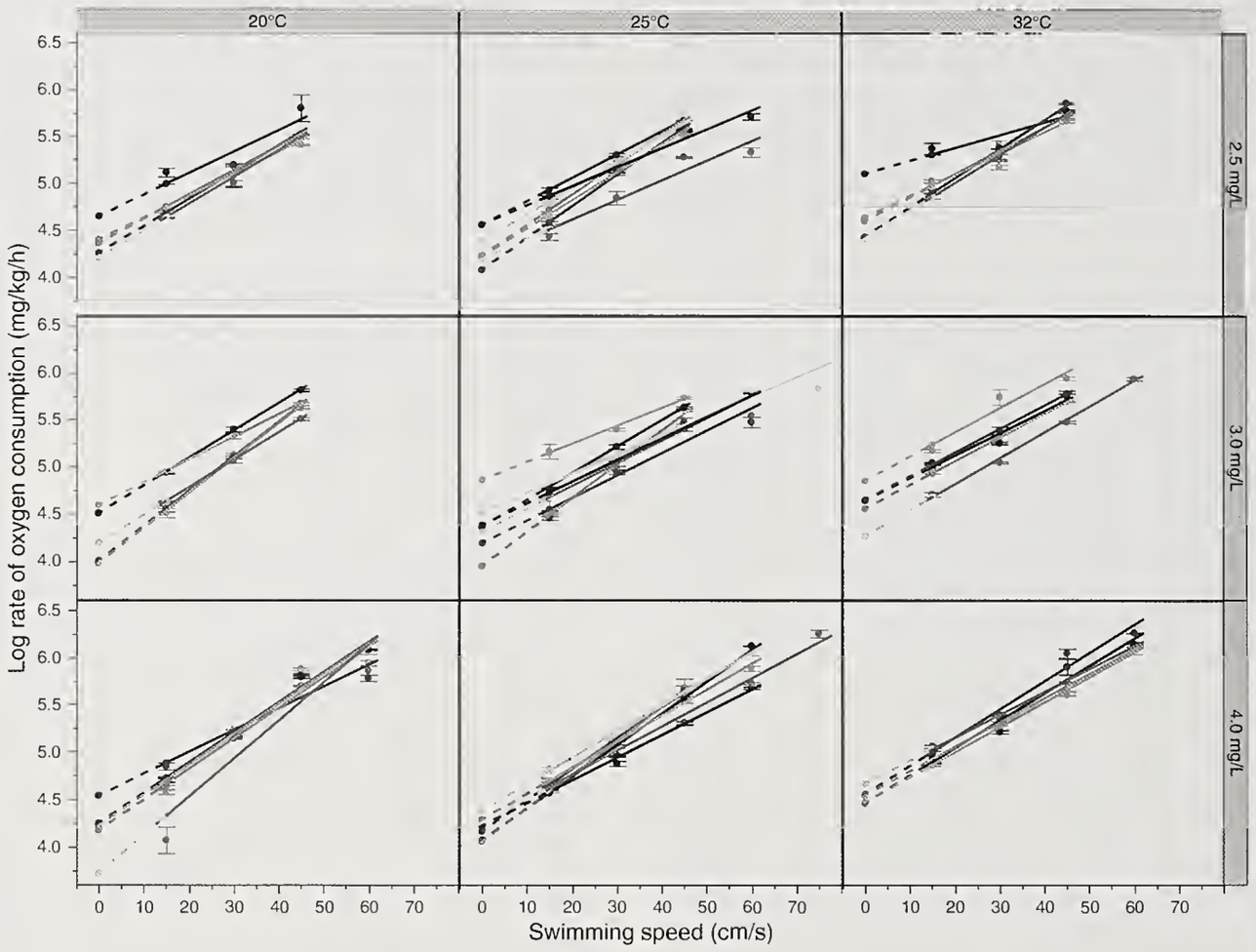

Figure 2

Mean log rate of oxygen consumption by striped bass (*Morone saxatilis*) as a function of swimming speed for each treatment combination of temperature and dissolved oxygen (DO) level. Individual replicates are differentiated by differently shaded lines within each panel. The dashed lines on the left side of each panel show the extrapolation of log standard metabolic rate to a speed of zero. Error bars indicate the standard error of mean oxygen consumption at each speed for each individual. Trials were conducted in aquarium tanks at the Marine Resources Research Institute, South Carolina Department of Natural Resources, from June through December 2014.

by using analysis of variance with the Tukey's honestly significant difference (HSD) test (Table 1). The *Kn* was calculated with the following equation:

$$Kn = \left(\frac{W}{\hat{W}}\right), \quad (2)$$

where W = weight (in grams) and

$\hat{W}$ = the fish weight (in grams) predicted from the least squares regression of log W on the log of the fish TL.

Measures of SMR, MMR, AMS, and exhaustion time were log transformed to meet assumptions of normality of residuals and homogeneity of variance, which were verified by using Shapiro-Wilk and Levene tests, respectively. Separate linear models that use standard least squares were used to test the effects of treatment temperature, DO concentration, weight, *Kn*, and acclimation time of fish on SMR, MMR, AMS, and exhaustion time. A similar set of linear models were also generated with the PO_2 in place of DO concentration; this second set of models was used to examine the effect of uneven PO_2 across combinations of temperature and dissolved oxygen on the metabolism and exhaustion time. This entire analysis was repeated except the SMR, MMR, and AMS values were not adjusted for weight (i.e., values were not divided by fish weight; therefore, they were absolute, or raw, metabolic rates in milligrams per hour). This second round of analysis with unadjusted values was done to understand differences in the effects of temperature or DO concentration due to estimating SMR, MMR, and AMS as ratios (with weight in the denominator) rather than using raw metabolic rates. For all analyses, Tukey's HSD tests were used where appropriate to assess differences among treatments. For all statistical tests, the significance level or alpha level was set at 0.05.

Ethical approval

All applicable international, national, and institutional guidelines for the care and use of animals were followed. All procedures in this study involving animals were performed in accordance with the ethical standards of the institution or practice at which the procedures were conducted. Procedures used in this research were covered under College of Charleston Institutional Animal Care and Use Committee protocol 2016-01-29-081028.

Results

During all trials, the decrease in oxygen saturation in the chamber during the measurement period was linear (mean coefficient of determination [r^2]: 0.99 [SD 0.01]), indicating that the chamber had no leakage (Svendsen et al., 2016). The decrease in oxygen saturation observed while measuring background oxygen consumption was also linear (mean r^2: 0.92 [SD 0.13]). Groups of fish used to compare among treatment temperatures had significantly different wet weights ($F_{2,46}$=16.76, P<0.01), TL ($F_{2,46}$=12.60, P<0.01), and *Kn* ($F_{2,46}$=6.31, P<0.01) (Table 1), although these same factors were similar across all DO-concentration treatments (weight: $F_{2,46}$=0.50, P=0.61; TL: $F_{2,46}$=1.12, P=0.34; *Kn*: $F_{2,46}$=1.05, P=0.36; Table 1).

Strong linear relationships of the log of oxygen consumption on swimming speed allowed for calculation of SMR by extrapolation to zero for each individual (mean r^2: 0.95 [SD 0.07]). The SMRs of striped bass were significantly different across temperatures, with the SMR at 25°C being significantly lower than the SMR at 32°C and with the SMR at 20°C being intermediate and not significantly different from the SMRs at the other temperatures (Tables 1 and 2, Fig. 3A). Standard metabolic rate was not significantly affected by treatment DO concentration, the interaction of temperature and DO level, weight, or *Kn* (Table 2). The results were slightly different when DO concentration was replaced with PO_2 in the linear models: PO_2 was marginally negatively related to SMR (Table 2), and the SMR was higher for the 32°C treatment than for the 20°C and 25°C treatments. The models that used raw SMR were qualitatively similar (Table 2), with the exception that fish wet weight was positively related to SMR as would be expected.

The MMRs were significantly different across temperature and DO-level treatments, although the interaction of these 2 factors was not significant (Table 2). The MMR at 20°C was significantly lower than the MMR at 32°C, and the MMR at 25°C was intermediate and not significantly different from the MMRs at other temperatures (Table 1, Fig. 3). The MMRs increased significantly with increasing DO concentration (Table 1, Fig. 3). Maximum metabolic rate was negatively related to *Kn* but not to weight (Table 2). When DO level was replaced with PO_2 in the linear models, PO_2 was positively related and *Kn* was still negatively related to MMR. However, treatment

Table 2

Results from linear models used to test the effects of treatment temperature, dissolved oxygen (DO) concentration, partial pressure of oxygen (PO_2), fish wet weight, fish relative condition factor (*Kn*), and acclimation time of striped bass (*Morone saxatilis*) on standard metabolic rate (SMR), maximum metabolic rate (MMR), aerobic metabolic scope (AMS), and exhaustion time. The top half of the table shows results for models with DO concentration at fixed-level treatments (2.5, 3.0, and 4.0 mg/L). The bottom half shows actual PO_2 in each treatment (a continuous variable). Values for SMR, MMR, and AMS were calculated by dividing oxygen consumption per hour by fish wet weight. Absolute or raw SMR, MMR, and AMS were calculated as metabolic rates not divided by fish wet weight. The degrees of freedom (df) numerator and denominator used to test each parameter in each model are separated by a comma. An alpha level of 0.05 was used to establish significance. Data used in models came from trials conducted at the Marine Resources Research Institute, South Carolina Department of Natural Resources, from June through December 2014.

	SMR		MMR		AMS		Raw SMR		Raw MMR		Raw AMS		Exhaustion time		
Model	*F*	*P*	*F*	*P*	*F*	*P*	*F*	*P*	*F*	*P*	*F*	*P*	*F*	*P*	df
Temperature	8.55	<0.01	8.42	<0.01	4.02	0.03	9.18	<0.01	9.16	<0.01	4.21	0.02	3.13	0.05	2,39
DO (mg/L)	2.22	0.12	54.0	<0.01	72.4	<0.01	2.23	0.12	52.6	<0.01	71.8	<0.01	15.2	<0.01	2,39
Temp*DO	0.24	0.91	0.29	0.88	0.68	0.61	0.22	0.92	0.33	0.86	0.73	0.58	0.23	0.92	4,39
Acclimation	2.24	0.14	0.70	0.41	0.13	0.72	2.56	0.12	1.08	0.31	0.04	0.85	1.70	0.20	1,39
Kn	0.21	0.65	4.89	0.03	3.81	0.06	0.09	0.76	3.63	0.06	2.95	0.09	3.66	0.06	1,39
Wet weight	0.41	0.53	1.87	0.18	4.03	0.05	16.6	<0.01	26.1	<0.01	11.0	<0.01	5.70	0.02	1,39
Temperature	10.4	<0.01	0.85	0.44	0.69	0.51	11.2	<0.01	1.31	0.28	0.37	0.69	6.87	<0.01	2,42
PO_2 (kPa)	4.49	0.04	116	<0.01	150	<0.01	4.45	0.04	113	<0.01	148	<0.01	30.9	<0.01	1,42
Temp*PO_2	0.21	0.77	0.03	0.97	0.11	0.90	0.22	0.81	0.04	0.96	0.10	0.91	0.75	0.48	2,42
Acclimation	2.88	0.10	0.60	0.44	0.31	0.58	3.26	0.08	0.97	0.33	0.14	0.71	2.02	0.16	1,42
Kn	0.31	0.58	5.26	0.03	3.55	0.07	0.14	0.71	3.73	0.06	2.58	0.12	4.76	0.03	1,42
Wet weight	0.44	0.51	1.96	0.17	3.92	0.05	18.4	<0.01	30.9	<0.01	13.2	<0.01	5.44	0.02	1,42

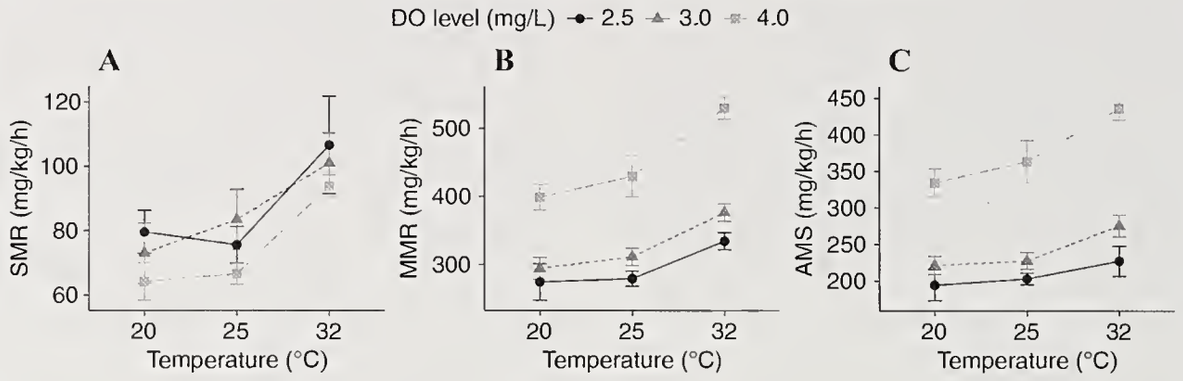

Figure 3

Effects of temperature and dissolved oxygen (DO) level on (**A**) standard metabolic rate (SMR), (**B**) maximum metabolic rate (MMR), and (**C**) aerobic metabolic scope (AMS) of juvenile striped bass (*Morone saxatilis*) during trials conducted in aquarium tanks at the Marine Resources Research Institute, South Carolina Department of Natural Resources, from June through December 2014. Error bars indicate standard errors of the mean.

temperature was no longer related to MMR (Table 2). The results were similar when these analyses were run with raw MMR as the response, except that the MMR at 32°C was significantly greater than the MMRs at both 20°C and 25°C, *Kn* was not related to raw MMR, and weight was positively related to raw MMR (Table 2).

The values of AMS were significantly different across temperatures and DO levels, although the interaction between treatments was not significant (Table 2). The AMS at 20°C was significantly lower than the AMS at 32°C, and the AMS at 25°C was intermediate and not significantly different from the AMS values at other temperatures (Table 1, Fig. 3). The AMS values increased with increasing DO concentration (Table 1, Fig. 3). Aerobic metabolic rate was negatively related to weight but was not related to *Kn* (Table 2). The results were similar when DO level was replaced with PO_2 in the linear model, except that treatment temperature was no longer related to AMS and PO_2 was positively related to AMS (Table 2). The results were similar when raw AMS was used as the response, except that fish wet weight was positively related to AMS (Table 2).

Exhaustion time was significantly different across DO levels (Table 2). Fish in the 4.0-mg/L treatment had significantly longer exhaustion times compared with fish in the 3.0-mg/L and 2.5-mg/L treatments (Table 1). Neither temperature nor the interaction between treatments were significant terms in the model (Table 2). Exhaustion time was positively related to fish wet weight (Table 2). When DO concentration was replaced with PO_2 in the linear model, PO_2 and fish wet weight were both positively related to exhaustion time and *Kn* was negatively related to exhaustion time. Treatment temperature was a significant predictor of exhaustion time when PO_2 was used (Table 2), with exhaustion times significantly longer at 25°C than at 32°C and with exhaustion time at 20°C being intermediate and not significantly different from the exhaustion times at 25°C or 32°C.

Discussion

This study is the first to investigate the effects of temperature and DO concentration on the metabolism of striped bass in coastal waters of the southeastern United States. Within the range tested, SMR was greatest at 32°C. The SMRs increased with increasing temperature at DO levels of 3.0 and 4.0 mg/L (Fig. 2), supporting our first prediction. Notably, at a DO concentration of 2.5 mg/L, SMR was lowest at 25°C, a result that may have been influenced by high variability and small sample size. The MMRs increased with increasing temperature at all DO levels. Contrary to our second prediction, MMR was highest at 32°C at every DO level. The increase in both SMR and AMS with temperature caused a net increase in AMS across temperature. Again, contrary to predictions, AMS was highest at 32°C. Although increases in SMR and MMR are predicted within a normal temperature range, the magnitude of these changes was lower than expected. The Q_{10} temperature coefficient is a measure of the rate of change of a process as a consequence of increasing the temperature by 10°C. In a normal temperature range, Q_{10} values of 2–3 are expected, but in this study a Q_{10} value of approximately 1.3 was observed for SMR and MMR. The relatively parallel changes in SMR and MMR led to a Q_{10} value of 1.2 for AMS, indicating wide thermal breadth for striped bass in the study area. This result may indicate that southern stocks of striped bass are well equipped to cope with temperature fluctuations, which are common in their estuarine habitat.

The results of previous studies of northern populations of striped bass indicate an optimum temperature in the mid-20s (degrees Celsius) (Coutant and Carrol, 1980; Coutant et al., 1984) and a lethal temperature in the lower 30s (degrees Celsius), depending on life stage (Tagatz[4]; Gift, 1970). These findings indicate that our highest treatment temperature (32°C) may be approaching the lethal

limit. In this study, MMR increased with temperature all the way up to 32°C (Table 1, Fig. 3). The rise in MMR, in concurrence with the smaller increase in SMR, resulted in a steady rise in AMS across all temperatures. In effect, the decrease in MMR and, therefore, in AMS at high temperatures that should signal the onset of thermal intolerance (Pörtner, 2001, 2002) was absent in our sample of juvenile striped bass.

Although high temperature did not decrease the AMS available for striped bass, low DO levels did decrease it, with both MMR and AMS declining at the lower DO levels tested. These results support our third prediction. In fact, DO concentration clearly played an important role in limiting MMR and AMS. Most notably, the sharp differences between the values of AMS at the DO level of 4.0 mg/L and the values of AMS at DO levels of 2.5 or 3.0 mg/L (Fig. 3, B–D) indicate that DO level has a greater influence on AMS than the range of water temperatures used in our study. Even when DO concentration remained above a level that would directly cause fish mortality (e.g., 2 mg/L), the reduction in AMS that was observed in this study with low environmental DO concentration could limit the capacity of striped bass for locomotion, foraging, growth, or reproduction (Coutant, 1990; Neill and Bryan, 1991). These conclusions are further supported by the results of our analyses based on PO_2 because, in models that used it, PO_2 was significantly positively related to AMS and MMR but temperature was not (Table 2).

Fish that were exercised at lower DO levels had shorter exhaustion times, further supporting the findings that low DO concentration plays a larger role in limiting metabolic capacities than temperature. At every temperature tested, fish exercised at a DO level of 4.0 mg/L had significantly longer exhaustion times (Table 1). Although there was no statistically significant effect of temperature on exhaustion time, fish that were acclimated and exercised at 25°C had slightly longer exhaustion times on average, and swam to greater speeds, than their counterparts at other temperatures (Table 1, Fig. 2). This trend is more pronounced when PO_2 is substituted in the model, with exhaustion time being significantly longer at 25°C (Table 2). This result indicates that, although AMS may not be optimal at 25°C, swimming performance may be higher at this intermediate temperature.

The overall effects of high temperature on survival of southern populations of striped bass remain unknown; however, the striped bass used in this study were not likely to have been metabolically limited in the Ashley River. Temperatures above 32°C are rare and brief in this river. Although DO levels between 3.0 and 4.0 mg/L are common, DO concentrations below 3.0 mg/L account for only 1% of all values recorded at water-quality stations during June–August (M. Denson, unpubl. data). Several caveats, however, should be noted.

First, because of the decline in AMS with decreasing DO concentration, occupancy of hypoxic habitats (DO levels <3 mg/L) may have long-term metabolic costs, which could eventually affect growth and reproduction depending on the amount of time spent under such conditions. Second, temperatures in the southeastern United States are projected to increase by 2.2–4.4°C by the end of this century, with an additional 10–40 d over 35°C per year in South Carolina (Carter et al., 2014). The maximum temperature that fish will be exposed to and the amount of time spent at high temperatures will increase. If 32°C is near the optimum for AMS, an increase in temperature by a few degrees could drastically decrease AMS, limiting available summer habitat for wild striped bass in rivers of the southeastern United States. Lastly, metabolic tolerances in relation to temperature and DO concentration may change as fish grow and age. In northern populations, adult striped bass have a lower temperature tolerance than juveniles. Additionally, Johnson (2015) found that age-0 striped bass in the Ashley River have positive growth rate potential over a wider range of temperatures than older fish. It is reasonable to conclude that in southern populations, AMS of adult striped bass will decrease at a lower temperature than it would for juveniles. Lower AMS at high temperatures will likely increase mortality and reduce the reproductive potential of a population.

Larger fish had greater raw MMR and AMS and longer exhaustion times, a finding similar to those of several previous studies (Clarke and Johnston, 1999; Killen et al., 2006; Norin and Malte, 2011). This observation reflects the greater abilities of larger individuals. Although raw AMS is greater in larger fish, larger fish will also face absolutely greater metabolic demands from the physiological systems that support swimming. Therefore, the larger AMS of larger fish may not convey a greater ability to deal with variable environmental conditions. Conversely, heavier fish had lower relative AMS and MMR (i.e., size-adjusted metabolic rates). The negative relationship between weight and size-adjusted active metabolism can be explained by the supposition that heavier fish contain more stored reserves that are not involved in active metabolism (Brett, 1964). Lapointe et al. (2014) measured the AMS of larger Chesapeake Bay striped bass (mean weight: 1300g) under hypoxic conditions with a DO level of 3 mg/L. At 20°C, the striped bass used in our study had 80% greater AMS than the larger striped bass used by Lapointe et al. (2014), although a portion of this difference could be due to differences between northern and southern populations. We note that the aim of our study was to determine the AMS of striped bass that were most comparable to large age-1 or small age-2 wild fish during the summer in South Carolina. Therefore, a relatively small range of weights and Kn were intentionally used in this study. The consequence of this narrow size range is that the significant relationship between weight and AMS may not hold for striped bass of other sizes in South Carolina.

Given trends in the recapture of striped bass by the SCDNR in the Ashley River and knowledge of the physical conditions within this river, juvenile striped bass are occupying habitats that, during the warmest days of summer, are near the edge of their thermal tolerance. We predict

that these same habitats will become less tolerable as fish age. Additionally, they will likely become less habitable, even for juveniles, as the warm periods of summer increase in duration and in maximum temperature as a result of climate change.

Acknowledgments

This work was supported by funds from the South Carolina Saltwater Fishing License Funds and the U.S. Fish and Wildlife Service State Wildlife Grant Program. Larvae of striped bass were provided by the Jack D. Bayless Hatchery in South Carolina. Many thanks are due to the staff of the SCDNR mariculture program for providing the animals used in this study and for aiding in setup and execution of experimental trials. This manuscript is contribution number 816 from the SCDNR MRRI.

Literature cited

Bjorgo, K. A., J. J. Isely, and C. S. Thomason.
2000. Seasonal movement and habitat use by striped bass in the Combahee River, South Carolina. Trans. Am. Fish. Soc. 129:1281–1287.

Brett, J. R.
1964. The respiratory metabolism and swimming performance of young sockeye salmon. J. Fish. Res. Board Can. 21:1183–1226.

Bulak, J. S., C. S. Thomason, K. Han, and B. Ely.
2004. Genetic variation and management of striped bass populations in the coastal rivers of South Carolina. North Am. J. Fish. Manage. 24:1322–1329.

Carter, L. M., J. W. Jones, L. Berry, V. Burkett, J. F. Murley, J. Obeysekera, P. J. Schramm, and D. Wear.
2014. Southeast and the Caribbean. *In* Climate change impacts in the United States: the third national climate assessment (J. M. Melillo, T. C. Richmond, and G. W. Yohe, eds.), p. 396–417. U.S. Global Chang. Res. Program, Washington, DC.

Clark, T. D., K. M. Jeffries, S. G. Hinch, and A. P. Farrell.
2011. Exceptional aerobic scope and cardiovascular performance of pink salmon (*Oncorhynchus gorbuscha*) may underlie resilience in a warming climate. J. Exp. Biol. 214:3074–3081.

Clark, T. D., E. Sandblom, and F. Jutfelt.
2013. Aerobic scope measurements of fishes in an era of climate change: respirometry, relevance and recommendations. J. Exp. Biol. 216:2771–2782.

Clarke, A., and N. M. Johnston.
1999. Scaling of metabolic rate with body mass and temperature in teleost fish. J. Anim. Ecol. 68:893–905.

Coutant, C. C.
1985. Striped bass, temperature, and dissolved oxygen: a speculative hypothesis for environmental risk. Trans. Am. Fish. Soc. 114:31–71.
1990. Temperature-oxygen habitat for freshwater and coastal striped bass in a changing climate. Trans. Am. Fish. Soc. 119:240–253.

Coutant, C. C., and D. S. Carroll.
1980. Temperatures occupied by ten ultrasonic-tagged striped bass in freshwater lakes. Trans. Am. Fish. Soc. 109:195–202.

Coutant, C. C., and D. L. Benson.
1990. Summer habitat suitability for striped bass in Chesapeake Bay: reflections on a population decline. Trans. Am. Fish. Soc. 119:757–778.

Coutant, C. C., K. L. Zachman, D. K. Cox, and B. L. Pearman.
1984. Temperature selection by juvenile striped bass in laboratory and field. Trans. Am. Fish. Soc. 113:666–671.

Farquhar, B. W., and S. Gutreuter.
1989. Distribution and migration of adult striped bass in Lake Whitney, Texas. Trans. Am. Fish. Soc. 118: 523–532.

Farrell, A. P., and J. G. Richards.
2009. Defining hypoxia: an integrative synthesis of the responses of fish to hypoxia. *In* Hypoxia. Fish physiology, vol. 27 (J. G. Richards, A. P. Farrell, and C. J. Brauner, eds.), p. 487–503. Academic Press, London.

Farrell, A. P., S. G. Hinch, S. J. Cooke, D. A. Patterson, G. T. Crossin, M. Lapointe, and M. T. Mathes.
2008. Pacific salmon in hot water: applying aerobic scope models and biotelemetry to predict the success of spawning migrations. Physiol. Biochem. Zool. 81:697–709.

Fry, F. E. J.
1947. Effects of the environment on animal activity. Univ. Toronto Stud., Biol. Ser. 55, Publ. Ontario Fish. Res. Lab. 68, 62 p.
1971. The effect of environmental factors on the physiology of fish. *In* Fish physiology, vol. 6 (W. S. Hoar and D. J. Randall, eds.), p. 1–98. Academic Press, New York.

Fry, F. E. J., and J. S. Hart.
1948. The relation of temperature to oxygen consumption in the goldfish. Biol. Bull. 94:66–77.

Gift, J. J.
1970. Responses of some estuarine fishes to increasing thermal gradients. Ph.D. diss., 199 p. Rutgers Univ., New Brunswick, NJ.

Hochachka, P. W., and G. N. Somero.
2002. Biochemical adaptation: mechanism and process in physiological evolution, 480 p. Oxford Univ. Press, New York.

Johnson, S. P.
2015. Field validation and application of two bioenergetics models to evaluate relative habitat quality for coastal striped bass (*Morone saxatilis*) in the southeastern United States. M.S. thesis, 105 p. Coll. Charleston, Charleston, SC. [Available from website.]

Killen, S. S., I. Costa, J. A. Brown, and A. K. Gamperl.
2006. Little left in the tank: metabolic scaling in marine teleosts and its implications for aerobic scope. Proc. Royal Soc. B. 274:431–438.

Lapointe, D., W. K. Vogelbein, M. C. Fabrizio, D. T. Gauthier, and R. W. Brill.
2014. Temperature, hypoxia, and mycobacteriosis: effects on adult striped bass *Morone saxatilis* metabolic performance. Dis. Aquat. Org. 108:113–127.

Le Cren, E. D.
1951. The length-weight relationship and seasonal cycle in gonad weight and condition in the perch (*Perca fluviatilis*). J. Anim. Ecol. 20:201–219.

Merriman, D.
1941. Studies on the striped bass (*Roccus saxatilis*) of the Atlantic coast. Fish. Bull. 50:1–77.

Metcalfe, N. B., T. E. Van Leeuwen, and S. S. Killen.
2016. Does individual variation in metabolic phenotype predict fish behaviour and performance? J. Fish Biol. 88:298–321.

Neill, W. H., and J. D. Bryan.
1991. Responses of fish to temperature and oxygen, and response integration through metabolic scope. *In* Aquaculture and water quality: advances in world aquaculture, vol. 3 (D. E. Brune and J. R. Tomasso, eds.), p. 30–57. World Aquac. Soc., Baton Rouge, LA.

Norin, T., and H. Malte.
2011. Repeatability of standard metabolic rate, active metabolic rate and aerobic scope in young brown trout during a period of moderate food availability. J. Exp. Biol. 214:1668–1675.

Norin, T., and T. D. Clark.
2016. Measurement and relevance of maximum metabolic rate in fishes. J. Fish Biol. 88:122–151.

Pörtner, H. O.
2001. Climate change and temperature-dependent biogeography: oxygen limitation of thermal tolerance in animals. Naturwissenschaften 88:137–146.
2002. Climate variations and the physiological basis of temperature dependent biogeography: systemic to molecular hierarchy of thermal tolerance in animals. Comp. Biochem. Physiol. A. 132:739–761.
2010. Oxygen- and capacity-limitation of thermal tolerance: a matrix for integrating climate-related stressor effects in marine ecosystems. J. Exp. Biol. 213:881–893.

Pörtner, H. O., and R. Knust.
2007. Climate change affects marine fishes through the oxygen limitation of thermal tolerance. Science 315:95–97.

Pörtner, H. O., and A. P. Farrell.
2008. Physiology and climate change. Science 322:690–692.

Reidy, S. P., S. R. Kerr, and J. A. Nelson.
2000. Aerobic and anaerobic swimming performance of individual Atlantic cod. J. Exp. Biol. 203:347–357.

Ruane, R. J., G. E. Hauser, and A. F. Sawyer.
2013. Water quality modelling as a management tool for striped bass and hybrid striped bass. Am. Fish. Soc. Symp. 80:161–179.

Schaffler, J. J., J. J. Isely, and W. E. Hayes.
2002. Habitat use by striped bass in relation to seasonal changes in water quality in a southern reservoir. Trans. Am. Fish. Soc. 131:817–827.

Setzler, E. M., W. R. Boynton, K. V. Wood, H. H. Zion, L. Lubbers, N. K. Mountford, P. Frere, L. Tucker, and J. A. Mihursky.
1980. Synopsis of biological data on striped bass, *Morone saxatilis* (Walbaum). NOAA Tech. Rep. NMFS Circ. 433, 69 p.

Svendsen, M. B. S., P. G. Bushnell, and J. F. Steffensen.
2016. Design and setup of intermittent-flow respirometry system for aquatic organisms. J. Fish Biol. 88:26–50.

Young, S. P., and J. J. Isely.
2002. Striped bass annual site fidelity and habitat utilization in J. Strom Thurmond Reservoir, South Carolina–Georgia. Trans. Am. Fish. Soc. 131:828–837.

Zale, A. V., J. D. Weichman, R. L. Lochmiller, and J. Burroughs.
1990. Limnological conditions associated with summer mortality of striped bass in Keystone Reservoir, Oklahoma. Trans. Am. Fish. Soc. 119:72–76.

National Marine
Fisheries Service
NOAA

Fishery Bulletin
established in 1881

Spencer F. Baird
First U.S. Commissioner
of Fisheries and founder
of *Fishery Bulletin*

Fine-scale behavior and habitat use of the endangered smalltooth sawfish (*Pristis pectinata*): insights from accelerometry

Karissa O. Lear (contact author)[1,2]
Gregg R. Poulakis[3]
Rachel M. Scharer[3]
Adrian C. Gleiss[2]
Nicholas M. Whitney[1,4]

Email address for contact author: k.lear@murdoch.edu.au

[1] Behavioral Ecology and Physiology Program
Mote Marine Laboratory
1600 Ken Thompson Parkway
Sarasota, Florida 34236

[2] Centre for Sustainable Aquatic Ecosystems
Harry Butler Institute
Murdoch University
90 South Street
Murdoch, Western Australia 6150, Australia

[3] Charlotte Harbor Field Laboratory
Fish and Wildlife Research Institute
Florida Fish and Wildlife Conservation Commission
585 Prineville Street
Port Charlotte, Florida 33954

[4] Anderson Cabot Center for Ocean Life
New England Aquarium
1 Central Wharf
Boston, Massachusetts 02110

Abstract—Determining movement, behavior, and activity patterns is of central importance to conservation efforts for threatened and endangered species because this knowledge is crucial for prioritizing management actions. In this study, we used acceleration data loggers (ADLs) concurrently with passive acoustic monitoring to examine behavior, activity patterns, and habitat use of juvenile smalltooth sawfish (*Pristis pectinata*) in a Florida nursery. Data from the ADLs indicate that smalltooth sawfish were more active and that more burst events indicative of foraging occurred during the evening and night than during the day. Smalltooth sawfish were also most active at depths <1 m and during low tides. The locations of individuals derived from acoustic monitoring techniques indicate that they were less active while in mangrove creek habitats and were more active and more likely to engage in burst activity in habitats within the main stem of the Peace River. This study is the first one to deploy ADLs on smalltooth sawfish, and results describe their fine-scale activity and behavior, clarifying patterns of habitat use by this endangered species in one of their few remaining nurseries.

Manuscript submitted 19 March 2019.
Manuscript accepted 7 November 2019.
Fish. Bull. 117:348–359 (2019).
Online publication date: 17 December 2019.
doi: 10.7755/FB.117.4.7

The views and opinions expressed or implied in this article are those of the author (or authors) and do not necessarily reflect the position of the National Marine Fisheries Service, NOAA.

Sawfish species compose what is considered one of the most threatened groups of chondrichthyans worldwide, with all 5 species listed as endangered or critically endangered by the International Union for the Conservation of Nature (IUCN) (Dulvy et al., 2014, 2016). The smalltooth sawfish (*Pristis pectinata*) is a coastal elasmobranch that inhabits estuaries and nearshore environments in the western Atlantic Ocean and Gulf of Mexico. Once common in the United States from Texas to North Carolina (Bigelow and Schroeder, 1953), this species is now restricted to less than 20% of its former range (Dulvy et al., 2016). Like that of other sawfish species, the decline in this population can largely be attributed to mortality from bycatch because their rostrum is easily entangled in fishing gear. Declines in populations of sawfish species have also been partially attributed to habitat destruction (Dulvy et al., 2016). In 2003, the smalltooth sawfish was federally protected and listed as endangered under the U.S. Endangered Species Act (Federal Register, 2003), and this species is listed as critically endangered on the IUCN Red List of Threatened Species (Carlson et al., 2013).

Although there is widespread concern regarding the protection and rebuilding of populations of smalltooth sawfish, little is known about their behavior and activity patterns. Previous studies have determined that smalltooth sawfish use the lower reaches of rivers, estuaries, and coastal bays as nurseries for about the first 3 years of life (Scharer et al., 2012). This species is particularly vulnerable to anthropogenic factors during this part of the juvenile stage, given that most of their known nurseries are surrounded by developed areas or subject to multiple fisheries (Norton et al., 2012). As a result, interactions with humans or recreational fishing gear are common (Seitz and Poulakis, 2006), and habitat destruction, pollution, and coastal

developments are likely to have substantial, cumulative negative effects. Additionally, the high site fidelity of juveniles (Poulakis et al., 2016; Huston et al., 2017) means that these fish must cope with a wide range of environmental conditions (Poulakis et al., 2011, 2013), including extreme weather events (Scharer et al., 2017; Poulakis and Grubbs, 2019).

Acoustic tracking and monitoring of smalltooth sawfish in nursery habitats has provided valuable information regarding the long-term horizontal movement patterns of these animals (e.g., Simpfendorfer et al., 2011; Poulakis et al., 2013; Scharer et al., 2017); for example, this technique has been used to identify hotspots that represent the most productive habitats within nurseries (Poulakis et al., 2011, 2013; Huston et al., 2017). However, acoustic monitoring provides information only about the use of horizontal space by individuals, and as a result, little is known about the behavior of smalltooth sawfish or why they use specific microhabitats within their nurseries. One method of determining such fine-scale behavioral patterns is to use acceleration data-loggers (ADLs), which in recent years have been proven to be effective in linking behavior and physiology of species similar to the smalltooth sawfish (Gleiss et al., 2017; Whitney et al., 2018). This technology can be used to produce information about behavior and activity patterns without the need to continuously track or observe individuals.

In this study, to determine fine-scale habitat use and behavioral patterns, we deployed triaxial ADLs and acoustic transmitters concurrently on juvenile smalltooth sawfish in the Peace River, Florida, one of the known nurseries for this species. Behavioral and activity patterns measured by the ADLs were examined in combination with horizontal movement patterns measured by the acoustic transmitters, and the results of this analysis provide information on how smalltooth sawfish used specific habitats and depth ranges within this nursery.

Materials and methods

Between May 2014 and November 2015, 10 smalltooth sawfish were caught in gill nets with 152-mm stretch meshes in the Peace River (Fig. 1). Nets were set for 1 h and constantly monitored. As soon as a sawfish was caught, it was carefully removed from the net, measured for stretch total length (STL) in millimeters, and tagged. All individuals were tagged with 1 ADL and at least

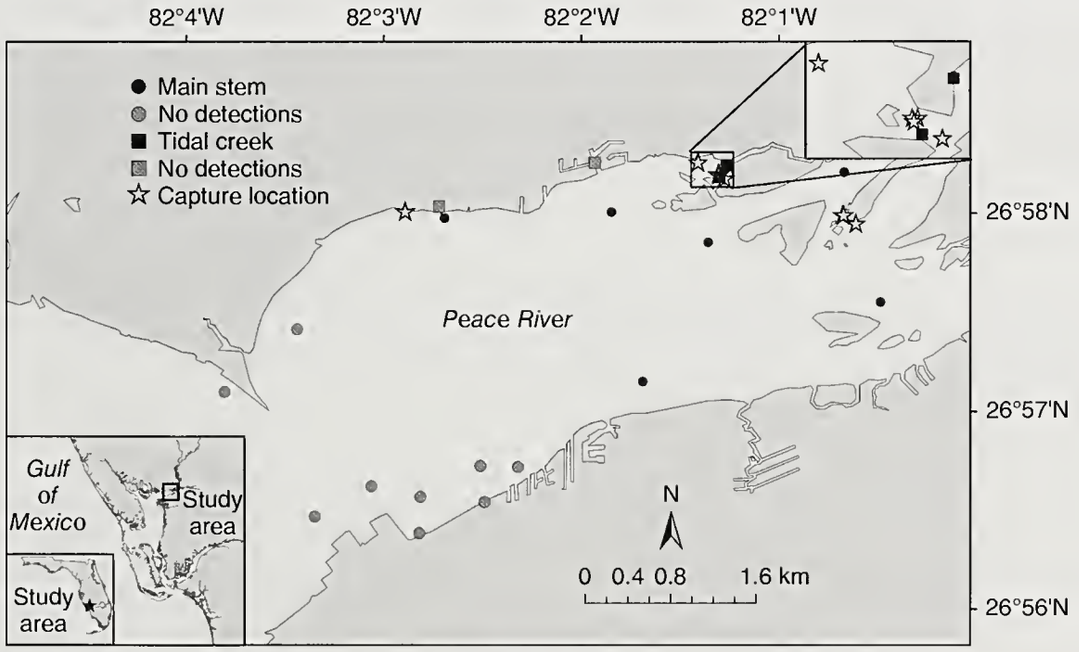

Figure 1

Map of the study area in the Peace River, Florida, showing locations (gray stars) where smalltooth sawfish (*Pristis pectinata*) were captured and tagged with acceleration data loggers and acoustic transmitters between May 2014 and November 2015 and some of the locations where acoustic receivers were deployed. The receivers shown were part of an array of 35 receivers in the Peace River. Locations where receivers were deployed in areas used by smalltooth sawfish were designated as either creeks lined with red mangroves (*Rhizophora mangle*) (black squares) or habitats in the main stem of the river (black circles). Gray squares and circles indicate receivers that did not detect individuals tagged in this study.

1 acoustic transmitter. The ADLs (G6a+[1], Cefas Technology Ltd., Lowestoft, UK) were programmed to record triaxial acceleration at 25 Hz, depth at 1 Hz, and temperature at 0.033 Hz. If possible, ADLs were paired with externally attached continuous acoustic transmitters (V9, Vemco, Bedford, Canada) with 5-s delays, to facilitate recovery of the ADLs through recapture after 5–7 d. Most of these tags were attached to the first dorsal fin directly by using monofilament (Fig. 2A). Alternatively, 2 ADLs were indirectly attached to the dorsal fin of individuals by tethering them to custom float packages (Fig. 2B). Float packages incorporated both a very high frequency (VHF) transmitter (MM110, Advanced Telemetry Systems Inc., Isanti, MN) and a galvanic timed release (GTR; International Fishing Devices Inc., Jupiter, FL). The GTRs were set to corrode after approximately 7 d, allowing the float package to detach and rise to the surface, where the VHF transmitter facilitated recovery following the technique of Lear and Whitney (2016), and eliminating the need for recapture.

All animals were tagged with a coded 69-kHz acoustic transmitter (V9), which was epoxied to a rototag and externally attached to the second dorsal fin following the methods of Poulakis et al. (2013). These transmitters emitted unique acoustic signals on a random delay between 80 and 160 s to minimize interference of signals from multiple tags and to maximize battery life. These transmitters communicated to an array of 35 omnidirectional VR2W acoustic receivers (Vemco) placed throughout the Peace River estuary (Fig. 1). They were also used to facilitate recovery of the ADLs through recapture if necessary. After tagging, smalltooth sawfish were released at their site of capture.

Work with animals was conducted under endangered species permit no. 15802, issued by the National Marine Fisheries Service.

Data processing and analyses: data loggers

Once ADLs were recovered, raw data were downloaded from them and prepared for analysis by using Igor Pro (vers. 6.22; WaveMetrics Inc., Portland, OR) and the application Ethographer (Sakamoto et al., 2009). Data from the first 12 h of ADL deployments were excluded to eliminate any behavioral effects of capture stress following tagging and release (Whitney et al., 2012). Static and dynamic acceleration were separated by using a 3-s box smoother, which was sufficient to remove the tailbeat signal from the static acceleration traces (Shepard et al., 2008), and both components were used to analyze body movement and position throughout the monitoring periods. *K*-means clustering analyses were run on the sway (tailbeat) acceleration axis to separate resting and active periods (Sakamoto et al., 2009; Whitney et al., 2010). Overall dynamic body acceleration (ODBA) (Wilson et al., 2006; Gleiss et al., 2011) was calculated as the sum of the absolute value of the 3 dynamic acceleration axes. We used ODBA to determine burst events, calculating the 98th percentile of ODBA for each individual by using means for each 1-s segment of data and subsequently classifying burst events as periods during which ODBA was continuously above this threshold for more than 3 s (Gleiss et al., 2017).

Because of permitting restrictions, no validation (ground-truthing) trials were run for this species to specifically link behaviors to their corresponding acceleration traces; however, ground-truthing has been conducted for the largetooth sawfish (*Pristis pristis*) (senior author and A. Gleiss, unpubl. data), as well as for the lemon shark (*Negaprion brevirostris*) (Brewster et al., 2018). These studies established that chafe behavior (dorsal rubbing) is defined by a distinctive *W*-shaped trace in the heave acceleration axis. Therefore, burst events with similar distinctive *W*-shaped

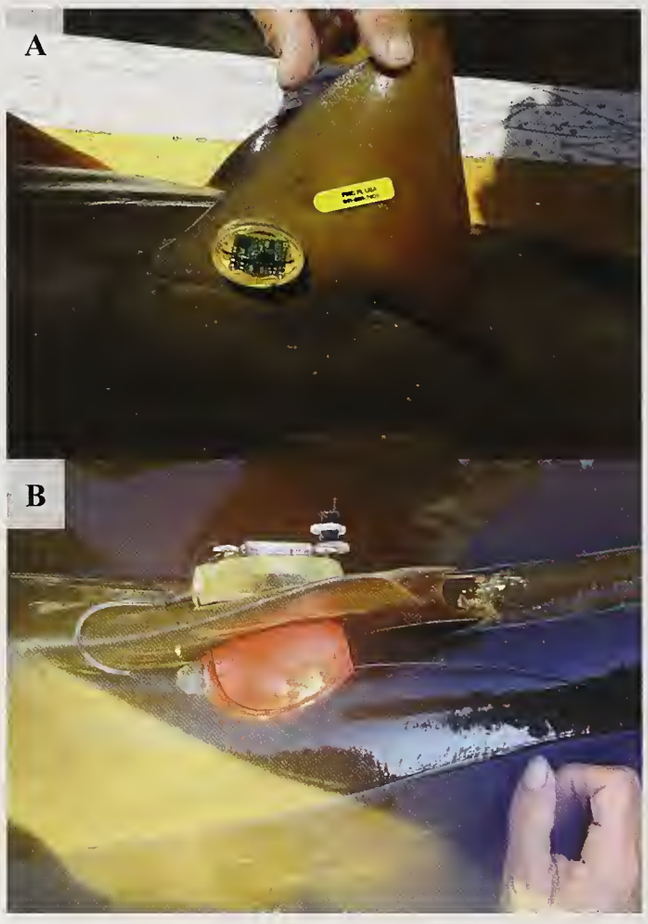

Figure 2

Photographs of acceleration data loggers (ADLs) attached to the first dorsal fins of 2 of the 10 smalltooth sawfish (*Pristis pectinata*) caught and tagged in the Peace River, Florida, from May 2014 through November 2015. (**A**) An ADL on an individual that was 1.7-m stretch total length (STL), paired with a continuous acoustic transmitter (not shown) to enable recapture and recovery of the logger. (**B**) A 1.8-m-STL individual, with the logger tethered to a float package that incorporated a very high frequency transmitter. A galvanic timed release was used to attach these float packages, allowing recovery of the ADL without recapture.

[1] Mention of trade names or commercial companies is for identification purposes only and does not imply endorsement by the National Marine Fisheries Service, NOAA.

traces (Fig. 3A) were removed from the burst event mask for each individual, leaving only burst events designated by large-amplitude and high-frequency lateral body movements for further analysis (Fig. 3, B and C). Mean depth, mean temperature, percentage of time spent active, and total number of burst events were summarized for each hour of the deployment for each individual.

Generalized additive mixed models (GAMMs) were built by using the mcgv package (vers. 1.8-28; Wood et al., 2017) in R, vers. 3.5.2 (R Core Team, 2018), and were used to analyze patterns in activity and bursting with respect to 5 fixed effects: depth, temperature, time of day, tide, and age class. Tidal period was split into 6 discrete phases—high, low, first ebb, second ebb, first flood, and second flood—by using tide data reported by NOAA's National Ocean Service for the Peace River (available from the Tides and Currents website). Periods of low and high tide were designated as the 2 h surrounding the minimum and maximum tide height within a cycle, and each bridging ebb and flood period was evenly divided into a first and second phase, with each tidal phase lasting approximately 2 h. Smalltooth sawfish were split by age class into either a group for young of the year (YOY; <1.5 m STL) or a group for individuals age 1 or older (≥1.5 m STL) (Scharer et al., 2012), with 4 individuals in each group (Table 1).

To determine informative drivers of activity, a series of GAMMs were built for predicting the percentage of time sawfish were active by using different combinations and interactions of the 5 fixed effects. The Akaike information criterion corrected for small sample sizes (AICc) and log likelihood of each model were used to determine the best-fit model and the predictors that should be maintained in the model. The number of burst events observed in each hour was highly zero inflated; therefore, to describe patterns in burst events, a 2-step process was used following methods described by Gleiss et al. (2017). First, a series of GAMMs with binomial distributions was built to determine which fixed effects affected the probability of a burst event. Similar to what was done for the model for activity, the fit of different combinations of these predictor variables was assessed by using AICc, and the model

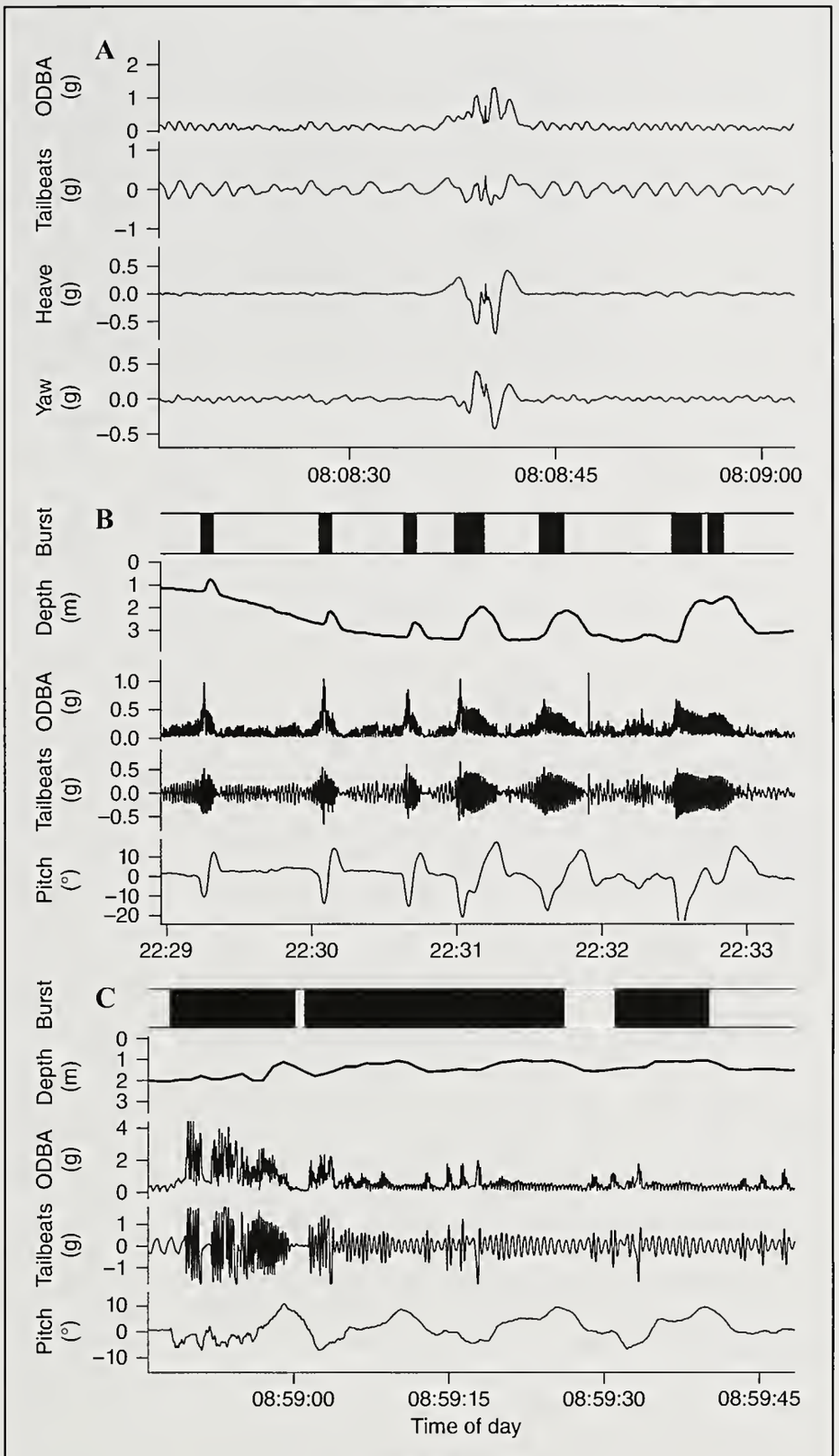

Figure 3

(**A**) Dynamic acceleration traces and overall dynamic body acceleration (ODBA) data that show a typical chafe event (dorsal rubbing) for the smalltooth sawfish (*Pristis pectinata*), characterized by a distinctive *W* shape in the heave acceleration axis. These events were excluded from the burst event mask for each individual. Burst events included in the mask were generally characterized by either (**B**) short bursts accompanied by sharp ascents or (**C**) longer bursts without distinct changes in depth. Data used in these graphs were collected from acceleration data loggers deployed on smalltooth sawfish caught and tagged in the Peace River, Florida, between May 2014 and November 2015.

Table 1

Details for the 8 recovered acceleration data loggers (ADLs) and the smalltooth sawfish (*Pristis pectinata*) on which they were deployed between May 2014 and November 2015 in the Peace River, Florida. Individuals were classified as either young of the year (YOY) or individuals age 1 or older, on the basis of stretch total length (Scharer et al., 2012). In this study, ADLs were attached either directly to the first dorsal fin, requiring recapture for retrieval, or were tethered to pop-off float packages that were retrieved while floating on the surface by using a very high frequency transmitter signal (Fig. 2). The asterisks (*) indicate the same individual caught 5 months after it was initially tagged. M=male; F=female.

Sawfish ID	Date tagged	Sex	Length (mm)	Age class	Deployment duration (d)	Retrieval method
1	9 May 2014	M	808	YOY	5.03	Recapture
2	12 Jun 2014	M	1735	≥age 1	5.37	Recapture
3	12 Jun 2014	F	1575	≥age 1	5.09	Recapture
4	11 Jun 2015	M	980	YOY	5.06	Recapture
5*	11 Jun 2015	F	1025	YOY	5.13	Recapture
6	11 Jun 2015	F	1049	YOY	5.12	Recapture
7	10 Nov 2015	F	1831	≥age 1	5.23	Pop-off
8*	20 Nov 2015	F	1531	≥age 1	5.42	Pop-off

with the lowest AICc was determined to have the best fit. Following the formation of this model describing the burst probability, the hours during which no burst events were detected were removed from the analysis, and the number of bursts observed in the remaining hours was modeled by using a GAMM with a negative binomial distribution. This model included the same predictor variables used in the previously described models, and the best-fit combination of fixed-effect predictor variables was determined by using AICc.

In all GAMMs, normality of residuals was confirmed by using the gam.check function in the mcgv package in R, and autocorrelation was accounted for by using the CorAR1 function. Cyclic smoothers were used for time of day to reflect the circular nature of the 24-h clock. Fixed effects that were maintained in the chosen model were further examined with Tukey's honestly significant difference (HSD) tests by using the multcomp package, vers. 1.4-10 (Hothorn et al., 2008). Additionally, to determine whether there was a shift in depth distributions with size, the frequency distributions of hourly depths of YOY and individuals age 1 or older were compared by using a Kolmogorov–Smirnov test.

Data processing and analyses: passive acoustic monitoring

Acoustic transmitter data were downloaded from acoustic receivers and examined to provide location data concurrent with ADL-derived behavioral data. Positions derived from acoustic data were matched with those from ADL data by using time stamps, and a location was designated for each hour that acoustic transmissions were received. Receivers were deployed in 2 habitats: creeks, lined with red mangroves (*Rhizophora mangle*), that are generally shallow, enclosed habitats (with depths <1 m at most tides) and habitats within the main stem (or main channel) of the Peace River that are generally deeper (with depths of 1–3 m at most tides), more open areas with less habitat complexity (Fig. 1). If acoustic transmissions were received from multiple habitats during the same hour of deployment or if they were not received during an hour of deployment, data were not included in location analyses. The percentage of time smalltooth sawfish were active and the probability and frequency of burst events were compared between the 2 types of habitats by using analysis of variance (ANOVA), with depth, temperature, time of day, tide, and age class included as fixed-effect predictors in the models and individual included as a random effect. The dredge function in the MuMIn package (vers. 0.12.0; Bartoń, 2009) in R was used to determine which factors should be included as informative predictors of activity and burst events.

To visualize the overall area and habitat use by smalltooth sawfish while they carried ADLs, a contour map was created by using Surfer 13 (Golden Software LLC, Golden, CO) following the methods of Huston et al. (2017). Age classes were combined because all individuals used the same area of the river regardless of size during the 5-d ADL deployments.

Results

Between May 2014 and November 2015, ADLs were deployed on 10 smalltooth sawfish (Table 1). Eight of these tags were recovered, and over 994 h of high-resolution behavioral data were collected from them (Fig. 4). Acoustic detections were received during 225 h of the ADL deployments, providing concurrent position and behavior data for these hours. Burst events were identified for all sawfish, with 6–58 burst events observed per day for individuals. These burst events composed 2 main categories: repeated,

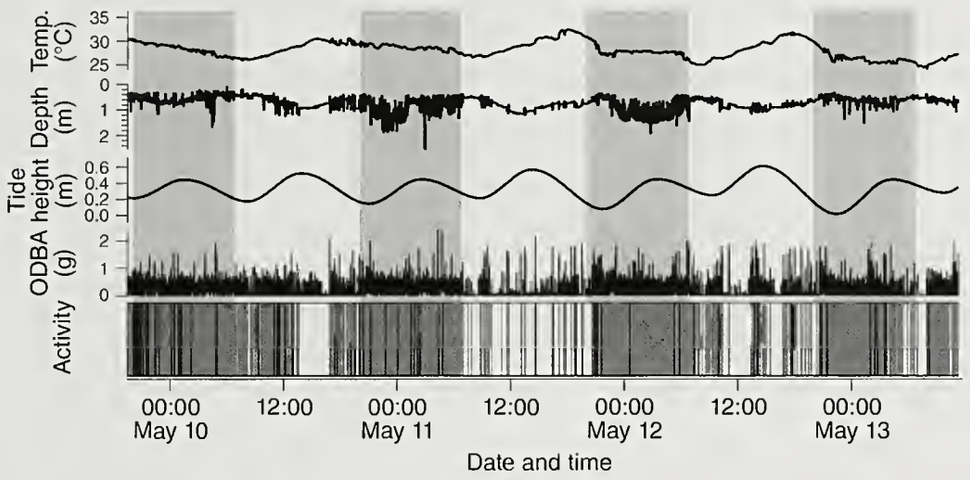

Figure 4

Representation of acceleration and environmental data from an acceleration data logger that was attached to a young-of-the-year smalltooth sawfish (*Pristis pectinata*) caught in the Peace River, Florida, and tagged on 9 May 2014 (sawfish ID 1, see Table 1). Vertical shading indicates periods of day (white) and night (light gray). Temperature and depth values show a diel pattern of depth use in which this individual remained in relatively shallow depths during the day and made repeated ventures to deeper water at night. Overall dynamic body acceleration (ODBA) was used to establish activity (dark gray bars) and burst patterns (black bars) that depict putative foraging activity; white bars indicate resting periods.

short (5–10 s) bursts accompanied by sharp ascents (Fig. 3B), accounting for approximately 24% of observed burst events, and bursts of variable duration up to 45 s without predictable changes in depth (Fig. 3C). Water temperatures during deployments were 24.5–32.7°C for sawfish tagged in May and June and 20.6–28.9°C for individuals tagged in November.

The model that best described activity included depth, temperature, time of day, and tide as fixed-effect predictors (Table 2). Smalltooth sawfish were significantly more active during the evening and night hours, with a peak in activity around 2200, a few hours after typical sunset, and a second smaller peak around 0500, near sunrise (Fig. 5). Activity increased with temperature. Individuals were also more active at depths around 0.8 m (Fig. 5), with decreased activity in shallower and deeper areas, and were more active during the lower half of the tidal cycle (i.e., second ebb, low tide, and first flood) than during the higher half of the tidal cycle (i.e., second flood, high tide, and first ebb) (Tukey's HSD: $P<0.05$; Fig. 5). Hourly mean depth of sawfish was significantly shallower at low tide (mean: 0.57 m [standard error (SE) 0.04]) than at high tide (mean: 0.75 m [SE 0.04]) (ANOVA: $P<0.001$, df=1, $F=11.94$), although there was no difference in mean depth between day and night (ANOVA: $P>0.05$, df=1, $F=2.40$).

The best-fit model describing the probability of a burst event included only age class as a predictor, with bursts more likely to occur in YOY smalltooth sawfish than in individuals age 1 or older. However, time of day was the most important predictor of burst frequency and the only predictor maintained in the best-fit model (Table 2). This result indicates that, although the likelihood that bursts would occur was the same for all hours of the day, the burst frequency increased substantially during evening and night hours, with the highest burst frequency observed around 2200, coinciding with the peak in percentage of time sawfish were active.

The distributions of the recorded depths of YOY and individuals age 1 and older were significantly different (Kolmogorov–Smirnov test: $P<0.0001$). An overall mean depth of 0.5 m was observed for YOY, with an hourly mean depth range of 0.1–1.5 m. Larger individuals (age 1 or older) made occasional excursions into deeper water, with an overall mean depth of 0.8 m and an hourly mean depth range of 0.2–3.6 m (Fig. 6).

Although acoustic tags were concurrently deployed with ADLs on all smalltooth sawfish, detections were sparse for some individuals during ADL deployments, with location categorized in 226 h of ADL deployments (126 h in the main stem of the Peace River and 100 h in mangrove creek habitats). This lack of detections for some fish made it difficult to link specific locations with behaviors, but data were sufficient to compare behaviors between broad habitat categories. Habitat type was an informative predictor of activity, along with tidal period and depth, with individuals more active in the main channel than in mangrove creek habitats (Tukey's HSD: $P<0.05$; Fig. 7). Habitat type was also an informative predictor of burst frequency, along with tide and depth, and of the burst probability, along with tide, depth, and age class. Smalltooth

Table 2

The top-5 combinations of fixed effects in generalized additive mixed models used to predict 1) the percentage of time smalltooth sawfish (*Pristis pectinata*) were active (Activity), 2) burst probability, and 3) burst frequency. Degrees of freedom (df), log likelihood (logLik), and the corrected Aikake's information criterion (AICc) were used to determine the best-fit models, which are indicated with asterisks. The burst frequency model described by only hour of day (HOD) was selected as the most parsimonious model, with relative differences between AICc values (ΔAICc) <2 for the top model. All models included individual as a random effect. Data used in the models were collected during deployments of acceleration data loggers in the Peace River, Florida, between May 2014 and November 2015.

Model	df	logLik	AICc	ΔAICc
Activity				
~HOD + Temp + Depth + Tide*	13	−4068.5	8137.0	
~HOD + Temp + Depth + Tide + Age class	14	−4068.1	8137.9	1.2
~HOD + Temp + Tide	11	−4072.8	8140.9	4.5
~HOD + Temp	6	−4082.2	8150.3	13.4
~HOD + Temp + Age class	7	−4082.1	8150.9	17.5
Burst probability				
~Age class*	3	−1914.6	3835.3	
~Depth	4	−1915.9	3839.7	4.4
~Depth + Age class	5	−1915.2	3840.4	5.1
~Tide	7	−1916.0	3845.9	10.6
~Tide + Age class	8	−1915.2	3846.4	11.1
Burst frequency				
~HOD + Age class	5	−1021.6	2053.2	
~HOD*	4	−1022.8	2053.6	0.4
~HOD + Tide	9	−1018.0	2053.9	0.7
~HOD + Depth + Age class	7	−1020.3	2054.6	1.4
~HOD + Depth + Tide + Age class	12	−1015.5	2054.9	1.7

sawfish were more likely to burst in the main stem of the river than in mangrove creek habitats (Tukey's HSD: $P<0.05$; Fig. 7), and a greater burst frequency was observed in the main channel; however, this difference was not significant (Tukey's HSD: $P>0.05$; Fig. 7).

Smalltooth sawfish that were fitted with ADLs remained in a small portion of the Peace River (Figs. 1 and 7). Both size classes remained in enclosed creek habitats during the day and in more open habitats in the main stem of the river at night.

Discussion

This study, the first to deploy ADLs on smalltooth sawfish, provides behavioral data that describes their fine-scale activity and behavior patterns, including potential foraging strategies. Acceleration data indicate that a number of factors, including time of day, tidal period, depth, age class, and habitat, affect activity and foraging rates in this species. These data will increase our understanding of how this critically endangered species behaves in its nursery habitats throughout juvenile life stages and will assist in management and conservation of crucial nursery areas.

Purported foraging behavior

Foraging behavior of sawfish species is seldom observed in natural habitats and is generally not well documented, although the toothed rostrum is known to aid in stunning and pinning prey as well as in electroreception (Wueringer et al., 2011, 2012). Because validation trials could not be performed to match acceleration traces with specific behaviors in our study, it was impossible to identify foraging activity with certainty from the acceleration data we collected (Whitney et al., 2018). However, by examining video footage of feeding sawfish in captivity (Wueringer et al., 2011, 2012), and by considering the results of ground-truthing trials for data collected on acceleration behavior of the largetooth sawfish (senior author and A. Gleiss, unpubl. data), we made some deductions about the relation of the burst events observed in our study to putative foraging activity. Conservatively, it is likely that any foraging activity displayed by ADL-tagged smalltooth sawfish was included in the 98th percentile burst event mask determined for each fish, although bursts tied to predator escape or startle responses may also be included in this subset of data.

Many of the burst events we recorded were accompanied by acute ascents (see Fig. 3B), indicating that smalltooth

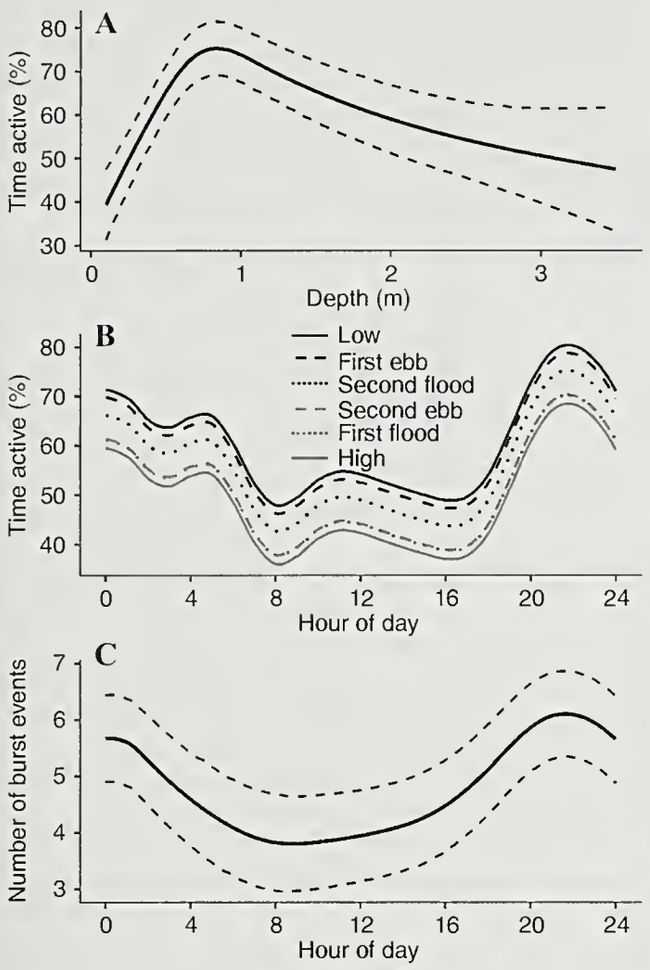

Figure 5

Patterns of activity of smalltooth sawfish (*Pristis pectinata*) in the Peace River, Florida, with percentage of time fish were active in relation to (**A**) depth and (**B**) time of day and tidal period, from data analysis conducted with generalized additive mixed models (GAMMs). The lines for first ebb and second flood are essentially the same and overlay each other. (**C**) The relationship of the number of burst events of smalltooth sawfish with time of day, the only predictor of the burst frequency included in the best-fit GAMM. Dashed lines in panels A and C show standard error of the GAMM smoother; standard errors are not shown in panel B in the interest of clarity. Data used in the models were collected from acceleration data loggers deployed on smalltooth sawfish caught and tagged in the Peace River between May 2014 and November 2015.

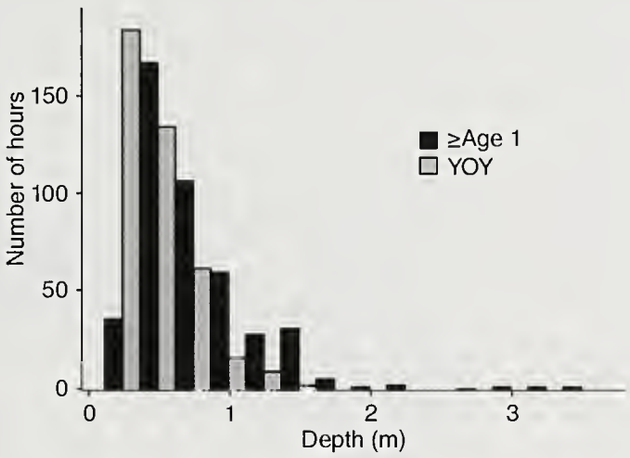

Figure 6

Frequency of use of depths by smalltooth sawfish (*Pristis pectinata*), by age class, in the Peace River, Florida, from May 2014 through November 2015. Depth values are mean depths (in paired bins of 0.25 m) from all hours of deployment of acceleration data loggers. The age classes were young of the year (YOY, <1.5 m stretch total length [STL]) and individuals ≥age 1 (≥1.5 m STL). The youngest individuals used shallower depths than those used by older individuals, and they did not occur below 1.5 m; older individuals made occasional excusions up to 3.6 m.

sawfish may travel or wait near the bottom and quickly burst upward into the water column, potentially in pursuit of teleost fishes, their primary prey (Poulakis et al., 2017). Other burst events were not accompanied by predictable changes in depth, instead occurring at relatively constant depths, presumably on or near the bottom. We hypothesize that these events indicate benthic prey capture or *pinning* behavior, in which smalltooth sawfish pin prey, such as rays, on the substrate (Poulakis et al., 2017), using their rostrum until they can maneuver prey into their mouths (Wueringer et al., 2012). These high-acceleration amplitude signals could also represent sawfish avoiding predation by bull sharks (*Carcharhinus leucas*), which are one of the main predators of smalltooth sawfish in Florida (Brame et al., 2019). However, predation pressure on smalltooth sawfish in the Peace River is considered low because of the divergent salinity affinities between bull sharks and smalltooth sawfish (Poulakis et al., 2011).

Environmental drivers of activity and foraging

Temperature and time of day were the most influential drivers of activity, with both factors included in the top-5 candidate models for activity. The highest activity rates were observed at higher water temperatures and during evening and night hours. That activity increased with water temperature was not unexpected because ectothermic animals, including elasmobranchs, often increase activity as temperatures increase and, therefore, muscle performance capacity and metabolic needs increase (Halsey et al., 2015; Lear et al., 2017, 2019). The crepuscular and nocturnal activity observed in the smalltooth sawfish is also similar to that observed in many elasmobranchs (reviewed by Hammerschlag et al., 2017), activity that is often attributed to the exceptional sensory capabilities of elasmobranchs (Hueter et al., 2004).

Similar crepuscular and nocturnal activity has been observed in other sawfish species (Gleiss et al., 2017; Whitty et al., 2017), and these findings confirm hypotheses of diel activity patterns in juvenile smalltooth sawfish formed during previous studies that included passive and active acoustic monitoring (Hollensead et al., 2016;

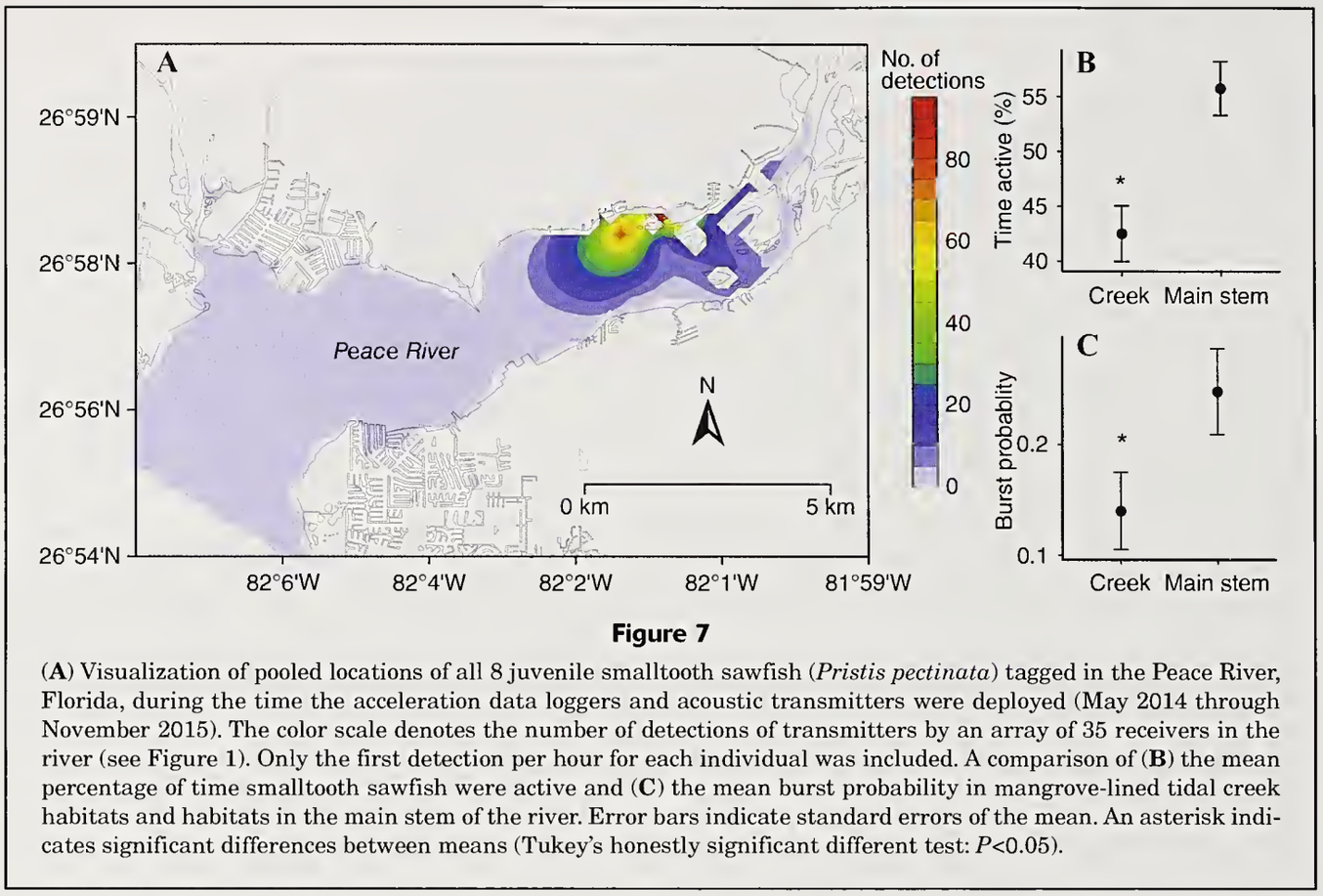

Figure 7

(**A**) Visualization of pooled locations of all 8 juvenile smalltooth sawfish (*Pristis pectinata*) tagged in the Peace River, Florida, during the time the acceleration data loggers and acoustic transmitters were deployed (May 2014 through November 2015). The color scale denotes the number of detections of transmitters by an array of 35 receivers in the river (see Figure 1). Only the first detection per hour for each individual was included. A comparison of (**B**) the mean percentage of time smalltooth sawfish were active and (**C**) the mean burst probability in mangrove-lined tidal creek habitats and habitats in the main stem of the river. Error bars indicate standard errors of the mean. An asterisk indicates significant differences between means (Tukey's honestly significant different test: $P<0.05$).

Huston et al., 2017; Scharer et al., 2017). The results of these previous studies indicate that juveniles rest in shallow creeks during the day and are active in the main channel of a river at night. Although data from the use of these monitoring techniques describe horizontal movements, it can be difficult to use acoustic data to accurately assess activity levels because movements are recorded during passive acoustic monitoring only when sawfish travel between receivers, not when they travel within the area covered by an individual receiver. In our study, data from ADLs directly confirmed these diel patterns.

In addition to time of day and temperature, depth and tide also significantly affected activity. Smalltooth sawfish were more active in the middle range of depths observed during ADL deployments and in the lower half of the tidal cycle. Decreased activity in the shallowest depths likely reflects sawfish refuging in the shallowest habitats. The decrease in activity at depths >1 m by fish could be a method of predator avoidance, given that bull sharks are more common in these deeper areas (Heupel et al., 2010), or it could indicate a lie-in-wait hunting strategy in deeper water. Alternatively, smalltooth sawfish could use deeper areas only for transiting through different habitats, as suggested by May et al. (2019), and could forage more actively in relatively shallow habitats of approximately 1 m. The relationship between activity levels and tidal stage observed in our study has not been indicated by results of previous studies (e.g., Hollensead et al., 2016). In our study, increased activity at lower tide heights could have been due to lower refuging potential at low tide because some shallow mangrove habitats that sawfish use as refuges may not be available at low tide (Simpfendorfer et al., 2010), forcing individuals to leave refuge locations and become more active as the tide drops. This pattern emerged despite a relatively small daily change in tide height, with daily tidal variance <1 m.

Time of day was also an important predictor of burst activity, with the greatest number of burst events observed during evening and night hours. However, although individuals generally adhered to these patterns, some foraging events also occurred during the day, timing that has been confirmed by using baited-rod-and-reel-derived public encounter data (Poulakis and Seitz, 2004), indicating that smalltooth sawfish opportunistically feed during the day and at night. Time of day was the only factor included in the final model describing burst frequency; however, burst probability was best described by age class, with YOY more likely to burst than individuals age 1 or older. Smalltooth sawfish are known to double in length by the end of their first year (Scharer et al., 2012); therefore, YOY may need to feed more often, on smaller prey items, than older individuals to achieve these growth rates. In addition, YOY individuals could be less experienced feeders and are under higher predation pressure in comparison with individuals age 1 or older. As a result, there may be more unsuccessful feeding attempts and a higher frequency of predator escape behavior (or startle responses) in YOY fish, contributing to their higher rate of burst activities.

In addition to differences in burst activity between age classes, there were also significant differences between the

depth distributions of YOY and older fish, with fish age 1 and older venturing deeper than YOY. This ontogenetic shift in depth use has been reported in a number of previous studies of both smalltooth and largetooth sawfish, indicating that YOY individuals stayed in shallow areas close to shore while larger fish that have less predation risk ventured farther from shorelines to use deeper habitats (Whitty et al., 2009; Simpfendorfer et al., 2010; Huston et al., 2017).

Habitat use and foraging ecology

The patterns of activity and putative foraging effort, combined with knowledge about depth and habitat use, reveal important insights into the foraging ecology of these animals. Increased activity and putative foraging of smalltooth sawfish was tied to habitats in the main stem of the Peace River, and refuging was more common in shallow habitats. This pattern is the opposite of that observed in the morphologically similar largetooth sawfish (Gleiss et al., 2017; Whitty et al., 2017). Largetooth sawfish studied in the Fitzroy River, Australia, are thought to use shallow sandbar habitats, which are generally devoid of woody debris, to forage because of increased abundance of prey, and snags and woody debris in the deeper areas of the river offer better refuging habitats from crocodilians, which are common along shorelines (Morgan et al., 2017; Whitty et al., 2017). Although foraging in shallow habitats could be similarly beneficial for smalltooth sawfish, some shallow habitats in the Peace River, such as red-mangrove-lined tidal creeks, have increased habitat complexity and are spatially restricted, possibly limiting overall foraging success. Moving away from these shallow habitats into the slightly deeper main channel at night may improve foraging success in the Peace River, and the shallow mangrove creeks and shorelines may provide more of a protection function from bull sharks; these habitats are known to be used as refuging areas in multiple nurseries in Florida (Simpfendorfer et al., 2010; Poulakis et al., 2013, 2016). Shallow creek habitats in the Peace River may offer protection from boat traffic and noise as well as from predators.

A similar diel pattern in habitat use has been reported from passive acoustic monitoring conducted over many years in the Peace River (Huston et al., 2017; Scharer et al., 2017; May et al., 2019), as well as from active and passive acoustic tracking conducted in other Florida nurseries (Simpfendorfer et al., 2010, 2011; Poulakis et al., 2013, 2016; Hollensead et al., 2016). All of these studies confirm that juvenile smalltooth sawfish refuge during the day in protected creek habitats, especially those lined with red mangroves (Norton et al., 2012). Although the authors of some of these studies have proposed that smalltooth sawfish use deeper habitats to forage because of increased nighttime detections by receivers in main channels (e.g., Poulakis et al., 2016; Huston et al., 2017), the use of alternative shallow nighttime foraging grounds has been observed in other studies. For example, May et al. (2019) found that, although smalltooth sawfish in the Peace River crossed the deeper main stem of the river at night, they did so in large part to use shallow habitats that included oyster reefs on the shoreline opposite to their protected daytime refuge. Shallow mud flats and habitats within the main river channel have also been reported as possible nighttime foraging areas for smalltooth sawfish in different Florida nurseries (Hollensead et al., 2016; Poulakis et al., 2016). Therefore, food availability and acquisition success may play roles in influencing where juveniles forage. For example, juveniles may forage in or near refuge locations when sufficient prey is available but venture farther into or across the main stem of the river if there is not sufficient prey or if densities of conspecifics near refuge locations are too high.

In our study, burst events were recorded at depths ranging from 0.1 to 3.6 m, indicating that a variety of habitats are important foraging areas for this species. However, regardless of foraging location, the timing of heightened activity and foraging appears to be maintained across nursery habitats and populations, given that all previous studies have found heightened activity at night in the Peace River and other nurseries (Poulakis et al., 2013, 2016; Hollensead et al., 2016; Huston et al., 2017; Scharer et al., 2017; May et al., 2019).

Conservation implications and future directions

This new information that relates putative foraging activity to habitat use has improved our understanding of the early life history of the smalltooth sawfish and validated previous hypotheses about activity patterns developed through acoustic monitoring studies. Increasing ADL deployment times and deploying ADLs throughout the year in future studies would help to identify long-term foraging and activity patterns, particularly in association with seasonal changes in abiotic variables, such as temperature and salinity. Additionally, deploying ADLs concurrently with a tracking system that can detect movements on a scale as small as meters, such as a Vemco Positioning System, would help to determine habitat use on a fine scale by enabling the matching of behaviors to specific sites within a nursery. Finally, conducting laboratory trials for validation of acceleration signals of smalltooth sawfish or deploying video cameras concurrently with ADLs in the field would help to conclusively determine feeding and other behaviors.

Even with its limitations, the information describing habitat use and potential foraging strategies provided by this study is valuable for understanding the habitat requirements of this species and emphasizes the importance of preserving a variety of habitats, including mangrove-lined creeks used by smalltooth sawfish as refuging areas and less complex habitats used as foraging grounds within nurseries. This information will help to guide crucial management and conservation efforts for the smalltooth sawfish in the Peace River and throughout the range of this species.

Acknowledgments

This research was supported by funding from the National Marine Fisheries Service (grant NA13NMF4720047) under

Section 6 of the U.S. Endangered Species Act (Cooperation with the States) and from Mote Marine Laboratory. We thank the staff at the Charlotte Harbor Field Laboratory, Florida Fish and Wildlife Conservation Commission, for assistance with capturing and tagging smalltooth sawfish. The senior author was supported by the Forrest Research Foundation and an Australian Government Research Training Program Scholarship.

Literature cited

Bartoń, K.
2009. MuMIn: multi-model inference. R package, vers. 0.12.0. [Available from website, accessed January 2018.]

Bigelow, H. B., and W. C. Schroeder.
1953. Fishes of the western North Atlantic, part 2: sawfishes, guitarfishes, skates, rays and chimaeroids, 514 p. Yale Univ., New Haven, CT.

Brame, A. B., T. R. Wiley, J. K. Carlson, S. V. Fordham, R. D. Grubbs, J. Osborne, R. M. Scharer, D. M. Bethea, and G. R. Poulakis.
2019. Biology, ecology, and status of the smalltooth sawfish *Pristis pectinata* in the USA. Endanger. Species Res. 39:9–23.

Brewster, L. R., J. J. Dale, T. L. Guttridge, S. H. Gruber, A. C. Hansell, M. Elliott, I. G. Cowx, N. M. Whitney, and A. C. Gleiss.
2018. Development and application of a machine learning algorithm for classification of elasmobranch behaviour from accelerometry data. Mar. Biol. 165:62.

Carlson, J., T. Wiley, and K. Smith.
2013. *Pristis pectinata* (errata version published in 2019). The IUCN Red List of Threatened Species 2013: e.T18175A141791261. [Available from website.]

Dulvy, N. K., S. L. Fowler, J. A. Musick, R. D. Cavanagh, P. M. Kyne, L. R. Harrison, J. K. Carlson, L. N. K. Davidson, S. V. Fordham, M. P. Francis, et al.
2014. Extinction risk and conservation of the world's sharks and rays. eLife 3:e00590.

Dulvy, N. K., L. N. K. Davidson, P. M. Kyne, C. A. Simpfendorfer, L. R. Harrison, J. K. Carlson, and S. V. Fordham.
2016. Ghosts of the coast: global extinction risk and conservation of sawfishes. Aquat. Conserv. 26:134–153.

Federal Register.
2003. Endangered and threatened species; final endangered status for a distinct population segment of smalltooth sawfish (*Pristis pectinata*) in the United States. Fed. Regist. 68:15674–15680. [Available from website.]

Gleiss, A. C., R. P. Wilson, and E. L. C. Shepard.
2011. Making overall dynamic body acceleration work: on the theory of acceleration as a proxy for energy expenditure. Methods Ecol. Evol. 2:23–33.

Gleiss, A. C., D. L. Morgan, J. M. Whitty, J. J. Keleher, S. Fossette, and G. C. Hays.
2017. Are vertical migrations driven by circadian behaviour? Decoupling of activity and depth use in a large riverine elasmobranch, the freshwater sawfish (*Pristis pristis*). Hydrobiologia 787:181–191.

Halsey, L. G., P. G. D. Matthews, E. L. Rezende, L. Chauvaud, and A. A. Robson.
2015. The interactions between temperature and activity levels in driving metabolic rate: theory, with empirical validation from contrasting ectotherms. Oecologia 177:1117–1129.

Hammerschlag, N., R. A. Skubel, H. Calich, E. R. Nelson, D. S. Shiffman, J. Wester, C. C. Macdonald, S. Cain, L. Jennings, A. Enchelmaier, et al.
2017. Nocturnal and crepuscular behavior in elasmobranchs: a review of movement, habitat use, foraging, and reproduction in the dark. Bull. Mar. Sci. 93:355–374.

Heupel, M. R., B. G. Yeiser, A. B. Collins, L. Ortega, and C. A. Simpfendorfer.
2010. Long-term presence and movement patterns of juvenile bull sharks, *Carcharhinus leucas*, in an estuarine river system. Mar. Freshw. Res. 61:1–10.

Hollensead, L. D., R. D. Grubbs, J. K. Carlson, and D. M. Bethea.
2016. Analysis of fine-scale daily movement patterns of juvenile *Pristis pectinata* within a nursery habitat. Aquat. Conserv. 26:492–505.

Hothorn, T., F. Bretz, and P. Westfall.
2008. Simultaneous inference in general parametric models. Biomet. J. 50:346–363.

Hueter, R. E., D. A. Mann, K. P. Maruska, J. A. Sisneros, and L. S. Demski.
2004. Sensory biology of elasmobranchs. *In* Biology of sharks and their relatives (J. C. Carrier, J. A. Musick, and M. R. Heithaus, eds.), p. 325–368. CRC Press, Boca Raton, FL.

Huston, C. A., P. W. Stevens, R. M. Blaxton, S. G. Tolley, R. M. Scharer, B. M. Tornwall, and G. R. Poulakis.
2017. Diel movements of juvenile smalltooth sawfish: implications for defining the size of a nursery hotspot. Endanger. Species Res. 34:311–322.

Lear, K. O., and N. M. Whitney.
2016. Bringing data to the surface: recovering data loggers from large sample sizes in marine vertebrates. Anim. Biotelem. 4:12.

Lear, K. O., N. M. Whitney, L. R. Brewster, J. J. Morris, R. E. Hueter, and A. C. Gleiss.
2017. Correlations of metabolic rate and body acceleration in three species of coastal sharks under contrasting temperature regimes. J. Exp. Biol. 220:397–407.

Lear, K. O., N. M. Whitney, D. L. Morgan, L. R. Brewster, J. M. Whitty, G. R. Poulakis, R. M. Scharer, T. L. Guttridge, and A. C. Gleiss.
2019. Thermal performance responses in free-ranging elasmobranchs depend on habitat use and body size. Oecologia 191:829–842.

May, R. K., S. G. Tolley, R. M. Scharer, B. Dye, F. Jose, and G. R. Poulakis.
2019. Automated monitoring of fine-scale movements of the endangered smalltooth sawfish (*Pristis pectinata*). Fish. Bull. 117:360–371.

Morgan, D. L., R. Somaweera, A. C. Gleiss, S. J. Beatty, and J. M. Whitty.
2017. An upstream migration fought with danger: freshwater sawfish fending off sharks and crocodiles. Ecology 98:1465–1467.

Norton, S. L., T. R. Wiley, J. K. Carlson, A. L. Frick, G. R. Poulakis, and C. A. Simpfendorfer.
2012. Designating critical habitat for juvenile endangered smalltooth sawfish in the United States. Mar. Coast. Fish. 4:473–480.

Poulakis, G. R., and J. C. Seitz.
2004. Recent occurrence of the smalltooth sawfish, *Pristis pectinata* (Elasmobranchiomorphi: Pristidae), in Florida Bay and the Florida Keys, with comments on sawfish ecology. Fla. Sci. 67:27–35.

Poulakis, G. R., and R. D. Grubbs.
2019. Biology and ecology of sawfishes: global status of research and future outlook. Endanger. Species Res. 39:77–90.

Poulakis, G. R., P. W. Stevens, A. A. Timmers, T. R. Wiley, and C. A. Simpfendorfer.
2011. Abiotic affinities and spatiotemporal distribution of the endangered smalltooth sawfish, *Pristis pectinata*, in a south-western Florida nursery. Mar. Freshw. Res. 62:1165–1177.

Poulakis, G. R., P. W. Stevens, A. A. Timmers, C. J. Stafford, and C. A. Simpfendorfer.
2013. Movements of juvenile endangered smalltooth sawfish, *Pristis pectinata*, in an estuarine river system: use of non-main-stem river habitats and lagged responses to freshwater inflow-related changes. Environ. Biol. Fish. 96:763–778.

Poulakis, G. R., P. W. Stevens, A. A. Timmers, C. J. Stafford, D. D. Chapman, K. A. Feldheim, M. R. Heupel, and C. Curtis.
2016. Long-term site fidelity of endangered smalltooth sawfish (*Pristis pectinata*) from different mothers. Fish. Bull. 114:461–475.

Poulakis, G. R., H. Urakawa, P. W. Stevens, J. A. DeAngelo, A. A. Timmers, R. D. Grubbs, A. T. Fisk, and J. A. Olin.
2017. Sympatric elasmobranchs and fecal samples provide insight into the trophic ecology of the smalltooth sawfish. Endanger. Species Res. 32:491–506.

R Core Team.
2018. R: a language and environment for statistical computing. R Foundation for Statistical Computing, Vienna, Austria. [Available from website, accessed December 2018.]

Sakamoto, K. Q., K. Sato, M. Ishizuka, Y. Watanuki, A. Takahashi, F. Daunt, and S. Wanless.
2009. Can ethograms be automatically generated using body acceleration data from free-ranging birds? PLoS ONE 4(4):e5379.

Scharer, R. M., W. F. Patterson III, J. K. Carlson, and G. R. Poulakis.
2012. Age and growth of endangered smalltooth sawfish (*Pristis pectinata*) verified with LA-ICP-MS analysis of vertebrae. PLoS ONE 7(10):e47850.

Scharer, R. M., P. W. Stevens, C. P. Shea, and G. R. Poulakis.
2017. All nurseries are not created equal: large-scale habitat use patterns in two smalltooth sawfish nurseries. Endanger. Species Res. 34:473–492.

Seitz, J. C., and G. R. Poulakis.
2006. Anthropogenic effects on the smalltooth sawfish (*Pristis pectinata*) in the United States. Mar. Pollut. Bull. 52:1533–1540.

Shepard, E. L. C., R. P. Wilson, L. G. Halsey, F. Quintana, A. G. Laich, A. C. Gleiss, N. Liebsch, A. E. Myers, and B. Norman.
2008. Derivation of body motion via appropriate smoothing of acceleration data. Aquat. Biol. 4:235–241.

Simpfendorfer, C. A., T. R. Wiley, and B. G. Yeiser.
2010. Improving conservation planning for an endangered sawfish using data from acoustic telemetry. Biol. Conserv. 143:1460–1469.

Simpfendorfer, C. A., B. G. Yeiser, T. R. Wiley, G. R. Poulakis, P. W. Stevens, and M. R. Heupel.
2011. Environmental influences on the spatial ecology of juvenile smalltooth sawfish (*Pristis pectinata*): results from acoustic monitoring. PLoS ONE 6(2): e16918.

Whitney, N. M., H. L. Pratt Jr., T. C. Pratt, and J. C. Carrier.
2010. Identifying shark mating behaviour using three-dimensional acceleration loggers. Endanger. Species Res. 10:71–82.

Whitney, N. M., Y. P. Papastamatiou, and A. C. Gleiss.
2012. Integrative multisensor tagging: emerging techniques to link elasmobranch behavior, physiology, and ecology. *In* Biology of sharks and their relatives, 2nd ed. (J. C. Carrier, J. A. Musick, and M. R. Heithaus, eds.), p. 265–289. CRC Press, Boca Raton, FL.

Whitney, N. M., K. O. Lear, A. C. Gleiss, N. Payne, and C. F. White.
2018. Advances in the application of high-resolution biologgers to elasmobranch fishes. *In* Shark research: emerging technologies and applications to the field and laboratory (J. C. Carrier, M. R. Heithaus, and C. A. Simpfendorfer, eds.), p. 45–70. CRC Press, Boca Raton, FL.

Whitty, J. M., D. L. Morgan, S. C. Peverell, D. C. Thorburn, and S. J. Beatty.
2009. Ontogenetic depth partitioning by juvenile freshwater sawfish (*Pristis microdon*: Pristidae) in a riverine environment. Mar. Freshw. Res. 60:306–316.

Whitty, J. M., J. Keleher, B. C. Ebner, A. C. Gleiss, C. A. Simpfendorfer, and D. L. Morgan.
2017. Habitat use of a Critically Endangered elasmobranch, the largetooth sawfish *Pristis pristis*, in an intermittently flowing riverine nursery. Endanger. Species Res. 34:211–227.

Wilson, R. P., C. R. White, F. Quintana, L. G. Halsey, N. Liebsch, G. R. Martin, and P. J. Butler.
2006. Moving towards acceleration for estimates of activity-specific metabolic rate in free-living animals: the case of the cormorant. J. Anim. Ecol. 75:1081–1090.

Wood, S. N.
2017. Generalized additive models: an introduction with R, 2nd ed., 476 p. Chapman and Hall/CRC, Boca Raton, FL.

Wueringer, B. E., S. C. Peverell, J. Seymour, L. Squire Jr., S. M. Kajiura, and S. P. Collin.
2011. Sensory systems in sawfishes. 1. The ampullae of Lorenzini. Brain Behav. Evol. 78:139–149.

Wueringer, B. E., L. Squire Jr., S. M. Kajiura, N. S. Hart, and S. P. Collin.
2012. The function of the sawfish's saw. Curr. Biol. 22: R150–R151.

National Marine
Fisheries Service
NOAA

Fishery Bulletin
established in 1881

Spencer F. Baird
First U.S. Commissioner
of Fisheries and founder
of *Fishery Bulletin*

Automated monitoring of fine-scale movements of the endangered smalltooth sawfish (*Pristis pectinata*)

Rebecca K. May[1]
S. Gregory Tolley[1]
Rachel M. Scharer[2]
Bass Dye[1]
Felix Jose[1]
Gregg R. Poulakis (contact author)[1,2]

Email address for contact author: gregg.poulakis@MyFWC.com

[1] Department of Marine and Ecological Sciences
Florida Gulf Coast University
10501 FGCU Boulevard South
Fort Myers, Florida 33965

[2] Charlotte Harbor Field Laboratory
Fish and Wildlife Research Institute
Florida Fish and Wildlife Conservation Commission
585 Prineville Street
Port Charlotte, Florida 33954

Abstract—Juvenile smalltooth sawfish (*Pristis pectinata*) were monitored in the Peace River, Florida. A series of 37 acoustic receivers was used throughout the river, 9 of which were time synchronized. In 2016, 20 individuals were tagged and tracked from 27 May through 26 October. Most juveniles resided along the northern shoreline during the day, and some individuals crossed the river at night. Eleven smalltooth sawfish were detected on the southern shoreline, and 6 individuals used it extensively. Estimates of the sawfish positions were sorted into 3 habitat types: shallow, deep, and oyster reef. While at the southern shoreline, all sawfish tended to occupy shallow water, and most of them visited the oyster reefs. These results 1) improve our understanding of how the most productive nursery habitats function within the overall nursery, 2) will continue to influence decisions regarding management in this unique nursery, and 3) have implications for recovery planning for other nurseries of this endangered species.

Manuscript submitted 13 February 2019.
Manuscript accepted 22 November 2019.
Fish. Bull. 117:360–371 (2019).
Online publication date: 19 December 2019.
doi: 10.7755/FB.117.4.8

The views and opinions expressed or implied in this article are those of the author (or authors) and do not necessarily reflect the position of the National Marine Fisheries Service, NOAA.

The term *hotspot* has been used in many contexts and on a variety of spatial scales to refer to important regions of terrestrial and aquatic ecosystems. Hotspots have been used to describe areas of high plant and animal biodiversity on a global scale (Myers, 1988; Mittermeier et al., 2011), aggregation areas of non-native and native vertebrates, including elasmobranchs, on regional scales (Semmens et al., 2004; Southall et al., 2005; Polovina et al., 2006; Huveneers et al., 2018), and areas of emerging diseases on local scales (Waruhiu et al., 2017). Recently, the term has been used to refer to the most productive nursery habitats for marine fauna (Nagelkerken et al., 2015). Regardless of terminology, a key aspect of this work acknowledges that some portions of nurseries of well-studied species are used more than others; therefore, results from models that use a single habitat or single life stage can be misleading. For example, Heupel et al. (2007, 2018) attempted to define elasmobranch nurseries, and, although their criteria may have improved previous definitions, their model is not adaptable because it applies only to young of the year (YOY) and fails to provide a mechanism for recognizing the most productive habitats within the broader nursery, if they exist. In general, there is much to learn about how marine species use nurseries; therefore, models that attempt to explain this and other complex concepts must be adaptable to acknowledge the myriad ways in which nature sometimes solves the same problems.

> In versatility and elegance, Nature's creative effort provides a never-ending source of astonishment and delight. She is tireless and imaginative in her innovations. Having evolved a happy solution to a given problem, it might be expected that she would rest content, adopting her discovery universally. Instead, she seems determined to demonstrate that the same problem can be solved, and solved brilliantly, in many ways and always with a great show of virtuosity (Greenewalt, 1960).

Most of the occupied nurseries of the smalltooth sawfish (*Pristis pectinata*), listed as endangered under the U.S. Endangered Species Act (Federal Register, 2003), are in southwest Florida. Charlotte Harbor, located on the Gulf of Mexico, has been identified as 1 of 2 units that compose the critical habitat for promoting recovery of juveniles (Norton et al., 2012). The Charlotte Harbor estuarine system contains 2 distinct nurseries: 1 nursery associated with the Peace River (~10 km long) in the northern portion of the system, and 1 nursery in the Caloosahatchee River in the southern portion (~25 km long) (Scharer et al., 2017). In the Caloosahatchee River nursery, there are multiple hotspots, whereas in the Peace River there is only one (Poulakis et al., 2011). These nursery hotspots are important because adult females give birth nearby biennially and the young stay for 1–2 years; as a result, these areas contain multiple year classes and are prioritized for conservation, especially when the entire nursery cannot be preserved (Poulakis et al., 2016; Feldheim et al., 2017). Because criteria to establish broad nurseries and hotspots within nurseries are complementary (Poulakis and Grubbs, 2019), data from nursery hotspots have already influenced key decisions regarding management in southwest Florida (NMFS[1]).

The single hotspot in the Peace River was identified by using public encounter, scientific catch, and acoustic data and was initially thought to be confined to the northern shoreline (Poulakis et al., 2011). However, the boundaries of this hotspot were expanded after active tracking revealed nightly excursions toward the southern shoreline of the river (Huston et al., 2017). Interestingly, smalltooth sawfish have remained associated with this nursery hotspot regardless of seasonal changes in abiotic conditions (Scharer et al., 2017).

In August 2015, the Nature Conservancy began a pilot oyster restoration project along the southern shoreline of the Peace River, given the importance of oysters to overall estuarine health (Beck et al., 2011). Oysters contribute to the health of estuaries by providing water filtration, 3-dimensional habitats, and storm buffering (Coen et al., 2007; Rodriguez et al., 2014). Because the restoration area was within designated critical habitat of juvenile smalltooth sawfish, it became important to determine how juveniles were using this area and to document any interactions they had with the developing reefs.

To document habitat use by smalltooth sawfish in and around the southern shoreline of the Peace River, time-synchronized acoustic receivers were added to a preexisting receiver array to obtain estimates of the position of sawfish accurate to within 5 m. The specific goals of this study were 1) to determine if juveniles were regularly using the southern shoreline of the river, 2) to determine if the timing of river crossing to the southern shoreline was related to the tidal cycle, and 3) to identify any patterns of habitat use and movement along the southern shoreline by different age classes (YOY and ≥age 1). These data will improve our understanding of how hotspots function as the most productive habitats within smalltooth sawfish nurseries.

Materials and methods

Study area

Charlotte Harbor is one of the largest estuaries in Florida with an area of about 700 km^2 (Hammett, 1990). The main study area was along the southern shoreline of the Peace River, where an oyster restoration site was located (Fig. 1). Prior to this study, 3 oyster reefs were constructed by the Nature Conservancy 16 m from shore. The shoreline was dominated by red mangroves (*Rhizophora mangle*), and the water depth ranged from 0.1 m along the central and easternmost portions of the main study area to 1.2 m along the westernmost portion. The tidal regime is mixed semidiurnal, generally resulting in 2 high and 2 low tides of variable heights each day (Zheng and Weisberg, 2004).

Field sampling

Gill-net sampling for smalltooth sawfish was conducted from February through September 2016 as part of an ongoing research program (Poulakis et al., 2011). Each month, 2 random sampling trips (4 sites per trip) and an average of 2 directed sampling trips (3 sites per trip) were made in upper Charlotte Harbor, including in the Peace River (for details, see Scharer et al., 2017). Directed sampling sites were selected on the basis of historic capture locations or recent encounters reported by the public. All nets were soaked for 1 h and checked after 0.5 h or when animals were observed in the net, whichever came first. Sawfish were measured to the nearest millimeter in stretch total length (STL) and tagged prior to release.

Acoustic transmitters

All captured smalltooth sawfish were externally tagged with 69-kHz Vemco[2] (Bedford, Canada) V9 acoustic transmitters (hereafter referred to as *tags*; tag family: V9-2H; code space ID: A69-1303; length: 29 mm; weight in water: 2.9 g). Tags were programmed to emit a unique acoustic sequence every 80–160 s. Delays were used to reduce signal collisions when multiple individuals were within range of the same acoustic receivers and to maximize battery life (~12 months). The 69-kHz tags also functioned with the existing acoustic receivers deployed broadly throughout the estuary (see the "Acoustic monitoring" section).

[1] NMFS. 2019. Unpubl. data. Southeast Reg. Off., Natl. Mar. Fish. Serv., NOAA. 263 13th Ave. S., St. Petersburg, FL 33701.

[2] Mention of trade names or commercial companies is for identification purposes only and does not imply endorsement by the Florida Fish and Wildlife Conservation Commission or the National Marine Fisheries Service, NOAA.

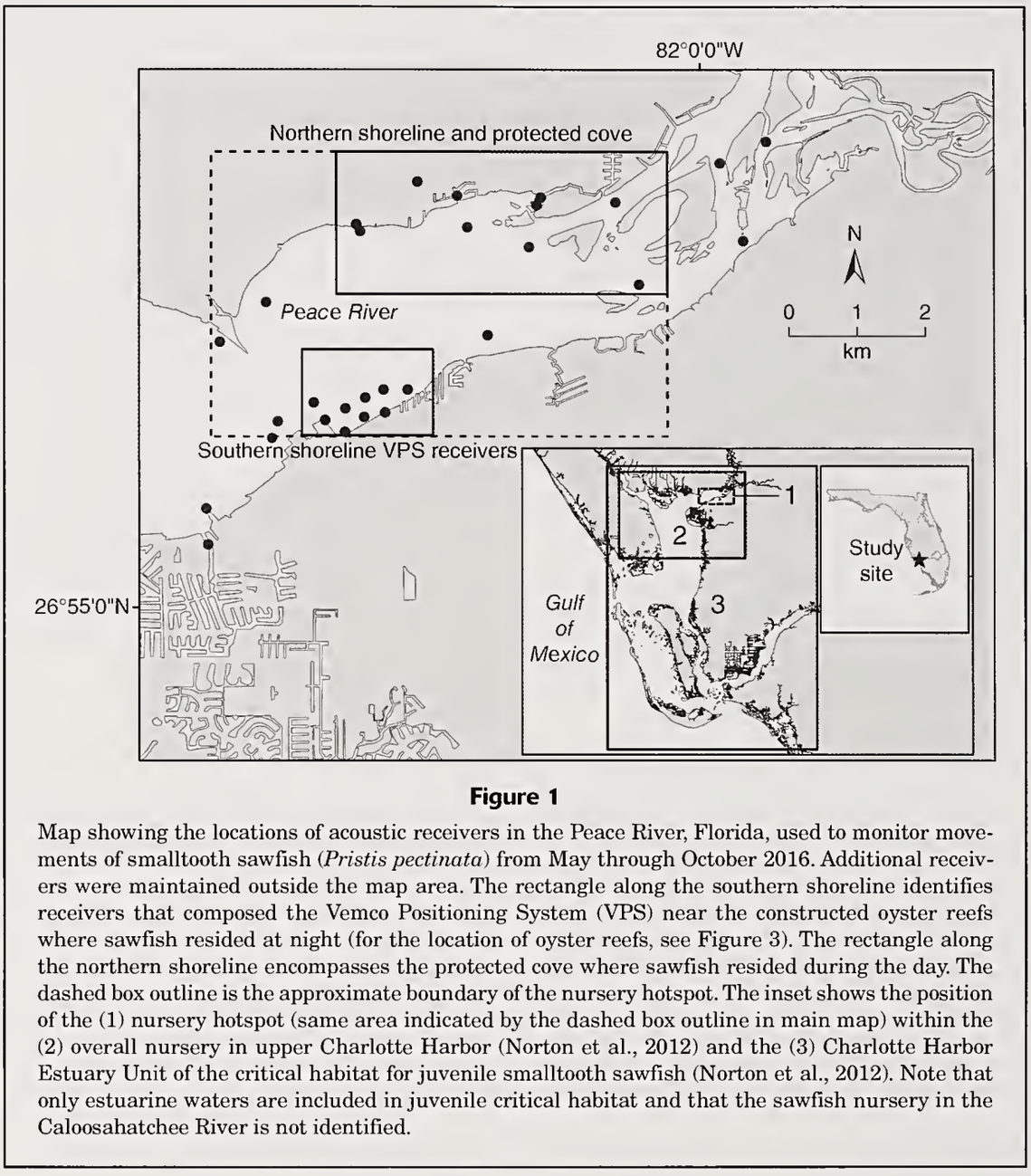

Figure 1

Map showing the locations of acoustic receivers in the Peace River, Florida, used to monitor movements of smalltooth sawfish (*Pristis pectinata*) from May through October 2016. Additional receivers were maintained outside the map area. The rectangle along the southern shoreline identifies receivers that composed the Vemco Positioning System (VPS) near the constructed oyster reefs where sawfish resided at night (for the location of oyster reefs, see Figure 3). The rectangle along the northern shoreline encompasses the protected cove where sawfish resided during the day. The dashed box outline is the approximate boundary of the nursery hotspot. The inset shows the position of the (1) nursery hotspot (same area indicated by the dashed box outline in main map) within the (2) overall nursery in upper Charlotte Harbor (Norton et al., 2012) and the (3) Charlotte Harbor Estuary Unit of the critical habitat for juvenile smalltooth sawfish (Norton et al., 2012). Note that only estuarine waters are included in juvenile critical habitat and that the sawfish nursery in the Caloosahatchee River is not identified.

Acoustic tags were prepared in the laboratory for external attachment prior to field sampling by using a cable tie covered with an epoxy gel to attach the acoustic tag to the flat half of a plastic dorsal fin tag (Rototag Identification Tag, 35 mm long by 9 mm wide, Dalton ID Systems Ltd., Henley-on-Thames, UK). Tags were applied to the thicker anterior margin of the second dorsal fin: a leather punch was used to make a hole for the projecting half of the Rototag, and then the 2 halves were attached (e.g., Whitty et al., 2009; Poulakis et al., 2013).

Acoustic monitoring

A total of 37 moored, single-frequency, omnidirectional VR2W or VR2Tx acoustic receivers (Vemco) were maintained in northern Charlotte Harbor, including in the Peace River, to monitor tagged smalltooth sawfish (Fig. 1; Huston et al., 2017; Scharer et al., 2017). When the signal of a tagged sawfish was detected by a receiver (maximum and mean detection ranges: 800 m and 450 m, respectively; Collins et al., 2008), date, time, and tag number were recorded. Data were downloaded from all receivers, and accumulated biofouling was removed every other month.

Positioning system

To accurately estimate positions of tagged smalltooth sawfish (hereafter referred to as *position estimates*) along the southern shoreline of the Peace River, with respect to the constructed oyster reefs, 3 VR2Tx acoustic receivers, 6 VR2W receivers, and 2 spatial reference tags were used to form a Vemco Positioning System (VPS; Fig. 1). These receivers were time synchronized to estimate positions of tagged sawfish on the basis of the times signals were received at each receiver (Özgül et al., 2015). The 6 VR2W

receivers required time-synchronization tags, which were placed 1 m from each receiver. VR2Tx receivers did not require external time-synchronization tags. Moored spatial reference tags were used to improve accuracy of position estimates. Functionality of the VPS was tested by using a V9 tag attached to the bottom of a pole to mimic the location of a sawfish.

Tide modeling

To investigate the influence of tidal fluctuations on habitat use by smalltooth sawfish near the shallow oyster reefs, a 2-dimensional hydrodynamic model (MIKE 21/3 Flow Model-FM, DHI Water and Environment, Hørsholm, Denmark) was calibrated to the study area (Dye et al., in press). This model simulated water transport when forced by variations in wind, temperature, salinity, freshwater discharges, and tides (Allahdadi et al., 2017). For the initial model, bathymetric data were obtained from the South Florida Water Management District (100-ft digital elevation model for the Lower West Coast region, available from website) and the General Bathymetric Chart of the Oceans (GEBCO_2014 Grid, available from website). To calibrate the model to the study site, water depth measurements were taken along 5 transects perpendicular to shore (6 or 7 measurements per transect), and latitude, longitude, and time of day were recorded to relate water depth to the tidal cycle. Tide data from the Tides and Currents website of NOAA's National Ocean Service for 2 stations, Locust Point (available from website) and Port Boca Grande (available from website), were also used to validate the modeled tidal heights. The model was run for the entire study period (27 May–26 October 2016) to discern when and where the receivers may have been too shallow to function effectively or were exposed at low tide.

For analyses, tidal phase was separated into two 6-h categories: ebbing and flooding. Position estimates for smalltooth sawfish were analyzed by using these 2 categories and were standardized as counts of detections per hour during each period (O'Shea et al., 2010). One test compared flooding to ebbing. Two other tests were conducted in recognition of the mixed semidiurnal tides of the study area: first and second occurrences were compared for both flooding and ebbing. Slack water was not investigated because the model outputs were hourly. These analyses were conducted by using Statgraphics Centurion 18 (Statpoint Technologies Inc., The Plains, VA). Because variances were unequal and the normality assumption was violated, non-parametric Kruskal–Wallis tests were used to test for differences in number of position estimates by tidal stage.

Analyses of movement and habitat use

Acoustic data were collected from 27 May through 26 October 2016 within the VPS. Raw detection data were sent to Vemco for determination of position estimates for individual smalltooth sawfish. Before further analysis, position estimates were filtered on the basis of their horizontal positioning errors (HPEs) following Scheel and Bisson (2012); only position estimates with HPE values <20 were analyzed because these estimates were likely within 5 m of the actual location.

Next, to determine habitat use within the VPS, polygons corresponding to 3 habitat types were created and defined as shallow (≤1 m), deep (>1 m), and oyster reef (all oyster restoration areas combined) for grouping position estimates. One meter was used to separate shallow and deep habitats because shallow depths are important for small juveniles (Norton et al., 2012). A likelihood ratio chi-square test (Cressie and Read, 1989; Rogers and White, 2007) was used to compare position estimates between shallow, deep, and oyster polygons (by using JMP 14, SAS Institute Inc., Cary, NC). This test was based on the area of the polygons (shallow: 0.12 km^2; deep: 1.74 km^2; and oyster: 0.002 km^2), with a significance level of 0.05, and compared the ratios of actual use of these habitats to what would be expected on the basis of random chance. Tests were run for all position estimates combined and then for position estimates for each individual sawfish separately because pooling position estimates would have eliminated the ability to identify individual variation. Bonferroni-adjusted confidence intervals (CIs) were also calculated to explore variation around the selection ratios and provide a conservative measure of reliability (Neu et al., 1974; Rogers and White, 2007). In general, ratios >1 indicate selection for a habitat type, and ratios <1 indicate selection against a habitat type.

By using river-wide data, contour maps were created with the software Surfer 13 (Golden Software LLC, Golden, CO) to visualize large-scale patterns of habitat use and movement, with regard to the nursery hotspot boundary (see inset in Figure 1). Raw data were reduced by selecting the first detection per hour per receiver for each individual, by using SAS 9.4 (SAS Institute Inc.), to eliminate the chance of data for 1 or 2 individuals biasing the results (Huston et al., 2017). These maps were used to visualize presence of smalltooth sawfish throughout the river by time period (day: 0900–1659; night: 2100–0559; crepuscular periods were omitted following Poulakis et al., 2013) and by age class following Scharer et al. (2012). Age classes were based on length (YOY: <1500 mm STL; ≥age 1: ≥1500 mm STL).

Results

In 2016, 20 smalltooth sawfish (726–1770 mm STL) were caught and tagged in upper Charlotte Harbor during daytime sampling (Peace River: number of tagged fish [n]=19; Myakka River: n=1; Table 1). Most individuals were caught along the northern shoreline of the Peace River within the nursery hotspot, and none were captured along the southern shoreline portion of the hotspot near the VPS. Both age classes, YOY (n=16) and ≥age 1 (n=4), were represented. Of the 20 tagged individuals, 11 sawfish (55%) were detected within the VPS on the

Table 1

Details for smalltooth sawfish (*Pristis pectinata*) caught and tagged with acoustic transmitters in upper Charlotte Harbor, Florida, including in the Peace River, in 2016, by tagging date (month/day/year). All individuals received uniquely coded 69-kHz acoustic tags. An asterisk indicates an individual that was detected within the array of acoustic receivers in the Vemco Positioning System (VPS) along the southern shoreline or that spent enough time in the area of the VPS to be analyzed in detail. STL=stretch total length.

Sawfish ID number	Sex	Date tagged	Date of last detection	STL (mm)	Detected by VPS	Used VPS area
1	M	3/8/2016	1/4/2017	1432	*	
2	F	3/8/2016	7/31/2016	1321	*	
3	M	3/15/2016	8/20/2016	1435	*	*
4	F	4/22/2016	4/14/2017	726	*	
5	F	4/26/2016	6/11/2016	952		
6	M	4/26/2016	10/28/2016	988		
7	M	4/26/2016	5/16/2016	957		
8	M	4/26/2016	2/18/2017	1028		
9	M	4/26/2016	7/7/2016	1001		
10	M	4/26/2016	6/20/2016	943		
11	F	5/9/2016	6/28/2016	889		
12	F	5/9/2016	8/5/2016	1010		
13	F	5/9/2016	4/26/2017	891	*	
14	F	5/9/2016	6/27/2016	903	*	
15	M	5/9/2016	5/30/2017	1160	*	*
16	F	5/18/2016	8/23/2016	1032	*	*
17	M	5/18/2016	3/2/2017	915	*	*
18	F	6/3/2016	12/5/2016	1019	*	*
19	F	6/28/2016	12/29/2016	897	*	*
20	F	7/5/2016	8/15/2016	1770		

southern shoreline (mostly at night), and 6 sawfish spent enough time there to be analyzed in detail. Throughout the 153-d study period (27 May–26 October), there were 115 d (75%) during which the VPS detected at least 1 sawfish. During 85 d (56%), multiple sawfish were detected.

Positioning system

The tide model validated water depths recorded in the field. Most modeled water depths were within 0.5 m of the measured depths, and results from the model indicate that the shallowest receiver remained submerged during the entire study (receiver depth: 0.1 m; lowest water depths were 0.2 m on 4 d in October). Therefore, water level should not have affected overall functioning of the array of acoustic receivers in the VPS.

Once the tide model was validated, the relationship between the presence of juveniles and tide stage was quantified (Fig. 2). Detections of tagged smalltooth sawfish occurred during 95 of the 295 flood tide stages (32%) and 99 of the 296 ebb stages (34%). There was no significant difference in median detections per hour along the southern shoreline between flood and ebb tides (Kruskal–Wallis test: H=0.7417, P=0.4). However, there was a significant difference in median detections per hour between the first and second tide occurrences for both flood (Kruskal–Wallis test: H=63.23, P<0.0001) and ebb (Kruskal–Wallis test: H=12.88, P=0.0003) periods. The majority of the first flood and first ebb tides occurred at night (75% and 74%, respectively, excluding crepuscular occurrences).

Habitat polygons created for the major habitat types found within the study area provided insight into how juveniles used shallow, deep, and oyster habitats, with a significant difference in the ratio of observed to expected frequencies detected among pooled position estimates (likelihood ratio chi-square test: G^2=3465, P<0.0001, df=2; Table 2).

To explore differences indicated by results from the likelihood ratio chi-square tests (Table 2), selection ratios were calculated. All but 1 juvenile selected the shallow or oyster habitats. This pattern was consistent when analyzing position data for all 6 sawfish combined, with a selection ratio of 3.770 (95% CI: 2.223–5.317) for shallow habitats, 0.828 (95% CI: 0.726–0.930) for deep habitats, and 3.570 (95% CI: 1.058–6.082) for oyster habitats. These data indicate that smalltooth sawfish were selecting against the deep habitat type and for shallow and

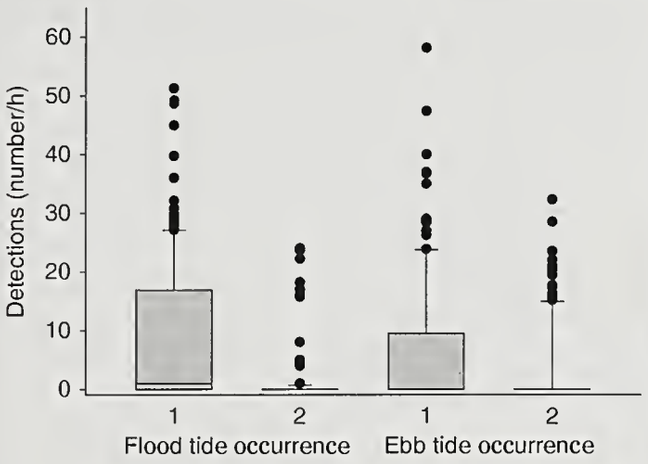

Figure 2

Activity of tagged smalltooth sawfish (*Pristis pectinata*) relative to the mixed semidiurnal tidal regime of the study area in the Peace River, Florida, from May through October 2016. Box plots from Kruskal–Wallis tests compare the median number of detections per hour of 6 sawfish within an array of acoustic receivers between the first and second flood tides each day and between the first and second ebb tides each day. The bottom and top boundaries of the box represent the 25th and 75th percentiles, respectively, of the number of detections per hour. The line within the box is the median value. Whiskers above the boxes indicate the 90th percentiles. Black circles indicate outlying values for upper ranges. Significantly more position estimates were placed on the southern shoreline during the first flood and first ebb tides (regardless of height), which typically occurred at night. Because these first tides typically occurred at night, the primary driver for the across-river movement was likely diel, rather than tidal.

oyster habitats. The wide CI for oyster habitats reflects greater variability in associations of sawfish with this habitat.

Although there were differences in habitat use among individuals, both size classes used all available habitats, and 5 of 6 individuals crossed over the oyster habitats (Table 2; Fig. 3). Furthermore, because most juveniles crossed the constructed oyster reefs, they were not actively avoiding the developing reefs.

Use of the southern shoreline varied ontogenetically, with detections of age-1 or older individuals peaking in June. Although a small number of detections of YOY occurred in June and July, detections in the VPS of YOY peaked in August and September.

Hotspot-wide movement patterns

In general, smalltooth sawfish made diel movements in the Peace River (Fig. 4). During the day, sawfish were concentrated near the protected cove portion of the northern shoreline as well as farther downriver along the northern shoreline. At night, they were still concentrated in these 2 areas but were more numerous downriver.

Table 2

Comparison of results from likelihood ratio chi-square tests (G^2) and selection ratio tests ($\hat{w}_{ij}$) for the 6 smalltooth sawfish (*Pristis pectinata*) detected frequently from May through October 2016 near the constructed oyster reefs along the southern shoreline of the Peace River, Florida. Sawfish were tagged with acoustic transmitters and tracked with an array of acoustic receivers in 3 habitat types: shallow (≤1 m), deep (>1 m), and oyster reef. Selection ratios >1 indicate selection for a habitat type; ratios <1 indicate selection against a habitat type. Sawfish ID numbers correspond to those in Table 1. For habitat descriptions, see the "Materials and methods" section.

Sawfish ID number	G^2	df	P	$\hat{w}_{ij}$		
				Shallow	Deep	Oyster
3	1983.25	2	<0.01	4.84	0.76	5.56
15	1030.70	2	<0.01	4.03	0.81	3.39
16	30.50	2	<0.01	1.82	0.89	2.32
17	38.50	2	<0.01	1.53	0.98	0.00
18	447.83	2	<0.01	7.75	0.57	5.81
19	507.82	2	<0.01	4.22	0.80	4.62

Although some individuals moved only along the northern shoreline, smalltooth sawfish used both shorelines (Fig. 5). The majority (91%) of detections at the VPS occurred at night, and over half (63%) of the daytime detections were of the largest individual. Sample size was low, but this finding suggests that there are ontogenetic differences in hotspot-wide habitat use: larger juveniles (>1500 mm STL) were more likely to make farther excursions during the day.

Diel movements were evident within the entire nursery hotspot over short time scales (e.g., 1 week; Fig. 6) and over the course of the entire study (Fig. 7). Individuals generally remained along the northern shoreline during the day and made nightly excursions toward the middle of the river, sometimes to the southern shoreline, and back.

Discussion

Currently, for the smalltooth sawfish in the United States, habitat use by juveniles is monitored and related management actions can be implemented on 3 spatial scales (see inset in Fig. 1). First, nursery hotspots are relatively discrete areas within the broader nursery where YOY and juveniles age 1 or older commonly occur over many years (i.e., the most productive nursery habitats; Nagelkerken et al., 2015). Young may be born elsewhere in the broader nursery, but they tend to go to nursery hotspots and spend most of their time there, even when disturbances, such as tropical storms or cold fronts, temporarily disrupt normal patterns of habitat use (Poulakis et al., 2016; Scharer et al., 2017). Therefore, nursery hotspots often contain at least 2 year classes and become

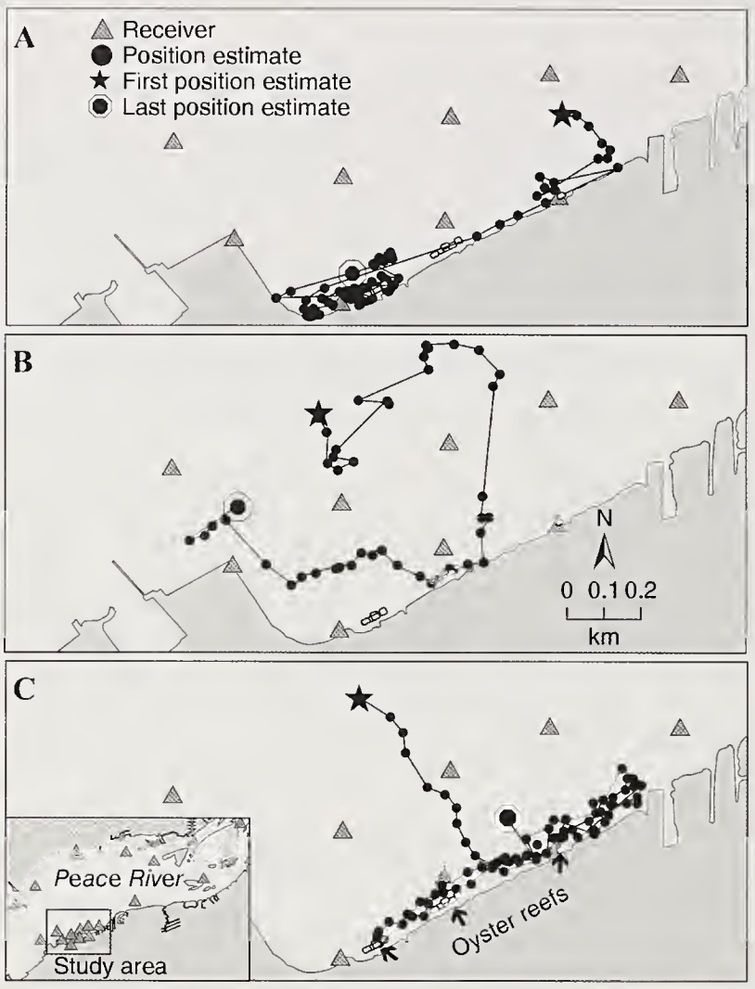

Figure 3

Maps showing the receiver locations and position estimates for 3 tagged young-of-the-year smalltooth sawfish (*Pristis pectinata*) when they interacted with the constructed oyster reefs in 2016 in the Peace River, Florida. Receivers shown were time synchronized to estimate positions of tagged sawfish based on the time that signals were received at each receiver. Each map presents position estimates during a short time segment for each sawfish: (**A**) sawfish 18, detected on 7 June from 0423 to 1359; (**B**) sawfish 16, detected on 5 July from 0100 to 0803; and (**C**) sawfish 19, detected on 9 October from 0043 to 0622 (sawfish ID numbers correspond to those in Table 1). The inset in the lower left corner shows the entire study area.

conservation priorities when preserving the entire nursery is not possible. Second, the nursery itself encompasses any hotspots, and the corridors between them, where young may remain for their first 2–3 years (Norton et al., 2012). Third, for this species, juvenile *critical habitat* is purely a management designation required in the United States as part of the Endangered Species Act and encompasses all nurseries and the non-nursery habitats that connect them. There are 2 large units of juvenile critical habitat for this species, 1 unit encompasses the Charlotte Harbor estuarine system, where this study was conducted, and the other includes the entire Ten Thousand Islands region and Everglades National Park (Norton et al., 2012). Other elasmobranchs are likely to have variations of these spatial scales and the life history stages within them; therefore, adapting these ideas as results from future studies emerge would be expected.

Within the Charlotte Harbor Estuary Unit of critical habitat for smalltooth sawfish, there are 2 distinct nurseries in the Peace and Caloosahatchee Rivers (Norton et al., 2012; Feldheim et al., 2017). Within those sawfish nurseries, 5 hotspots have been identified (Poulakis et al., 2011, 2016). The Peace River has only one known hotspot, and its approximate boundaries, within the broader nursery, have been refined through recent research (Huston et al., 2017). In our study, using relatively new technology, we further refined habitat use within the hotspot and identified sawfish behavior associated with the southern shoreline of the Peace River. Collectively, the results of these studies have already resulted in management decisions (NMFS[1]) and have served to enhance our understanding of the early life history of this endangered species. This research has never been used to restrict previous nursery designations, as was recently suggested by Heupel et al. (2018). In fact, the concepts of nursery and nursery hotspot are complementary and help prioritize areas for management and conservation actions (Poulakis and Grubbs, 2019). Both of these concepts should be considered as more research is conducted on this and other elasmobranch species, especially if they occur in regions where substantial habitat loss could occur and data to support management and conservation actions may be required to sustain or recover populations.

As in previous studies (Poulakis et al., 2016; Huston et al., 2017; Lear et al., 2019), diel behaviors were observed in this study. In general, smalltooth sawfish resided along the northern shoreline of the Peace River in a protected cove during the day and ventured away from the cove and toward the southern shoreline at night. However, because of the increased accuracy of the time-synchronized array of acoustic receivers, which provided continuous tracking data for this study, complete crossing of the river was documented for the first time with near-exact, autonomously recorded GPS locations of the sawfish. Both size classes remained along the northern shoreline during the day, but individuals age 1 or older began to use the entire hotspot, including the southern shoreline, well before YOY, a difference that may relate to known ontogenetic changes in the areas where individuals are active and in the depths where they occur throughout the range of this species (Simpfendorfer et al., 2010; Poulakis et al., 2011, 2013; Brame et al., 2019).

Restoration projects have become necessary to promote recovery of oyster populations and to enhance accretion rates (Coen et al., 2007; Rodriguez et al., 2014). Juvenile smalltooth sawfish are known to frequent shallow

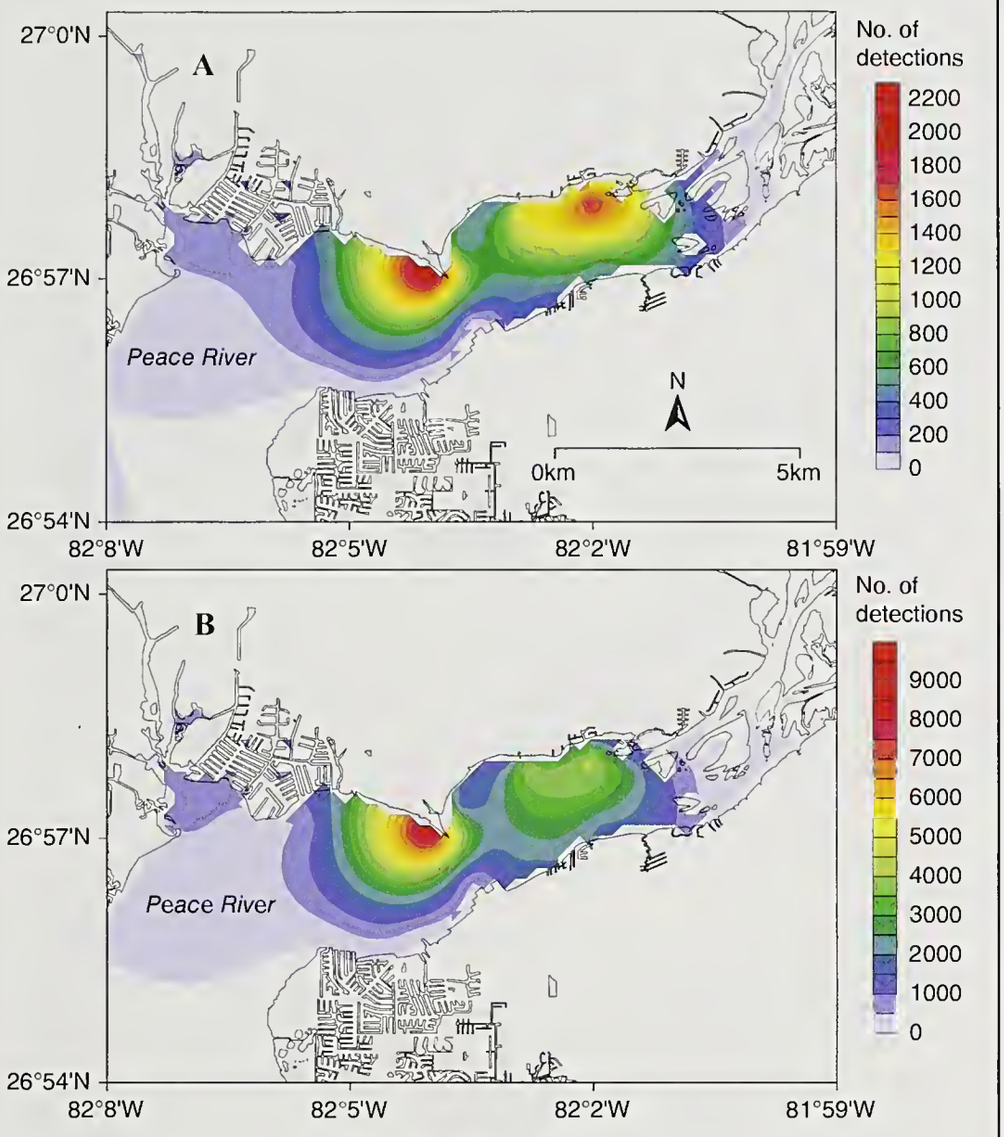

Figure 4

Visualization of diel movements from pooled locations of all 20 juvenile smalltooth sawfish (*Pristis pectinata*) caught and tagged with acoustic transmitters in upper Charlotte Harbor (Peace and Myakka Rivers), Florida, during (**A**) day (0900–1659) and (**B**) night (2100–0559) from May through October 2016. The color scale denotes the number of first detections per hour, per receiver, for each individual. The light blue color indicates areas where a range of 0–100 or 0–500 detections was recorded, and the white color indicates areas with no detections.

shoreline habitats, yet this study is the first to explore interactions with oyster reefs. Although juveniles did not select the restored oyster habitats more often than other available shallow habitats, as the reefs mature, perhaps juveniles will interact with them more often as habitat complexity increases and more potential forage species reside in the area (Harding and Mann, 2001).

Throughout the mixed semidiurnal tidal regime of the Charlotte Harbor estuarine system, smalltooth sawfish were detected on the southern shoreline significantly more often during the first flood and first ebb tides of the day, regardless of height. Because these first tides typically occurred at night, the primary driver for the across-river movement was likely diel, rather than tidal.

This study is the first to use an automated positioning system on a sawfish species, and results indicate that this technology is effective in the shallow habitats where individuals in the early life history stages of this and other relatively large fish species reside. The array of acoustic receivers allowed tracking data that traditionally have been collected manually to be automatically recorded 24 h a day. On the basis of the results of this preliminary, summer-focused study, similar arrays will be deployed in this and other nursery hotspots, including on the northern shoreline

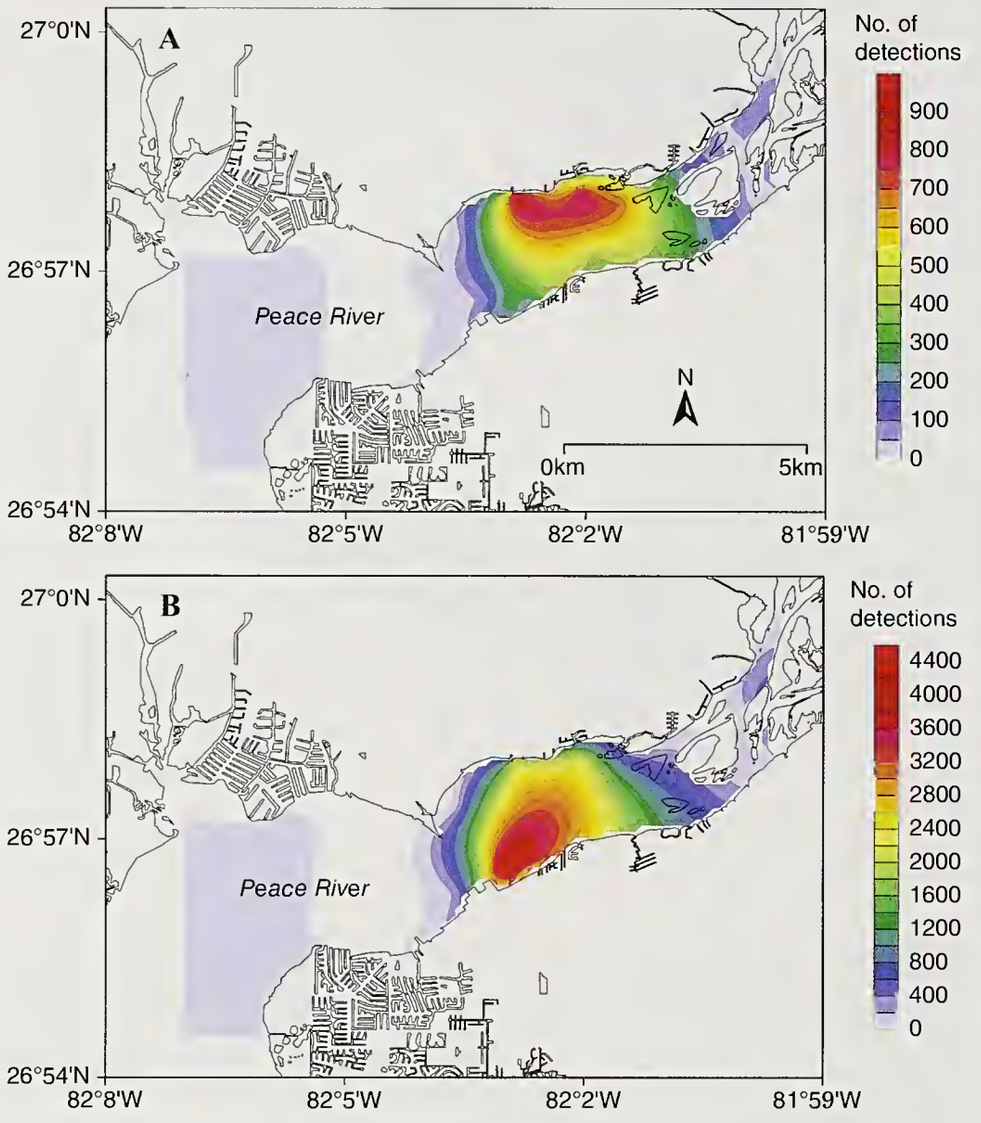

Figure 5

Visualization of diel movements from pooled locations of 6 tagged juvenile smalltooth sawfish (*Pristis pectinata*) that used the southern shoreline of the Peace River, Florida, extensively between 27 May and 26 October 2016 during (**A**) day (0900–1659) and (**B**) night (2100–0559). These individuals regularly crossed from the northern shoreline, where they resided during the day, to the southern shoreline at night. The color scale denotes the number of first detections per hour, per receiver, for each individual. The light blue color indicates areas where a range of 0–50 or 0–200 detections was recorded, and the white color indicates areas with no detections.

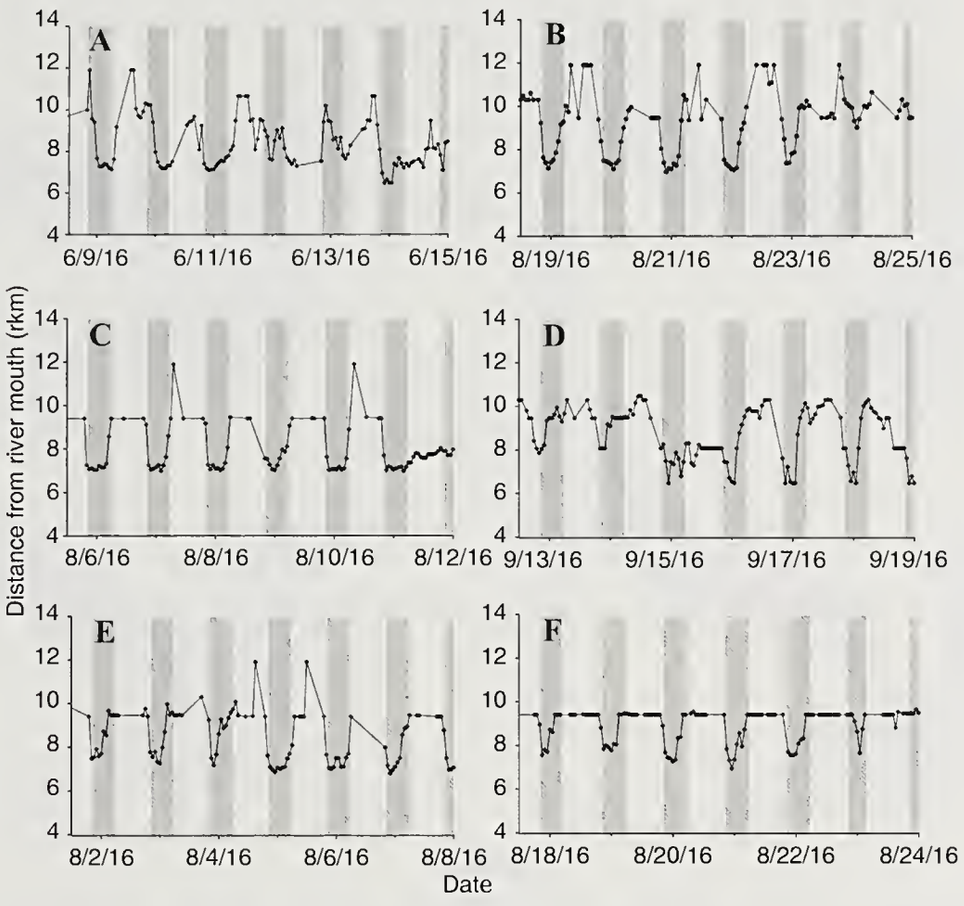

Figure 6

Example patterns of weekly diel movements of 6 tagged smalltooth sawfish (*Pristis pectinata*) in the Peace River, Florida, by hour and date: (**A**) ≥1 year old (sawfish 3), (**B**) young of the year (YOY, sawfish 17), (**C**) ≥1 year old (sawfish 15), (**D**) YOY (sawfish 18), (**E**) YOY (sawfish 16), and (**F**) YOY (sawfish 19). River kilometer (rkm) refers to distance from the river mouth (i.e., rkm 0), and gray bars indicate night. The Vemco Positioning System (VPS) was located at rkm 6–8. Sawfish ID numbers correspond to those in Table 1. In general, individuals of both age classes remained in or near the protected cove (rkm 9–11) during the day and moved downriver and toward the southern shoreline, where they were detected within the VPS, at night.

of the Peace River, to obtain fine-scale data on where juvenile smalltooth sawfish reside during the day. In addition, results of recent work indicate that internally placed acoustic tags can eliminate tag retention issues and allow collection of year-round data over multiple years (Poulakis and Grubbs, 2019); therefore, the tracking data from these arrays will provide a more complete picture of how juveniles use the most productive habitats within their broader nurseries. Although this technology offers many benefits, we recognize that it may not be accessible to all researchers because of the cost and maintenance involved, but it may be worth the investment if the most productive habitats can be identified for a species of interest.

Acknowledgments

This research was supported primarily by grant NA13NMF4720047 from the National Marine Fisheries Service (NMFS) under Section 6 of the U.S. Endangered Species Act (Cooperation with the States) and grant no. 02012016-001 from the Nature Conservancy. Research was conducted pursuant to NMFS endangered species permit no. 15802. C. Saari and 3 anonymous reviewers improved earlier versions of the manuscript. Statements, findings, conclusions, and recommendations are those of the authors and do not necessarily reflect the views or policies of the funding agencies.

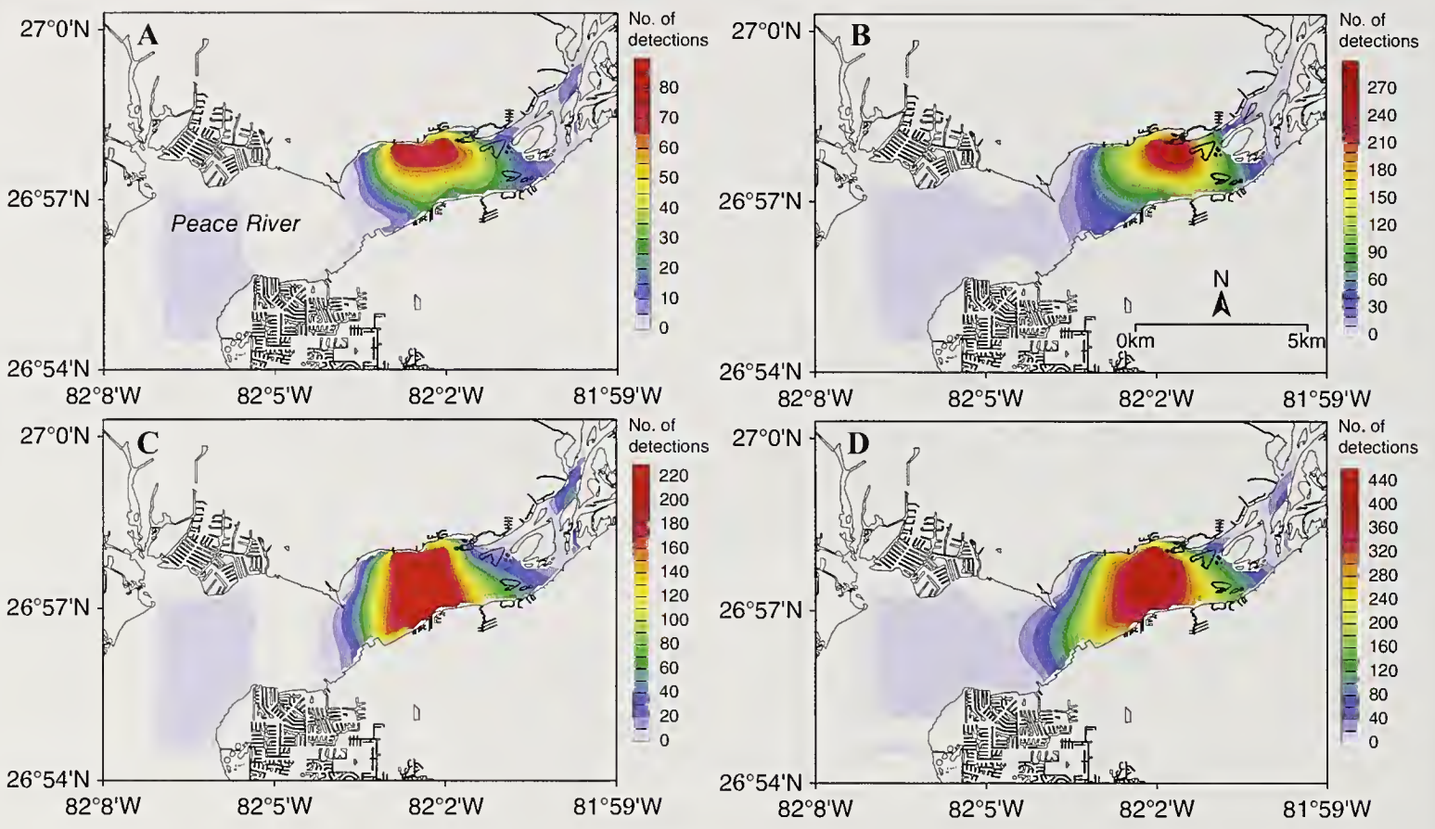

Figure 7

Visualization of diel movements of 2 tagged smalltooth sawfish (*Pristis pectinata*) in the Peace River, Florida, from May through October 2016: sawfish 16, a young of the year with a stretch total length [STL] of 1032 mm, during (**A**) day and (**C**) night, and sawfish 3, a smalltooth sawfish with an age ≥1 year and STL of 1435 mm, during (**B**) day and (**D**) night (sawfish ID numbers correspond to those in Table 1). These sawfish generally remained along the northern shoreline during the day, making nightly excursions across the river, sometimes to the southern shoreline. The color scale denotes the number of first detections per hour, per receiver, for each individual. The light blue color indicates areas where a range of 0–5, 0–10, or 0–20 detections was recorded, and the white color indicates areas with no detections.

Literature cited

Allahdadi, M. N., F. Jose, E. J. D'Sa, and D. S. Ko.
2017. Effect of wind, river discharge, and outer-shelf phenomena on circulation dynamics of the Atchafalaya Bay and shelf. Ocean Eng. 129:567–580.

Beck, M. W., R. D. Brumbaugh, L. Airoldi, A. Carranza, L. D. Coen, C. Crawford, O. Defeo, G. J. Edgar, B. Hancock, M. C. Kay, et al.
2011. Oyster reefs at risk and recommendations for conservation, restoration, and management. BioScience 61:107–116.

Brame, A. B., T. R. Wiley, J. K. Carlson, S. V. Fordham, R. D. Grubbs, J. Osborne, R. M. Scharer, D. M. Bethea, and G. R. Poulakis.
2019. Biology, ecology, and status of the smalltooth sawfish *Pristis pectinata* in the USA. Endanger. Species Res. 39:9–23.

Coen, L. D., R. D. Brumbaugh, D. Bushek, R. Grizzle, M. W. Luckenbach, M. H. Posey, S. P. Powers, and S. G. Tolley.
2007. Ecosystem services related to oyster restoration. Mar. Ecol. Prog. Ser. 341:303–307.

Collins, A. B., M. R. Heupel, and C. A. Simpfendorfer.
2008. Spatial distribution and long-term movement patterns of cownose rays *Rhinoptera bonasus* within an estuarine river. Estuar. Coasts 31:1174–1183.

Cressie, N., and T. R. C. Read.
1989. Pearson's X^2 and the loglikelihood ratio statistic G^2: a comparative review. Int. Stat. Rev. 57:19–43.

Dye, B., F. Jose, and M. N. Allahdadi.
In press. Circulation dynamics and seasonal variability for the Charlotte Harbor estuary, southwest Florida coast. J. Coast. Res.

Federal Register.
2003. Endangered and threatened species; final endangered status for a distinct population segment of smalltooth sawfish (*Pristis pectinata*) in the United States. Fed. Regist. 68:15674–15680. [Available from website.]

Feldheim, K. A., A. T. Fields, D. D. Chapman, R. M. Scharer, and G. R. Poulakis.
2017. Insights into reproduction and behavior of the smalltooth sawfish *Pristis pectinata*. Endanger. Species Res. 34:463–471.

Greenewalt, C. H.
1960. Hummingbirds, 250 p. Doubleday and Co. Inc., New York.

Hammett, K. M.
1990. Land use, water use, streamflow characteristics, and water-quality characteristics of the Charlotte Harbor inflow area, Florida. U.S. Geol. Surv. Water-Supply Pap. 2359-A, 64 p. [Available from website.]

Harding, J. M., and R. Mann.
2001. Oyster reefs as fish habitat: opportunistic use of restored reefs by transient fishes. J. Shellfish Res. 20:951–959.

Heupel, M. R., J. K. Carlson, and C. A. Simpfendorfer.
2007. Shark nursery areas: concepts, definition, characterization and assumptions. Mar. Ecol. Prog. Ser. 337: 287–297.

Heupel, M. R., S. Kanno, A. P. B. Martins, and C. A. Simpfendorfer.
2018. Advances in understanding the roles and benefits of nursery areas for elasmobranch populations. Mar. Freshw. Res. 70:897–907.

Huston, C. A., P. W. Stevens, R. M. Blaxton, S. G. Tolley, R. M. Scharer, B. M. Tornwall, and G. R. Poulakis.
2017. Diel movements of juvenile smalltooth sawfish: implications for defining the size of a nursery hotspot. Endanger. Species Res. 34:311–322.

Huveneers, C., K. Apps, E. E. Becerril-García, B. Bruce, P. A. Butcher, A. B. Carlisle, T. K. Chapple, H. M. Christiansen, G. Cliff, T. H. Curtis, et al.
2018. Future research directions on the "elusive" white shark. Front. Mar. Sci. 5:455.

Lear, K. O., G. R. Poulakis, R. M. Scharer, A. C. Gleiss, and N. M. Whitney.
2019. Fine-scale behavior and habitat use of the endangered smalltooth sawfish (*Pristis pectinata*): insights from accelerometry. Fish. Bull. 117:348–359.

Mittermeier, R. A., W. R. Turner, F. W. Larsen, T. M. Brooks, and C. Gascon.
2011. Global biodiversity conservation: the critical role of hotspots. *In* Biodiversity hotspots (F. E. Zachos and J. C. Habel, eds.), p. 3–22. Springer-Verlag, Berlin, Germany.

Myers, N.
1988. Threatened biotas: "hot spots" in tropical forests. Environmentalist 8:187–208.

Nagelkerken, I., M. Sheaves, R. Baker, and R. M. Connolly.
2015. The seascape nursery: a novel spatial approach to identify and manage nurseries for coastal marine fauna. Fish Fish. 16:362–371.

Neu, C. W., C. R. Byers, and J. M. Peek.
1974. A technique for analysis of utilization–availability data. J. Wildl. Manage. 38:541–545.

Norton, S. L., T. R. Wiley, J. K. Carlson, A. L. Frick, G. R. Poulakis, and C. A. Simpfendorfer.
2012. Designating critical habitat for juvenile endangered smalltooth sawfish in the United States. Mar. Coast. Fish. 4:473–480.

O'Shea, O. R., M. J. Kingsford, and J. Seymour.
2010. Tide-related periodicity of manta rays and sharks to cleaning stations on a coral reef. Mar. Freshw. Res. 61: 65–73.

Özgül, A., A. Lök, A. Ulaş, F. O. Düzbastılar, T. T. Tanrıkul, and C. Pelister.
2015. Preliminary study on the use of the Vemco Positioning System to determine fish movements in artificial reef areas: a case study on *Sciaena umbra* Linnaeus, 1758. J. Appl. Ichthyol. 31(S3):41–47.

Polovina, J., I. Uchida, G. Balazs, E. A. Howell, D. Parker, and P. Dutton.
2006. The Kuroshio Extension Bifurcation Region: a pelagic hotspot for juvenile loggerhead sea turtles. Deep Sea Res., II 53:326–339.

Poulakis, G. R., and R. D. Grubbs.
2019. Biology and ecology of sawfishes: global status of research and future outlook. Endanger. Species Res. 39:77–90.

Poulakis, G. R., P. W. Stevens, A. A. Timmers, T. R. Wiley, and C. A. Simpfendorfer.
2011. Abiotic affinities and spatiotemporal distribution of the endangered smalltooth sawfish, *Pristis pectinata*, in a south-western Florida nursery. Mar. Freshw. Res. 62:1165–1177.

Poulakis, G. R., P. W. Stevens, A. A. Timmers, C. J. Stafford, and C. A. Simpfendorfer.
2013. Movements of juvenile endangered smalltooth sawfish, *Pristis pectinata*, in an estuarine river system: use of non-main-stem river habitats and lagged responses to freshwater inflow-related changes. Environ. Biol. Fish. 96: 763–778.

Poulakis, G. R., P. W. Stevens, A. A. Timmers, C. J. Stafford, D. D. Chapman, K. A. Feldheim, M. R. Heupel, and C. Curtis.
2016. Long-term site fidelity of endangered smalltooth sawfish (*Pristis pectinata*) from different mothers. Fish. Bull. 114:461–475.

Rodriguez, A. B., F. J. Fodrie, J. T. Ridge, N. L. Lindquist, E. J. Theuerkauf, S. E. Coleman, J. H. Grabowski, M. C. Brodeur, R. K. Gittman, D. A. Keller, et al.
2014. Oyster reefs can outpace sea-level rise. Nat. Clim. Chang. 4:493–497.

Rogers, K. B., and G. C. White.
2007. Analysis of movement and habitat use from telemetry data. *In* Analysis and interpretation of freshwater fisheries data (C. S. Guy and M. L. Brown, eds.), p. 625–676. Am. Fish. Soc., Bethesda, MD.

Scharer, R. M., P. W. Stevens, C. P. Shea, and G. R. Poulakis.
2017. All nurseries are not created equal: large-scale habitat use patterns in two smalltooth sawfish nurseries. Endanger. Species Res. 34:473–492.

Scheel, D., and L. Bisson.
2012. Movement patterns of giant Pacific octopuses, *Enteroctopus dofleini* (Wülker, 1910). J. Exp. Mar. Biol. Ecol. 416–417:21–31.

Simpfendorfer, C. A., T. R. Wiley, and B. G. Yeiser.
2010. Improving conservation planning for an endangered sawfish using data from acoustic telemetry. Biol. Conserv. 143:1460–1469.

Semmens, B. X., E. R. Buhle, A. K. Salomon, and C. V. Pattengill-Semmens.
2004. A hotspot of non-native marine fishes: evidence for the aquarium trade as an invasion pathway. Mar. Ecol. Prog. Ser. 266:239–244.

Southall, E. J., D. W. Sims, J. D. Metcalfe, J. I. Doyle, S. Fanshawe, C. Lacey, J. Shrimpton, J.-L. Solandt, and C. D. Speedie.
2005. Spatial distribution patterns of basking sharks on the European shelf: preliminary comparison of satellite-tag geolocation, survey and public sightings data. J. Mar. Biol. Assoc. U.K. 85:1083–1088.

Waruhiu, C., S. Ommeh, V. Obanda, B. Agwanda, F. Gakuya, X.-Y. Ge, X.-L. Yang, L.-J. Wu, A. Zohaib, B. Hu, et al.
2017. Molecular detection of viruses in Kenyan bats and discovery of novel astroviruses, caliciviruses and rotaviruses. Virol. Sinica 32:101–114.

Whitty, J. M., D. L. Morgan, S. C. Peverell, D. C. Thorburn, and S. J. Beatty.
2009. Ontogenetic depth partitioning by juvenile freshwater sawfish (*Pristis microdon*: Pristidae) in a riverine environment. Mar. Freshw. Res. 60:306–316.

Zheng, L., and R. H. Weisberg.
2004. Tide, buoyancy, and wind-driven circulation of the Charlotte Harbor estuary: a model study. J. Geophys. Res. 109:C06011.

National Marine
Fisheries Service
NOAA

Fishery Bulletin
established in 1881

Spencer F. Baird
First U.S. Commissioner
of Fisheries and founder
of *Fishery Bulletin*

Simple gear modifications for achieving greater than 40% bycatch reduction in an estuarine shrimp trawl fishery

H. Kevin Brown (contact author)[1]
Blake Price[2]
Laura Lee[3]
M. Scott Baker Jr.[4]
Sara E. Mirabilio[5]

Email address for contact author: kevin.h.brown@ncdenr.gov

[1] Division of Marine Fisheries
North Carolina Department of
Environmental Quality
3441 Arendell Street
Morehead City, North
Carolina 28557

[2] Riverside Technology Inc.
Beaufort Laboratory
Southeast Fisheries Science Center
National Marine Fisheries Service, NOAA
101 Pivers Island Road
Beaufort, North Carolina 28516

[3] Division of Marine Fisheries
North Carolina Department of Environmental
Quality
3441 Arendell Street
Morehead City, North Carolina 28557

[4] North Carolina Sea Grant Extension Program
University of North Carolina Wilmington Center
for Marine Science
601 S. College Road
Wilmington, North Carolina, 28409

[5] North Carolina Sea Grant Extension Program
P.O. Box 699
Manteo, North Carolina 27954

Abstract—Penaeid shrimp fisheries, particularly those operating with bottom otter trawls, can generate high levels of bycatch. In 2014, a workgroup was formed to devise and test gear modifications in Pamlico Sound and the nearshore waters of North Carolina with the goal of improving bycatch reduction rates. Trials were conducted in 2015 and 2016 on large (>12 m), double-rigged industry vessels, and trials were conducted in 2017 on 1 double-rigged vessel and 3 smaller, twin-rigged vessels. A paired *t*-test and a randomization test were used to compare tows. The results of both tests indicate that 4 of the 14 gears tested achieved an average rate of finfish bycatch reduction that was 40% greater than that of the control gear. Shrimp loss in most gears tested was minimal. Three of the 4 gears that met the reduction goal for finfish bycatch employed a combination of increased codend mesh size and larger finfish escape openings relative to the control configuration. Relying on industry input and expert opinions as well as on past research to guide the selection of test gears and their design, the workshop members developed gear combinations that appear to meet the management objective for bycatch reduction. The results of this work provide direction for future testing in similar fisheries.

Manuscript submitted 2 April 2019.
Manuscript accepted 4 December 2019.
Fish. Bull. 117:372–385 (2019).
Online publication date: 19 December 2019.
doi: 10.7755/FB.117.4.9

The views and opinions expressed or implied in this article are those of the author (or authors) and do not necessarily reflect the position of the National Marine Fisheries Service, NOAA.

Bycatch in commercial fisheries remains an important and controversial topic in fisheries management and marine conservation both in the United States and around the world (Andrew and Pepperell, 1992; Crowder and Murawski, 1998; Hall et al., 2000; Kelleher, 2005; Davies et al., 2009; Portley et al.[1]). Warm-water penaeid shrimp fisheries, particularly those operating with bottom otter trawls, can generate high levels of bycatch (Andrew and Pepperell, 1992). Importantly, bycatch in the shrimp trawl fishery can have ecological, economic, and management repercussions (Hall et al., 2000).

Efforts to reduce bycatch in shrimp trawl fisheries span decades (Watson and McVea, 1977; Vieira et al., 2017), and the conventional approach to addressing bycatch has been through gear modification to achieve bycatch reduction rather than elimination of trawl gear (Watson et al., 1999; Broadhurst, 2000; Eayrs, 2012). Gear modifications that are easy to deploy, are inexpensive, reduce bycatch, and maintain shrimp catch are more acceptable to the fishing industry than area or seasonal closures (Murray et al., 1992). Some of the earliest work focused on the development of the trawl efficiency device (TED), also known as the turtle excluder device, in efforts to exclude sea turtles from the gear (Watson and McVea, 1977). Subsequently, bycatch reduction devices (BRD) have been developed and tested in an attempt to exclude bycatch by size or behavior (Broadhurst, 2000). The use

[1] Portley, N., M. Westmeyer, and J. M. Garcia Caudilo. 2015. SFP report on the wild shrimp sector: bycatch in global shrimp fisheries, 15 p. Sustainable Fish. Partner. Found., Honolulu, HI. [Available from website.]

of TEDs and BRDs has been required by federal and state law since the early 1990s in all commercial shrimp trawl fisheries in the southeastern United States.

In the United States, penaeid shrimp account for approximately 11% of the $5.3 billion total ex-vessel value reported for domestic fisheries in 2016 (NMFS[2]). Approximately 70% of domestic shrimp harvest occurs in the Gulf of Mexico, and North Carolina is typically the top producer among states on the East Coast. From 2013 through 2017, commercial fishermen in North Carolina landed an average of 4130 Mg of shrimp with an ex-vessel value of $20.0 million (NCDMF[3]).

The fishery in North Carolina targets brown (*Farfantepenaeus aztecus*), pink (*F. duorarum*), and white (*Litopenaeus setiferus*) shrimp. All 3 species are considered annual crops, implying that natural mortality rather than fishing pressure has the greatest effect on population size (NCDMF, 2015). This fishery is unique among those in East Coast states and much of the Gulf of Mexico in that approximately 75% of the shrimp harvest comes from inshore, estuarine waters (NCDMF, 2015). Approximately 92% of the harvest is captured with bottom otter trawls because other gears, such as channel nets, skimmer trawls, and shrimp pots, are not generally suitable for operating in the deeper, often muddy estuarine systems (e.g., Pamlico Sound, North Carolina) (NCDMF, 2015).

The shrimp fishery in North Carolina is controversial because of the amount of finfish bycatch in the fishery and the resulting discard of commercially and recreationally valuable fish species, such as the southern flounder (*Paralichthys lethostigma*), summer flounder (*P. dentatus*), Gulf flounder (*P. albigutta*), weakfish (*Cynoscion regalis*), spot (*Leiostomus xanthurus*), and Atlantic croaker (*Micropogonias undulatus*) (Murray et al., 1992; SAFMC, 1996; NCDMF, 2015).

Management and research efforts to curb bycatch in North Carolina are longstanding and significant. In 1992, North Carolina became the first state on the East Coast to require BRDs in shrimp trawls (NCDMF, 2015). State fisheries biologists have tested existing BRDs (Holland[4]; McKenna and Monaghan[5]; Brown[6]), experimented with modified trawls (He et al.[7]), and conducted statewide bycatch characterization studies (Brown[8]). Academic scientists have partnered with industry to reduce bycatch on multiple occasions (Murray et al., 1992; Rulifson et al., 1992). Likewise, members of the commercial shrimp industry have participated in numerous collaborative research projects addressing bycatch issues, including at least 21 short-term projects funded by the North Carolina Sea Grant from 1995 through 2013 (information about these projects is available from website).

In 2014, the North Carolina shrimp fishery management plan was amended by the North Carolina Marine Fisheries Commission (NCMFC) to focus exclusively on reducing finfish bycatch in the bottom otter trawl fishery (NCDMF, 2015). The overall objective of the research reported here was to address this management goal by evaluating gear modifications capable of achieving bycatch reductions relative to control trawl gears while minimizing shrimp loss. To achieve this goal, the project team set forth the following objectives: 1) convene a workgroup to devise and prioritize experimental gears to be tested, 2) conduct comparable paired tows aboard commercial fishing vessels, and 3) compare results to catch data observed in control nets. The desired outcome was to develop technical solutions within 3 years that met a bycatch reduction target of 40% (above that achieved with a control gear), as recommended by the NCMFC, while maintaining shrimp catches.

Materials and methods

Workgroup

Prior to gear selection and testing, we convened a 12-member workgroup consisting of commercial fishermen, net makers, and industry representatives from North Carolina. Multiple international gear experts attended the first meeting and provided advice relevant to the needs of the fishery in North Carolina (Brown et al.[9]). The purpose of this workgroup was to provide feedback throughout the project, from gear

[2] NMFS (National Marine Fisheries Service). 2017. Fisheries of the United States, 2016. NOAA Curr. Fish. Stat. 2016, 147 p. [Available from website.]

[3] NCDMF (North Carolina Division of Marine Fisheries). 2019. 2019 license statistics annual report, 424 p. Div. Mar. Fish., North Carolina Dep. Environ. Qual., Morehead City, NC. [Available from website.]

[4] Holland, B. F., Jr. 1989. Evaluation of certified trawl efficiency devices (TEDs) in North Carolina's nearshore ocean. North Carolina Dep. Nat. Resour. Comm. Dev., Div. Mar. Fish., Compl. Rep. Proj. 2-439-R, 38 p. [Available from website.]

[5] McKenna, S. A., and J. P. Monaghan Jr. 1993. Gear development to reduce bycatch in the North Carolina trawl fisheries. North Carolina Dep. Environ. Health Nat. Res., Div. Mar. Fish., Compl. Rep. Coop. Agreement No. NA90AA-H-SK052, 59 p. [Available from website.]

[6] Brown, K. 2010. Interstate fisheries management program implementation for North Carolina. Study 2: documentation and reduction of bycatch in North Carolina fisheries. Job 1: compare catch rates of shrimp and bycatch of other species in standard (control) and modified (experimental) otter trawls in the Neuse River and Pamlico Sound, North Carolina. North Carolina Dep. Environ. Nat. Res., Div. Mar. Fish., Compl. Rep. NOAA Award No. NA08NMF474076, 23 p. [Available from website.]

[7] He, P., C. Rillahan, K. Brown, T. Lewis. 2016. Design and test of a topless shrimp trawl to reduce finfish bycatch in Pamlico Sound, North Carolina, 55 p. Final report submitted to NOAA Saltonstall-Kennedy Grant Program for grant SMAST-CE-REP-2016-057. [Available from School Mar. Sci. Technol., Univ. Mass. Dartmouth, 285 Old Westport Rd., New Bedford, MA 02747-2300.]

[8] Brown, K. 2015. Characterization of the commercial shrimp otter trawl fishery in the estuarine and ocean (0–3 miles) waters of North Carolina, 165 p. Final report to the National Fish and Wildlife Foundation and the National Oceanic and Atmospheric Administration National Marine Fisheries Service for the study period August 2012–August 2015. Div. Mar. Fish., North Carolina Dep. Environ. Qual., Morehead City, NC. [Available from website.]

[9] Brown, K., B. Price, L. Lee, S. Baker, and S. Mirabilio. 2017. Technical solutions to reduce bycatch in the North Carolina shrimp trawl fishery, 50 p. Final Report to the North Carolina Marine Fisheries Commission and the National Oceanic and Atmospheric Administration Bycatch Reduction Engineering Program for the study period June–July 2015 and July–September 2016. Div. Mar. Fish., North Carolina Dep. Environ. Qual., Morehead City, NC. [Available from website.]

Table 1

Characteristics of the control and the 9 experimental shrimp otter trawls (gears) that were tested in Pamlico Sound and nearshore waters off North Carolina during 2015–2017. The state and federal fisheye bycatch reduction devices (BRDs), as constructed for this study, created openings of 131 cm^2 and 258 cm^2, respectively. All experimental gears included a typical net body, a trawl efficiency device (TED), one or more BRDs, and a codend. Some of the gears had TEDs with reduced bar spacing. The cost for an industry manufacturer to construct a single control gear for this study was $3000. N/A=not applicable.

		Configuration			
Year	Gear description	TED bar spacing (cm)	BRD	Codend mesh size (cm)	Costs to retrofit one control net
All	Control	10.16	1 state fisheye	3.81	N/A
2015	Composite panel	10.16	Composite panel, spooker cone, 1 state fisheye	3.81	$400
	Reduced-bar TED	7.62	1 state fisheye	3.81	$700
	Reduced-bar TED + square mesh panel + 4.76-cm codend	7.62	1 state fisheye, square mesh panel	4.76	$1250
	Ricky BRD	10.16	Ricky	3.81	$110
	Double federal fisheyes + 4.76-cm codend	10.16	2 federal fisheyes	4.76	$600
2016	Virgil Potter BRD	10.16	1 state fisheye, Virgil Potter	3.81	$275
	Double federal fisheyes + 4.45-cm codend	10.16	2 federal fisheyes	4.45	$600
	Reduced-bar TED + double federal fisheyes + 4.45-cm codend	7.62	2 federal fisheyes	4.45	$1250
	Virgil Potter BRD + 4.45-cm codend	10.16	1 state fisheye, Virgil Potter	4.45	$800
2017	Reduced-bar TED	7.62	1 state fisheye	3.81	$700
	Reduced-bar TED + 4.13-cm codend	7.62	1 state fisheye	4.13	$1225
	Reduced-bar TED + double state fisheyes + 4.13-cm codend (summer)	7.62	2 state fisheyes	4.13	$1250
	Reduced-bar TED + double state fisheyes + 4.13-cm codend (autumn)	7.62	2 state fisheyes	4.13	$1250
	Reduced-bar TED + double federal fisheyes + 4.13-cm codend	7.62	2 federal fisheyes	4.13	$1250

selection and testing to overall evaluation of the gear results and of an acceptable amount of shrimp loss. Meetings were held at the beginning of the project and following annual testing trials.

Selection of BRDs and gear combinations for testing in this study was guided by multiple factors, including existing state regulations, advice from international gear experts, and feedback from workgroup members and industry representatives. Additionally, a state management regulation issued by proclamation in 2015 after the start of this study mandated that shrimp fishermen install an additional BRD, for a total of 2 devices, allowing various BRD combinations (NCDMF[10]). The workgroup selected 14 gears by consensus for testing in 2015, 2016, and 2017 (Table 1).

Gear testing procedures

A formal procedure for comparing tows (experimental versus control) was developed and closely followed the procedure outlined in the NOAA BRD testing manual (NMFS[11]). A target of 60 successful paired tows was set for sampling in 2015, as mandated by the NCMFC, and a minimum target of 30 successful paired tows was set for the fishing seasons in 2016 and 2017 (NMFS[11]). A successful tow was defined as the control and experimental trawl fishing without indication of occurrence of problematic events (e.g., hangs or gear malfunction) that could have influenced fishing efficiency (i.e., catch). All paired tows were performed on 9 commercial shrimp vessels equipped with bottom otter trawls (3 vessels in 2015, 2 vessels in 2016, and 4 vessels in 2017). During the trials in 2015 and 2016, all vessels were greater than 12 m long and were rigged with 4 trawl nets (double rigged) (Figs. 1 and 2), and the vessels from which trials were conducted in 2017 ranged from 10.5 m to 18 m in length and were rigged with 2 trawl nets (twin rigged). The control and experimental nets were tested in the outside positions on double-rigged vessels, and trials conducted on double-rigged vessels

[10] NCDMF (North Carolina Division of Marine Fisheries). 2015. Re: Shrimp trawl BRD requirements. Proclamation SH-2-2015. Div. Mar. Fish., North Carolina Dep. Environ. Nat. Resour., Morehead City, NC. [Available from website.]

[11] NMFS (National Marine Fisheries Service). 2016. Bycatch reduction device testing manual, 8 p. Southeast Reg. Off., Natl. Mar. Fish. Serv., NOAA, St. Petersburg, FL. [Available from website.]

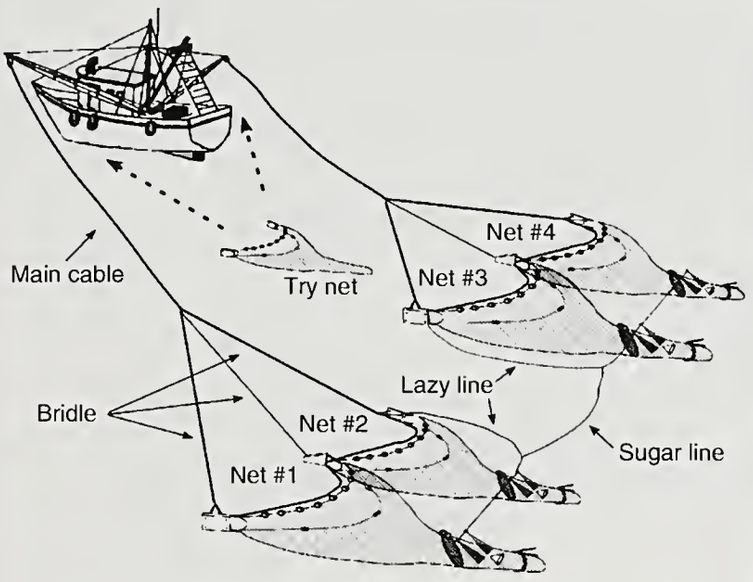

Figure 1

Illustration of a typical shrimp vessel equipped with 4 trawl nets. Double-rigged vessels like this one were used during the trials conducted in 2015 and 2016 in Pamlico Sound, North Carolina. Control and experimental gear were placed in the outside positions (i.e., Net #1 or Net #4). Note that try nets were not used in this study. Image source: Scott-Denton et al. (2012).

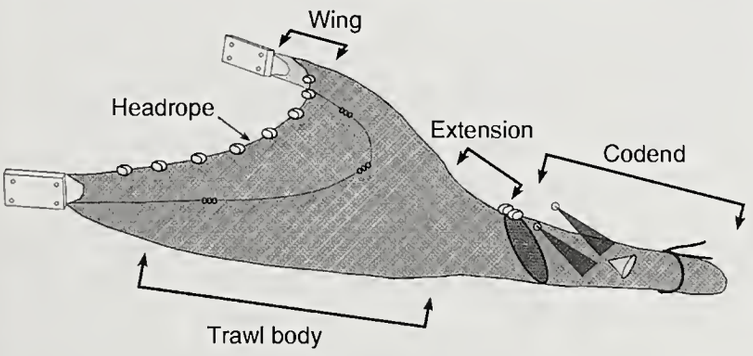

Figure 2

Illustration of the components of a trawl net. Several modifications of the trawl net typically used in the shrimp fishery were tested for this study aboard commercial vessels in Pamlico Sound and nearshore waters off North Carolina during 2015–2017. Image source: Scott-Denton et al. (2012).

minimized or eliminated the use of try nets to mitigate potential effects from their use (Eayrs, 2012; Figs. 1 and 2). To coincide with the peak shrimp seasons, testing was conducted during June–July 2015, July–September 2016, and July 2017 in Pamlico Sound and from August through November 2017 in the nearshore waters of North Carolina (Fig. 3). All paired tows were performed under normal fishing conditions.

Observers were hired and trained to collect data under NCDMF protocols and met or exceeded National Marine Fisheries Service (NMFS) guidelines (NMFS[12]). Two observers were assigned to each trial. Personnel from the Beaufort Laboratory, NOAA Southeast Fisheries Science Center, trained observers to handle, transport, identify, resuscitate, tag, and release protected sea turtles in accordance with federal standards of the U.S. Endangered Species Act.

Prior to formal field trials, tows were made to calibrate the nets on each side of the vessel to ensure that the nets fished evenly. To reduce the potential for side bias, protocol required that experimental and control modifications be switched periodically from one side to the other side to achieve an equal number of successful tows on each side of the vessel. Specifically, only the gear modifications being tested (i.e., BRDs and TEDs with reduced bar spacing) were switched while the body of the net remained to mitigate any net effect. Gear specification data were collected for both experimental and control nets and included fabrication costs, head rope length, mesh size of wing and codend, TED type, TED bar spacing, BRD type, and location, duration, and time of day of tow.

At the request of industry collaborators, data were collected for whole hauls (i.e., catches were not subsampled). Specifically, industry collaborators were concerned about the public perception of sampling a portion of the catch versus obtaining a census of harvest from each tow. Following each paired tow, the catches from each net (experimental and control) were counted and weighed separately in their entirety. Because of the volume of catch, organisms were not identified to species; instead, catches were grouped into shrimp and finfish categories for counting and weighing. In 2015, the total weight (in kilograms) of shrimp and finfish were recorded. In 2016 and 2017, smaller catches allowed further categorization that included groups for penaeid shrimp, finfish, non-shrimp invertebrates, sharks and rays, and miscellaneous organisms.

Description of control and experimental gears

All control and experimental nets were built to have identical head rope length, footrope length, and net bodies. The control net configuration for this project consisted of a shrimp otter bottom (2-seam) trawl with a state fisheye, a TED with 10.16-cm bar spacing, and a 3.81-cm stretched mesh codend (Fig. 4). This configuration was considered the most typical gear

[12] NMFS (National Marine Fisheries Service). 2010. Characterization of the US Gulf of Mexico and southeastern Atlantic otter trawl and bottom reef fish fisheries: observer training manual, 186 p. Galveston Lab., Southeast Fish. Sci. Cent., Natl. Mar. Fish. Serv., NOAA, Galveston, TX. [Available from website.]

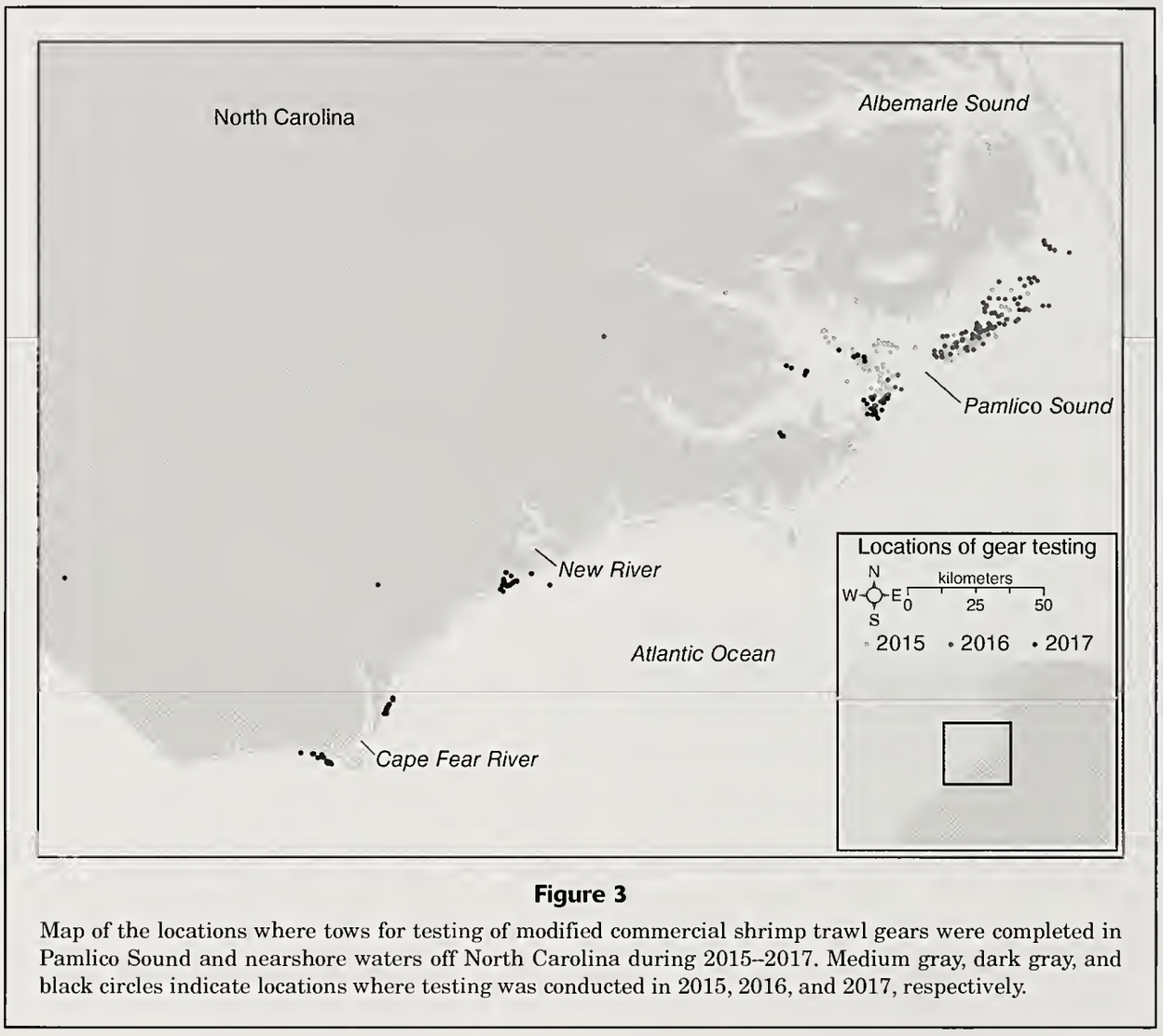

Figure 3

Map of the locations where tows for testing of modified commercial shrimp trawl gears were completed in Pamlico Sound and nearshore waters off North Carolina during 2015–2017. Medium gray, dark gray, and black circles indicate locations where testing was conducted in 2015, 2016, and 2017, respectively.

configuration used by the industry at the time of the start of this study and was dictated by the NCMFC's preferred management strategy.

The type, shape, frame size, and cover type (double or single) of TEDs were standardized on each test vessel. The orientation, either top or bottom, was identical for both control and test TEDs on each vessel; however, both bottom-opening and top-opening TEDs were tested throughout the study. Bar spacing of TEDs varied among control and experimental configurations as indicated in the next paragraph.

Five experimental gear configurations were tested in 2015, 4 configurations were tested in 2016, and 5 configurations were tested in 2017 (Table 1, Fig. 4). The first BRD tested in 2015 was a federally certified (by NOAA) composite panel with a fish spooker cone (Table 1, Fig. 4). This gear consists of 2 composite panels installed in the lower part of the extension. The panels taper inward, creating an area with slow water flow that allows escape of fish through 2 triangular openings. Each composite panel is composed of 2 overlapping panels, a diamond mesh panel and a square mesh panel. The diamond mesh panel reduces the water flow, and the square mesh panel provides support, preventing obstruction of the escape openings (NMFS[13]). This net was also equipped with a single state fisheye. The next gear tested was equipped with a TED with reduced, 7.62-cm bar spacing (hereafter referred to as *reduced-bar TED*) (Table 1, Fig. 4). However, following a week of testing with this gear during which less than desired reductions in finfish bycatch were observed, the trial was terminated. The next gear tested was equipped with a reduced-bar TED and included a square mesh panel (on the codend) and a larger 4.76-cm stretch mesh codend (Table 1, Fig. 4). The square mesh panel was constructed of 8.89-cm stretch mesh and was 5 meshes wide and 12 meshes long. This net was also equipped with a single state fisheye.

The fourth gear tested in 2015 was the Ricky BRD (Fig. 4), which is composed of a pair of diamond-shaped, federal fisheye BRDs (each with a 258-cm^2 opening) (hereafter referred to as *federal fisheye*) with a float

[13] NMFS (National Marine Fisheries Service). 2008. Recommended construction and installation instructions for the composite panel bycatch reduction device, 8 p. Harvest. Syst. Eng. Branch, Natl. Mar. Fish. Serv., NOAA, Pascagoula, MS. [Available from website.]

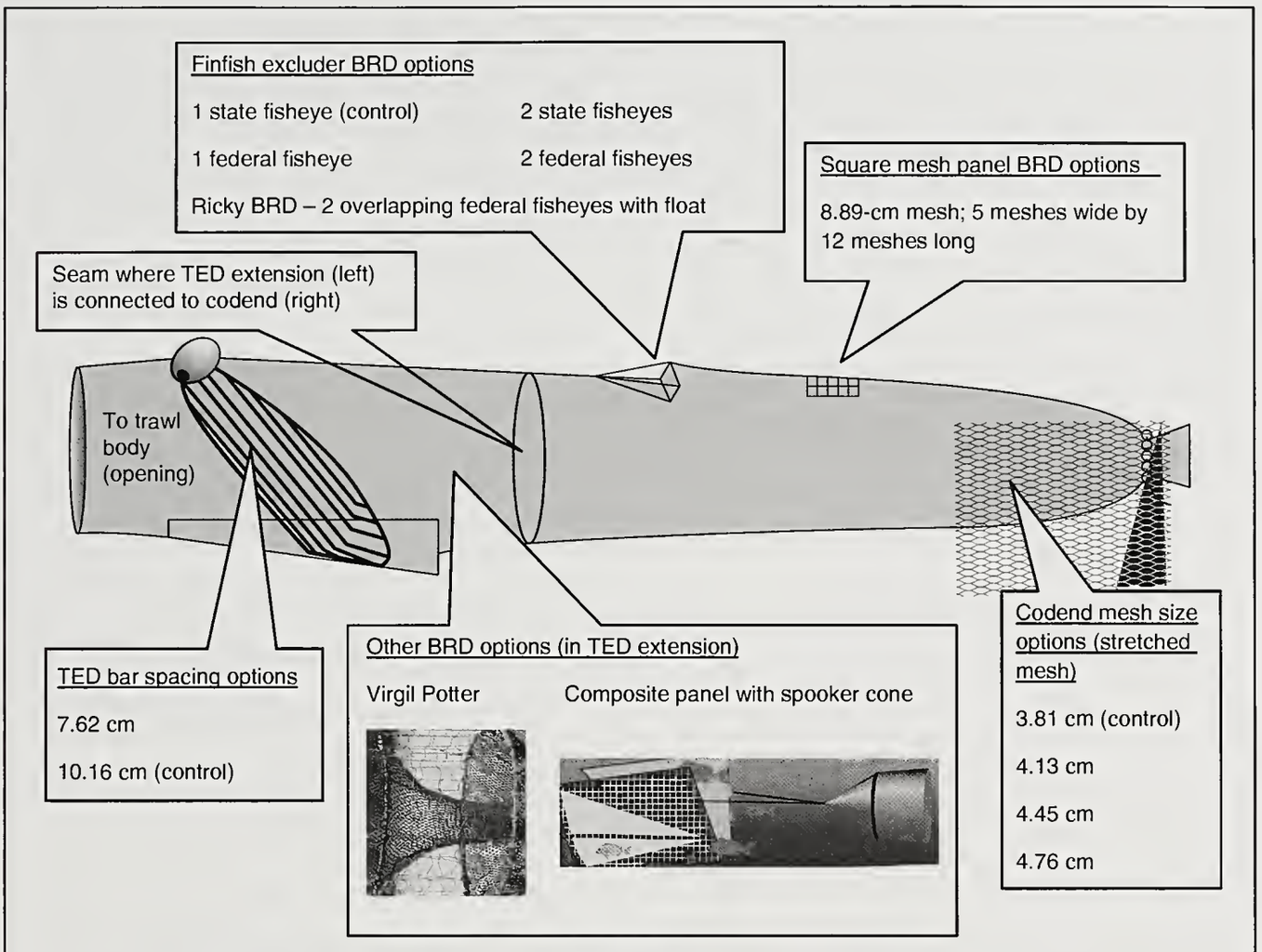
Finfish excluder BRD options
1 state fisheye (control)
2 state fisheyes
1 federal fisheye
2 federal fisheyes
Ricky BRD – 2 overlapping federal fisheyes with float
Square mesh panel BRD options
8.89-cm mesh; 5 meshes wide by 12 meshes long
Seam where TED extension (left) is connected to codend (right)
To trawl body (opening)
TED bar spacing options
7.62 cm
10.16 cm (control)
Other BRD options (in TED extension)
Virgil Potter
Composite panel with spooker cone
Codend mesh size options (stretched mesh)
3.81 cm (control)
4.13 cm
4.45 cm
4.76 cm

Figure 4

Illustration of individual components (not drawn to scale) of modified shrimp trawl gears tested in Pamlico Sound and nearshore waters off North Carolina during 2015–2017. All experimental gears included a typical net body (not shown) and, from the options shown, a trawl efficiency device (TED), one or more bycatch reduction devices (BRDs), and a codend. The fisheye BRDs were diamond shaped with a square, 4-sided base. The areas of a single state fisheye and a single federal fisheye were 131 cm^2 and 258 cm^2, respectively.

(Helies et al.[14]). The first federal fisheye BRD was installed 3.05 m from the codend tie-off rings. A second federal fisheye was installed 30 cm forward of the first federal fisheye, so that the aft of the forward fisheye touched the forward section of the aft fisheye. A 20.3-cm, hard plastic float was placed inside the codend, just forward of the tip of the most forward fisheye. The gear was tested and yielded less than satisfactory results; therefore, the trial was terminated. The next gear tested was designed with double federal fisheyes placed in the position required by North Carolina Division of Marine Fisheries: the first fisheye was placed 68 meshes forward of tie-off rings, and the second fisheye was placed 5 meshes forward of the forward edge of the first fisheye. In addition, the codend mesh size was increased to 4.76 cm (Table 1, Fig. 4).

Four gears were tested in 2016. The first gear was composed of 1 state fisheye and the Virgil Potter BRD (Table 1, Fig. 4). This gear consisted of a radial escape section constructed of 21.6-cm stretch mesh that was 5 meshes long. A funnel constructed of 3.81-cm stretch mesh was also part of this design. The next BRD tested included 2 federal fisheyes in the state-required position (as described previously) and a 4.45-cm stretch mesh codend (Table 1, Fig. 4). The next BRD combination tested included a reduced-bar TED, double federal fisheyes in the state-required position (as described previously), and a 4.45-cm stretch mesh codend (Table 1, Fig. 4). The final gear tested in 2016 was the Virgil Potter BRD with 1 state fisheye and a 4.45-cm stretch mesh codend (Table 1, Fig. 4).

[14] Helies, F., J. Jamison, and B. Gallaway. 2015. Continued development and assessment of bycatch reduction devices within the southeastern shrimp trawl fishery, 36 p. Final report to the National Oceanic and Atmospheric Administration National Marine Fisheries for NOAA Award NA10NMF4540108 (GSAFFI #115). [Available from Gulf and South Atlantic Fish. Found. Inc., Ste. 997, Lincoln Cent., 5401 W. Kennedy Blvd., Tampa, FL 33609.]

In the summer of 2017, 3 experimental gears were tested, with each including a reduced-bar TED, 1 state fisheye, and a 3.81-cm codend (Table 1, Fig. 4). Following 5 paired tows with less than desired reductions of finfish bycatch observed, the experimental gear in the trial was changed to include a reduced-bar TED, 1 state fisheye, and a 4.13-cm stretch mesh codend (Table 1, Fig. 4). The next tested gear, in the summer of 2017, was a reduced-bar TED with 2 state fisheyes and a 4.13-cm stretch mesh codend (Table 1, Fig. 4). In the autumn of 2017, 2 experimental gears were tested. The first included a reduced-bar TED, 2 state fisheyes, and a 4.13-cm stretch mesh codend (Table 1, Fig. 4). Finally, a modification of that gear, consisting of a reduced-bar TED, 2 federal fisheyes, and a 4.13-cm stretch mesh codend, was tested (Table 1, Fig. 4).

Analyses

Any problematic tows (as described previously) were dropped. Catch per unit of effort (CPUE) was calculated as weight divided by tow time; observed weights were standardized to either a 2-h tow time (2015–2016) or a 1-h tow time (2017) to adjust for differences in tow times. The CPUE values were calculated with the assumption that there were no differences in spread ratio between trawls with various BRD and TED configurations. The 1-h tow time was used in 2017 because of the smaller vessel and net size. The average weight of catch was computed for each gear (control and experimental) and taxonomic group along with the differences in average weight of catch and percent change in CPUE.

Paired *t*-tests were used to evaluate any differences in average CPUE values between the control and experimental nets by using the SURVEYSELECT procedure in the software SAS 9.4[15] (SAS Institute Inc., Cary, NC). The null hypothesis for the *t*-test was that there was no difference in CPUE between the control and experimental nets (significance level of 0.05). The procedure was used to account for any uneven number of tows by gear type per vessel side made during trials and to randomly select an even number of tows to minimize side-bias. This procedure resulted in the random exclusion of tows for some analyses.

One of the assumptions of the *t*-test is that the dependent variable (in this case, CPUE) is normally distributed within each group. Because ecological data are often non-normal, a second test that does not require normality of the data distribution was applied to the data. Specifically, a randomization procedure (Manly, 2007) was also used to compare CPUE between control and experimental nets for each gear and taxonomic group. The null hypothesis for the randomization test was that there was no difference in CPUE between the control and experimental nets. The test statistic evaluated was the difference in average CPUE between the control and experimental nets. Data were randomized and resampled 10,000 times for each gear and taxonomic group. The *P*-value from the randomization test for a 2-tailed test was the proportion of test statistics (including those computed from the original data) that were as large or larger in absolute value than the absolute value of the statistic computed from the original data. Code for this test was written and run in the R statistical program (vers. 3.4.3; R Core Team, 2017).

[15] Mention of trade names or commercial companies is for identification purposes only and does not imply endorsement by the National Marine Fisheries Service, NOAA.

Results

A total of 412 paired tows were made by using 14 experimental gear configurations. Testing occurred on 39 trips across 104 fishing days by a total of 9 different industry fishing vessels. A trip was defined as the time period that began when a vessel departed port to conduct fishing operations and ended with a return to port. Observers sampled and weighed over 142,000 kg of fish, shrimp, and other marine organisms. An even number of tows by side of vessel was not achieved for most gears (Table 2), and 81% of paired tows were made during the day (Table 2). The results of both the paired *t*-tests and the randomization tests for testing completed from 2015 through 2017 can be found in Tables 3–5.

Paired *t*-tests

None of the 5 experimental gears tested in 2015 lost a significant amount of shrimp ($P>0.05$; Table 3). Only with the Ricky BRD did we fail to achieve a significant reduction in finfish bycatch compared with that achieved by using the control gear (6.6% reduction with Ricky BRD, $P=0.503$). However, testing of this gear was discontinued after only 15 tows. Only by using the configuration with double federal fisheyes and a 4.76-cm codend was a greater than 40% reduction in bycatch (40.8%) achieved while maintaining shrimp catch (1.0% gain).

In 2016, no significant shrimp loss was observed during tows of the 4 gears tested (Table 4). With the Virgil Potter gear, we achieved a significant gain in shrimp harvest over that during tests with the control net (9.9% gain, $P=0.050$). Significant reduction in finfish bycatch was observed with the use of all test BRDs in 2016, and the use of 3 of the 4 gears resulted in bycatch reduction in excess of the 40% target in a range of 43–57%.

In 2017, 1 of the 5 gears tested was not analyzed by using the *t*-test, because of low sample size. When 3 of the remaining 4 gears were tested in 2017, significant shrimp loss was observed (Table 5). Tests of the gear with a reduced-bar TED, double state fisheyes, and a 4.13-cm codend during summer, the gear with a reduced-bar TED, double state fisheyes, and a 4.13-cm codend during autumn, and the gear with a reduced-bar TED, double federal fisheyes, and a 4.13-cm codend resulted in shrimp losses of 6.8%, 14.9%, and 9.0%, respectively. By using 2 of these gears, the reduced-bar TED with a 4.13-cm codend and the reduced-bar TED

Table 2

Number of port and starboard tows made with control and experimental gears in Pamlico Sound in June and July 2015, July–September 2016, and July 2017 and in nearshore waters off North Carolina in August–November 2017. Some of the gears had trawl efficiency devices (TEDs) with reduced bar spacing, and bycatch reduction devices (BRDs) included the Ricky BRD, Virgil Potter BRD, and state and federal fisheyes. An asterisk (*) indicates that 1 tow made with this gear configuration was dropped from analysis.

			Number of tows	
Year	Gear description	Net	Port	Starboard
2015	Composite panel	Control	37	22
		Experimental	22	37
	Reduced-bar TED	Control	10	9
		Experimental	9	10
	Reduced-bar TED + square mesh panel + 4.76-cm codend	Control	31	20
		Experimental	20	31
	Ricky BRD	Control	10	5
		Experimental	5	10
	Double federal fisheyes + 4.76-cm codend*	Control	19	13
		Experimental	14	19
2016	Virgil Potter BRD	Control	18	15
		Experimental	15	18
	Double federal fisheyes + 4.45-cm codend	Control	20	3
		Experimental	3	20
	Reduced-bar TED + double federal fisheyes + 4.45-cm codend	Control	15	15
		Experimental	15	15
	Virgil Potter BRD + 4.45-cm codend	Control	11	14
		Experimental	14	11
2017	Reduced-bar TED	Control	5	5
		Experimental	5	5
	Reduced-bar TED + 4.13-cm codend	Control	10	15
		Experimental	15	10
	Reduced-bar TED + double state fisheyes + 4.13-cm codend (summer)	Control	15	15
		Experimental	15	15
	Reduced-bar TED + double state fisheyes + 4.13-cm codend (autumn)	Control	15	15
		Experimental	15	15
	Reduced-bar TED + double federal fisheyes + 4.13-cm codend	Control	15	15
		Experimental	15	15

with double state fisheyes and a 4.13-cm codend that was tested in summer, we achieved significant bycatch reduction (22.8%, P=0.019, and 32.6%, P<0.001, respectively), although we did not obtain the desired 40% reduction.

Randomization tests

In the randomization tests, no significant loss of shrimp catch was observed among the 5 gears tested in 2015 (Table 3). Significant (P<0.05) decreases in finfish catch were found in all gears tested in 2015 except for the reduced-bar TED and Ricky BRD. Of the gears for which a significant reduction in finfish CPUE was detected, only the use of the double federal fisheye with a 4.76-cm codend resulted in a reduction greater than the target of 40% (40.1%, P<0.001).

No significant loss of shrimp catch was detected for the 4 gears tested in 2016, on the basis of the results of the randomization tests (Table 4). Tests with all 4 gears resulted in a significant (P<0.05) decrease in the catch of finfish. The use of the double federal fisheye (54.0%), the reduced-bar TED with a double federal fisheye and a 4.45-cm codend (44.9%), and the Virgil Potter BRD with a 4.45-cm codend (44.3%) all resulted in reductions greater than the 40% target. According to the results of the randomization tests, no significant changes were detected in the CPUE of invertebrates or elasmobranchs in 2016.

None of the 5 gears tested in 2017 had a significant loss of shrimp catch, on the basis of the results of the randomization tests (Table 5). Only when the gear with a reduced-bar TED, double state fisheyes, and a 4.13-cm codend was tested in summer was a significant decrease in finfish catch (32.6%) observed, although the decrease was less than the 40% target. Significant decreases in the catches of invertebrates (65.1%) and elasmobranchs (57.3%) were achieved when the gear with the reduced-bar TED,

Table 3

Results of the paired *t*-tests and randomization tests used to compare catch per unit of effort (CPUE), weight divided by tow time, between the control gear and 5 experimental (Exp.) gears tested in 2015 in Pamlico Sound, North Carolina. Some of the gears had trawl efficiency devices (TEDs) with reduced bar spacing, and bycatch reduction devices (BRDs) included a composite panel, the Ricky BRD, and a federal fisheye. Mean values of CPUE are reported in kilograms. *n*=number of tows.

		Control	Exp.	*t*-test			Control	Exp.	Randomization	
Gear	Taxonomic group	*n*	Mean	Mean	Change (%)	*P*-value	*n*	Mean	Mean	Change (%)	*P*-value
Composite panel	Finfish	44	178.1	132.1	−25.83	<0.001	60	177.3	128.4	−27.60	<0.001
	Shrimp	44	64.3	63.9	−0.65	0.754	60	67.3	65.2	−3.13	0.776
Reduced-bar TED	Finfish	16	107.3	70.0	−16.18	0.029	19	112.8	89.8	−20.40	0.217
	Shrimp	16	49.6	46.0	−7.35	0.078	19	48.2	45.5	−5.63	0.739
Reduced-bar TED + square mesh panel + 4.76-cm codend	Finfish	40	104.8	78.2	−25.34	<0.001	51	102.3	74.1	−27.50	0.007
	Shrimp	40	65.7	64.4	−1.94	0.309	51	67.3	65.2	−3.04	0.775
Ricky BRD	Finfish	10	110.6	103.3	−6.61	0.503	15	100.0	95.5	−4.55	0.793
	Shrimp	10	35.3	31.8	−9.87	0.449	15	35.4	33.3	−6.06	0.728
Double federal fisheyes + 4.76-cm codend	Finfish	25	90.0	53.3	−40.81	<0.001	32	88.3	52.9	−40.10	<0.001
	Shrimp	25	61.3	61.9	1.00	0.778	32	60.6	61.9	2.16	0.862

Table 4

Results of the paired *t*-tests and randomization tests used to compare catch per unit of effort (CPUE), weight divided by tow time, between the control gear and 4 experimental (Exp.) gears tested in 2016 in Pamlico Sound, North Carolina. One of the gears had a trawl efficiency device (TED) with reduced bar spacing, and bycatch reduction devices included the Virgil Potter and federal fisheye. Mean values of CPUE are reported in kilograms. Values for invertebrates are for all non-commercial shrimp invertebrates. *n*=number of tows.

		Control	Exp.	*t*-test			Control	Exp.	Randomization	
Gear	Taxonomic group	*n*	Mean	Mean	Change (%)	*P*-value	*n*	Mean	Mean	Change (%)	*P*-value
Virgil Potter	Finfish	30	146.3	106.9	−26.92	<0.001	33	149.4	106.9	−28.50	0.005
	Shrimp	30	62.6	68.8	9.92	0.050	33	61.8	67.0	8.51	0.696
	Invertebrates	10	3.3	2.7	−18.79	0.384	33	1.0	0.8	−18.80	0.681
	Elasmobranchs	7	5.3	5.9	11.11	0.589	33	1.1	1.2	11.10	0.912
Double federal fisheye + 4.45-cm codend	Finfish	6	201.5	86.3	−57.19	0.001	23	164.5	75.6	−54.00	<0.001
	Shrimp	6	23.0	20.2	−12.11	0.215	23	28.1	23.6	−16.20	0.280
	Invertebrates	6	7.2	6.1	−15.67	0.081	23	5.4	5.1	−4.85	0.833
	Elasmobranchs	6	1.8	2.6	45.79	0.509	23	2.1	2.5	18.80	0.573
Reduced-bar TED + double federal fisheye + 4.45-cm codend	Finfish	30	115.4	63.6	−44.91	<0.001	30	115.4	63.6	−44.90	0.007
	Shrimp	30	27.0	25.7	−4.85	0.435	30	27.0	25.7	−4.85	0.706
	Invertebrates	30	2.1	1.8	−13.26	0.418	30	2.1	1.8	−13.30	0.601
	Elasmobranchs	27	1.8	1.4	−18.62	0.404	30	1.6	1.3	−18.60	0.568
Virgil Potter + 4.45-cm codend	Finfish	22	189.1	107.4	−43.20	<0.001	25	172	96.1	−44.30	0.001
	Shrimp	22	33.2	31.3	−5.46	0.055	25	31.3	29.5	−5.78	0.691

double state fisheyes, and a 4.13-cm codend was tested in autumn; however, the observed catches were relatively small.

Test comparison

A comparison of the results from the paired *t*-tests and randomization tests (relative to the results of each other and to the raw data as collected) is provided in Tables 3–5. In general, both tests produced similar results. A paired *t*-test detected a significant decrease in finfish CPUE for the reduced-bar TED (tested in 2015) and the reduced-bar TED with a 4.13-cm codend (tested in 2017), whereas the results of the randomization tests indicate no significant difference in finfish bycatch between these gears (Tables 3 and 5). Additionally, a paired *t*-test detected a significant increase in shrimp catch for the Virgil Potter gear (tested in 2016), but in a randomization test, no significant change

Table 5

Results of the paired *t*-tests and randomization tests used to compare catch per unit of effort (CPUE), weight divided by tow time, between the control gear and 5 experimental (Exp.) gears tested in 2017 in Pamlico Sound and nearshore waters off North Carolina. Each of the 5 gears had a trawl efficiency device (TED) with reduced bar spacing, and bycatch reduction devices included state and federal fisheyes. Mean values of CPUE are reported in kilograms. An asterisk (*) indicates that data for a taxonomic group were not analyzed with a *t*-test because of low sample size. Values for invertebrates are for all non-commercial shrimp invertebrates. *n*=number of tows.

			Control	Exp.	*t*-test			Control	Exp.	Randomization	
Gear	Taxonomic group	*n*	Mean	Mean	Change (%)	*P*-value	*n*	Mean	Mean	Change (%)	*P*-value
Reduced-bar TED	Finfish	*	*	*	*	*	5	12.3	12.9	5.06	0.732
	Shrimp	*	*	*	*	*	5	18.7	17.3	−7.79	0.827
	Invertebrates	*	*	*	*	*	5	4.9	6.8	38.78	0.281
	Elasmobranchs	*	*	*	*	*	4	0.2	0.4	75.00	0.487
Reduced-bar TED + 4.13-cm codend	Finfish	20	34.6	26.7	−22.80	0.019	22	34.9	27.8	−20.42	0.341
	Shrimp	20	12.1	11.2	−7.82	0.294	22	11.6	10.6	−9.04	0.556
	Invertebrates	18	2.3	2.1	−6.06	0.692	22	2.07	2.06	−0.444	0.993
	Elasmobranchs	*	*	*	*	*	3	0.3	0.1	−80.00	0.397
Reduced-bar TED + double state fisheyes + 4.13-cm codend (summer)	Finfish	30	146.0	98.5	−32.60	<0.001	30	146.0	98.5	−32.61	0.002
	Shrimp	30	2.9	2.7	−6.80	0.039	30	2.9	2.7	−6.64	0.598
	Invertebrates	30	17.2	15.9	−7.58	0.086	30	17.2	15.9	−7.59	0.505
	Elasmobranchs	29	3.0	2.5	−16.3	0.184	30	2.87	2.4	−16.70	0.425
Reduced-bar TED + double state fisheyes + 4.13-cm codend (autumn)	Finfish	30	57.5	54.9	−4.57	0.670	30	57.5	54.9	−4.58	0.890
	Shrimp	30	9.8	8.3	−14.90	<0.001	30	9.75	8.3	−14.83	0.365
	Invertebrates	30	8.2	2.9	−65.10	0.001	30	8.20	2.9	−65.07	<0.001
	Elasmobranchs	28	4.4	1.9	−57.10	0.009	29	4.26	1.8	−57.29	0.014
Reduced-bar TED + double federal fisheyes + 4.13-cm codend	Finfish	30	75.6	97.7	29.30	0.204	30	75.6	97.7	29.30	0.250
	Shrimp	30	17.3	15.7	−9.04	0.002	30	17.3	15.1	−12.48	0.234
	Invertebrates	25	2.2	2.7	21.90	0.276	30	2.29	2.9	25.15	0.455
	Elasmobranchs	15	1.3	1.0	−24.30	0.271	28	0.904	0.7	−24.50	0.360

was found when this gear was used (Table 4). The paired *t*-test results indicate a significant decrease in shrimp catch for the gear with a reduced-bar TED, double state fisheyes, and a 4.13-cm codend that was tested in summer, the gear with a reduced-bar TED, double state fisheyes, and a 4.13-cm codend that was tested in autumn, and the gear with a reduced-bar TED, double federal fisheyes, and a 4.13-cm codend (all tested in 2017), whereas results of the randomization tests indicate no significant difference in shrimp CPUE for these gears (Table 5).

The results of both tests indicate that the double federal fisheye with a 4.76-cm codend (tested in 2015), the double federal fisheye with a 4.45-cm codend (tested in 2016), the gear with a reduced-bar TED, double federal fisheye, and a 4.45-cm codend (tested in 2016), and the Virgil Potter BRD with a 4.45-cm codend (tested in 2016) exceeded the target of 40% reduction in finfish bycatch (Tables 3–5). None of those gears had a significant decrease in shrimp catches in either the paired *t*-tests or randomization tests.

Gear costs

Relative to the material and labor costs associated with constructing a single control trawl ($3000), additional costs associated with modifying the control gear to that of each experimental gear ranged from $110 to $1250 (Table 1). An additional $600 per trawl above the cost of a typical control net was the minimum investment required to achieve reduction >40% in finfish bycatch in this study.

Discussion

Gear performance

The goal to achieve a reduction of 40% in finfish bycatch did not allow this study to evaluate the effects of single gear modifications, as is typically conducted in BRD testing (Brewer et al., 1998). However, the bycatch reduction goal was achieved by using BRD combinations chosen through a collaborative process that relied on expert opinions and past research. Four of the 14 gear combinations that were tested met the immediate project goal, and the results of this study provide direction for future testing and for making interim management recommendations (Tables 3 and 4). In fact, the NCMFC voted in May 2018 to implement these gear combinations as a requirement, beginning in 2019 on larger vessels (>12 m) fishing in

Pamlico Sound, North Carolina (NCDMF[16]). A proclamation was issued for these requirements, which went into effect by July 2019.

Although we cannot attribute observed reductions in finfish bycatch to one element, all 4 gears that achieved the target of greater than 40% bycatch reduction (Tables 3–5) used a combination of increased codend mesh size and larger finfish escape openings relative to the control configuration. The simple use of 2 federal fisheyes provided a combined opening size of 516 cm^2, almost 4 times the opening of the industry-standard state fisheye (131 cm^2). In addition to allowing larger fish to escape the trawl, the larger escape openings likely create a larger area for the flow of disturbed water, a difference that has been shown to result in higher rates of escape (Wardle, 1986; Engaas et al., 1999; Watson et al., 1999; Winger et al., 2010). The use of each of these 4 gears did not result in a significant decrease in shrimp catch relative to that from the use of the control net, but the use of the gear with the double federal fisheyes and a 4.45-cm codend produced a reduction in shrimp catch that was greater than the 5% threshold for shrimp loss identified by workgroup members from industry (Table 4).

The use of a reduced-bar TED in several gear configurations also appears to have contributed to overall finfish bycatch reduction. The reduction of finfish bycatch achieved with this gear was more substantial after the mesh size of the codend was increased, following a week-long trial of just a reduced-bar TED. The increase in codend mesh size may have resulted in increased water flow through the codend, allowing smaller finfish species to escape (Isaksen et al., 1992; Engaas et al., 1999).

Similar improvements in bycatch reduction from the use of reduced-bar TEDs have been found in the Gulf of Mexico (Hataway et al., 2017), Australia (Noell et al., 2018), and the nearshore waters of coastal North Carolina (Broome et al.[17]). Broome et al.[17] documented that the use of a trawl equipped with a TED with 5.08-cm bar spacing and a state fisheye reduced total bycatch weight by 40% with insignificant loss of shrimp catch (6%) in 43 paired tows conducted in nearshore waters of the Atlantic Ocean, compared with the reduction achieved with a control trawl that was similar to the control gear in this study: an otter trawl equipped with a TED with standard 10.16-cm bar spacing and a state fisheye. Although the gear tested by Broome et al.[17] met the bycatch reduction target that was set for our study, a majority of the workgroup members felt that such a reduction in TED bar spacing would not be feasible for use in the estuarine fishery because of potential clogging associated with debris and grasses that are typically found in the estuarine waters of North Carolina. In fisheries outside of this test area, similar improvements in bycatch reduction have been observed when the mesh or grid size of the Nordmore grates have been reduced (Broadhurst, 2000; Silva et al., 2011, 2012).

The use of a radial escape panel in conjunction with a funnel behind the TED (both versions of the Virgil Potter gear) also showed great promise. Perhaps most encouraging is that this gear was developed by a local fisherman (V. Potter) that participated in the workgroup process. Use of the Virgil Potter BRD with a 3.81-cm mesh codend resulted in lower bycatch reduction, relative to that from the use of the Virgil Potter BRD with a 4.45-cm codend, but resulted in a gain in shrimp catch, on average, compared with the average loss in shrimp catch from use of the version with the codend that has the larger mesh size (Table 4).

Testing in 2017 focused on smaller vessels (<14 m) and the nearshore waters of North Carolina. Unlike the outcome of previous testing in 2015 and 2016 (Brown et al.[9]), the results from testing in 2017 fell short of achieving the additional 40% reduction in finfish bycatch with the gear combinations used. Although the catch was not separated by species during trials, we did observe that striped anchovy (*Anchoa hepsetus*) made up the majority of the finfish catch for several tows conducted in ocean waters but were not observed in catch of tows conducted during the inshore testing in Pamlico Sound. Differences in species composition were likely a contributing factor in the underperformance of similar gears that had reached the 40% reduction goal during testing in inshore waters in previous years. Although the target for reduction of finfish bycatch was not achieved with the gears tested in our study in 2017, the use of a TED with 7.62-cm bar spacing in conjunction with 2 state fisheyes did show promise during testing in the summer on a small vessel. On the basis of results from testing in 2015 and 2016, it is anticipated that testing of a gear composed of a TED with 7.62-cm bar spacing, 2 state fisheyes, and a codend with a larger stretch mesh (4.45-cm) would result in reductions in finfish bycatch greater than the 40% target. Further testing with this gear combination is needed in the small-boat fleet to accurately assess this expectation.

Study design

The use of a workgroup throughout this project played a critical role in achieving the finfish reduction goal set forth by the NCMFC. The fact that international trawl experts provided all participants with a basic understanding of trawl gear dynamics, fish behavior in trawls, results from recent research, and an overview of the scientific testing protocol to be used was instrumental in these achievements (Brown et al.[9]; NMFS[11]). Workgroup members from the fishing industry then provided ideas to be tested that they believed would work best within the parameters of Pamlico Sound, a shallow, muddy-bottom estuarine environment. Finally, facilitated discussion techniques were

[16] NCDMF (North Carolina Division of Marine Fisheries). 2018. Marine Fisheries Commission briefing book for business meeting; New Bern, NC, 16–17 May, 659 p. Div. Mar. Fish., North Carolina Dep. Environ. Nat. Resour., Morehead City, NC. [Available from website.]

[17] Broome, J. D., J. W. Anderson, and D. W. Anderson. 2011. Bycatch volume reduction through turtle excluder device (TED) reduced grid spacing, 37 p. Final report for North Carolina Sea Grant proj. 10-FEG-03. [Available from North Carolina Sea Grant, 303 College Circle, Morehead City, NC 28557.]

used to ensure consensus in the selection of gears to be tested. This process engaged industry participants and created ownership in the selections made, contributing to the project's success.

Some elements of the study design mandated by the NCMFC differed from typical collaborative research methods and BRD testing. For example, paired tow testing is best conducted during normal fishing conditions so that the true effects of experimental gear, relative to the standard gears used, can be determined (Eayrs, 2012). A condition of the award that sponsored the testing in 2015 required that industry partners contribute a 50% cost match. Requiring large industry matching funds can change the perceptions and expectations of the industry sector relative to those of scientific collaborators (Harte, 2001). Specifically, projects that deviate from a collaborative approach (e.g., requesting that fishermen fish out of season or, more importantly, fish by using experimental gear during normal conditions) operate outside of established parameters (Conway and Pomeroy, 2006). Collaborative research is difficult at best, and expectations of scientists and industry participants often do not align when only one of the partners—in this case, the shrimp industry—is asked to make concessions (Stephenson et al., 2016).

Our methods followed NOAA BRD testing protocols with a few exceptions. First, the establishment of a goal of 40% bycatch reduction over that achieved by the current industry trawl with TED and BRD installed was above and beyond normal testing design, requiring BRD combinations to be evaluated. Federal certification of a BRD prototype requires the use of the BRD to result in a consistent reduction of total finfish bycatch of at least 30%, by weight, when compared with the use of a naked (TED, but no BRD) control net (NMFS[11]). Assuming, for instance, that by using our control net with a BRD we achieved a 30% reduction of finfish bycatch and by using our experimental net we achieved our goal of a 40% reduction of finfish bycatch by weight, we theoretically would have achieved the equivalent of 58% reduction over a naked net or nearly twice the federal requirement. Second, the protocol for regular switching of experimental gear to each side of the vessel was not always followed for a variety of reasons: lack of performance for a given gear, weather, or vessel captains not following agreed upon protocols. Finally, NOAA testing protocols require that testing achieve a minimum of 30 successful paired tows. The sponsor of our field season in 2015 requested that 60 successful paired tows be attempted but offered no scientific basis for deviation from the NOAA testing protocol of 30 paired tows (NMFS[11]).

Although the level of decrease in shrimp catch is not part of the NOAA testing protocol, it was discussed during workgroup meetings. The results of previous collaborative testing with industry in the Gulf of Mexico indicate that a 10% loss in shrimp catch may be acceptable, as long as bycatch is greatly reduced by the gear (Crowley, 2014). During discussions in our study, members of the workgroup from the fishing industry indicated that a 3–5% decrease in shrimp catch would likely be acceptable but that acceptable loss would ultimately depend upon the level of bycatch reduction achieved. Because discussions on this topic happened largely before preliminary results were obtained, it will be worthwhile to reexamine the issue of shrimp loss in future collaborations now that significant finfish bycatch reductions have been observed.

Gear evaluation

The use of 2 statistical procedures to evaluate the paired tows resulted in similar outcomes in most cases. Unlike the paired *t*-test, the randomization test did not assume that the data were normally distributed. Another advantage of the randomization procedure was that it did not require tows to be dropped from the analysis. Finally, the *P*-values computed in the randomization procedure are exact and not asymptotic.

Experimental gear costs

Fabrication and installation costs of the 14 experimental gear configurations varied considerably. However, cost was not a good predictor of performance. The estimates of gear costs included in Table 1 were provided by a local net maker and workgroup member; lower costs may be expected if fishermen build and install their own shrimp trawls. Further, we do not have costs for building a new experimental gear (costs are only for modifying control gear). Shrimp trawl components, particularly codends, have a finite life span and must be replaced with heavy use. Additional cost savings are likely if new gear is to be built rather than existing gear is to be modified.

Recommendations

Although our initial findings are promising, continued testing is necessary for repeatability and to ensure consistent and reliable performance by gears under variable conditions prior to widespread voluntary adoption (Murray et al., 1992). Shrimp catch and bycatch results varied considerably by vessel and between 2015 and 2016, although fishing was conducted in the same general area during the relatively short shrimp season.

Further, we recommend continuing the industry workgroup and evaluation of experimental gears and gear combinations on both smaller class vessels (<12 m) and vessels that operate in the nearshore Atlantic Ocean (<4.83 km from shore) in both the summer brown shrimp and autumn white shrimp fisheries. Smaller vessels accounted for approximately 66% of the fleet and for 64% of the effort by number of trips over the 5-year period 2013–2017 in North Carolina (Bianchi[18]). Although the majority of shrimp trawling effort in North Carolina typically occurs in estuarine waters, approximately 25% occurs in the nearshore Atlantic Ocean primarily <4.83 km from shore (i.e., in state managed waters).

[18] Bianchi, A. 2017. Personal commun. Div. Mar. Fish., North Carolina Dep. Environ. Qual., 3441 Arendell St., Morehead City, NC 28557.

Given additional time and funding, it would be worthwhile to explore bycatch reduction strategies beyond those tested here. The results of testing gear combinations in this study provide a strong basis by which to make adjustments. Despite the high levels of bycatch reduction achieved, *t*-test results indicate that the decrease of shrimp catch never exceeded 12.1% relative to that of the control net (Tables 3 and 4). In fact, loss of shrimp catch was significant only in 2 of 10 *t*-tests, indicating that even more radical approaches could be considered. For example, would a 20% decrease in shrimp catch be acceptable if finfish bycatch could be reduced by 80% in the estuarine shrimp fishery? Given that significant shrimp loss (>15%) would likely occur during the course of testing, future studies should consider funding that would compensate industry partners for lost revenue while adhering to strict testing protocols.

The importance of using a collaborative process for gear testing cannot be overstated. Projects that can combine the interests of both industry and resource management can often obtain multiple objectives and create successful cooperation between stakeholders (Yochum et al., 2011; Thornton and Scheer, 2012; O'Keefe and DeCelles., 2013). It would not have been possible to test 14 gears in the course of 3 sampling seasons without substantial and consistent industry input, involvement, and cost sharing of vessel time.

Acknowledgments

We thank the fishing vessel owners, captains, and crews and all workshop and workgroup members that participated in this collaborative effort. Special gratitude is extended in memory of the late S. Parrish, who served as a highly respected member of this workgroup and similar groups in the past. Funding was made available through the NCMFC's Conservation Fund, the North Carolina Sea Grant Program, the NOAA Bycatch Reduction Engineering Program (Award NA15NMF4720376), and the National Fish and Wildlife Foundation Fisheries Innovation Fund (Award 47988).

Literature cited

Andrew, N. L., and J. G. Pepperell.
1992. The by-catch of shrimp trawl fisheries. Oceanogr. Mar. Biol. Annu. Rev. 30:527–565.

Brewer, D., N. Rawlinson, S. Eayrs, and C. Burridge.
1998. An assessment of bycatch reduction devices in a tropical Australian prawn trawl fishery. Fish. Res. 36: 195–215.

Broadhurst, M. K.
2000. Modifications to reduce bycatch in prawn trawls: a review and framework for development. Rev. Fish Biol. Fish. 10:27–60.

Conway, F. D. L., and C. Pomeroy.
2006. Evaluating the human—as well as the biological—objectives of cooperative fisheries research. Fisheries 31:447–454.

Crowder, L. B., and S. A. Murawski.
1998. Fisheries bycatch: implications for management. Fisheries 23(6):8–17.

Crowley, M.
2014. Towing trends: making strides in bycatch, bottom impacts, fuel savings. Natl. Fisherman 94(11):32–33, 37.

Davies, R. W. D., S. J. Cripps, A. Nickson, and G. Porter.
2009. Defining and estimating global marine fisheries bycatch. Mar. Policy 33:661–672.

Eayrs, S.
2012. Comparative testing of bycatch reduction devices in tropical shrimp-trawl fisheries: a practical guide, 122 p. FAO, Rome.

Engaas, A., D. Foster, B. D. Hataway, J. W. Watson, and I. Workman.
1999. The behavioral response of juvenile red snapper (*Lutjanus campechanus*) to shrimp trawls that utilize water flow modifications to induce escapement. Mar. Tech. Soc. J. 33(2):43–50.

Hall, M. A., D. L. Alverson, and K. I. Metuzals.
2000. By-catch: problems and solutions. Mar. Pollut. Bull. 41:204–219.

Harte, M.
2001. Opportunities and barriers for industry-led fisheries research. Mar. Policy 25:159–167.

Hataway, D., D. Foster, and L. Saxon.
2017. Evaluations of turtle excluder devices (TEDs) with reduced bar spacing in the inshore penaeid shrimp fishery in the northern Gulf of Mexico. NOAA Tech. Memo. NMFS-SEFSC-707, 13 p.

Isaksen, B., J. W. Valdemarsen, R. B. Larsen, and L. Karlsen.
1992. Reduction of fish by-catch in shrimp trawl using a rigid separator grid in the aft belly. Fish. Res. 13: 335–352.

Kelleher, K.
2005. Discards in the world's marine fisheries: an update. FAO Fish. Tech. Pap. 470, 131 p. FAO, Rome.

Manly, B. F. J.
2007. Randomization, bootstrap, and Monte Carlo methods in biology, 3rd ed., 480 p. Chapman and Hall/CRC, Boca Raton, FL.

Murray, J. D., J. J. Bahen, and R. A. Rulifson.
1992. Management considerations for by-catch in the North Carolina and southeast shrimp fishery. Fisheries 17(1):21–26.

NCDMF (North Carolina Division of Marine Fisheries).
2015. North Carolina shrimp fishery management plan, Amendment 1, 366 p. Div. Mar. Fish., North Carolina Dep. Environ. Nat. Resour., Morehead City, NC. [Available from website.]

Noell, C. J., M. K. Broadhurst, and S. J. Kennelly.
2018. Refining a Nordmøre-grid bycatch reduction device for Spencer Gulf penaeid-trawl fishery. PLoS ONE 13(11):e0207117.

O'Keefe, C. E., and G. R. DeCelles.
2013. Forming a partnership to avoid bycatch. Fisheries 38:434–444.

R Core Team.
2017. R: a language and environment for statistical computing. R Foundation for Statistical Computing, Vienna, Austria. [Available from website, accessed December 2017.]

Rulifson, R. A., J. D. Murray, and J. J. Bahen.
1992. Finfish catch reduction in the South Atlantic shrimp trawls using three designs of by-catch reduction devices. Fisheries 17(1):9–20.

SAFMC (South Atlantic Fishery Management Council).
1996. Final amendment 2 (bycatch reduction) to the fishery management plan for the shrimp fishery of the

South Atlantic region, including a final supplemental environmental impact statement, regulatory impact review, and social impact assessment, 108 p. SAFMC, Charleston, SC. [Available from website.]

Scott-Denton, E., P. F. Cryer, M. R. Duffy, J. P. Gocke, M. R. Harrelson, D. L. Kinsella, J. M. Nance, J. R. Pulver, R. C. Smith, and J. A. Williams.
2012. Characterization of the U.S. Gulf of Mexico and South Atlantic penaeid and rock shrimp fisheries based on observer data. Mar. Fish. Rev. 74(4):1–27.

Silva, C. N. S., M. K. Broadhurst, A. Schwingel, J. H. Dias, A. P. Cattani, and H. L. Spach.
2011. Refining a Nordmøre-grid for a Brazilian artisanal penaeid-trawl fishery. Fish. Res. 109:168–178.

Silva, C. N. S., M. K. Broadhurst, J. H. Dias, A. P. Cattani, and H. L. Spach.
2012. The effects of Nordmøre-grid bar spacings on catches in a Brazilian artisanal shrimp fishery. Fish. Res. 127–128: 188–193.

Stephenson, R. L., S. Paul, M. A. Pastoors, M. Kraan, P. Holm, M. Wiber, S. Mackinson, D. J. Dankel, K. Brooks, and A. Benson.
2016. Integrating fishers' knowledge research in science and management. ICES J. Mar. Sci. 73:1459–1465.

Thornton, T. F., and A. M. Scheer.
2012. Collaborative engagement of local and traditional knowledge and science in marine environments: a review. Ecol. Soc. 17(3):8.

Vieira, W. J., M. M. Domingos, J. L. Rodrigues-Filho, and E. G. Gentil de Farias.
2017. Kite escape device: a new approach to reduce bycatch in shrimp trawls. Mar. Coast. Fish. 9:396–403.

Wardle, C. S.
1986. Fish behaviour and fishing gear. *In* The behaviour of teleost fishes (T. J. Pitcher, ed.), p. 463–495. Springer, Boston, MA.

Watson, J. W., Jr., and C. McVea Jr.
1977. Development of a selective shrimp trawl for southeastern United States penaeid shrimp fisheries. Mar. Fish. Rev. 39(10):18–23.

Watson, J., D. Foster, S. Nichols, A. Shah, E. Scoll-oenlon, and J. Nance.
1999. The development of bycatch reduction technology in the southeastern United States shrimp fishery. Mar. Technol. Soc. J. 33(2):51–56.

Winger, P. D., S. Eayrs, and C. W. Glass.
2010. Fish behavior near bottom trawls. *In* Behavior of marine fishes: capture processes and conservation challenges (Pingguo He, ed.), p. 65–103. Blackwell Publishing, Ames, IA.

Yochum, N., R. M. Starr, and D. E. Wendt.
2011. Utilizing fishermen knowledge and expertise: keys to success for collaborative fisheries research. Fisheries 36:593–605.

Acknowledgment of reviewers

The editorial staff of *Fishery Bulletin* would like to acknowledge the scientists who reviewed manuscripts in 2018–2019. Their contributions have helped ensure the publication of quality science.

Dustin Addis
Matthew Ajemian
Robert Allman
Michael Andres
Allen Andrews
Mayumi Arimitsu
Jerald Ault

M. Scott Baker Jr.
Luiz Barbieri
Henry Bart Jr.
William Bechtol
Arnaud Bertrand
Reginald Blaylock
Christopher Bonzek
Matthew Breece
Matt Broadhurst
Nancy Brown-Peterson
Jeffrey Buckel
Vincent Buonaccorsi
Erin Burge

Matthew Campbell
Shannon Cass-Calay
Elizabeth Chilton
J. Howard Choat
Mary Christman
Mark Collins
Christina Conrath
Jason Cope
Anthony Courtney

Kevin Dillon
David Dippold
William Driggers III
J. Marcus Drymon

Jim Ellis

Mariam Feki
James Franks
Richard Fulford
Gregory Fulling

Francisco García-Rodríguez
Trika Gerard
François Gerlotto
Melissa Gibbs
R. Grant Gilmore Jr.
M. Teresa González
Gretchen Grammer
Donald Gunderson

Dana Haggarty
Reginal Harrell
Chris Harvey
Joe Heublein
Allan Hicks
Scott Hinch
Eric Hoffmayer
Thomas Hurst
John Hyde

Kelsey James
Christopher Jerde
Christian Jones
Adrian Jordaan

Neosha Kashef
Bryan Keller
David Kerstetter
Christopher Koenig

Richard Langton
Dominique Lapointe
Kari Lavalli
Lyndsey Lefebvre
John Logan
Stuart Ludsin

Katey Marancik
Atsushi Maruyama
Mary Matta
Richard McBride
Andrew McDougall
W. David McElroy
Stephen McIninch
Richard Merrick
Richard Methot
Todd Miller
Michael Murphy

Lisa Natanson
Gavin Naylor
Sandra Neidetcher
Daniel Nichol

Jill Olin

Yannis Papastamatiou
Mark Peterson
Nicole Phillips
Richard Pillans
Adam Pollack
Jennifer Potts
Gregg Poulakis
Imants Priede

Joseph Quattro

Victor Restrepo
R. Anne Richards
Martin Robards
Paul Rudershausen

Skyler Sagarese
David Sampson
David Secor
William Slack
Thomas Sminkey
John Stieglitz
William Stockhausen
Christoph Stransky
James Sulikowski

Todd Tenbrink
Kenneth Tiffan

Donald Van Doornik
Jeremy Vaudo
Hannah Verkamp
Jon Vølstad

John Walter III
Chantel Wetzel
Sasha Whitmarsh
Bruce Wright
Mark Wuenschel

Joseph Zydlewski

Fishery Bulletin

Guidelines for authors

Contributions published in *Fishery Bulletin* describe original research in marine fishery science, fishery engineering and economics, and marine environmental and ecological sciences (including modeling). Preference will be given to manuscripts that examine processes and underlying patterns. Descriptive reports, surveys, and observational papers may occasionally be published but should appeal to an audience outside the locale in which the study was conducted.

Although all contributions are subject to peer review, responsibility for the contents of papers rests upon the authors and not on the editor or publisher. *Submission of an article implies that the article is original and is not being considered for publication elsewhere.*

All submissions are subject to a double-blind review to remove the identity of author and reviewer during the review process.

Plagiarism and double publication are considered serious breaches of publication ethics. To verify the originality of the research in papers and to identify possible previous publication, manuscripts may be screened with plagiarism-detection software.

Manuscripts must be written in English; authors whose native language is not English are strongly advised to have their manuscripts checked by English-speaking colleagues before submission.

Once a paper has been accepted for publication, online publication takes approximately 2 weeks.

There is no cost for publication in *Fishery Bulletin*.

Types of manuscripts accepted by the journal

Articles generally range from 20 to 30 double-spaced typed pages (12-point font) and describe an original contribution to fisheries science, engineering, or economics. Tables and figures are not included in this page count, but the number of figures should not exceed 1 figure for every 4 pages of text. Articles contain the following divisions: abstract, introduction, methods, results, and discussion.

Short contributions are generally less than 15 double-spaced typed pages (12-point font) and, like articles, describe an original contribution to fisheries science. They follow the same format as that for articles: abstract, introduction, methods, results, and discussion, but the results and discussion sections may be combined. They are distinguished from full articles in that they report a noteworthy new observation or discovery—such as the first report of a new species, a unique finding, condition, or event that expands our knowledge of fisheries science, engineering, or economics—and do not require a lengthy discussion.

Companion articles should be submitted together and are published together as a scientific contribution. Both articles should address a closely related topic and may be articles that result from a workshop or conference.

Preparation of manuscript

Title page should include authors' full names, mailing addresses, and the senior author's email address.

Abstract should be limited to 200 words (one-half typed page), state the main scope of the research, and emphasize the authors' conclusions and relevant findings. Do not review the methods of the study or list the contents of the paper. Because abstracts are circulated by abstracting agencies, it is important that they represent the research clearly and concisely.

General text must be typed in 12-point Times New Roman font throughout. A brief introduction should convey the broad significance of the paper; the remainder of the paper should be divided into the following sections: Materials and methods, Results, Discussion, and Acknowledgments. Headings within each section must be short, reflect a logical sequence, and follow the rules of subdivision (i.e., there can be no subdivision without at least 2 subheadings). The entire text should be intelligible to interdisciplinary readers; therefore, all acronyms, abbreviations, and technical terms should be written out in full and defined the first time they are mentioned. Abbreviations should be used sparingly because they are not carried over to indexing databases and slow readability for those readers outside a discipline. They should never be used for the main subject (species, method) of a paper.

For general style, follow the U.S. Government Publishing Office *Style Manual* (2016, available at website) and *Scientific Style and Format: the CSE Manual for Authors, Editors, and Publishers* (2014, 8th ed.) published by the Council of Science Editors. For scientific nomenclature, use the current edition of the American Fisheries Society's *Common and Scientific Names of Fishes from the United States, Canada, and Mexico* and its companion volumes (*Crustaceans, Mollusks, Cnidaria and Ctenophora*, and *World Fishes Important to North Americans*). For species not found in the above mentioned AFS publications and for more recent changes in nomenclature, use the Integrated Taxonomic Information System (ITIS, available at website), or, secondarily, the California Academy of Sciences *Catalog of Fishes* (available at website) for species names not included in ITIS. Common (vernacular) names of species should be lowercase. Citations must be given for the identification of specimens. For example, "Fish species were identified according to Collette and

Klein-MacPhee (2002); sponges were identified according to Stone et al. (2011)."

Dates should be written as follows: 11 November 2018. Measurements should be expressed in metric units, for example, "58 metric tons (t);" if other units of measurement are used, please make this fact explicit to the reader. Use numerals, not words, to express whole and decimal numbers in the general text, tables, and figure captions (except at the beginning of a sentence). For example, "We considered 3 hypotheses. We collected 7 samples in this location." Use American spelling. Refrain from using the shorthand slash (/), an ambiguous symbol, in the general text.

Cite all software, special equipment, and chemical solutions used in the study within parentheses in the general text, for example, "SAS, vers. 6.03 (SAS Institute Inc., Cary, NC)."

Word usage and grammar that may be useful are the following:

- *Aging*
  For our journal, the word *aging* is used to mean both age determination and the aging process (senescence). Authors should make clear which meaning is intended where ambiguity may arise.

- *Fish and fishes*
  The plural of the word fish (a collective noun that implies individuals without regard to species) is *fish*.
  Example: The *fish* were collected by trawl net.
  Example: The numbers of *fish* collected that season were less than the numbers from previous years.

  The plural for *fish species* is *fishes* (a contrived plural used by taxonomists to mean several or more *fish species*) or one can use *fish species* (which is preferred in this journal for clarity across disciplines).
  Example: The *fishes* of Puget Sound [biodiversity is implied] or
  Example: The *fish species* of Puget Sound [preferred plural for clarity across disciplines].

- *Crab and crabs, squid and squids, etc.*
  The plural of the word *crab* (i.e., many individuals without regard to species) is *crab*.
  Example: The crab were sorted by weight.
  Example: Many red king *crab* were dying [Many individuals of one species of crab.]

  The plural of *crab species* is *crabs* (a word used by taxonomists) or *crab species* (the latter is preferred in this journal for clarity).
  Example: These *crabs* were selected for treatment. [Different crab species are implied.]
  Example: These *crab species* were selected for treatment. [Preferred word choice for clarity of meaning.]
  Example: Snow *crabs* are found throughout the North Pacific Ocean and Bering Sea. [There are 2 species of snow crab and therefore the word *crabs* can be used here.]
  Example: *Two species* of snow *crab* are found throughout the North Pacific Ocean and Bering Sea. [Preferred usage for clarity.]
  Example: Three crabs were selected for treatment. [3 species of crab are implied.]
  Example: Three crab species were selected for treatment. [Preferred word choice for clarity.]

- *Fisherman and fisher*
  We use *fisherman* and *fishermen* in this journal not *fisher* and *fishers*. One can always use crew member, vessel operator, and angler (the latter for recreational fishing.

- *The definite article with common names of species*
  When the singular common name of a species represents the entire class or group to which it belongs, use the definite article.
  Example: Only one species of the genus *Salmo* is found in the Atlantic Ocean—*the* Atlantic salmon (*Salmo salar*).
  Example: The sonic emissions of *the* bottlenose dolphin are complex.

  For plural common names, this rule does not apply.
  Example: Chinook salmon are found throughout the Pacific Ocean.
  Example: Bottlenose dolphins are found in temperate and tropical waters.

- *Sex*
  For the meaning of male and female, use the word *sex*, not *gender*. Do not write "fish were sexed." Write, "sex was determined."

- *Participles*
  As adjectives, participles must modify a specific noun or pronoun.
  Example: Using mark-recapture methods, these scientists determined the size of the population. [Correct. The participle *using* modifies the word *scientists*.]
  Example: These scientists, based on the collected data, concluded that the mortality rate of these fish had increased. [Incorrect. The scientists were not based on the collected data.]
  Example: These scientists concluded, on the basis of collected data, that the mortality rate of these fish had increased. [Correct. The offending participle has been eliminated and an adverbial phrase modifies the verb *concluded*.]

Equations and mathematical symbols should be set from a standard mathematical program (MathType or Equation Editor). Equations formatted in LaTex are not acceptable. For mathematical symbols in the general text (α, χ^2, π, $\pm$, etc.), use the symbols provided by

the MS Word program and italicize all variables, except those variables represented by Greek letters and the superscript and subscript parts of variables and expressions. Do not use photo mode when creating these symbols in the general text, and do not cut and paste equations, letters, or symbols from a different software program.

Number equations (if there are more than one) for future reference by scientists; place the number within parentheses at the end of the first line of the equation.

Literature cited section comprises published works and those accepted for publication (in press) in peer-reviewed journals. Follow the name and year system for citation format in this section (i.e., citations should be listed alphabetically by the authors' last names, and then by year if there is more than one citation by the same author. A list of abbreviations for citing journal titles can be found at this website.

Authors are responsible for the accuracy and completeness of all citations. Literature citation format: Authors (last name, followed by initials for first name and, if given, middle name of first author; then list names of additional authors with initials before last names). Year. Title of article. Abbreviated title of the journal in which it was published. Always include either the range of page numbers (for a journal article) or a total number of pages (for a book or other type of publication). List a sequence of citations in the general text chronologically, for example, "(Smith, 1932: Green. 1947; Smith and Jones, 1985)." Avoid the use of multiple citations when a single citation sufficiently supports a statement; cite the work that first reported the information that supports a statement, not all of the subsequent works.

Acknowledgments should be no more than 6 lines of text. Only those who have contributed in an outstanding way should be acknowledged by name. For recognition of other persons or groups, use a general term, such as *crew*, *observers*, or *research coordinators*, and do not include names with these terms.

Digital object identifier (doi) code ensures that a publication has a permanent location online. A doi link (which may include a doi code) should be included at the end of citations of published literature. Authors are responsible for submitting accurate doi links. Faulty links will be deleted at the page-proof stage.

Footnotes are used for all documents that have not been formally peer reviewed and for observations and personal communications, but these types of references should be cited sparingly in manuscripts submitted to the journal.

All reference documents, administrative reports, internal reports, progress reports, project reports, contract reports, personal observations, personal communications, unpublished data, manuscripts in review, and council meeting notes are footnoted in 9-point font and placed at the bottom of the page on which they are first cited. Footnote format is the same as that for formal literature citations. A link to the online source (e.g., [Available from http://www... , accessed July 2017.]), or the mailing address of the agency or department holding the document, should be provided so that readers may obtain a copy of the document.

Tables are often overused in scientific papers; it is seldom necessary to present all the data associated with a study. Tables should not be excessive in size and must be cited in numerical order in the text. Headings should be short but ample enough to allow the table to be intelligible on its own.

All abbreviations and unusual symbols must be explained in the table legend. Other incidental comments may be footnoted with numeral footnote markers. Use asterisks only to indicate significance in statistical data. Do not put a table legend on a page separate from the table; place the legend above the table. *Do not submit tables in photo mode.*

- Note probability with a capital, italic *P*.
- Provide a zero before all decimal points for values less than one (e.g., 0.07).
- Round all values to 2 decimal points.
- Use a comma in numbers of 5 digits or more (e.g., 13,000 but 3000).

Figures must be cited in numerical order in the text. Graphics should aid in the comprehension of the text, but they should be limited to presenting patterns rather than raw data. The number of figures should not exceed 1 figure for every 4 pages of text. Place panel labels **A, B, C,** etc., within the upper-left area of graphs and photos. Avoid placing labels vertically.

Figure legends should explain all symbols and abbreviations seen in the figure and should be double spaced on a separate page at the end of the manuscript.

Line art and halftone figures should be saved at resolutions >600 dots per inch (dpi) and >300 dpi, respectively. Color is allowed in figures to show morphological differences among species (for species identification), to show stain reactions, to show gradations (such as those of temperature and salinity within maps), and to distinguish between numerous lines and symbols in graphs. Figures approved for color should be saved in CMYK format.

All figures must be submitted as PDF, TIFF, or EPS files.

- Capitalize only the first letter of the first word and proper nouns in all labels within figures.
- Do not use overly large font sizes in maps and for axis labels in graphs.

- Do not use bold fonts or bold lines in figures.
- Do not place outline rules around graphs.
- Place a north arrow and label degrees latitude and longitude (e.g., 170°E) in all maps.
- Use symbols, shadings, or patterns (not clip art) in maps and graphs.

Supplementary materials that are considered essential, but are too large or impractical for inclusion in a paper (e.g., metadata, figures, tables, videos, and websites), may be provided at the end of an article. These materials are subject to the editorial standards of the journal. A URL to the supplementary material and a brief explanation for including such material should be sent at the time of initial submission of the paper to the journal.

- **Metadata, figures, and tables** should be submitted in standard digital format (MS Word or PDF file) and should be cited in the general text, for example, as "... was determined (Suppl. Table 3, Suppl. Fig. 1)."
- **Websites** should be cited with a URL in the general text.
- **Videos** must not be larger than 30 MB to allow a swift technical response for viewing the video. Authors should consider whether a short video uniquely captures what text alone cannot capture for the understanding of a process or behavior under examination in the article. Supply an online link to the location of the video.

Copyright law does not apply to *Fishery Bulletin*, which falls within the public domain. However, if an author reproduces any part of an article from *Fishery Bulletin*, reference to source is considered correct form (e.g., Source: Fish. Bull. 97:105).

Failure to follow these guidelines and failure to correspond with editors in a timely manner will delay publication of a manuscript.

Submission of manuscript

Submit a manuscript online at the ScholarOne Manuscripts website for *Fishery Bulletin*. Commerce Department authors should submit papers under a completed NOAA Form 25-700. For further details on electronic submission, please contact the associate editor, Cara Mayo, at

cara.mayo@noaa.gov.

When requested, the text and tables should be submitted in MS Word format. Each figure should be sent as a separate PDF, TIFF, or EPS file. Send a copy of a figure in the original software if conversion to any of these formats yields a degraded version of the figure.

Questions? If you have questions regarding these guidelines, please contact the managing editor, Kathryn Dennis, at

kathryn.dennis@noaa.gov.

Questions regarding manuscripts under review should be addressed to Associate Editor Cara Mayo.

Please note that Sharyn Matriotti has retired after serving for 29 years as the managing editor of *Fishery Bulletin*.

Fishery Bulletin

Subscription form

Superintendent of Documents **Publications** Order Form

*5178

☐ YES, please send me the following publications:

____ Subscriptions to *Fishery Bulletin*
for $32.00 per year ($44.80 foreign)

The total cost of my order is $ _____ . Prices include regular domestic postage and handling and are subject to change.

_____
(Company or Personal Name) (Please type or print)

_____
(Additional address/attention line)

_____
(Street address)

_____
(City, State, ZIP Code)

_____
(Daytime phone including area code)

_____
(Purchase Order No.)

Charge your order. IT'S EASY!

VISA

MasterCard

Please Choose Method of Payment:

☐ Check payable to the Superintendent of Documents
☐ GPO Deposit Account ☐☐☐☐☐☐☐–☐
☐ VISA or MasterCard Account
☐☐☐☐☐☐☐☐☐☐☐☐☐☐☐☐
☐☐☐☐ (Credit card expiration date)

To fax your orders (202) 512-2104

_____
(Authorizing Signature)

Mail to: Superintendent of Documents
P.O. Box 979050, St. Louis, Missouri 63197
Tel. no. (U.S. callers): 866-512-1800
Tel. no. (International callers): 1-202-512-1800

Thank you for your order!

Also available online at
http://bookstore.gpo.gov/actions/GetPublication.do?stocknumber=703-023-00000-2
email: ContactCenter@gpo.gov

SMITHSONIAN LIBRARIES
3 9088 01818 1545